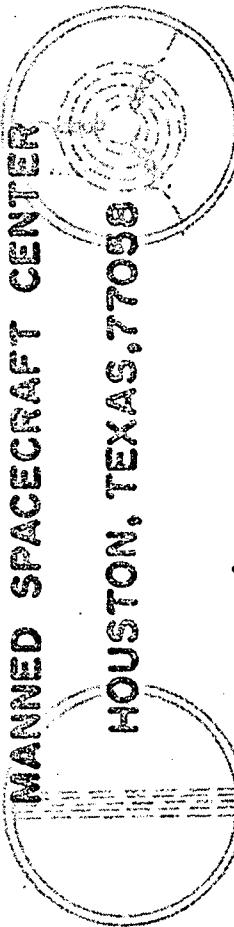


HEAT PIPE  
DESIGN

HANDBOOK  
PART I  
PREPARED FOR

NASA



W74-22569

HEAT PIPE DESIGN  
NASA-CR-134264  
(NASA-HANDBOOK, PART I)  
DYNATHERM  
CORPORATION  
Cockeysville, Maryland 21030

Unclassified  
SCL 20N G3/33 38187

Dynatherm

CORPORATION  
Cockeysville, Maryland 21030

REPRODUCED BY  
NATIONAL TECHNICAL  
INFORMATION SERVICE  
U.S. DEPARTMENT OF COMMERCE  
SPRINGFIELD, VA 22261

N O T I C E

THIS DOCUMENT HAS BEEN REPRODUCED FROM THE  
BEST COPY FURNISHED US BY THE SPONSORING  
AGENCY. ALTHOUGH IT IS RECOGNIZED THAT CERT-  
AIN PORTIONS ARE ILLEGIBLE, IT IS BEING RE-  
LEASED IN THE INTEREST OF MAKING AVAILABLE  
AS MUCH INFORMATION AS POSSIBLE.

DRL-2  
DRD No. SE-354T  
DTM 72-3

HEAT PIPE DESIGN HANDBOOK

Contract No. NAS9-11927

August 1972

Prepared For

National Aeronautics and Space Administration  
Manned Spacecraft Center  
Houston, Texas

Prepared By

Dynatherm Corporation Engineering Staff

Submitted By E. A. Skrabek

E. A. Skrabek  
Principal Investigator

Approved By W. B. Bienert

W. B. Bienert  
Engineering Manager

FOREWARD

This Handbook was prepared under NASA Contract NAS9-11927, "Preparation of a Heat Pipe Design Handbook." The work is administered by the Manned Spacecraft Center, Houston, Texas, and Mr. Richard Bullock is the NASA Technical Monitor.

The program is being conducted by the Dynatherm Corporation, Cockeysville, Maryland, with Dr. Walter B. Blenert serving as Program Manager and Dr. Emanuel A. Skrabek as Principal Investigator.

The following members of the Dynatherm engineering staff contributed significantly to the Program: Mr. Patrick J. Brennan, Mr. Noel L. Lee, and Mr. Edward J. Kroliczek. Mr. Milton F. Pravda provided a major contribution in ensuring the overall continuity and accuracy of the Handbook. Special thanks are due Mrs. Mary E. Brezinski, who checked and typed nearly the entire final manuscript; Mr. Theodore P. Zarnoch, who prepared all of the figures and tables; and Mr. Robert W. Spangler, who developed the performance curves.

NOTE TO THE USER

This volume is intended basically to be a loose-leaf reference document capable of continuous expansion and revision as new data become available. It has been temporarily bound as an economical means of assembly and distribution. It is punched for standard three-ring binders.

The computer program user's manuals are bound separately as Part II as a convenience to the user.

FOREWORD  
NOTE TO THE USER

TABLE OF CONTENTS

I. 0	INTRODUCTION . . . . .	I-2
I. 1	History . . . . .	I-1
I. 2	Principles of Operation . . . . .	I-2
I. 3	Types . . . . .	I-4
I. 4	Operating Ranges . . . . .	I-4
I. 5	Applications . . . . .	I-5
I. 6	Arrangement of Handbook . . . . .	I-8
I. 7	Nomenclature . . . . .	I-10
I. 8	Units and Conversion Tables . . . . .	I-16
T. 0	HEAT PIPE THEORY . . . . .	T-1
T. 1	Introduction . . . . .	T-1
T. 2	Fundamental Considerations . . . . .	T-4
T. 3	Capillary Pressure . . . . .	T-8
T. 4	Pressure Gradients in the Liquid . . . . .	T-11
T. 4. 1	Viscous Pressure Gradients in the Liquid . . . . .	T-11
T. 4. 2	Body Forces in the Liquid . . . . .	T-13
T. 5	Pressure Gradient in the Vapor . . . . .	T-15
T. 5. 1	Viscous Pressure Gradients in the Vapor . . . . .	T-15
T. 5. 2	Dynamic Pressure Gradients in the Vapor . . . . .	T-16
T. 5. 3	Non-Laminar Flow and Compressibility Effects . . . . .	T-17
T. 5. 4	Body Forces in the Vapor . . . . .	T-17
T. 6	Capillary Heat Transport Limit . . . . .	T-18
T. 6. 1	General Approach . . . . .	T-18
T. 6. 2	Heat Transport Factor and Heat Transport Capability Factor . . . . .	T-23
T. 6. 3	Closed Form Solution . . . . .	T-27
T. 7	Other Heat Transport Limitations . . . . .	T-31
T. 7. 1	Sonic Limit . . . . .	T-31
T. 7. 2	Entrainment Limit . . . . .	T-33
T. 7. 3	Heat Flux Limit . . . . .	T-34
T. 8	Heat Transfer . . . . .	T-36
T. 9	Variable Conductance Heat Pipes . . . . .	T-43
T. 9. 1	Techniques for Varying Heat Pipe Conductance . . . . .	T-44
T. 9. 2	Categories of Variable Conductance Heat Pipes . . . . .	T-46
T. 9. 3	Variable Conductance Through Condenser Flooding with Gas . . . . .	T-47
T. 9. 4	Self-Controlled VCHP's . . . . .	T-53
(Wicked, Uncontrolled Storage Reservoir -- Non-Wicked Storage Reservoir -- Wicked, Temperature Controlled Storage Reservoir)		
T. 9. 5	Feedback Self-Controlled VCHP's . . . . .	T-60
(Mechanical Feedback -- Electrical Feedback)		
T. 9. 6	Variable Set Point Heat Pipes . . . . .	T-67
T. 9. 7	Active VCHP . . . . .	T-69

T.9.8	Diffusion Effects . . . . .	T-69
	(Flat Front Model -- Diffuse Front Model -- Numerical Analysis of Diffuse Vapor/Gas Front)	
T.9.9	Notes on Transients . . . . .	T-78
	(Wicked Reservoir Heat Pipe -- Non-Wicked Reservoir Heat Pipe -- Feedback Controlled VCHP's)	
T.9.10	Other Variable Conductance Techniques . . . . .	T-82
	(Condenser Flooding with Liquid -- Liquid Flow Control -- Vapor Flow Control)	
D.0	HEAT PIPE DESIGN PROCEDURE . . . . .	D-1
D.1	Introduction . . . . .	D-1
D.2	Problem Definition and Design Criteria . . . . .	D-1
D.2.1	Problem Definition . . . . .	D-3
	(Heat Pipe vs. Conductive Heat Transfer -- Heat Pipe vs. Forced Flow Systems -- Heat Pipe as a Temperature Control System)	
D.2.2	Design Criteria . . . . .	D-9
	(Operating Temperature Range -- Thermal Load -- Transport Length -- Temperature Uniformity and Overall $\Delta T$ -- Physical Requirements -- Acceptance and Qualification Testing -- Ground Testing -- Dynamic Environment -- Man Rating -- Thermal Environment -- Mechanical Interfacing -- Transient Behavior -- Reliability -- Temperature Sensitivity)	
D.3	Performance Limit Evaluation . . . . .	D-16
D.3.1	Capillary Transport Limit . . . . .	D-17
	(Category 1. General One Dimensional Heat Pipe -- Category 2. General One Dimensional Heat Pipe -- Category 3. Special Closed Form Solution -- Case 1. Heat Pipe in Zero Gravity -- Case 2. Conventional Heat Pipe Operating Against Gravity)	
D.3.2	Sonic Limit . . . . .	D-29
D.3.3	Entrainment Limit . . . . .	D-30
D.3.4	Heat Flux Limit . . . . .	D-30
D.4	Conventional Heat Pipe Design Procedures . . . . .	D-31
D.4.1	Selection of Working Fluid . . . . .	D-31
	(Operating Temperature -- Operating Pressure -- Liquid Transport Capabilities -- Fluid Wicking Capability in a Body-Force Field -- Heat Transfer Requirements -- Fluid Compatibility and Stability)	
D.4.2	Wick Design . . . . .	D-40
	(Conventional Wick Design -- Composite Wick Design)	
D.4.3	Container Design . . . . .	D-54
	(Material Selection -- Configuration Selection -- Structural Consideration)	
D.4.4	Fluid Inventory . . . . .	D-56

D.5	Variable Conductance Heat Pipe Design . . . . .	D-58
D.5.1	General . . . . .	D-58
(Wicked Reservoir Systems -- Cold Reservoir -- Constant		
Temperature Reservoir -- Feedback VCHP -- Non-Wicked		
Reservoirs)		
D.5.2	Design Considerations . . . . .	D-65
D.5.3	Design Procedure . . . . .	D-66
P.0	PERFORMANCE CURVES . . . . .	P-1
P.1	Conventional Heat Pipes . . . . .	P-1
P.2	Variable Conductance Heat Pipes . . . . .	P-5
W.0	WICK DATA . . . . .	W-1
W.1	Basic Properties . . . . .	W-1
W.2	Prediction of Properties . . . . .	W-1
W.2.1	Effective Pore Radius . . . . .	W-1
W.2.2	Permeability of Various Wicks . . . . .	W-5
W.3	Composite Wicks . . . . .	W-10
W.4	Experimental Values . . . . .	W-15
W.4.1	Effective Pore Radius . . . . .	W-15
W.4.2	Permeability . . . . .	W-20
W.5	Suppliers of Wick Materials . . . . .	W-22
F.0	FLUID PROPERTIES . . . . .	F-1
1.	Hydrogen . . . . .	F-4
2.	Neon . . . . .	F-6
3.	Nitrogen . . . . .	F-8
4.	Oxygen . . . . .	F-12
5.	Methane . . . . .	F-14
6.	Freon-21 . . . . .	F-16
7.	Ammonia . . . . .	F-18
8.	Freon-11 . . . . .	F-22
9.	Acetone . . . . .	F-24
10.	Methanol . . . . .	F-26
11.	Benzene . . . . .	F-28
12.	Water . . . . .	F-30
13.	Mercury . . . . .	F-34
14.	Cesium . . . . .	F-36
15.	Potassium . . . . .	F-38
16.	Sodium . . . . .	F-40
17.	Lithium . . . . .	F-44
18.	Silver . . . . .	F-46
M.0	MATERIALS COMPATIBILITY . . . . .	M-1
M.1	Introduction . . . . .	M-1
M.2	Low Temperature Corrosion . . . . .	M-3
M.3	High Temperature Corrosion . . . . .	M-6

M.3.1	Oxygen Corrosion . . . . .	M-6
M.3.2	Simple Solution Corrosion . . . . .	M-7
M.4	Cleaning Methods . . . . .	M-8
M.5	Experimental Results . . . . .	M-9
B.0	BIBLIOGRAPHY . . . . .	B-1
B.1	Introduction . . . . .	B-1
I.0	INDEX . . . . .	X-1
C.0	COMPUTER CODES USER'S MANUALS (BOUND SEPARATELY AS PART II) . . . . .	C-1
C.1	Heat Pipe Analysis and Design (HPAD) . . . . .	C.1-1
C.2	Data Acquisition Code (DAC) . . . . .	C.2-1
C.3	Variable Conductance Heat Pipe Analysis (VCHPA) . . . . .	C.3-1

I.1 History

In 1944, Gaugler (2) patented a lightweight heat transfer device which was essentially the present heat pipe. However, the technology of that period presented no clear need for such a device and it lay dormant for two decades. The idea was resurrected in connection with the space program, first as a suggestion by Trefethen (6) in 1962 and then form of a patent application by Wyatt in 1963. It was not until Grover and his co-workers (3) of the Los Alamos Scientific Laboratory rediscovered the concept in late 1963 and built prototypes that the impetus was provided to this technology. Grover also coined the name "heat pipe" and stated that "Within certain limitations on the manner of use, a heat pipe may be regarded as a synergistic engineering structure which is equivalent to a material having a thermal conductivity greatly exceeding that of any known metal."

The first heat pipe which Grover built used water as the working fluid and was followed shortly by a liquid-sodium heat pipe for operation at 1100°K. Both the high temperature and ambient temperature regimes were soon explored by many workers in the field. It was not until 1966 that the first cryogenic heat pipe was developed by Haskin of the Air Force Flight Dynamic Laboratory at Wright-Patterson Air Force Base.

The concept of a Variable Conductance or Temperature Controlled Heat Pipe was first described by Hall of RCA in a patent application dated October 1964. However, although the effect of a noncondensing gas was shown in Grover's original publication, its significance for achieving variable conductance was not immediately recognized. In subsequent years the theory and technology of Variable Conductance Heat Pipes was greatly advanced, notably by Bienert and Brennan at Dynatherm and Marcus at TRW.

On April 5, 1967, the first zero "g" demonstration of a heat pipe was conducted by a group of engineers of the Los Alamos Scientific Laboratory. This first successful flight experiment overcame the initial hesitation that many spacecraft

designers had for using this new technology to solve the ever-present temperature control problems on spacecraft. Subsequently, more and more spacecrafts have relied on heat pipes either to control the temperature of individual components or of the entire structure. Recent examples of this trend are the ATS-E, OAO, ATS F&G spacecrafts, and the Sky Lab.

The development of terrestrial applications of heat pipes progressed at a much slower pace. In 1968, RCA developed a heat pipe heat sink for transistors used in aircraft transmitters. This probably represented the first commercial application of heat pipes. In the meantime, many other applications have firmly established that heat pipes can solve many critical problems in heat transfer and temperature control.

### 1.2 Principles of Operation

The basic heat pipe is a closed container which has been evacuated of all noncondensable gases and which contains a capillary wick structure and a small amount of vaporizable fluid. The heat pipe employs a boiling-condensing cycle and the capillary wick pumps the condensate to the evaporator. This is shown schematically in

Figure 1-1.

The vapor pressure drop between the evaporator and the condenser is very small; and, therefore, the boiling-condensing cycle is essentially an isothermal process. Furthermore, the temperature losses between the heat source and the vapor and between the vapor and the heat sink can be made small by proper design. Therefore, one feature of the heat pipe is that it can be designed to transport heat between the heat source and the heat sink with very small temperature losses.

The amount of heat that can be transported as latent heat of vaporization is usually several orders of magnitude larger than can be transported as sensible heat in a conventional convective system with an equivalent temperature difference. Therefore, a second feature of the heat pipe is that relatively large amounts of heat can be transported with small lightweight structures.

The capillary pumping head is derived from a difference in the radii of curvature of the fluid surfaces in the capillary pores in the evaporator and condenser

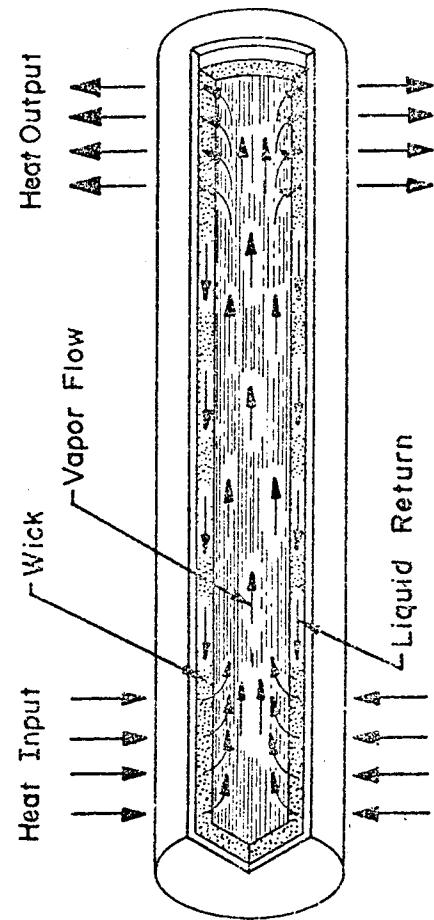


Figure I-1. Schematic Representation of the Heat Pipe

wick sections. In order for the available capillary pumping head to be able to provide adequate circulation of the working fluid, it must be sufficient to overcome the viscous and dynamic losses of the system and it must compensate for adverse gravity effects. Capillary pumping heads are normally small when compared to the pumping heads available in dynamic systems. Therefore, certain restrictions must be imposed on the application of heat pipes in gravity environments.

Hydrodynamics is important in the overall functioning of the heat pipe, since the interaction between the working fluid and the wick (and the container walls) essentially determines the flow rate of the fluid. Heat transfer theory provides information on the conductance of thermal energy into and out of the heat pipe through its various components (container, wick, and working fluid) and the thermal interfaces of the heat pipe with the heat source and heat sink. Therefore, the designer must be acquainted with basic hydrodynamic and heat transport concepts before he can intelligently design a device. All of the above points are discussed in detail in the Theory Chapter (Sections T. 1 through T. 8).

### 1.3 Types

Heat pipes are classified into two general types -- "Conventional" and "Variable Conductance". The conventional heat pipe is a device of very high thermal conductance with no fixed operating temperature. Its temperature rises or falls according to variations in the heat source or heat sink.

It was recognized rather early <sup>(1)</sup> in the history of heat pipe research that techniques could be developed which would provide for control of the effective thermal conductance of the heat pipe. This was first envisioned as a blocking of a portion of the condenser by a noncondensable gas. More recently several other types of control have been proposed. These are discussed in Section T. 9. Such techniques enable the device to be operated at a fixed temperature independent of source and sink conditions, or even allows programmable temperature to be used.

### 1.4 Operating Ranges

In this manual, the operating temperature ranges of the heat pipes are

referred to as "cryogenic" ( $0^{\circ}$  to  $150^{\circ}$ K) ( $-459^{\circ}$  to  $-189^{\circ}$ F), "low temperature" ( $150^{\circ}$  to  $750^{\circ}$ F) ( $-189^{\circ}$  to  $+890^{\circ}$ F), and "high temperature" ( $750^{\circ}$  to  $3000^{\circ}$ F) ( $890^{\circ}$  to  $5432^{\circ}$ F). These ranges have been defined somewhat arbitrarily such that the currently known working fluids are generally of the same type within each range, and each range is roughly four times as large as the preceding one. Working fluids are usually elemental or simple organic gases in the cryogenic range, mainly polar molecules or halocarbons in the low temperature range, and liquid metals in the high temperature range.

The approximate useful range of the eighteen fluids whose properties are presented in this Handbook in the limits of the three regimes are indicated in Figure I-2. Also indicated are the limits of the three regimes as defined above. The limits of the ranges should only be considered as approximate since some of the fluids overlap into the next temperature range.

The properties of the fluids are not constant over the temperature ranges indicated, but most of them peak somewhat above their boiling point. The Maximum Heat Transport Capability (a function of fluid properties and heat pipe geometry) also varies widely through these temperature regimes. The abscissa of Figure I-2 indicates the order of increasing Maximum Heat Transport Capability of these fluids in similar geometry heat pipes but is not drawn to any scale. For example, in the cryogenic range approximately  $10$  watt-meters ( $400$  watt-inches) can be attained, while in the low temperature regime it is on the order of  $10^4$  watt-meters ( $40 \times 10^4$  watt-inches), and for the best of the high temperature fluids it approaches  $10^6$  watt-meters ( $40 \times 10^6$  watt-inches).

### I.5 Applications

Heat pipes have been used in many varied applications during the first decade of their existence, and future applications seem limited only by the ingenuity of the designer. They show to best advantage in situations which require the transport of large amounts of heat over large distances; but they are certainly not limited to such cases, as can be seen by the list of applications in Table I-0 most of which have already been reduced to practice.

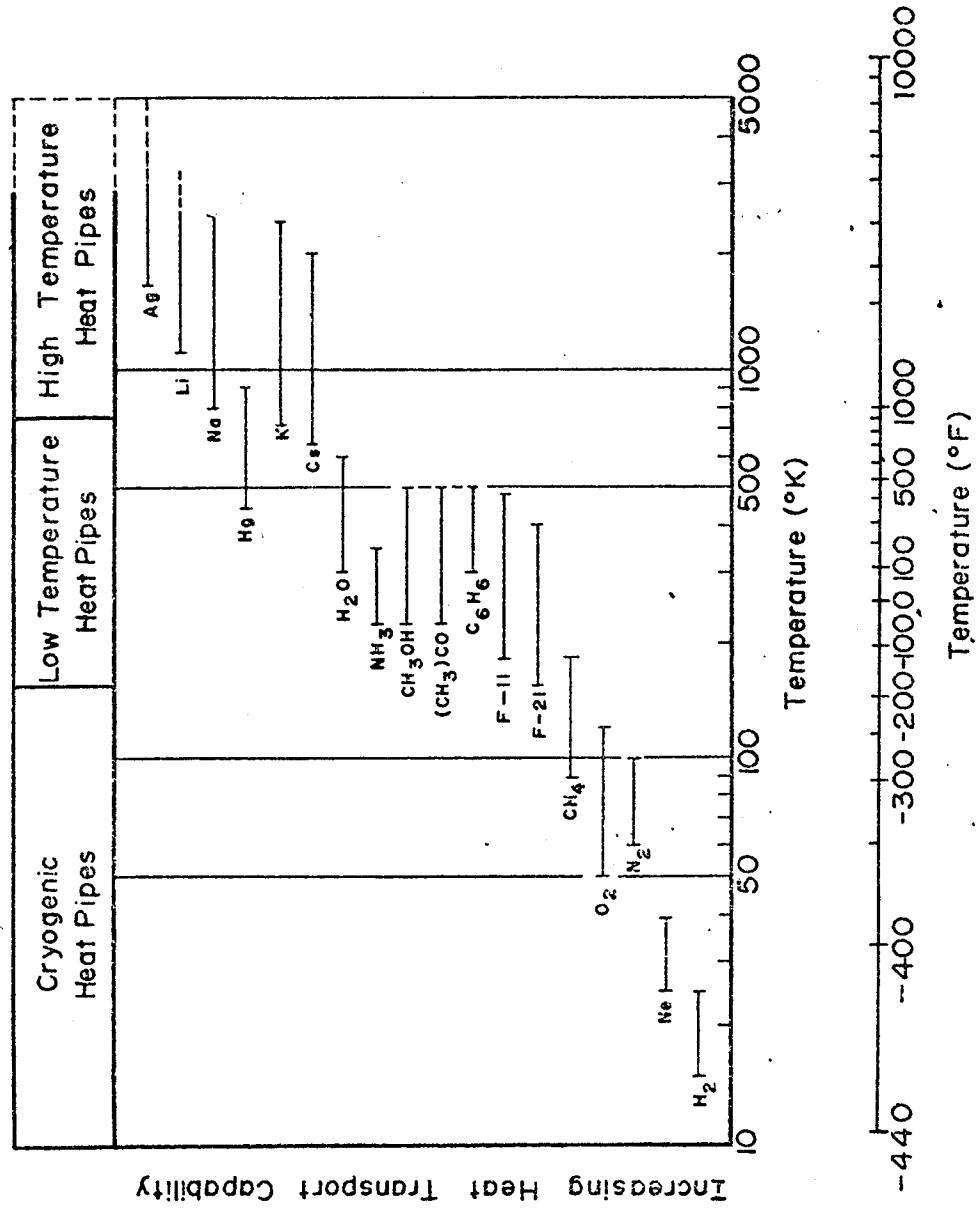


Figure I-2. Approximate Range of Applicability of Some Working Fluids in the Various Temperature Regimes

Table I-0. Application of Heat Pipes

Cooling	Heating	Spacecraft	Specialized Users
Arc Jets	Chemical Reactors	Temperature Regulation	Surgical Cryoprobes
Batteries	Coal Gasification	Isothermalization of Structures	Heat Exchangers
Brakes	Cooking Appliances	Electronically Cooling on:	Measurements:
Bus Bars	Dielectric Bridges	• ATS F&G	• Emissivity
Gold Traps	Isothermal Furnaces	• OAO-C	• Surface Tension
Drill Shafts	Thermionic Emitter	• Thermal Conductivity	• Vapor Pressure
Electric Motors			
Fuel Cells			
Leading Edges of Wings			
Castings Molds			
Radioisotope Power Sources			
Nuclear Reactors			
Turbine Shafts & Blades			

The topics included in this Handbook have been divided into relatively independent chapters. The internal numbering of pages, figures, etc., of each chapter starts from one (1) and is thus independent of the other sections. The chapters are indicated by letter, but it should be noted that they do not follow in alphabetic order, rather they are the initial letters of the chapter titles. This arrangement has been adopted so as to allow easy expansion and modification of format in any updated editions.

Most of the chapters have been written to be relatively self-sufficient for use by the designer. However, it is recommended that the theory and design procedures chapters be read before an attempt is made to apply any of the formulas given in the Handbook to an actual design.

The major topics considered in this Handbook are theory, design, data, and general information. The theory of heat pipes is considered in detail for conventional heat pipes in Sections T.1 through T.8 and for variable conductance heat pipes in Section T.9. Design techniques and aids are presented in the Design Procedures (D), Performance Curve (P), and Computer Code (C) Chapters. Much of the readily useable experimental data published to date has been included in the Wick Data (W), Fluid Properties (F), and Materials Compatibility (M) Chapters. The general information (nomenclature, units, conversion tables, references, and cross-index) are contained in the Introduction (I), Bibliography (B), and Index (X) Chapters.

The fluid properties needed for heat pipe analysis and design are presented for six fluids in each of the three temperature ranges. Much of the available experimental data on which properties is included in Chapter W (Wick Data). Since this data is relatively sparse, a series of equations are presented which will allow the designer to estimate values of the permeability and capillary pumping radius for some well defined wick system.

An estimate of the reliability of various combinations of container materials and working fluids can be obtained from a study of the final table in Chapter M (Materials Compatibility). This chapter also lists the types of problems which can

result from an injudicious selection of wick, container, weld material, and working fluid.

A collection of performance curves is also included to indicate the types of performance to be expected from various designs.

Several computer codes have been included to aid the designer with access to computer facilities. Included are a conventional heat pipe design code, a data acquisition code, and variable conductance heat pipe code.

A quick reference table to the articles listed in the Bibliography is included as an aid to easy access to articles dealing with particular topics. Also included are references to other sources of information. The index is cumulative for the whole Handbook.

The basic system of units (following recommendation of NBS and NASA) is the International Scientific (SI) system. However, important data is listed in both SI and English Engineering Units and conversion tables are included at the end of this chapter.

### I.7 Nomenclature

The following pages contain a listing of the symbols used throughout this Handbook. The units for each quantity are given in both the mks system and the English Engineering Units.

Table I-1. Nomenclature

Symbol	SI Unit	English Unit
A	Area $\text{m}^2$	$\text{ft}^2$
$A, A_o$ $B, B_o$	Constants for Beattie-Bridgman Equation	
$C_p$	Heat Capacity $\text{J kg}^{-1}\text{K}^{-1}$	$\text{Btu lbm}^{-1}\text{o F}^{-1}$
D	Diameter $\text{m}$	ft (in)
F	Body Force $\text{N}$	lbf
$F_1$	Pressure Drop Ratio	
G	Thermal Conductance $\text{W K}^{-1}$	$\text{Btu hr}^{-1}\text{o F}^{-1}$
G	Gibbs Free Energy $\text{J kg}^{-1}$	$\text{Btu lbm}^{-1}$
H	Wicking Height Factor $\text{m}^2$	$\text{ft}^2$
K	Permeability $\text{m}^2$	$\text{ft}^2$
L	Length $\text{m}$	ft (in)
M	Molecular Weight $\text{kg kmole}^{-1}$	$\text{lbm mole}^{-1}$
N	Mesh Number (of screens) $\text{m}^{-1}$	$\text{in}^{-1}$
N	Transport Factor $\text{W m}^{-2}$	$\text{W in}^{-2}$
Q	Axial Heat Flow Rate $\text{W}$	$\text{Btu hr}^{-1}$
QL	Heat Transport Factor $\text{W m}$	$\text{W in}$
R	Principal Radius of Curvature $\text{m}$	ft (in)
R	Thermal Impedance $\text{K W}^{-1}$	$\text{o F W}^{-1}$
Re	Reynolds Number	
Rg	Gas Constant ( $R_o/M$ ) $\text{J kg}^{-1}\text{K}^{-1}$	$\text{ft lbf lbm}^{-1}\text{o F}^{-1}$
$R_o$	Universal Gas Constant $\text{J kmole}^{-1}\text{K}^{-1}$	$\text{Btu mole}^{-1}\text{o F}^{-1}$

Table I-1. Nomenclature (Continued)

Symbol	SI Unit	English Unit
$S$	Crimping Factor	
$T$	Temperature	$^{\circ}\text{F}$
$V$	Volume	$\text{m}^3$ $\text{ft}^3$
$V'$	Defined in Section D.5.1	
$We$	Weber Number	ft
$a$	Area Per Unit Length	m
$a, b, c$	Constants for Beattie-Bridgman Equation	
$b$	Tortuosity Factor	
$d$	Wire Diameter	m $\text{in}$
$g$	Acceleration	$\text{m s}^{-2}$ $\text{ft s}^{-2}$
$h$	Heat Transfer Coefficient	$\text{W cm}^{-2}\text{K}^{-1}$ $\text{Btu hr}^{-1}\text{ft}^{-2}\text{o_F}^{-1}$
$h$	Wicking Height	m ft
$k$	Thermal Conductivity	$\text{W em}^{-1}\text{K}^{-1}$ $\text{Btu ft hr}^{-1}\text{ft}^{-2}\text{o_F}^{-1}$
$k$	Spring Constant of Bellows	$\text{N m}^{-1}$
$m$	Mass Flow Rate	$\text{kg s}^{-1}$ $\text{lbf ft}^{-1}$
$p$	Pressure	$\text{N m}^{-2}$ $(\text{psia}) \text{lbf in}^{-2}$
$q$	Radial Heat Flux/Unit Length	$\text{W m}^{-2}$ $\text{W in}^{-2}$
$r$	Radius	m ft
$t$	Thickness	m ft
$v$	Velocity	$\text{m s}^{-1}$ $\text{ft s}^{-1}$
$v$	Specific Volume	$\text{m}^3 \text{kg}^{-1}$ $\text{ft}^3 \text{lbf}^{-1}$

Table I-1. Nomenclature (Continued)

Symbol	SI Unit	English Unit
w	Groove Width m	in
x	Axial Coordinate m	ft
y	Perpendicular Coordinate m	ft
z	Characteristic Dimension (in We) m	in
$\alpha$	Groove Half Angle rad	deg
$\alpha$	Fraction of Impinging Molecules Sticking to Surface	
$\beta$	Heat Pipe Orientation with Respect to Gravity	rad
$\gamma$	Ratio of Specific Heats	
$\delta$	Depth of Grooves m	in
$\epsilon$	Porosity	
$\eta$	Gravity Factor	
$\theta$	Contact Angle rad	deg
$\lambda$	Heat of Vaporization J kg <sup>-1</sup>	Btu lbm <sup>-1</sup>
$\mu$	Viscosity (dynamic) N s m <sup>-2</sup>	lbf s ft <sup>-2</sup>
$\nu$	Kinematic Viscosity m <sup>2</sup> s <sup>-1</sup>	ft <sup>2</sup> s <sup>-1</sup>
$\rho$	Density kg m <sup>-3</sup>	lbm ft <sup>-3</sup>
$\sigma$	Surface Tension N m <sup>-1</sup>	lbf ft <sup>-1</sup>
$\tau$	Time Constant s	s
$\Psi$	Defined in Section D.5.1	
$\omega$	Angular Velocity rad s <sup>-1</sup>	deg s <sup>-1</sup>

Table I-1. Nomenclature (Continued)

<u>Symbol</u>		<u>SI Unit</u>	<u>English Unit</u>
$\Delta$	Incremental		
$\nabla$	Del Operator		
<u>Subscripts</u>			
a	A diabatic		
b	Bellows		
c	Condenser		
con	Condensation		
e	Evaporator		
ex	Excess		
ext	External		
h	Hydraulic		
i	Interface		
int	Internal		
j	Counter Index		
l	Liquid		
max	Maximum		
min	Minimum		
n	Nucleation Cavity		
o	Sink		
p	Pore		
r	Radial		

Table I. Nomenclature (Continued)

<u>Subscript</u>		<u>SI Unit</u>	<u>English Unit</u>
r	Reservoir		
s	Source		
st	Storage		
t	Total		
v	Vapor		
vap	Vaporization		
	Parallel		
l	Perpendicular		

## I.8 Units and Conversion Tables

The following values for physical constants and conversion factors are taken from NASA SP-7012 (revised 1969), The International System of Units. Both the National Bureau of Standards and NASA have adopted the policy of using SI units "except when the use of these units would obviously impair communication or reduce the usefulness of a report to the primary recipients". (NBS AB-64-6)

Table I-2. Common Units of the International Scientific System

<u>Physical Quantity</u>	<u>Name of Units</u>	<u>Symbol</u>
	<u>Basic Units</u>	
Length	meter	m
Mass	kilogram	kg
Time	second	s
Electric current	ampere	A
Temperature	kelvin	K
	<u>Derived Units</u>	
Area	square meter	$m^2$
Volume	cubic meter	$m^3$
Frequency	hertz	$Hz$ ( $s^{-1}$ )
Density	kilogram per cubic meter	$kg\ m^{-3}$
Velocity	meter per second	$m\ s^{-1}$
Angular velocity	radian per second	$rad\ s^{-1}$
Acceleration	meter per second squared	$m\ s^{-2}$
Angular acceleration	radian per second squared	$rad\ s^{-2}$
Force	newton	N ( $kg\ m\ s^{-2}$ )
Pressure	newton per sq. meter	$N\ m^{-2}$
Kinematic viscosity	sq. meter per second	$m^2\ s^{-1}$
Dynamic viscosity	newton-second per sq. m	$N\ s\ m^{-2}$
Work, energy, quantity of heat	joule	J ( $N\ m$ )
Power	watt	W ( $J\ s^{-1}$ )
Electric charge	coulomb	C ( $A\ s$ )
Voltage, potential diff., Emf.	volt	V ( $W\ A^{-1}$ )
Electric resistance	ohm	$\Omega$ ( $V\ A^{-1}$ )
Entropy	joule per kelvin	$J\ K^{-1}$
Specific heat	joule per kilogram kelvin	$J\ kg^{-1}K^{-1}$
Thermal conductivity	watt per meter kelvin	$W\ m^{-1}K^{-1}$
Radiant intensity	watt per steradian	$W\ sr^{-1}$
	<u>Supplementary Units</u>	
Plane angle	radian	$\hat{\theta}$ rad
Solid angle	steradian	sr

Table I-3. Prefixes Used to Indicate Multiples and Submultiples of SI Units

<u>Multiplying Factor</u>	<u>Prefix</u>	<u>Symbol</u>
$10^2$	tera	T
$10^9$	giga	G
$10^6$	mega	M
$10^3$	kilo	k
$10^2$	hecto	h
$10^1$	deka	da
$10^{-1}$	deci	d
$10^{-2}$	centi	c
$10^{-3}$	milli	m
$10^{-6}$	micro	$\mu$
$10^{-9}$	nano	n
$10^{-12}$	pico	p
$10^{-15}$	femto	f
$10^{-18}$	atto	a

Selected Physical Constants (1969 values)

<u>Quantity</u>	<u>Symbol</u>	<u>Value</u>	<u>Unit</u>
Avogadro constant	$N_A$	$6.022169 \times 10^{26}$	$\text{kmole}^{-1}$
Boltzmann constant	$k$	$1.380622 \times 10^{-23}$	$\text{J K}^{-1}$
Gas constant	$R$	$8.31434 \times 10^3$	$\text{J kmole}^{-1} \text{K}^{-1}$
Volume of ideal gas, STP	$V_0$	$2.24136 \times 10^4$	$\text{m}^3 \text{kmole}^{-1}$
Faraday constant	$F$	$9.648670 \times 10^7$	$\text{C kmole}^{-1}$
Stefan-Boltzmann constant	$\sigma$	$5.66961 \times 10^{-8}$	$\text{W m}^{-2} \text{K}^{-4}$

The following tables give conversion factors from some common cgs and English engineering units to International Scientific (SI) units and vice versa. The multiplier given in the table converts a quantity in the "Given unit" to the equivalent quantity in the "New unit". Thus in Table I.4 we determine that water with a nominal density of 1.0 g/cc has a density of  $(1.0) (1.0 \times 10^3) = 1.0 \times 10^3 \text{ kg/m}^3$  in SI units.

The arrows at the top of the table indicate the direction of the conversion.

Table I.4. Conversion from CGS or Engineering Units to SI Units

Quantity	convert from	To obtain	Multiply by	To convert from
Angle	degree	$1.745 \times 10^{-2}$	rad	
Area (Wicking Height factor)	$\text{cm}^2$	$1.0 \times 10^{-4}$	$\text{m}^2$	$9.290 \times 10^{-2}$ $6.452 \times 10^{-4}$ $\text{ft}^2$ $\text{in}^2$
Density	$\text{g cm}^{-3}$ $\text{g l}^{-1}$	$1.0 \times 10^3$ $1.0$	$\text{kg m}^{-3}$	$1.602 \times 10^1$ $2.768 \times 10^4$ $\text{lbm ft}^{-3}$ $\text{lbm in}^{-3}$
Energy (Work, Heat)	erg	$1.0 \times 10^{-7}$	J	$1.054 \times 10^3$ Btu
Force	calorie	$4.184$		
Heat Flux (Fluid Transport factor)	dyne	$1.0 \times 10^{-5}$	N	$4.448$ lbf
Heat Transfer Coefficient	$\text{W cm}^{-2} \text{K}^{-1}$	$1.0 \times 10^4$	$\text{W m}^{-2} \text{K}^{-1}$	$3.152$ $1.634 \times 10^3$ $\text{Btu hr}^{-1} \text{ft}^{-2}$ $\text{Btu s}^{-1} \text{in}^{-2}$
Heat of Vaporization	$\text{erg g}^{-1}$ $\text{cal g}^{-1}$	$1.0 \times 10^{-4}$ $4.184 \times 10^{-3}$	$\text{J kg}^{-1}$	$5.674$ $8.170 \times 10^2$ $\text{Btu hr}^{-1} \text{ft}^{-2} \text{F}^{-1}$ $\text{Btu hr}^{-1} \text{in}^{-2} \text{F}^{-1}$
Length	cm	$1.0 \times 10^{-2}$	m	$2.324 \times 10^3$ $\text{Btu lbm}^{-1}$
Mass	angstrom	$1.0 \times 10^{-10}$		
Power	g	$1.0 \times 10^{-3}$	kg	$4.536 \times 10^{-1}$ lbm
Pressure	W	$1.0$	W	$2.929 \times 10^{-1}$ $1.757 \times 10^1$ $1.054 \times 10^3$ $\text{Btu hr}^{-1}$ $\text{Btu min}^{-1}$ $\text{Btu s}^{-1}$
Surface Tension	dyne $\text{cm}^{-2}$ bar	$1.0 \times 10^{-1}$ $1.0 \times 10^5$	$\text{N m}^{-2}$	$6.895 \times 10^3$ psia
Thermal Conductivity	atm	$1.013 \times 10^5$		
Viscosity (dynamic)	erg cm	$1.233 \times 10^2$		
Viscosity (kinematic)	$\text{cm}^2 \text{s}^{-1}$	$1.0 \times 10^{-3}$	$\text{N m}^{-1}$	$1.459 \times 10^1$ lbf ft <sup>-1</sup>
Volume	$\text{cm}^3$	$1.0 \times 10^{-6}$	$\text{m}^3$	$2.832 \times 10^{-2}$ $1.639 \times 10^{-3}$ $\text{ft}^3$ $\text{in}^3$
Temperature		$(T_c + 273.15)$	$T_K$	$(T_F + 459.67) 5/9$ $5/9 T_R$

Table I.5. Conversion from SI Units to Cgs or Engineering Units

Quantity	To Obtain		Convert		To Obtain
	To	Multiply by	From	Multiply by	
Angle	degree	$5.730 \times 10^1$	rad		
Area (Wicking Height factor)	cm <sup>2</sup>	$1.0 \times 10^4$	m <sup>2</sup>	$1.076 \times 10^1$ $1.550 \times 10^3$	ft <sup>2</sup> in <sup>2</sup>
Density	g cm <sup>-3</sup> g l <sup>-1</sup>	$1.0 \times 10^{-3}$ 1.0	kg m <sup>-3</sup>	$6.243 \times 10^{-2}$ $3.613 \times 10^{-5}$	lbm ft <sup>-3</sup> lbm in <sup>-3</sup>
Energy (Work, Heat)	erg	$1.0 \times 10^7$	J	$9.485 \times 10^{-4}$	Btu
Force	calorie	$2.390 \times 10^{-1}$			
Force	dyne	$1.0 \times 10^5$	N	$2.248 \times 10^{-1}$	lbf
Heat Flux (Fluid Transport factor)	W cm <sup>-2</sup>	$1.0 \times 10^{-4}$	W m <sup>-2</sup>	$3.172 \times 10^{-1}$ $6.119 \times 10^{-4}$	Btu hr <sup>-1</sup> ft <sup>-2</sup> Btu s <sup>-1</sup> in <sup>-2</sup>
Heat Transfer Coefficient	W cm <sup>-2</sup> K <sup>-1</sup>	$1.0 \times 10^{-4}$	W m <sup>-2</sup> K <sup>-1</sup>	$1.762 \times 10^{-1}$ $1.224 \times 10^{-3}$	Btu hr <sup>-1</sup> ft <sup>-2</sup> F <sup>-1</sup> Btu hr <sup>-1</sup> in <sup>-2</sup> F <sup>-1</sup>
Heat of Vaporization	erg g <sup>-1</sup> cal g <sup>-1</sup>	$1.0 \times 10^4$ $2.390 \times 10^{-4}$	J kg <sup>-1</sup> $10^2$	$4.302 \times 10^{-4}$	Btu lbm <sup>-1</sup>
Length	cm	$1.0 \times 10^2$	m	$3.281 \times 10^1$	ft
Length	angstrom	$1.0 \times 10^{10}$		$3.937 \times 10^1$	in
Mass	g	$1.0 \times 10^3$	kg	$2.205 \times 10^3$	lbm
Power	W	$1.0 \times 10^3$	W	$3.414 \times 10^3$ $5.691 \times 10^{-2}$ $9.485 \times 10^{-4}$	Btu hr <sup>-1</sup> Btu min <sup>-1</sup> Btu s <sup>-1</sup>
Pressure	dyne cm <sup>-2</sup>	$1.0 \times 10^{-1}$	N m <sup>-2</sup>	$1.450 \times 10^{-4}$	psia
Pressure	bar	$1.0 \times 10^{-5}$			
Pressure	atm	$9.869 \times 10^{-6}$			
Pressure	torr (mm Hg, 0°C)	$7.501 \times 10^{-3}$			
Surface Tension	dyne cm <sup>-1</sup>	$1.0 \times 10^3$	N m <sup>-1</sup>	$6.852 \times 10^{-2}$	lbf ft <sup>-1</sup>
Surface Tension	erg cm <sup>-2</sup>	$1.0 \times 10^3$			
Thermal Conductivity	W cm <sup>-1</sup> K <sup>-1</sup>	$1.0 \times 10^{-2}$	W m <sup>-1</sup> K <sup>-1</sup>	$5.782 \times 10^{-1}$ 6.938	Btu hr <sup>-1</sup> ft <sup>-1</sup> F <sup>-1</sup> Btu hr <sup>-1</sup> ft <sup>-2</sup> F <sup>-1</sup>
Viscosity (dynamic)	g cm <sup>-1</sup> s <sup>-1</sup> (Poise)	$1.0 \times 10^1$	Ns m <sup>-2</sup>	$2.419 \times 10^3$ $2.089 \times 10^{-2}$	lbm hr <sup>-1</sup> ft <sup>-1</sup> lbf s ft <sup>-2</sup>
Viscosity (kinematic)	cm <sup>2</sup> s <sup>-1</sup>	$1.0 \times 10^4$	m <sup>2</sup> s <sup>-1</sup>	$3.875 \times 10^4$	ft <sup>2</sup> hr <sup>-1</sup>
Volume	cm <sup>3</sup>	$1.0 \times 10^6$	m <sup>3</sup>	$3.531 \times 10^1$ $6.102 \times 10^4$	ft <sup>3</sup> in <sup>3</sup>
Temperature	T <sub>c</sub> = T <sub>k</sub> - 273.15		T <sub>K</sub>	T <sub>F</sub> = $1.8 \frac{T_K - 459.67}{T_R}$	T <sub>R</sub> = 1.8 T <sub>K</sub>

T. 1 Introduction

After eight years of investigation, heat pipe theory as first presented by Cotter (11) remains unchanged. Two excellent works on heat pipes have recently been published by Winters and Barsch (39) and by Marcus (28). In addition to including up-to-date refinements and extensions to Cotter's original presentation, these recent publications also treat other topics such as heat pipe design, heat transfer, and variable conductance techniques.

Winters and Barsch present a detailed survey of many theoretical models, while Marcus offers a more selective approach, summarizing well accepted features of the basic theory which are of interest to heat pipe designers.

The following discussion will, in general, follow the approach taken by Marcus, but with somewhat altered emphasis in certain areas. The purpose of this Chapter is to give the heat pipe designer as firm a basis as is presently possible for designing and evaluating heat pipes.

The principle of operation of a heat pipe is best described by using the simple cylindrical geometry shown in Figure T-1. The essential components of a heat pipe are the sealed container, a wick, and a suitable working fluid which is in equilibrium with its own vapor. When heat is applied along one section of the pipe (evaporator), the local temperature is raised slightly and part of the working fluid evaporates. Because of the saturation condition this temperature difference results in a difference in vapor pressure which, in turn, causes vapor to flow from the heated section to a cooler part of the pipe (condenser). The rate of evaporation is commensurate with heat absorbed in the form of latent heat of evaporation. The excess vapor condenses at the cooler end and releases its latent heat. During steady-state operation, conservation of energy requires that the amount of heat absorbed is identical to the heat released. Return of the liquid condensate occurs through the wick. The wick provides a flow path for the liquid and is also responsible for the pumping. During evaporation the liquid recedes somewhat into the pores of the wick thus forming menisci of the liquid-vapor interface which are highly curved. On the other hand,

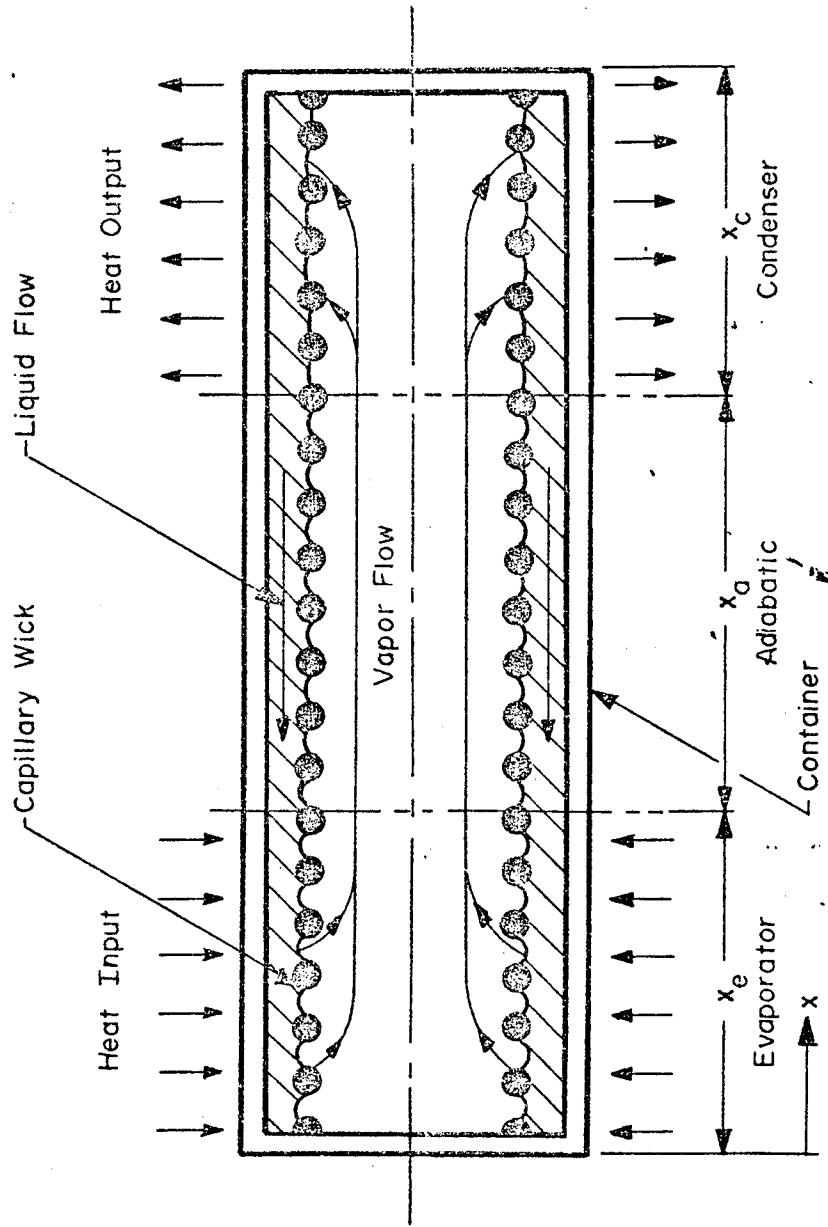


Figure T-1. Schematic Diagram of the Principle of Operation of a Heat Pipe

condensation occurs mainly on the surface of the wick with corresponding flat menisci.

In thermodynamic equilibrium, a pressure difference related to the radius of curvature exists across any curved liquid-vapor interface. Since the curvature is different at the evaporator from that at the condenser, a net pressure difference exists within the system. This capillary pumping pressure maintains circulation of the fluid against the liquid and vapor flow losses and the, sometimes adverse, effects of body forces.

In addition to evaporator and condenser, the heat pipe frequently also has an "adiabatic" section. It is characterized by zero heat exchange with the environment. It should also be noted that the heat pipe is not limited to having only one evaporator and condenser but may have several heat input and output areas distributed along its length.

As generally conceived, heat pipe theory consists of the description of concurrent hydrodynamic and heat transfer processes. Hydrodynamic theory is used to describe the circulation process. Its most important function is to establish the maximum circulation and, therefore, the maximum heat transport capability of the heat pipe. It also describes and sets bounds upon various factors affecting maximum circulation.

Heat transfer theory deals essentially with the conduction of heat into and out of the heat pipe. Primarily it is used to predict overall conductance. Since the heat pipe utilizes evaporation and condensation, it is subject to limitations which do not apply to solid conductors. Heat transfer theory is used to investigate these limitations and also to provide a model for the overall conductance.

Fundamentally, the internal heat transport process of a heat pipe is a thermodynamic cycle subject to the first and second laws of thermodynamics. A quantity of heat is introduced to the system at a temperature  $T_1$ , and the same quantity of heat is rejected at a lower temperature  $T_2$ . "Work" is generated internally but it is completely consumed in overcoming the hydrodynamic losses of the system. The energy conversion process occurs in the phase change across the curved liquid-vapor interface, where thermal energy is converted to mechanical energy with the appearance of a pressure head. The curvature of this interface adjusts automatically, such that the capillary pumping (the "work" of the system) is just adequate to meet the

flow requirement. As with every thermodynamic cycle a finite temperature difference must exist between heat source and heat sink; that is, heat rejection must occur at a lower temperature than heat addition. In most heat pipes this  $\Delta T$  associated with the circulation of the working fluid is small compared to other conductive temperature gradients. Nevertheless, even an ideal heat pipe can never be completely isothermal because this would violate the second law of thermodynamics.

Although its performance does have definite limitations, the heat pipe generally has very high heat transport capability. The limitations include maximum capillary pumping ability, choking of the vapor flow when it approaches sonic velocity, entrainment of liquid droplets in the vapor stream, and disruption of the liquid flow by the occurrence of boiling in the wick.

## T.2 Fundamental Considerations

Along the entire length of the heat pipe, the liquid and the vapor phases of the working fluid are in close contact with each other. Because of the circulation, the pressures in liquid and vapor are not constant, but vary along the length of the pipe. Furthermore, the pressure difference between the liquid and the vapor is also a function of the location. In order to maintain the pressure balance between liquid and vapor, the interface separating them must be curved. Any curved liquid-vapor interface creates a pressure difference which can be expressed in terms of the surface tension and the principal radii of curvature  $R_1$  and  $R_2$  of the interface as given in Equations T-1 and T-2 (1). The principal radii of the surface are shown in Figure T-2.

$$\Delta p_i(x) = p_v(x) - p_l(x)$$

$$\Delta p_i(x) = \sigma \left( \frac{1}{R_1(x)} + \frac{1}{R_2(x)} \right)$$

T-1

T-2

This interfacial pressure difference  $\Delta p_i$  maintains the pressure balance between vapor and liquid at any point along the length of the heat pipe. Since the interfacial pressure difference varies with location, the radii of curvature of the menisci also vary along the heat pipe. If the interface is concave with respect to the vapor, the pressure in the liquid will be lower than the pressure in the vapor.

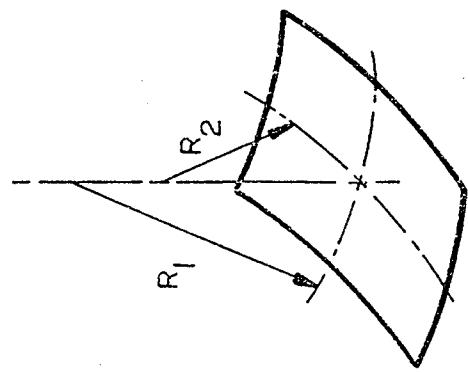


Figure T-2. Principal Radii of Curvature of Liquid-Vapor Interface

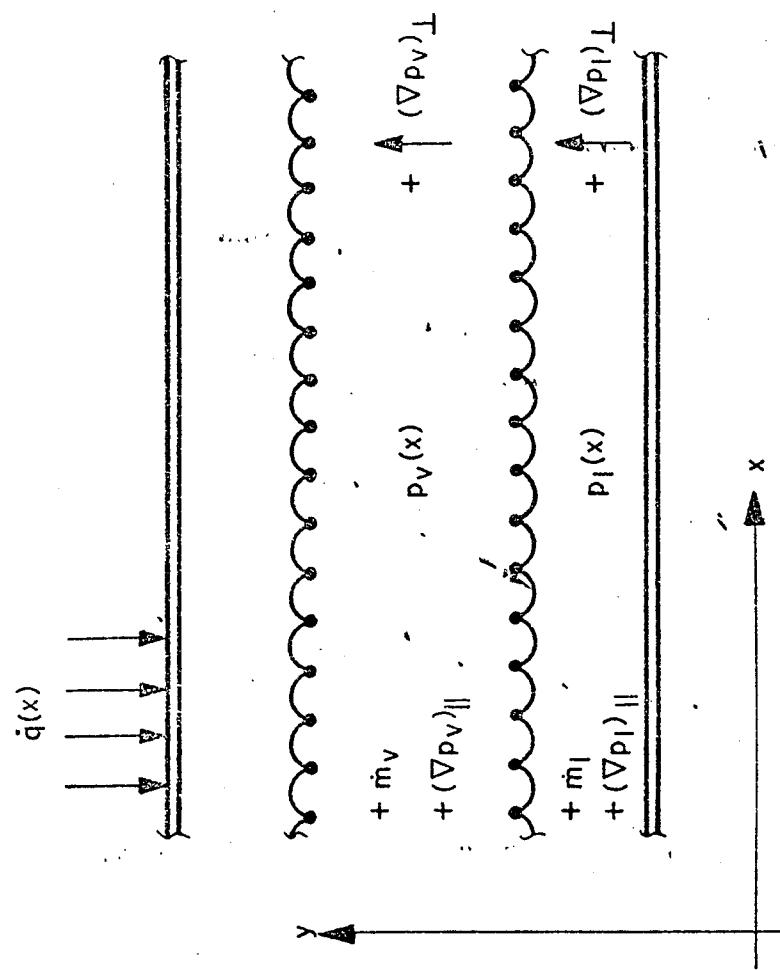


Figure T-3. Model of Heat Pipe Hydrodynamics

The function of the wick in a heat pipe is to provide a medium for establishing curved interfaces between liquid and vapor. It must be emphasized that the interfacial pressure difference  $\Delta p_i$  is independent of the wick properties and is only determined by the curvature of the interfacial surface. Wick properties such as pore size and contact angle only determine the upper bound of the interfacial pressure difference. This upper limit is frequently referred to as "capillary pressure".

In addition to pressure differences between liquid and vapor, there exist pressure gradients within both phases of the working fluid. These gradients are the result of viscous, momentum and body forces. It is convenient to group the gradients according to their origin; that is, whether they are associated with the flow or due to independent body forces.

$$\nabla p = (\nabla p)_{\text{flow}} + \frac{\overrightarrow{dF}}{dV} \quad \text{T-3}$$

The vector Equation T-3 applies to both the liquid and the vapor phase.

For a heat pipe with one-dimensional liquid and vapor flow, the gradients are given in Equations T-4 and T-5 in terms of their axial and perpendicular components.

$$(\nabla p)_{\parallel} = \frac{\partial p}{\partial x} = \left( \frac{\partial p}{\partial x} \right)_{\text{flow}} + \left( \frac{dF}{dV} \right)_{\parallel} \quad \text{(Axial)} \quad \text{T-4}$$

$$(\nabla p)_{\perp} = \frac{\partial p}{\partial y} = \left( \frac{dF}{dV} \right)_{\perp} \quad \text{(Perpendicular)} \quad \text{T-5}$$

The components of the pressure gradients are shown schematically in Figure T-3. This figure also establishes the sign convention adopted throughout the Handbook. The "x" coordinate is parallel to the heat pipe axis, and the "y" coordinate is perpendicular to the axis. The origin of the coordinate system is located at the bottom and at the evaporator end. All vector components, such as pressure gradients, mass flow rates and body forces shall have a positive sign if they are directed in the positive "x" or "y" direction.

In some cases, a different coordinate system may be more convenient. For example, in a heat pipe with a multitude of evaporators and condensers, one might

arbitrarily choose one end of the pipe as the origin of the coordinate system. All hydrodynamic equations are actually independent of the choice of the coordinate system. Care must be exercised, however, in selecting the proper sign for all vector components if a different system is selected.

Obviously the assumption of one-dimensional fluid flow does not hold in the areas where evaporation and condensation occurs, or in two-or-three dimensional heat pipes such as flat plates, cavities, etc. But for most conventional heat pipes, the one-dimensional model represents a very close approximation.

The body force term in Equations T-3, T-4, and T-5 consists of those mass action forces which are independent of flow; e.g., gravity, acceleration, and electric effects. This form of the equation does not include flow dependent body forces such as arise due to magnetic effects.

The pressure gradients give rise to mass transfer along the heat pipe. The two axial mass-flow rates,  $\dot{m}_v$  and  $\dot{m}_l$  are related through the continuity equation:

$$\dot{m}_v(x) + \dot{m}_l(x) = 0 \quad T-6$$

Equation T-6 simply states that during steady-state operation mass accumulation does not occur and vapor and liquid flow rates must be equal in magnitude but opposite in direction.

Finally, the mass-flow rates are related to the local heat exchange with the environment through the energy equation:

$$\frac{d\dot{m}_v(x)}{dx} = \frac{1}{\lambda} \dot{q}(x) \quad T-7$$

Equation T-7 is a simplified form of the first law of thermodynamics.  $\dot{q}(x)$  is the rate of heat addition (or removal) per unit length of the heat pipe. It is counted positive in the case of heat addition (evaporator) and negative for heat removal (condenser). In Equation T-7 the effects of conduction in the axial direction are neglected. It is also assumed that sensible heat transport is negligible. This assumption appears well justified because of the very small temperature differences along the heat pipe. In the

following sections the various terms used in describing the performance of heat pipes are examined in more detail.

### T.3 Capillary Pressure

The capillary pressure is defined as the maximum interfacial pressure differences which a given wick/liquid combination can develop, or:

$$\Delta p_{\text{cap}} \equiv (\Delta p_i)_{\text{max}} \quad \text{T-8}$$

The capillary pressure is related to the surface tension of the liquid, the contact angle between liquid and vapor, and the effective pore radius through (42):

$$\Delta p_{\text{cap}} = \frac{2 \sigma \cos \theta}{r_p} \quad \text{T-9}$$

With few exceptions, the wicks employed in heat pipes have no well defined pore geometries. Therefore, it is common practice to define an effective pore radius which is determined experimentally and which satisfies Equation T-9.

For some well defined pore geometries analytical expressions for the effective pore radius can be found. For circular pores, the meniscus is spherical and the two principal radii of curvature of the surface are equal. Referring to Figure T-4 we have:

$$(R_1)_{\text{min}} = (R_2)_{\text{min}} = \frac{r}{\cos \theta} \quad \text{T-10}$$

According to Equation T-2, the maximum interfacial pressure difference which the capillary forces are capable of handling is:

$$(\Delta p_i)_{\text{max}} = \sigma \left( \frac{1}{R_{1,\text{min}}} + \frac{1}{R_{2,\text{min}}} \right) = \frac{2 \sigma \cos \theta}{r} \quad \text{T-11}$$

A comparison of Equations T-9 and T-11, along with the Identity T-8, yields the result that for circular pores the effective pore radius  $r_p$  is equal to the physical pore radius  $r$ .

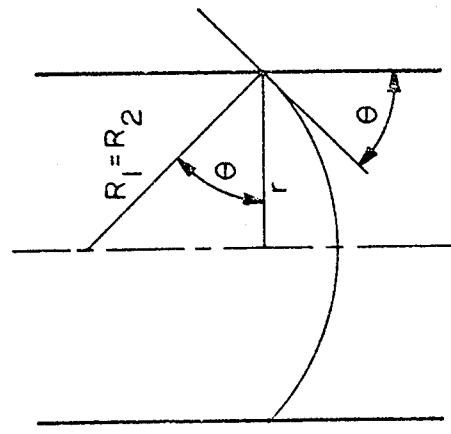


Figure T-4. Effective Pore Radius in Circular Capillary

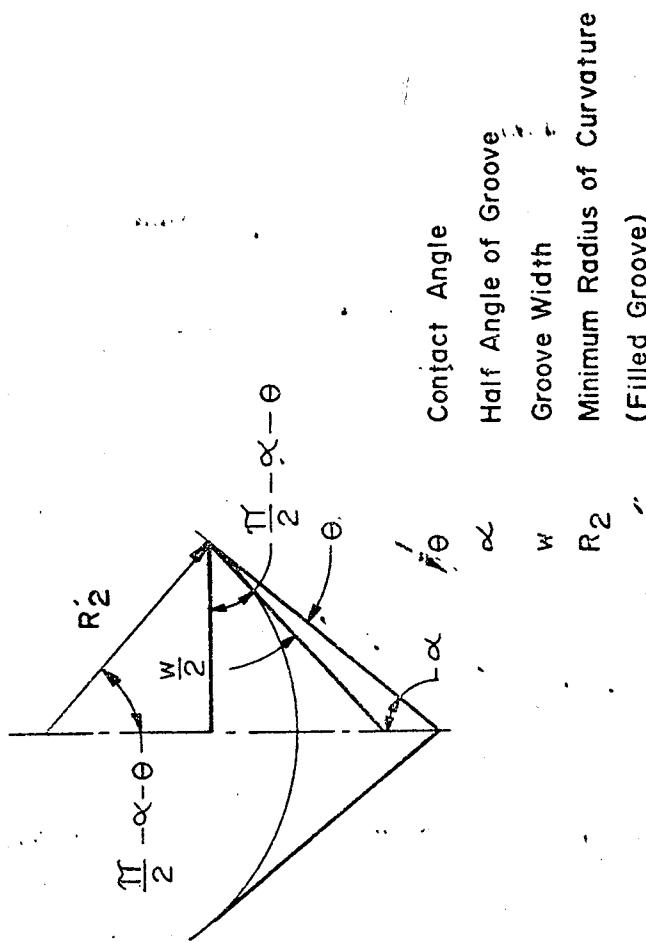


Figure T-5. Effective Pore Radius in Open Groove

In long, open channels one of the principal radii is infinite. Using Figure T-5 the minimum radii can readily be calculated:

$$R_1 = \infty, \quad (R_2)_{\min} = \frac{w/2}{\cos(\alpha + \theta)} \quad T-12$$

The maximum interfacial pressure difference becomes:

$$(\Delta p_i)_{\max} = \frac{\sigma \cos(\alpha + \theta)}{w/2} \quad T-13$$

In the limit of grooves with parallel walls ( $\alpha = 0$ ) Equation T-13 reduces to:

$$(\Delta p_i)_{\max} = \frac{2\sigma \cos \theta}{w} \quad T-14$$

If we compare Equations T-14 with T-9 (along with the Identity T-8), we see that the effective pore radius of a rectangular groove is equal to the groove width while for circular pores it was equal to half the pore diameter. The reason for this difference is, of course, the absence of curvature in the direction of the groove length.

The most common wicking material used in heat pipes is wire mesh. It would be natural to assume that the effective capillary radius is approximately equal to half the mesh opening. Experimental evidence has shown, however, that the capillary radius is larger and approaches the width of the mesh opening. Several empirical methods for estimating the effective radius will be discussed in Chapter W.

A voluminous literature exists on the contact angle, and many inconsistencies in experimental results are reported. However, it has been well established now (42) that much of the "inconsistent" behavior of the contact angle is due to very low level impurities in the liquid or on the surface being wetted. Thus, combinations of scrupulously clean surfaces and very pure liquids will exhibit no difference in advancing and receding contact angles; and water and other liquids with low surface tensions should exhibit a contact angle of approximately zero (2) on all clean metal surfaces with which they do not react chemically. The fact that much larger contact angles are often observed usually indicates the presence of adsorbed impurities on the surface, which is generally more difficult to clean than the working fluid.

The capillary pressure, as defined in this section, refers to the maximum interfacial pressure difference which a given wick/liquid combination can sustain; but, as pointed out earlier, the interfacial pressure varies along the heat pipe. It will be shown later that the upper and lower limit of the interfacial pressure difference must be known in order to determine the maximum heat transport capability. The lower limit corresponds to the maximum value of the radius of curvature of the meniscus. It can be determined that for wetting liquids the pressure in the liquid cannot exceed that of the vapor. Equal pressures in liquid and vapor correspond to an infinite radius of curvature which is equivalent to a flat meniscus. For nonwetting liquids the pressure in the liquid always exceeds that of the vapor.

The point of pressure equality in liquid and vapor represents a well-defined boundary condition for the integration of the flow equations. Frequently it is located at the end of the condenser of the heat pipe. In the presence of body forces and with complicated heat pipe geometries or distributed heat loads, this will not necessarily be the case and a careful analysis is required to determine its location. This subject will be discussed in more detail in conjunction with the integration of the flow equations.

#### T.4 Pressure Gradients in the Liquid

The liquid is subjected to a series of different forces, such as the shearing forces associated with viscous flow, the forces associated with momentum in a dynamic system, and the body force effects arising from external force fields. The actions of these forces upon the liquid result in pressure gradients along the heat pipe (as was indicated in Equation T-3).

The ratio of the dynamic-to-viscous flow pressure gradients in a capillary passage is of the order of magnitude of the Reynold's number determined using the average flow in a pore (14). Since this number will be small with respect to unity for heat pipes, the inertial (dynamic) forces in the liquid will be neglected.

##### T.4.1 Viscous Pressure Gradients in the Liquid

The pressure gradient resulting from viscous shear forces in an incompressible liquid with laminar flow through a porous media is given directly by Darcy's Law (35):

$$\frac{dp_1}{dx} = -\frac{\mu_1 \dot{m}_1(x)}{K A_w \rho_1} \quad T-15$$

For some geometries where the physical dimensions of the pores are known and well defined the permeability  $K$  may be expressed in terms of a hydraulic diameter  $D_h$  and the porosity of the wick  $\epsilon$  (21):

$$K = \frac{\epsilon D_h^2}{32} \quad T-16$$

The hydraulic diameter  $D_h$  is defined as:

$$D_h = \frac{4 \times \text{Area}}{\text{Wetted Perimeter}} \quad T-17$$

The above definition represents a good approximation for many geometries. More refined expressions are given in Chapter W.

For cylindrical passages with diameter  $D$  Equation T-17 yields for the hydraulic diameter:

$$D_h = D \quad T-18$$

and Equation T-15 reduces to a form of Poiseuille's Law:

$$\frac{dp_1}{dx} = \frac{-32 \mu_1 \dot{m}_1(x)}{\epsilon A_w \rho_1 D_h^2} \quad T-19$$

For many wick geometries the hydraulic diameter cannot be calculated, particularly for those which involve porous materials. In these cases it is best to resort to experimental measurements to obtain a value for the permeability.

Many literature references report the viscous pressure gradient in a form first introduced by Cotter (11):

$$\frac{dp_1}{dx} = -\frac{b \mu_1 \dot{m}_1(x)}{\epsilon r_p^2 A_w \rho_1} \quad T-20$$

T-12

The equation holds rigorously for parallel cylindrical capillaries having a tortuosity factor of  $b = 8$ . Much of the wick data in the literature is reported in terms of the parameters  $b$ ,  $\epsilon$ , and  $r_p$ . However, since all three of these parameters are subject to various definitions for different wicks, it is better to use Darcy's Law and lump all of the experimental determinations into one factor, the permeability,  $K$ .

#### T.4.2 Body Forces in the Liquid

The pressure gradients in the liquid resulting from body forces can either augment or diminish the gradients associated with viscous flow. The body forces result from external fields which can be applied in any direction with respect to the heat pipe's axis. The body force can be expressed as:

$$\overrightarrow{\left(\frac{dF}{dV}\right)} = \rho_1 \overrightarrow{g} \quad T-21$$

In a gravity field the heat pipe will experience two components of body force (Figure T-6). The obvious body force component is the axial component which is parallel to the mass flow along the heat pipe:

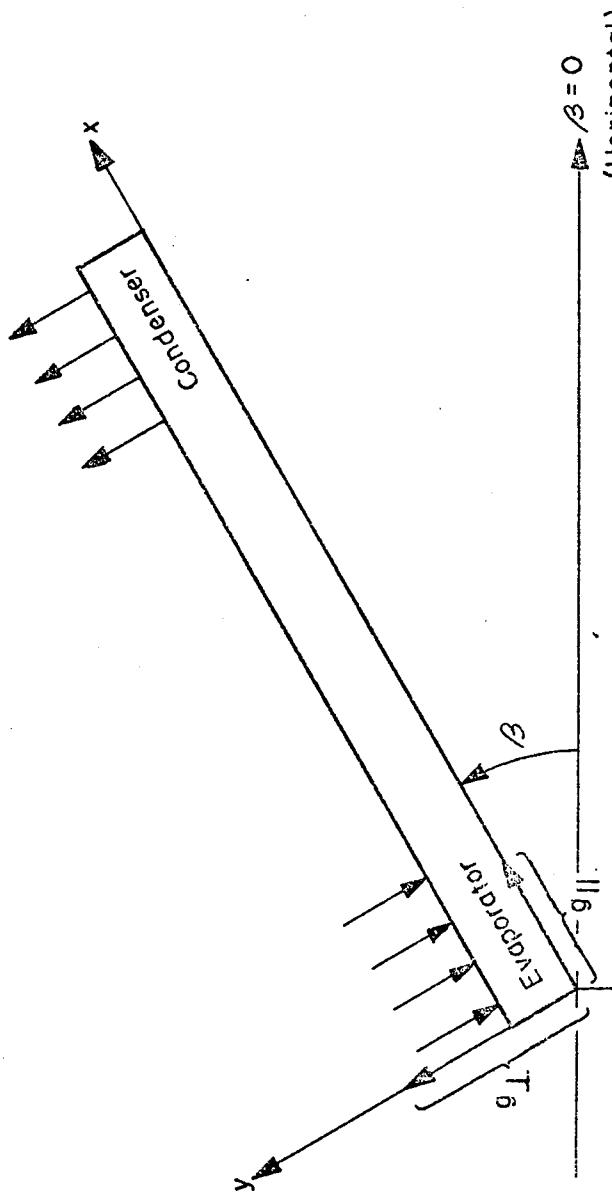
$$\left(\frac{dF}{dV}\right)_\parallel = \rho_1 g_\parallel = -\rho_1 g \sin \beta \quad T-22$$

Depending on whether the condenser ( $\beta > 0$ ) or the evaporator ( $\beta < 0$ ) is elevated, the axial body force component of gravity will either augment or impede the liquid flow. Less frequently considered is the perpendicular body force component:

$$\left(\frac{dF}{dV}\right)_\perp = \rho_1 g_\perp = -\rho_1 g \cos \beta \quad T-23$$

Unlike the axial body force component, this component will always act to the detriment of heat pipe operation. It generates a pressure gradient which is perpendicular to the liquid flow (Equation T-5). When integrating the flow equations, it is found that this perpendicular gradient always detracts from the capillary pumping (Section T.6).

Body forces originate not only from gravity but from any acceleration vector,  $\overrightarrow{g}$ . A typical, and frequently encountered non-gravitational body force is that



$$g_{||} = g \cos(\frac{\pi}{2} + \beta) = -g \sin \beta$$

$$g_{\perp} = g \cos(\frac{\pi}{2} - \beta) = -g \cos \beta$$

Figure T-6. ~ Body Force Components in Gravity Field

resulting from acceleration due to rotation. Its vector is directed in a radial direction from the axis of rotation and its magnitude is:

$$g_{\text{rot}} = \gamma \omega^2$$

where  $\gamma$  is the distance between the axis of rotation and the point where the body force is encountered.

### T.5 Pressure Gradients in the Vapor.

The pressure gradients in the vapor will also result from a combination of flow dependent (viscous and dynamic) effects, and flow independent external force fields or body forces. However, the effects on heat pipe performance of the various pressure gradients in the vapor phase are not as easily determined as those of the liquid. Much of this difficulty is attributable to the higher flow velocities in the vapor which make it more susceptible to the effects of mass addition and removal along the length of the heat pipe, to the frequently non-negligible dynamic effects, to the existence of turbulent flow, and to the compressibility of the vapor. All of these factors combine to produce a condition which does not permit simple, all encompassing, analytical expressions for the vapor pressure losses.

#### T.5.1 Viscous Pressure Gradients in the Vapor

Under conditions of low axial heat flow and high vapor density the vapor velocity will be low and viscous forces will predominate. If laminar, noncompressible flow occurs the vapor pressure gradient can also be expressed by Darcy's Law:

$$\frac{dp_v}{dx} = \frac{-\mu_v \dot{m}_v(x)}{K A_v \rho_v}$$

T-25

Since the vapor passages are generally of a simpler geometry than those of the liquid, the concept of the "hydraulic diameter" is especially useful. Substituting the hydraulic diameter for the permeability in Equation T-16 the pressure gradient in the vapor becomes:

T-15

$$\frac{dp_v}{dx} = - \frac{32 \mu_v \dot{m}_v(x)}{\rho_v A_v D_{h,v}^2}$$

T-26

By the definition of porosity  $\epsilon$  --i.e., the ratio of void volume to total volume -- the vapor space porosity is unity.

### T.5.2 Dynamic Pressure Gradients in the Vapor

Separation of viscous and dynamic effects in the vapor flow is not really possible. If the dynamic effects cannot be neglected, Equation T-26 should be replaced by Equation T-27 (11):

$$\frac{dp_v}{dx} = - \frac{32 \mu_v \dot{m}_v}{\rho_v A_v D_{h,v}^2} \left[ 1 + \frac{3}{4} Re_r - \frac{11}{27} Re_r^2 + \dots \right] \quad T-27$$

where the radial Reynolds number,  $Re_r$ , is defined by:

$$Re_r = \frac{1}{2\pi \mu_v} \frac{d\dot{m}_v}{dx} \quad T-28$$

The expansion in Equation T-27 accounts for momentum changes due to evaporation or condensation. It obviously holds only for small rates of evaporation and condensation, i.e., for  $[Re_r] < 1$ . The momentum effects cause the pressure gradient in the evaporator to be higher than for viscous shear alone and the pressure gradient in the condenser to be lower due to deceleration of the vapor flow. In the absence of mass addition or subtraction, as for instance in the adiabatic section of a heat pipe, Equation T-27 reduces to that of purely viscous flow.

For high evaporation and condensation rates the pressure distribution in the vapor is considerably more complex. Analytical solutions exist only for the limiting case, where the radial Reynolds number approaches infinity. For this limit the pressure gradient is given by (24):

$$\frac{dp_v}{dx} = - \frac{S \pi \dot{m}_v}{\rho_v A_v D_{h,v}^2} \frac{d\dot{m}_v}{dx} \quad T-29$$

T-16

The value for the numerical constant  $S$  is 1 for evaporation and  $4/\pi^2$  for condensation. Equation T-29 predicts approximately 40% recovery of the dynamic head in the condenser.

### T.5.3 Non-Laminar Flow and Compressibility Effects

Little is known about the onset of turbulence in vapor flow with high radial Reynolds numbers. In the adiabatic section, where the radial Reynolds number is zero, fully developed turbulent flow will occur if the axial Reynolds number exceeds 2000. The axial Reynolds number is defined in the usual manner as:

$$Re = \frac{D_v \dot{m}_v}{A_v \mu_v} \quad T-30$$

For turbulent flow the viscous pressure gradient is given by the empirical Blasius Law (35):

$$\frac{dp_v}{dx} = \frac{0.156 \mu_v^2}{\rho_v D_{h,v}^3} Re^{7/4} \quad T-31$$

In the transition region, i. e., at axial Reynolds numbers of approximately 2200, Blasius' empirical law holds only approximately and gives slightly different numerical values than the expression for laminar flow.

Compressibility effects can normally be ignored if the Mach number of the flow is less than approximately 0.2. This criterion applies for most heat pipes with the notable exception of liquid metal heat pipes during start-up. If compressibility effects are taken into account, the pressure recovery for high axial fluxes may be as high as 90% (32) instead of the 40% predicted by Equation T-29. Compressibility can certainly not be neglected when the vapor flow approaches sonic conditions. This has been considered by Levy (26), (27) and is discussed in Section T.7.1.

### T.5.4 Body Forces in the Vapor

The theory of body forces acting upon the vapor is identical to that of the liquid. However, because of the large difference in density between liquid and vapor (usually of the order of  $10^3$ ) the effect of body forces in the vapor is always negligible.

T.6.1 General Approach

The rate of circulation of the working fluid is determined by a balance between heat transport, capillary pumping, body forces, and viscous and dynamic flow losses. During normal operation the pumping adjusts itself to meet the circulation requirements. But since capillary pumping is limited to a maximum capillary pressure (see Section T. 3) a limit also exists for the rate of circulation and therefore for the heat transport capability.

The capillary limit is the most commonly encountered limit and it relates to the hydrodynamics previously discussed. When the required interfacial pressure exceeds the capillary pressure that the wick can sustain, the pumping rate is no longer sufficient to supply enough liquid to the evaporation sites. Consequently, more liquid is evaporated than replenished and local dryout of the wick occurs.

For high velocity vapor flows, other hydrodynamic limits may restrict the heat transport even before the capillary limit is reached. When the vapor velocity reaches the sonic point, further increase in the mass flow rate is not possible without raising the saturation vapor pressure and therefore the temperature of the evaporator (sonic limit). High velocity vapor flow may also interfere with the recirculating liquid causing liquid droplets to be entrained in the vapor and preventing sufficient liquid from returning to the evaporator (entrainment limit). Finally, high local heat fluxes can lead to nucleation within the liquid and result in wick dry-out (heat flux limit). Each one of these limitations will be discussed separately in subsequent sections.

In the preceding sections the pressures and forces affecting the circulation of the working fluid of a one-dimensional heat pipe have been presented in differential form. No restriction has been placed on the distribution of heat fluxes into and out of the heat pipe, its orientation with respect to body forces, and the geometry of the wick. In order to arrive at the capillary limit, i. e., the maximum heat transport capability of a heat pipe, the hydrodynamic equations must be integrated. In the general case, numerical methods have to be employed and the integration constants must be judiciously chosen, particularly when body forces and more than one evaporator and condenser are

involved. The following approach will always lead to the correct capillary limit and can readily be reduced to a closed form for specific geometries.

The pressure distribution in liquid and vapor is obtained by integrating the axial pressure gradients.

$$p_v(x) = \int_0^x (\nabla p_v)_{||} dx + p_v(0) \quad T-32$$

$$p_l(x) = \int_0^x (\nabla p_l)_{||} dx + p_l(0) \quad T-33$$

The integration is extended from one end of the heat pipe ( $x = 0$ ) to the specific location,  $x$ . The two integration constants must be determined before the absolute values of each pressure can be calculated. The two pressures are related at every point  $x$  through the interface equation T-1.

$$\Delta p_i(x) = p_v(x) - p_l(x) \quad T-1$$

Inserting the values for  $p_v(x)$  and  $p_l(x)$  from Equations T-32 and T-33 yields:

$$\Delta p_i(x) = \int_0^x [(\nabla p_v)_{||} - (\nabla p_l)_{||}] dx + p_v(0) - p_l(0) \quad T-34$$

Equation T-34 gives the required interfacial pressure difference  $\Delta p_i$  at any axial location  $x$  to within the additive constant  $[p_v(0) - p_l(0)]$ .

In general,  $\Delta p_i$  will vary along the length of the heat pipe and at some point  $x'$  will reach a lowest, or minimum value. It is generally assumed that this minimum interfacial pressure difference is zero (equal pressure in liquid and vapor, corresponding to a "flat" meniscus). The integration constant in Equation T-34 may then be evaluated as follows:

$$\Delta p_i(x') = 0 \quad T-35$$

$$p_v(0) - p_l(0) = - \int_0^{x'} [(\nabla p_v)_{||} - (\nabla p_l)_{||}] \quad T-36$$

The interfacial pressure difference becomes:

$$\Delta p_i(x) = \int_{x'}^x [(\nabla p_v)_\parallel - (\nabla p_l)_\parallel] dx \quad T-37$$

This last equation describes the interfacial pressure difference at any location,  $x$ , of the heat pipe with respect to the reference value at  $x'$  which, conveniently, is equal to zero.

There always exists at least one axial location  $x''$  at which the interfacial pressure difference  $\Delta p_i(x)$  reaches a highest, or maximum value. Once this point has been found (either by numerical or closed form solution) the maximum interfacial pressure difference can be expressed as:

$$(\Delta p_i)_{\max} = \Delta p_i(x'') = \int_{x'}^{x''} [(\nabla p_v)_\parallel - (\nabla p_l)_\parallel] dx \quad T-38$$

In the hydrodynamic limit the pumping requirement  $(\Delta p_i)_{\max}$  is equal to the maximum capillary pressure,  $\Delta p_{\text{cap}}$ , which the wick can develop. Proper circulation of the working fluid is assured if the pumping requirement is less than the maximum capillary pressure difference:

$$(\Delta p_i)_{\max} \leq \Delta p_{\text{cap}} \quad T-39$$

For a specified wick geometry and heat flux distribution, the above equation will in general be an inequality. In the course of a numerical analysis it establishes the criterion for a selected heat pipe and wick geometry to satisfy the heat transport requirement. Alternately, Equation T-39 may be used as an equality to determine the capillary pumping requirement. For most wicks, capillary pumping (pore size) and hydrodynamic pressure gradients are closely related. The approach is therefore to select a particular wick, compute the hydrodynamic requirements according to Equation T-38 and then compare the resulting  $(\Delta p_i)_{\max}$  with the capillary pumping capability  $\Delta p_{\text{cap}}$ . If the inequality is met, the selected wick will be adequate for the given heat transport requirement.

The preceding equations express the capillary pumping requirement in terms of integrated pressure gradients within liquid and vapor. These pressure gradients are related to the corresponding mass flow rates and the body forces (Sections

T.4 and T.5). The mass flow rates, in turn, are determined by the heat transport requirement.

For a specified distribution of heat inputs and outputs,  $\dot{q}(x)$ , the mass flow rates of vapor and liquid are obtained by integrating Equation T-7.

$$\frac{d\dot{m}(x)}{dx} = \frac{1}{\lambda} \dot{q}(x) \quad T-7$$

Integration yields:

$$\dot{m}_v(x) = \int_0^x \frac{1}{\lambda} \dot{q}(x) dx + \dot{m}_v(0) \quad T-40$$

The above equation gives the mass flow rate of the vapor for every axial location,  $x$ , when the integration is extended from one end of the heat pipe, ( $x = 0$ ), to the point  $x$ . Conservation of mass requires that the integration constant,  $\dot{m}_v(0)$ , goes identically to zero since no vapor enters or leaves the heat pipe. Thus:

$$\dot{m}_v(0) = 0 \quad T-41$$

The mass flow rate of the vapor is thus uniquely determined by the heat exchange with the environment. Because of the requirement of mass continuity (Equation T-6), the mass flow rate of the liquid is equal in magnitude and opposite in direction to the mass flow rate of the vapor.

$$\dot{m}_l(x) = -\dot{m}_v(x) \quad T-42$$

The net axial heat flow rate,  $\dot{Q}$ , is related to the  $\dot{m}_v$  and  $\dot{m}_l$  through a form of the first law of thermodynamics.

$$\dot{Q}(x) = \lambda \dot{m}_v(x) = -\lambda \dot{m}_l(x) \quad T-43$$

The theory as presented so far does not include the effects of perpendicular components of the body forces. Since the hydrodynamic model is one-dimensional, perpendicular body forces do not affect the axial pressure gradient. The perpendicular body

forces, however, create a pressure gradient within the liquid which is perpendicular to the flow direction. Referring to Equation T-23, this pressure gradient is:

$$\frac{\partial p_1}{\partial y} = - \frac{dF}{dV} = - \rho_1 g \cos \beta \quad T-23$$

The total pressure difference in the liquid across the heat pipe becomes:

$$(\Delta p_1)_1 = \int_0^D \frac{\partial p_1}{\partial y} dy = - \rho_1 g D \cos \beta \quad T-44$$

where the integration is extended from the bottom ( $y = 0$ ) to the top ( $y = D$ ) of the heat pipe. Equation T-44 holds for any axial location  $x$ . The negative sign in Equation T-44 indicates that the pressure within the liquid is lower at the top than at the bottom of the heat pipe.

This pressure difference creates an additional capillary pumping requirement. The wick must be capable of supporting the interfacial pressure difference between any two locations within the heat pipe (including those at different vertical positions). The datum point of equal pressure in liquid and vapor will always be located at the lower liquid-vapor interface of the heat pipe ( $x = x'$ ,  $y = 0 + t_w$ ). Conservatively, we locate it at the bottom of the heat pipe ( $y = 0$ ). The point of maximum interfacial pressure difference exists at  $x = x''$ ,  $y = D$ . The additional interfacial pressure difference  $\Delta p'_i$  due to the perpendicular pressure gradient is given by:

$$\Delta p'_i = (p_1)_{\text{top}} - (p_1)_{\text{bottom}} \neq \rho_1 g D \cos \beta \quad T-45$$

The amount of capillary pumping available for axial flow is therefore reduced and Equation T-39 must be modified as follows:

$$\left. \begin{aligned} (\Delta p_i)_{\text{max}} &\leq \Delta p_{\text{cap}} - \Delta p'_i \\ &\leq \Delta p_{\text{cap}} - \rho_1 g D \cos \beta \end{aligned} \right\} \quad T-46$$

Most heat pipes are operated very nearly in the horizontal position. The value of the

cosine is close to unity and the additional pumping requirement is approximately

$$\Delta p'_1 \sim \rho_1 g D$$

T-47

Thus, in a gravity field the pressure head corresponding to the perpendicular dimension D of the heat pipe must always be added to the capillary pumping requirement.

#### T.6.2 Heat Transport Factor and Heat Transport Capability Factor

Two very useful parameters in heat pipe design are the "Heat Transport Factor" and the "Heat Transport Capability Factor". A meaningful definition of these parameters requires that:

1. The flow regimes in liquid and vapor are laminar and momentum effects are negligible.
2. All geometrical properties of wick and heat pipe are constant along its length.
3. At least one of the following conditions are met:
  - (1) Body forces are absent, and/or
  - (2) The location of minimum ( $x'$ ) and maximum ( $x''$ ) interfacial pressure are independent of  $Q(x)$ .

The Heat Transport Factor and the Heat Transport Capability Factor shall be defined by referring to the pressure balance (Equation T-39) within the heat pipe. Using the applicable expressions (Equations T-4, T-15, T-22, and T-26) for the pressure gradients in liquid and vapor and Equation T-38 for the maximum interfacial pressure difference, the pressure balance (Equation T-39) can be written as follows:

$$\Delta p_{\text{cap}} \geq \int_{x'}^{x''} \left[ -\frac{32 \mu_y \dot{m}_v}{\rho_v A_v D_{h,v}} + \frac{\mu_1 \dot{m}_1}{K A_w \rho_1} + \rho_1 g \sin \beta \right] dx \quad T-48$$

The local mass flow rates  $\dot{m}_v$  and  $\dot{m}_1$  are related to the net axial heat flow rate,  $Q$ , through Equation T-43. Using the above assumptions, Equation T-48 can then be rearranged into the following simplified form:

T-23

$$\Delta p_{cap} \geq -C \int_{x'}^{x''} \dot{Q} dx + \int_{x'}^{x''} \rho_1 g \sin \beta dx \quad T-49$$

where the constant C combines the wick and working fluid properties and is given by:

$$C = \frac{32 \mu_v}{\rho_v A_v D_{h,v} 2 \lambda} + \frac{\mu_1}{K A_w \lambda} \quad T-50$$

In both Equations T-48 and T-49, the integration is extended from the point of minimum ( $x'$ ) to maximum ( $x''$ ) interfacial pressure difference. Further rearrangement of Equation T-49 yields:

$$\int_{x''}^{x'} \dot{Q}(x) dx \leq \frac{\Delta p_{cap}}{C} + \int_{x''}^{x'} \frac{\rho_1 g \sin \beta}{C} \quad T-51$$

The left side of Equation T-51 represents the heat transport requirement; i.e., the axial distribution of heat flow rates. The right side of Equation T-51 describes the capability of the heat pipe to meet these requirements for a specified orientation.

The Heat Transport Factor is defined as the integral on the left side of Equation T-51:

$$\dot{Q}_L = \int_{x''}^{x'} \dot{Q}(x) dx \quad T-52$$

It is completely described by the distribution of heat flow rates and is independent of the parameters of the heat pipe and the orientation. The Heat Transport Factor therefore defines the heat transport requirement.

If Equation T-51 is examined, it is seen that the right side is independent of the heat transport requirement. It contains only physical heat pipe properties; i.e., wick and fluid properties and the orientation with respect to gravity. But the right side also sets the upper limit for the Heat Transport Factor. It is therefore convenient to define the capability of the heat pipe in a form that permits a direct comparison with the requirements.

$$(\dot{Q}_L)_{max} \equiv \frac{\Delta p_{cap}}{C} + \int_{x''}^{x'} \frac{\rho_1 g \sin \beta}{C} \quad T-53$$

From the definition of  $(\dot{Q}L)_{\max}$ , it is observed that it is necessary to impose the restriction that either body forces are absent or  $x'$  and  $x''$  are independent of  $\dot{Q}(x)$ . If at least one of these conditions is not met,  $(\dot{Q}L)_{\max}$  will be dependent on the heat transport requirement, and Equation T-53 will not describe the capability of the heat pipe.

Using the two definitions, Equations T-52 and T-53, the pressure balance assumes a simple form:

$$\dot{Q}L \leq (\dot{Q}L)_{\max} \quad \text{T-54}$$

It must be emphasized again that  $\dot{Q}L$  represents the heat transport requirement as prescribed by the application and  $(\dot{Q}L)_{\max}$  represents the heat pipe's capability to meet these requirements. The symbol  $\dot{Q}L$  for both parameters has not been chosen arbitrarily. Both  $\dot{Q}L$  and  $(\dot{Q}L)_{\max}$  have the dimension of a heat flow rate  $\dot{Q}$  times a length  $L$ . Numerical values for  $\dot{Q}L$  and  $(\dot{Q}L)_{\max}$  are therefore given in watt-meter or, more commonly, in watt-inches.

The significance of the Heat Transport Factor and the Heat Transport Capability Factor can best be realized by examining two special but very important cases.

1. The first case involves a heat pipe operating in a "zero g" environment. No restrictions shall be placed on the shape of the heat pipe\* or the distribution of evaporators and condensers. Once this distribution has been specified, the net axial heat flow rate  $\dot{Q}(x)$  can be obtained from Equations T-40 and T-43. Because of the assumption of uniform wick properties and the absence of dynamic effects and body forces the interfacial pressure difference  $\Delta p_i(x)$  is proportional to  $\dot{Q}(x)$ . Thus the locations  $x'$  and  $x''$  of the lowest and highest value of  $\Delta p_i$  are completely determined by the distribution of  $\dot{Q}(x)$  and independent of the Heat Pipe geometry. The Heat Transport Factor  $\dot{Q}L$  is found from Equation T-52 and is also specified by the distribution of heat loads.

---

\* As long as the one-dimensional flow model applies.

The Heat Transport Capability Factor  $(\dot{Q}L)_{\max}$  is given by:

$$(\dot{Q}L)_{\max} = \frac{\Delta p_{\text{cap}}}{C} \quad \text{T-55}$$

Closed form solutions for  $(\dot{Q}L)_{\max}$  which apply to this special case may be found in Section T. 6. 3. Any distribution of heat inputs and outputs which results in a  $\dot{Q}L$  that is less than  $(\dot{Q}L)_{\max}$  for a given heat pipe will be compatible with that heat pipe design.

2. Another special, but frequently encountered, case is that of a straight heat pipe which is operating in a gravity field and in the "heat pipe mode". The latter shall be defined by the following two (2) conditions:

- (1) The angle between the positive x axis and the horizontal is less than zero ( $\beta < 0$ ), and
- (2) The net axial heat flow rate  $\dot{Q}$  is positive (or zero) at all axial locations x.

The above conditions state that the net axial heat flow rate should everywhere have a component in the direction of gravity. For this special case it can be shown (but will not be proven here) that the points of maximum and minimum interfacial pressure are always located at the ends of the heat pipe, i. e.,

$$x'' = 0, \quad x' = L \quad \text{T-56}$$

For this case, the Heat Transport Factor becomes

$$\dot{Q}L = \int_0^L \dot{Q}(x) dx \quad \text{T-57}$$

The Heat Transport Capability Factor  $(\dot{Q}L)_{\max}$  can be found by carrying out the integration in Equation T-53:

$$(\dot{Q}L)_{\max} = \frac{1}{C} (\Delta p_{\text{cap}} + \rho_1 g L \sin \beta) \quad \text{T-58}$$

The first term on the right side of Equation T-58 represents the Heat Transport Capability Factor in the absence of gravity. Equation T-58 can therefore be expressed as:

$$(\dot{Q}L)_{\max} = (\dot{Q}L)_{\text{max, zero } g} + \frac{\rho_1 g L}{C} \sin \beta \quad \text{T-59}$$

Gravity thus reduces the effective heat transport capability. (In the heat pipe mode,  $\beta$  is negative). Equation T-59 describes the reduction of the "zero g" Heat Transport Capability Factor due to the effects of gravity.

### T.6.3 Closed Form Solution

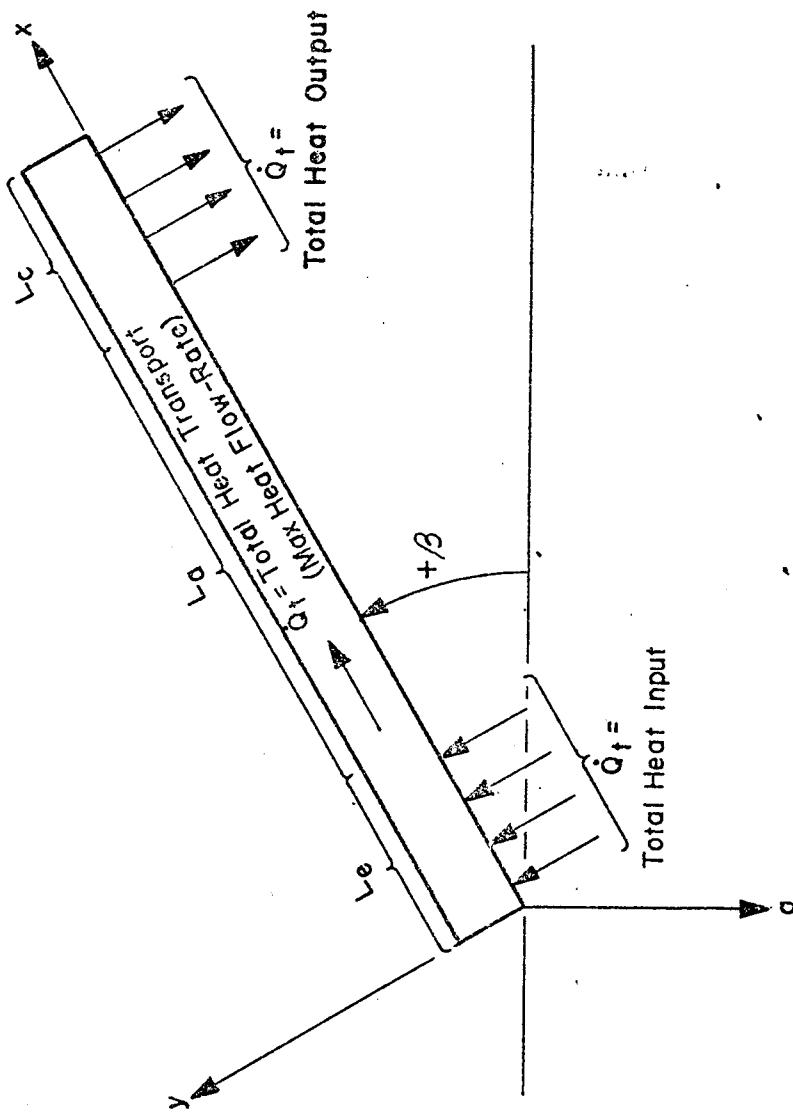
Closed form solutions of the hydrodynamic transport equations may be found for several heat pipe cases. One of these cases is the conventional heat pipe shown in Figure T-7 which has uniform heat addition and removal near the two ends, uniform wick properties along the length, and is operated in the "heat pipe mode" ( $\beta < 0$ , evaporator above condenser). Additional requirements necessary to perform a closed form solution are laminar flow in the liquid and the vapor and negligible momentum pressure gradients. Although the requirements of laminar flow and absence of momentum effects appear restrictive, good design practices usually avoid these regimes altogether. (Special modes of operation such as the start-up transients of liquid metal heat pipes are exceptions.) A large majority of all heat pipes fall into the category of the conventional heat pipe; and, therefore, the following closed form solution is developed.

The Heat Transport Capability Factor for this conventional heat pipe was given by Equation T-58. Using the appropriate expressions for the constant C (Equation T-50) and for  $\Delta p_{\text{cap}}$  (Equation T-9 in conjunction with Equation T-46),  $(\dot{Q}L)_{\max}$  becomes:

$$(\dot{Q}L)_{\max} = \frac{\frac{2 \sigma \cos \theta}{r_p} - \rho_1 g D \cos \beta + \rho_1 g L \sin \beta}{\frac{32 \mu_v}{\lambda A_v \rho_v D_{h,v}} + \frac{\mu_1}{\lambda A_w \rho_1 K}} \quad \text{T-60}$$

Equation T-52 can be rearranged and simplified:

$$(\dot{Q}L)_{\max} = \frac{2 K A_w (1 + \eta) \cos \theta F_1}{r_p} N_1 \quad \text{T-61}$$



Evaporator and Condenser

$$\bullet L = L_e + L_a + L_c$$

• Uniform Heat Flux  $\dot{Q}_f$

Figure T-7. Conventional Heat Pipe

The following abbreviations have been used in Equation T-61:

1. The parameter  $\eta$  is defined as the ratio of the sum of all pressure differences resulting from body forces to the available capillary pressure, i.e.,

$$\eta = -\frac{r_p D \cos \beta}{2 H \cos \theta} + \frac{r_p L \sin \beta}{2 H \cos \theta} \quad T-62$$

where  $H$ , the wicking height factor, is a property of the working fluid only and is defined as:

$$H = \frac{\sigma}{\rho_1 g} \quad T-63$$

2. The parameter  $F_1$  represents the ratio of the flow pressure drop in the liquid to the sum of the flow pressure drops in liquid and vapor.

$$F_1 = \frac{\Delta p_1}{\Delta p_1 + \Delta p_v} = \frac{1}{1 + \frac{\nu_v}{\nu_1} \frac{32 K}{D_{h,v}} \frac{A_w}{A_v}} \quad T-64$$

3. The Liquid Transport Factor  $N_1$  is a property of the working fluid and is defined as:

$$N_1 = \frac{\rho_1 \lambda \sigma}{\mu_1} \quad T-65$$

Equation T-61 defines the maximum heat transport capability of a conventional heat pipe provided that capillary pumping is the limiting factor. Since in most applications the capillary limit is the controlling one, Equation T-61 is one of the most useful expressions for the design of heat pipes.

In order to obtain an expression for the maximum amount of heat which the heat pipe can transport, the Heat Transport Factor is equated with the Heat Transport Capability Factor:

$$\int_0^L \dot{Q} dx = (\dot{Q}L)_{\max}$$

T-66

Referring to Figure T-7, the axial heat flow rate  $\dot{Q}(x)$  can be expressed in terms of the total heat input  $\dot{Q}_t$  for each of the following regions:

$$\left. \begin{array}{ll} \text{Evaporator} & \dot{Q}(x) = \dot{Q}_t x/L_e \\ \text{Transport Section} & \dot{Q}(x) = \dot{Q}_t \\ \text{Condenser} & \dot{Q}(x) = \dot{Q}_t L - x/L_c \end{array} \right\} \quad \text{T-67}$$

If the integration in Equation T-66 is carried out, an explicit expression is obtained for the total heat transport or heat flow rate  $\dot{Q}_t$ :

$$(\dot{Q}L)_{\max} = \dot{Q}_t \left( \frac{1}{2} L_e + L_a + \frac{1}{2} L_c \right) \quad \text{T-68}$$

It is often convenient to define an "effective length" of the heat pipe as follows:

$$L_{\text{eff}} = \frac{1}{2} L_e + L_a + \frac{1}{2} L_c \quad \text{T-69}$$

Equation T-66 then becomes:

$$\dot{Q}_t L_{\text{eff}} = (\dot{Q}L)_{\max} \quad \text{T-70}$$

Using Equations T-61 and T-70, the following expression for the maximum heat flow rate  $\dot{Q}_t$  is obtained:

$$\dot{Q}_t = \frac{2 K A_w (1 + \eta) \cos \theta F_1}{r_p L_{\text{eff}}} N_1 \quad \text{T-71}$$

It is important to note that the definition for the effective heat pipe length (Equation T-69) applies only for the special case of uniform heat input and heat output. For non-uniform heat distributions the integral of  $\dot{Q} dx$  in Equation T-66 must be solved in order to obtain an applicable effective length to be used in Equations T-70 or T-71.

T-30

If Equation T-70 is compared with Equation T-66, it is seen that  $\dot{Q}_t L_{\text{eff}}$  represents the Heat Transport Factor  $\dot{Q}_L$ . Thus for the special case for this conventional heat pipe:

$$\dot{Q}_L = \dot{Q}_t L_{\text{eff}} \quad \text{T-72}$$

Any combination of total heat load  $\dot{Q}_t$  and effective length  $L_{\text{eff}}$  which results in the same  $\dot{Q}_L$  will impose the same heat transport requirement on the heat pipe.

### T.7 Other Heat Transport Limitations

In addition to the capillary pumping limit discussed above, the circulation of the working fluid is restricted by several other limitations.

#### T.7.1 Sonic Limit

The evaporator section of a heat pipe represents a constant area vapor flow duct with mass addition through the evaporation process. The vapor velocity increases steadily along the length of the evaporator section due to the progressively increasing mass flow and reaches a maximum at the evaporator exit. It can be shown (27) that the limitations of such a flow regime are comparable to that of a converging nozzle with constant mass flow. The evaporator exit corresponds to the throat of the nozzle. The maximum vapor velocity which can exist at the evaporator exit corresponds to Mach 1. This choked flow condition is a fundamental limit on the axial vapor flow in a heat pipe. This limit does not exclude the possibility of supersonic flow in other sections of the heat pipe. In fact, Kemme (14) (15) has reported supersonic flow conditions in the condenser section of liquid metal heat pipes.

The axial heat flux for the sonic limit is obtained by calculating the mass flow rate at Mach 1:

$$\frac{\dot{Q}_t}{A_V} = \rho_v \lambda v_s \quad \text{T-73}$$

where the sonic velocity  $v_s$  is given by the familiar equation:

$$v_s = \sqrt{\frac{\gamma R_o T}{M}}$$

T-74

At the sonic limit, the mass flow rate per unit area and the corresponding axial heat flux are characteristic for every working fluid and are only a function of temperature. The limiting axial heat flux has, therefore, been included as a fluid property in Chapter F.

The axial heat flux at sonic conditions must be evaluated using the local temperature at the choking point. This temperature is considerably lower than the stagnation temperature which is measured at the entrance of the evaporator. Stagnation and local static temperature at Mach 1 are related through the expression:

$$T_{\text{stagn}} = T \left( 1 + \frac{\gamma - 1}{2} \right) \quad \text{T-75}$$

For liquid metals with a ratio of specific heats of 5/3 the static temperature is only 75% of the stagnation temperature at  $M = 1$ . Levy presents an equation which gives the limiting axial heat flux at sonic conditions in terms of the stagnation temperature (the temperature at the beginning of the evaporator) which is often more convenient to use:

$$\frac{\dot{Q}}{A_v} = \frac{\rho_v \lambda v_s}{\sqrt{2(\gamma + 1)}} \quad \text{T-76}$$

In Equation T-76, the fluid properties, e.g.,  $\rho_v$ ,  $\lambda$  and  $v_s$  (Equation T-74), are evaluated at the stagnation temperature.

Exceeding the sonic limit does not represent as catastrophic a failure as exceeding the capillary limit. When the sonic limit is reached, further increase in the mass flow rate and therefore the heat transfer rate can be realized only by increasing the stagnation pressure upstream of the choking point. To some extent this will occur automatically since the evaporator temperature will rise (and with it the saturation pressure and therefore the stagnation pressure) as soon as the total heat input and total heat output begin to diverge. Operation at or near the sonic limit results in large axial temperature differences along the heat pipe.

### T.7.2 Entrainment Limit

Like the sonic limit the entrainment limit is also a characteristic of high axial vapor velocities. Since liquid and vapor are in direct contact along the heat pipe, separated only by the meniscus of the interface, a mutual shear force exists between them. At low relative velocities, this shear force will only add to the viscous drag in both phases. Because the vapor velocity is usually much higher than that of the liquid, the effects will be most noticeable in the liquid phase. If the relative velocity becomes too great, the interface becomes unstable and liquid droplets are torn from the wick and "entrained" in the vapor. The first observation of this phenomenon was made at Los Alamos Scientific Laboratory through the sound made by droplets striking the condenser end of the heat pipe (13).

Entrainment may be described by the Weber number which is a ratio of the inertial forces in the vapor and tension forces in the liquid surface. The Weber number is defined as:

$$We = \frac{\rho_v \bar{v}^2}{\sigma'/z} \quad T-77$$

where  $\bar{v}$  is the average vapor velocity and  $z$  is a characteristic dimension for the surface. A Weber number of unity is generally believed to indicate the onset of entrainment. The corresponding axial heat flux is given by:

$$\frac{\dot{Q}}{A_v} = \left( \frac{\rho_v \sigma' z^2}{z} \right)^{\frac{1}{2}} \quad T-78$$

There is some uncertainty as to the proper choice of the characteristic dimension  $z$ . It is related to the wavelength of the perturbation on the liquid surface. Experimental data seem to indicate that a Weber number of unity corresponds to the onset of entrainment if  $z$  is approximately equal to the mesh size of the wick. Insufficient quantitative data are available to resolve the question of whether the characteristic dimension is related to the wire diameter (22) or the wire spacing (40).

The phenomenon of entrainment reduces the amount of liquid pumped to

the evaporator by prematurely returning it to the condenser. It thus increases the circulation losses (it might be considered an internal "leak") and reduces the heat transport capability. Of all the heat transport limitations the entrainment limit is probably the one that is the least severe.

### T.7.3 Heat Flux Limit

In addition to the capillary, the sonic, and the entrainment limits the heat pipe performance is also limited by the evaporator heat flux. Heat is transferred into and out of the heat pipe through the pipe wall and through at least part of the wick. If the radial heat flux becomes excessive, the circulation of the working fluid can be severely affected and the heat transport capability may be controlled by the radial heat flux rather than by the axial heat transport.

The limitation of the axial heat flux is not nearly as well understood as the truly hydrodynamic limits. There appears to be no limit to the heat flux at the condenser. High condenser heat fluxes contribute, of course, directly to the heat pipe conductance but they do not affect circulation of the working fluid. The evaporator heat flux, on the other hand, has definite upper bounds which limit the axial heat transport. Unlike the previously described limits, which specify a maximum axial heat transport  $\dot{Q}_t$ , the heat flux limit specifies the maximum radial evaporator heat flux  $\dot{q}_e$ . The two quantities are related through the evaporator area  $A_e$ :

$$\dot{Q}_t = \dot{q}_e A_e$$

Thus, for a given evaporator geometry, the heat flux limit also specifies the maximum axial heat transport.

The heat flux limit is generally considered to coincide with the onset of nucleate boiling in the wick. Heat is conducted from the heat pipe wall through the wick, and evaporation is assumed to occur at the liquid-vapor interface. This model has been substantiated by extensive experimental evidence (28) (38) (18). When boiling occurs within the wick the presence of the vapor bubbles that are generated reduce the liquid flow area and consequently decrease the transport capability.

With the onset of nucleate boiling, the hydrodynamic equations previously developed are no longer applicable since they were based on one-dimensional, laminar, liquid flow in a fully saturated wick. Breakdown of the mathematical model does not necessarily indicate a heat transfer limit. Since the hydrodynamic theory does not account for boiling in the wick, it is a good design practice to define the heat flux limit as the onset of nucleate boiling.

The boiling heat flux limit corresponds to the conduction heat flux which yields a "critical" super heat  $\Delta T_{\text{crit}}$  in the liquid. The boiling heat flux limit is therefore:

$$q_{\max} = \frac{K_{\text{eff}}}{t_w} \Delta T_{\text{crit}} \quad \text{T-80}$$

where  $K_{\text{eff}}$  is the effective thermal conductivity of the wick-liquid matrix. Models for the effective conductivity will be discussed in Section T. 8.

Marcus (30) has derived an expression for the critical super heat which is based on criteria similar to those which apply to nucleate boiling from planar surfaces:

$$\Delta T_{\text{crit}} = \frac{T_{\text{sat}}}{\lambda \rho_v} \left( \frac{25}{r_n} - (\Delta p_i)_{\max} \right) \quad \text{T-81}$$

where  $T_{\text{sat}}$  is the saturation temperature of the fluid and  $r_n$  is the effective radius of the critical nucleation cavity. This equation is based on the assumption that a bubble of a certain size will grow if its internal vapor pressure associated with the local super heat exceeds the restraining forces of saturation and capillary pressure. The radius of nucleation cavities,  $r_n$ , is a function of the boiling surface finish. Typical values for smooth surfaces are between  $10^{-4}$  and  $10^{-3}$  inches. For wicked surfaces, little is known about the critical radii of nucleation cavities but an upper bound is certainly the pore size of the wick.

The model predicts very conservative superheat tolerances. Even if the lower bound for the critical radius is used ( $10^{-4}$  inches), the calculated critical superheat is sometimes one order of magnitude lower than that actually measured. Marcus attributes this to the absence of a gaseous phase at the nucleation sites because heat

pipes contain a highly degassed working fluid. However, incipient boiling is difficult to detect through temperature measurements alone and many wicks which provide for adequate venting of internally generated vapor can tolerate some nucleate boiling without affecting the hydrodynamic limit.

A definite upper heat flux limit exists for every wick, and it is reached when the vapor generated within the wick is at such a high rate that it cannot escape fast enough from the heated surface. This is equivalent to the inability of the capillary forces to replenish liquid at a high enough rate. Boiling in the wick and the associated heat flux has been the subject of many investigations. Because of the present lack of a consistent theory that has been tested experimentally, it is premature to include this information in a handbook.

#### T.8 Heat Transfer

In the preceding sections the maximum heat transfer capability of the heat pipe was established. In this section the heat pipe performance during normal operation will be discussed; i. e., at heat loads which are below the hydrodynamic or heat flux limits.

When operated below any of its limits, the heat pipe represents a thermal conductor of extremely high conductance. In fact, heat pipes are frequently referred to as isothermal devices. In reality their conductance is, of course, finite but very high. In defining the conductance of a heat pipe, one has to distinguish between its internal conductance and that of the interfaces between the heat pipe and environment. Furthermore, the internal conductance is a composite of the radial heat transfer (at the evaporator and the condenser) and of the axial vapor mass transport. In most cases the conductance associated with the heat input and output mechanisms (external and internal) is much lower than the one associated with axial vapor and liquid transport. The overall conductance is therefore limited by input/output conductances -- a fact which is very important in heat pipe design.

The thermal model of a conventional heat pipe is shown in Figure T-8.

The total thermal resistance,  $R$ , is composed of a series of individual resistances:

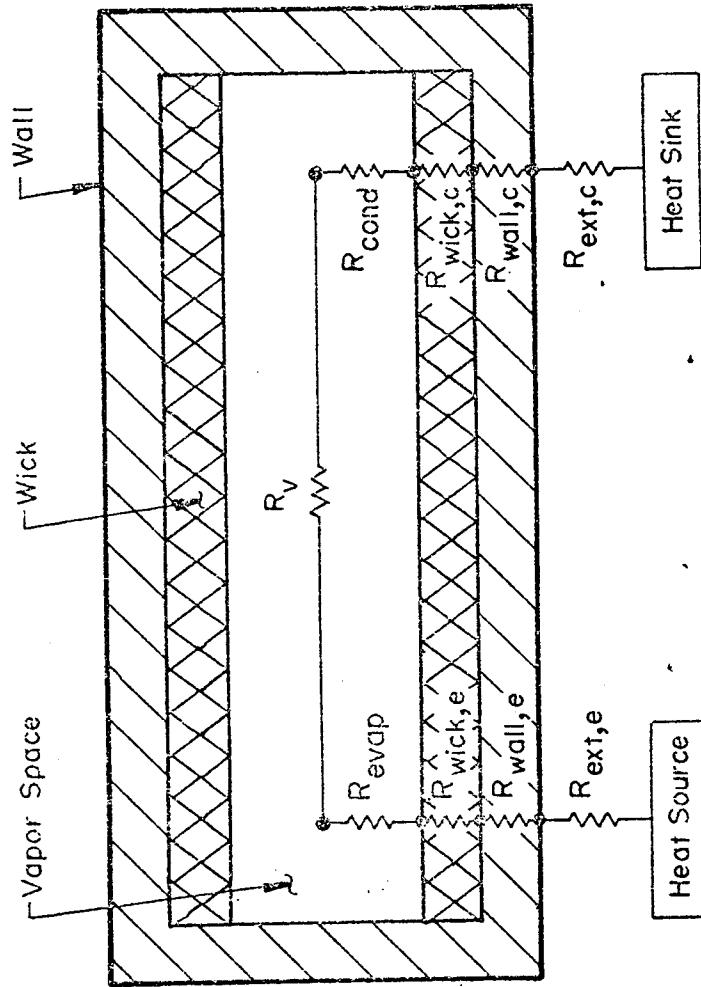


Figure T-8: Thermal Model of a Conventional Heat Pipe

$$R = R_{ext,e} + R_{wall,e} + R_{w,c} + R_{evap} + R_v + R_{cond} + \left. \right\} \quad T-82$$

$$R_{w,c} + R_{wall,c} + R_{ext,c}$$

Frequently, it is more convenient to describe the heat transfer characteristics by a conductance,  $G$ , rather than a resistance,  $R$ . The two are related through:

$$G = \frac{1}{R} \quad T-83$$

In terms of conductance, Equation T-82 becomes:

$$\frac{1}{G_t} = \frac{1}{G_{ext,e}} + \frac{1}{G_{wall,e}} + \frac{1}{G_{w,c}} + \frac{1}{G_{evap}} + \frac{1}{G_v} + \left. \right\} \quad T-84$$

$$\frac{1}{G_{cond}} + \frac{1}{G_{wall,e}} + \frac{1}{G_{ext,c}}$$

Unlike a solid conductor, the conductance of a heat pipe is dependent on the heat load,  $\dot{Q}$ . This dependency becomes very significant (in fact, catastrophic) when the heat load approaches any of the heat transport limits.

Each of the individual conductances, which are introduced by Equation T-84, will be discussed separately in the following paragraphs.

1.  $G_{ext,e}$  is the conductance between the heat source and the exterior of the evaporator. Its magnitude will, in general, depend on the application of the heat pipe. When it is closely coupled to the heat source, which is most frequently the case; this conductance is inversely proportional to the external evaporator area,

$$G_{ext,e} = h_{ext,e} A_{ext,e} \quad T-85$$

The external heat transfer coefficient,  $h_{ext,e}$ , is a function of the type of coupling and is best determined experimentally.

2.  $G_{wall,e}$  is the conductance of the heat pipe wall at the evaporator.

For cylindrical geometries this conductance is:

$$G_{\text{wall}, e} = \frac{2k_{\text{wall}, e}}{D_{\text{ext}}} \frac{A_{\text{ext}, e}}{\ln \frac{D_{\text{ext}}}{D_{\text{int}}}} \quad \text{T-86}$$

If the wall thickness is small compared to the diameter of the heat pipe this conductance reduces to:

$$G_{\text{wall}, e} = \frac{k_{\text{wall}, e}}{t_{\text{wall}, e}} \frac{A_{\text{ext}, e}}{} \quad \text{T-87}$$

3.  $G_{w, e}$  is the conductance of the wick at the evaporator. This term is usually the most difficult one to evaluate and is frequently a very significant contributor to the overall conductance. In the absence of nucleate boiling, heat is transmitted by conduction from the heat pipe wall, through the wick, and to the liquid-vapor interface which is the site of evaporation. This conductance can be expressed in terms of an internal heat transfer coefficient,  $h_{\text{int}, e}$ :

$$G_{w, e} = h_{\text{int}, e} A_{\text{int}, e} \quad \text{T-88}$$

For some geometries, analytical expressions or at least approximations can be found for the internal conductance. In the case of a porous wick located at the wall of the heat pipe, the internal evaporator conductance becomes:

$$G_{w, e} = \frac{2k_{w, e}}{D_{\text{int}, e}} \frac{A_{\text{int}, e}}{\ln \frac{D_{\text{int}, e}}{D_{v, e}}} \quad \text{T-89}$$

For thin wick structures, Equation T-89 reduces to a form similar to Equation T-87.

The effective wick conductivity  $k_w$  has been the subject of many studies (38) (19) (18). For a porous wick saturated with liquid, the effective conductivity is bracketed by the two extremes of parallel or series conduction paths:

$$\frac{k_s k_1}{\epsilon k_s + (1 - \epsilon) k_1} \leq k_w \leq (1 - \epsilon) k_s + \epsilon k_1 \quad T-90$$

(series) (parallel)

For metallic wicks and insulating liquids, the range of  $k_w$  covered by Equation T-90 is extremely broad. Conservative design would use the series conduction model. If the liquid conductivity  $k_1$  is much lower than that of the solid, the series model essentially represents the conductivity of a liquid layer whose thickness is weighted by the porosity of the matrix. For the case of an annular wick, Equation T-90 gives the correct result if  $\epsilon = 1$  is used.

In many high performance heat pipes, the bulk of the wick is removed from the wall in order to minimize the conductive temperature gradient. A secondary wick is then employed for circumferential distribution which consists of either a very thin layer of porous material or circumferential grooves. The latter design is used in most of the recently developed high performance heat pipes. At the present time, no satisfactory model exists for the thermal impedance of such grooves. The best design approach is to experimentally determine the heat transfer coefficient and then use Equation T-88 to compute the impedance.

The same arguments apply for wicks consisting of axial grooves in the wall. Although several theoretical models have been proposed (8) (9) (34), experimental determination of an effective film coefficient still represents the safest design approach.

There is some question concerning the validity of any model which is based purely on conduction. In the presence of axial mass-

flow of liquid within the wick, some radial convection effect is bound to exist. Chi and Cygnarowicz (10) have included convection effects in their heat transfer model of a cryogenic heat pipe; but, as yet, no comprehensive theory is available, and therefore the effective heat transfer coefficient of the wick must be determined experimentally.

4.  $G_{\text{evap}}$  is the conductance associated with the vaporization process at the liquid-vapor interface. This conductance is usually very large and contributes little to the overall conductance. Cotter (11) derived an expression, based on gas kinetics, for the pressure difference between the sites of vaporization and the bulk of the vapor. This expression, in terms of a heat transfer coefficient, is:

$$h = \frac{\alpha \lambda^2 \rho_v}{T} \sqrt{\frac{M}{R_o T 2\pi}} \quad \text{T-91}$$

The numerical factor ( $\alpha$ ) is of the order of 1. It accounts for probability of condensation of an impinging vapor molecule. The vaporization conductance  $G_{\text{evap}}$  is obtained from Equation T-91 using a relation similar to Equation T-88 but based on the area of the liquid vapor interface.

5.  $G_v$  is the thermal conductance associated with the axial vapor flow. This is the only term which is generally proportional to the length of the heat pipe when the pressure drop in the vapor is due to viscous losses. All other terms are proportional to the radial heat flux rather than the axial heat transport.

For a given vapor pressure drop, the corresponding temperature difference can be found. Based on the definition of  $G_v$  and using the Clausius-Clapeyron equation, the following expression may be obtained:

$$G_v = \frac{\lambda \rho_v}{T} \left( \frac{\dot{Q}}{\Delta P_v} \right) \quad \text{T-92}$$

If the vapor flow is predominantly viscous,  $\Delta p_v$  is proportional to  $\dot{Q}$  and to the length of the heat pipe.  $G_v$  then becomes a true, axial conductance which may be directly compared to that of a solid conductor. In fact, heat pipes have frequently been compared on this basis to other conductors. It must be noted, however, that  $G_v$  is only a small contributor to the overall heat pipe conductance and that the comparisons are therefore not very meaningful.

The expressions for the conductances at the condenser end of the heat pipe are identical to those at the evaporator. If the condenser geometry differs from that of the evaporator, the numerical values will be affected but the preceding Equations T-85 through T-91 will apply.

A combination of the individual contributions yields the overall conductance as expressed in Equation T-84. This expression can be simplified by neglecting the small terms  $1/G_{\text{evap}}$  and  $1/G_{\text{cond}}$  and by excluding the external interface conductances. The latter conductances are not really part of the heat pipe and should therefore be treated separately. It is also convenient to combine the contributions of wall and wick at the evaporator and at the condenser. The overall heat pipe conductance then becomes:

$$\frac{1}{G} = \frac{1}{A_e h_e} + \frac{1}{A_c h_c} + \frac{1}{G_v} \quad \text{T-93}$$

where  $A_e$  and  $A_c$  are the outside areas of evaporator and condenser and  $h_e$  and  $h_c$  are the respective combined heat transfer coefficients. The terms  $1/A_e h_e$  and  $1/A_c h_c$  are commonly much larger than  $1/G_v$ . Unlike in a solid conductor, the conductance of a heat pipe is dominated by the heat transfer at the heat input and the output regions.

Equation T-93 also illustrates that heat pipes are best utilized where heat is to be transported over relatively large distances. The terms  $1/(A_e h_e)$  and  $1/(A_c h_c)$  are independent of the heat transport length and only the relatively small term  $1/G_v$  is proportional to the heat pipe length. Thus, the overall conductance is fairly insensitive to length of the heat pipe. In the limit for very short heat pipes, this insensitivity to length sometimes renders the heat pipe inferior to solid conductors because the contributions of the evaporator and condenser do not vanish.

Up to this point, the absolute values of the temperature at any point of the heat pipe have not been established. Hydrodynamic theory only defines pressure and temperature differences but not their absolute values. Only the heat transfer relations provide the necessary boundary conditions for computing absolute temperatures. Source temperature  $T_s$ , sink temperature  $T_o$ , and heat transport  $\dot{Q}$  are related through:

$$T_s - T_o = \dot{Q} \frac{1}{G} \quad T-94$$

Once the heat pipe has been specified through its conductance  $G$  only two of the three operating parameters ( $T_s$ ,  $T_o$ ,  $\dot{Q}$ ) can be selected arbitrarily; the third one is defined through Equation T-94. For example, if source and sink temperature are specified, then the heat flow is completely defined. Similarly, if the sink temperature  $T_o$  and the heat transport  $\dot{Q}$  is specified, then the source temperature  $T_s$  is determined by Equation T-94. Once the environmental temperatures and the heat transport is defined, the absolute temperature of the vapor of the heat pipe is also determined through the following equations:

$$T_{v,e} = T_s - \dot{Q} \frac{1}{G_e} \quad T-95$$

$$T_{v,c} = T_o + \dot{Q} \frac{1}{G_c} \quad T-96$$

where  $T_{v,e}$  and  $T_{v,c}$  represent the vapor temperatures at the evaporator and at the condenser, respectively, and  $G_e$  and  $G_c$  are the conductances of the evaporator and the condenser. For the case of negligible temperature drop in the vapor, both equations yield the same vapor temperature:

#### T.9 Variable Conductance Heat Pipes

The preceding sections dealt with the heat transfer characteristics of heat pipes and with their ability to transport thermal energy. The conventional heat pipe discussed thus far is a completely passive device. It is not restricted to a fixed operating temperature but adjusts its temperature according to the heat load and the sink condition. Its thermal conductance is very high but, nevertheless, a nearly constant parameter.

With minor modifications, the heat pipe can be made a device of variable thermal conductance. Means of achieving variable conductance is discussed in this section along with the application of variable conductance to temperature control. The theory of variable conductance heat pipes is outlined. However, because of the complexity of this theory (in particular, in regard to transient phenomena), the reader is referred to special texts (29) for detailed derivations.

### T.9.1 Techniques for Varying Heat Pipe Conductance

The basic conductance model of a heat pipe is presented in Section T.8. For ease of reference, a slightly simplified model is shown in Figure T-9 in which some of the individual resistances are lumped together. In this model,  $R_e$  represents the sum of all resistances between the heat source and the vapor in the heat pipe,  $R_v$  the internal resistance along the length of the pipe, and  $R_c$  the sum of all resistances between the heat pipe vapor and the ultimate heat sink. The overall conductance  $G$  between the source and the sink is given by Equation T-97:

$$G = \frac{1}{\frac{1}{G_e} + \frac{1}{G_c} + \frac{1}{G_v}} \quad T-97$$

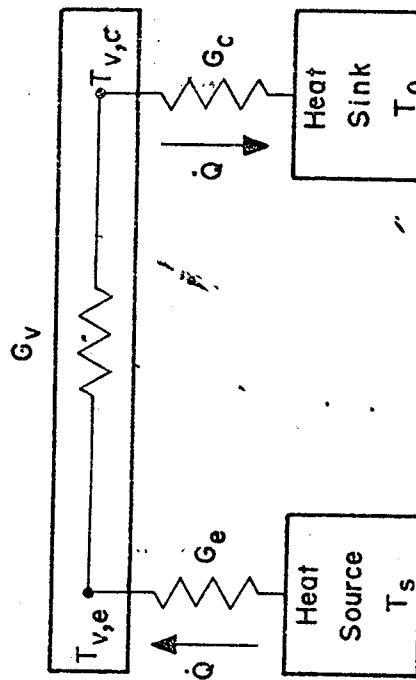


Figure T-9. Conductance Model of Heat Pipe

In principle, variable heat pipe conductance can be achieved by varying any one (or several) of the individual conductances which comprise to make up the overall conductances.

Various techniques have been proposed (and some of them demonstrated) to achieve variable conductance. These techniques can be conveniently grouped into the following three categories:

### 1. Liquid Flow Control

This technique involves either impeding or interrupting the liquid flow from the condenser to the evaporator. Impeding the liquid flow can result in an insufficient liquid supply at the evaporator and consequently can result in a partial dry-out. Since the evaporator resistance is a function of the area available for evaporation, this control technique functions by increasing the evaporator resistance  $R_e$  and thus decreasing the overall conductance  $G$ . Liquid flow control is a method which achieves control of the conductance by affecting the circulation of the working fluid in such a way as to create a partial hydrodynamic failure.

### 2. Vapor Flow Control

This technique involves throttling or interrupting the vapor flow from the evaporator to the condenser. The internal temperature drop along the heat pipe is directly related to the pressure drop in the vapor. Hence, by throttling the vapor flow, the pressure drop can be controlled and with it the internal resistance  $R_v$  of the heat pipe. Unlike the liquid flow control method, vapor flow control does not induce a partial hydrodynamic failure as long as certain control limits are not exceeded.

### 3. Condenser Flooding

Condenser flooding represents a control technique in which part of the condenser is blocked and thus rendered ineffective for heat rejection. The most common approach to condenser flooding is to use a noncondensing gas; but liquids, e.g., in the form of excess working fluid, have also been used. In either case, a partial blockage of the condenser results in

an increased condenser resistance  $R_c$  and therefore a decreased overall conductance  $G$ . Unlike the two previous techniques, condenser flooding does not adversely affect the circulation of the working fluid and does not represent a hydrodynamic failure.

Details of the various techniques are discussed in the following section. Because of the overwhelming importance of condenser blocking using a noncondensing gas, the major part of this discussion deals with this variable conductance control technique.

#### T.9.2 Categories of Variable Conductance Heat Pipes

Historically, the first application of variable conductance was to control the temperature of a heat source in the presence of fluctuating heat loads and sink temperatures. Indeed, the early heat pipe literature refers to variable conductance heat pipes frequently as temperature control heat pipes; but the concept of variable conductance has broader applicability. With reference to the function which they fulfill, variable conductance heat pipes (VCHP's) can be grouped into three (3) categories:

##### 1. Self-Controlled VCHP's

Self-controlled VCHP's are fairly effective in controlling the temperature of the heat source. The vapor pressure of the working fluid provides an internal reference for the selected operating temperature. The self-controlled VCHP maintains the vapor pressure nearly constant over a wide range of heat loads and sink conditions, and this results in a nearly constant internal vapor temperature. It is self-controlled in the sense that it constitutes a complete temperature control module with a built-in temperature reference.

##### 2. Feedback Controlled VCHP's

Feedback controlled VCHP's are also used for controlling temperatures. Unlike the self-controlled VCHP, the Feedback Controlled VCHP utilizes an external temperature reference. The temperature of the component to be controlled (e.g., the heat source) is monitored by an appropriate sensor (e.g., a thermocouple), the signal is then compared with

the reference, and the resulting error signal is used to vary the conductance of the heat pipe until the temperature deviation from the reference is corrected. Feedback systems generally provide much closer temperature control; however, this is at the expense of a more complex system.

### 3. Active Controlled VCHP's

The applications of VCHP's are not limited to temperature control.

As long as a technique for varying the conductance is employed which can be controlled externally, the VCHP represents a truly variable thermal conductor. It can be used to control the flow of heat to meet any requirement of a thermal system in the same manner as its electrical equivalent, the rheostat, is used to control the flow of electric current.

For each of the above categories of applications, one or several techniques of varying the conductance are available. The most important technique applicable to all three categories is condenser blocking by using a noncondensing gas. Other techniques have merits too and may even be preferable under certain circumstances. The selection of the most appropriate control technique can only be made on the basis of the requirements of the specific application.

#### T. 9.3 Variable Conductance Through Condenser Flooding With Gas

The principle of this technique is the formation of a gas plug at the condenser end of the pipe which prevents vapor from condensing in part of the condenser. This gas plug is the result of introducing a fixed amount of noncondensing gas in the heat pipe. In the absence of circulation of the working fluid (i.e., without heat transport) the gas is uniformly distributed within the vapor space except for a small amount which is dissolved in the liquid phase of the working fluid. During operation a steady flow of vapor exists from the evaporator to the condenser. The noncondensing gas is swept by the vapor to the condenser. Unlike the vapor, it does not condense but forms a "plug" at the condenser end of the heat pipe. The gas and vapor distributions for the nonoperating and operating condition are shown schematically in Figure T-10. As indicated in that figure, the transition between vapor and gas is not a sharp one. It is controlled by diffusion and axial conduction effects which are discussed elsewhere.

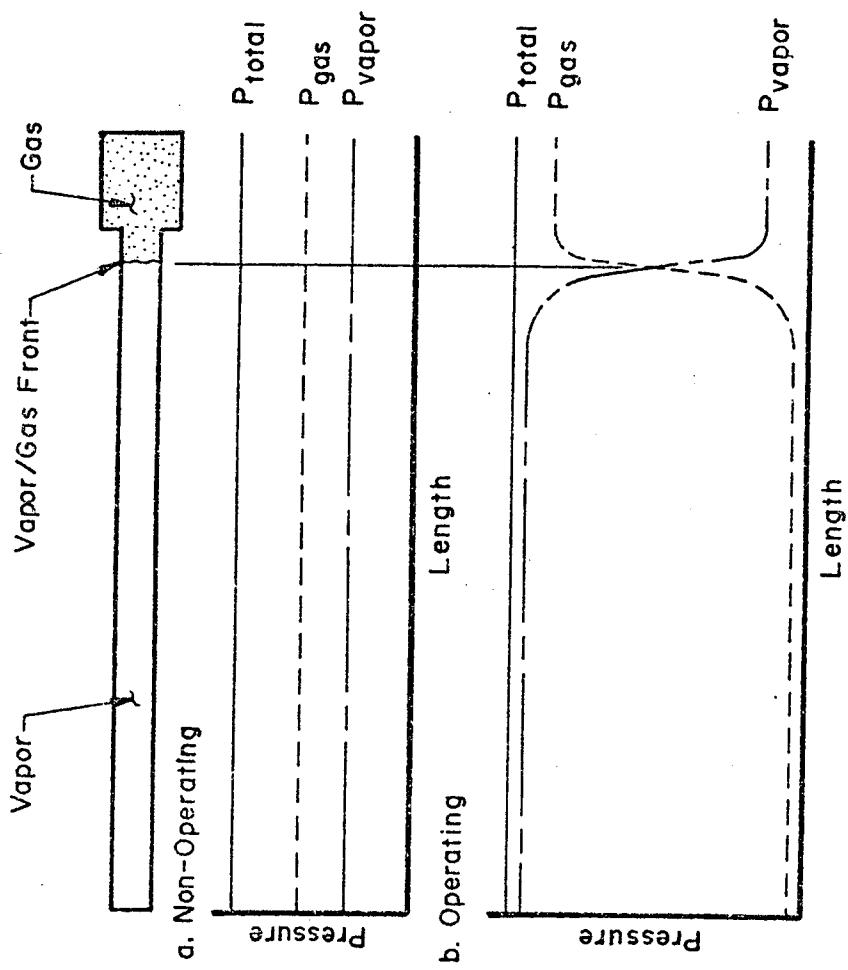


Figure T-10. Distribution of Gas and Vapor

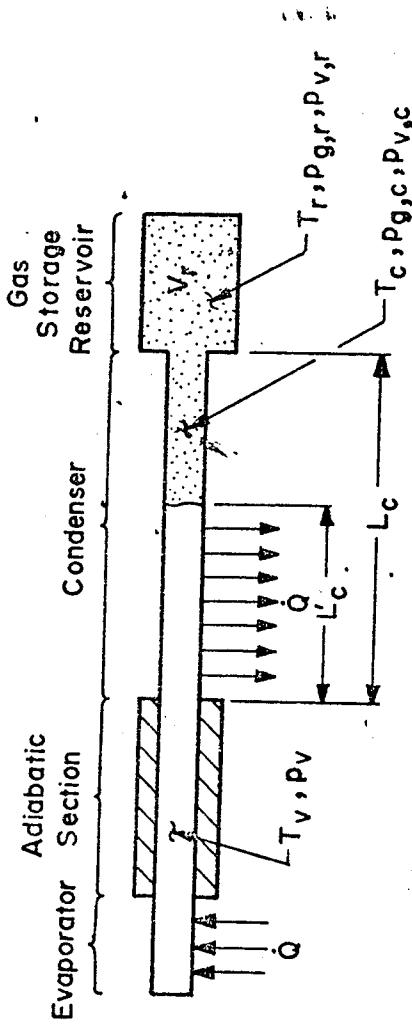


Figure T-11. Condenser Flooding with Gas

However, a good understanding of many of the operational characteristics of gas controlled VCHP's can be obtained by studying the simplified model of a flat front between the vapor and the noncondensing gas.

Conductance variation through addition of noncondensing gas is particularly attractive because it accomplishes self-control of its vapor temperature. In a conventional (fixed conductance) heat pipe, the vapor temperature adjusts itself in order to meet the heat rejection requirements for a given sink condition. Thus, if the heat load and/or sink temperature increases, the vapor temperature will also rise. In a gas loaded heat pipe, the fixed amount of gas occupies part of the condenser; the length of the gas plug being dependent on the vapor (and sink) temperature. If the heat load is increased, the vapor temperature tends to rise as in the fixed conductance heat pipe. However, the corresponding increase in vapor pressure of the working fluid compresses the gas plug, thereby increasing the size of the active condenser. This results in a higher conductance which effectively opposes the tendency of the vapor temperature to increase. Similarly, if the heat load and/or sink temperature decreases, the vapor temperature and pressure tend to drop which permits the gas plug to expand, the conductance of the heat pipe to decrease, and the vapor temperature decrease to be minimized. A gas loaded heat pipe therefore reduces fluctuations of the operating temperature and behaves as a self-controlled VCHP.

A simplified model of a heat pipe whose condenser is partially blocked with noncondensing gas is shown in Figure T-11. A sharp interface is assumed between the active and the inactive portion of the condenser. The noncondensing gas occupies both the inactive portion of the condenser and the gas storage volume. If the heat transfer to the environment is described through a heat transfer coefficient,  $h_c$ , the condenser conductance can be expressed in terms of the active condenser length  $L_c'$  as follows:

$$G_c = h_c a_c L_c'$$

T-98

In the more general case where heat is rejected from the condenser by a combination of convection, conduction and radiation, the heat transfer coefficient  $h_c$  and the conductance  $G_c$  become dependent on the operating temperature. But the principle of varying the conductance through condenser blockage applies equally for all modes of

heat rejection.

In order to arrive at a simple mathematical model for the gas controlled VCHP, the following additional assumptions are made:

- Steady state exists
- The gas-vapor mixture in the inactive part of the condenser and in the storage reservoir obeys the ideal gas law
- The total pressure within the heat pipe is uniform
- Axial conduction can be neglected

With these assumptions, the active length  $L'_c$  of the condenser can be calculated. In the model shown in Figure T-11, part of the gas resides in the inactive portion of the condenser and part in the storage reservoir. Applying the ideal gas law for both mass fractions yields the following expression for the total mass of the noncondensing gas:

$$m = \frac{p_{g,c} (L_c - L'_c) A_c}{R T_c} + \frac{p_{g,r} V_r}{R T_r} \quad T-99$$

where  $p_{g,c}$  and  $p_{g,r}$  are the partial pressures of the gas in the inactive condenser section and storage reservoir, respectively.

It follows from the assumption of uniform total pressure throughout the system that the sum of the partial pressures of gas and vapor in the inactive portion of the condenser and in the reservoir is equal to the vapor pressure in the active part of the heat pipe, i.e.:

$$p_{g,c} + p_{v,c} = p_v \quad T-100$$

and

$$p_{g,r} + p_{v,r} = p_v \quad T-101$$

where  $p_{v,c}$  and  $p_{v,r}$  are the partial pressures of the vapor in the inactive condenser section and the storage reservoir, respectively.

Within the inactive region of the condenser, the gas and liquid are at the sink temperature and the partial pressure of the vapor is equal to the saturation pressure of the vapor corresponding to the temperature of the sink. Thus we have:

$$T_c = T_o \quad \text{and} \quad p_{v,c} = p_{v,o} \quad \text{T-102}$$

With the help of Equations T-100, T-101 and T-102, Equation T-99 can be rearranged and solved for  $L'_c$ .

$$L'_c = L_c - \frac{m R T_o}{A_c (p_v - p_{v,o})} + \frac{T_o}{T_r} \frac{V_r}{A_c} \left( \frac{p_v - p_{v,r}}{p_v - p_{v,o}} \right) \quad \text{T-103}$$

The above expression may be substituted for  $L'_c$  in Equation T-98 in order to arrive at an equation for the conductance in terms of the various system parameters.

An easier way to show the effect of various parameters on the conductance of the heat pipe is to normalize the conductance with respect to its maximum value. The maximum value of conductance is attained when the entire condenser is active; i.e., no portion is blocked by noncondensing gas.

$$(G_c)_{\max} = h_c a_c L_c \quad \text{T-104}$$

The normalized conductance becomes (from Equations T-98, 103 and 104):

$$\frac{G_c}{(G_c)_{\max}} = \frac{L'_c}{L_c} = 1 - \frac{m R T_o}{V_c (p_v - p_{v,o})} + \frac{T_o}{T_r} \frac{V_r}{V_c} \left( \frac{p_v - p_{v,r}}{p_v - p_{v,o}} \right) \quad \text{T-105}$$

Keeping in mind that the various vapor pressures in Equation T-105 are completely determined by the corresponding temperatures, the conductance can be controlled by varying one or more of the following parameters:

$$\left. \begin{array}{l} \bullet m \\ \bullet V_r \\ \bullet T_r \end{array} \right\} \begin{array}{l} \text{Independent} \\ \text{Control} \\ \text{Parameters} \end{array} \quad \left. \begin{array}{l} \bullet T_o \\ \bullet T_v \end{array} \right\} \begin{array}{l} \text{Dependent} \\ \text{Control} \\ \text{Parameters} \end{array}$$

The above list excludes the condenser volume because it is normally fixed by the heat pipe design. The vapor temperature  $T_v$  is not an explicit variable in Equation T-105, but it controls the system pressure  $p_v$  and must therefore be included in the list of control parameters.

The left three parameters ( $m$ ,  $V_r$ , and  $T_r$ ) can be varied independently to control the heat pipe's conductance. The right two parameters ( $T_o$  and  $T_v$ ) affect the conductance also but normally cannot be varied independently. The sink temperature  $T_o$  is usually determined by the application, and the vapor temperature is determined by the heat load and the environment.

The effect on the conductance of increasing or decreasing any of the above parameters is shown in Table T-1.

Table T-1: Effect of Varying Control Parameters on Heat Pipe Conductance

Increases of:	Causes Conductance to:
Mass of Noncondensing Gas ( $m$ )	Decrease
Volume of Storage Reservoir ( $V_r$ )	Increase
Temperature of Storage Reservoir ( $T_r$ )	Decrease
Sink Temperature ( $T_o$ )	Decrease
Vapor Temperature ( $T_v$ )	Increase

Table T-1 can be verified by differentiating Equation T-105 with respect to the particular variable. In doing so, one must keep in mind that the sum of the last two terms in Equation T-105 is always negative. In principle, each one of the parameters in Table T-1 can be used to vary the conductance of the heat pipe. In the following sections, details of the various categories of VCHP's are given and the implementations of the above control parameters are presented.

T.9.4 Self-Controlled VCHPs

In the self-controlled VCHP the mass of the noncondensing gas and the volume of the storage reservoir is fixed. The temperature of the storage reservoir is either equal to the sink temperature or is maintained at some constant value. The principle of operation of a self-controlled VCHP was explained previously. The active length of the condenser is self-adjusting to maintain a nearly constant vapor temperature. Variable conductance is used to compensate for changes of the heat load  $\dot{Q}$  and/or the sink temperature  $T_o$ . The vapor temperature should be insensitive to changes in  $\dot{Q}$  and  $T_o$ .

$$\frac{dT_v}{d\dot{Q}} \sim 0 \quad \text{and} \quad \frac{dT_v}{dT_o} \sim 0 \quad \text{T-106}$$

The vapor temperature  $T_v$  is related to the heat flow rate  $\dot{Q}$  and the sink temperature  $T_o$  through the equation:

$$\dot{Q} = G_c (T_v - T_o) \quad \text{T-107}$$

Combining the above equation with the expression for the condenser conductance, Equation T-105 yields:

$$\dot{Q} = (G_c)_{\max} (T_v - T_o) \left[ 1 - \frac{m R T_o}{V_c (p_v - p_{v,o})} + \frac{T_o}{T_r} \frac{V_r}{V_c} \left( \frac{p_v - p_{v,r}}{p_v - p_{v,o}} \right) \right] \quad \text{T-108}$$

The preceding equation completely describes the behavior of a self-controlled VCHP. It relates the vapor temperature  $T_v$  to the heat load  $\dot{Q}$ , the sink temperature  $T_o$ , and the reservoir temperature  $T_r$ . Unfortunately, Equation T-108 is implicit with respect to  $T_v$ , since the vapor temperature enters the equation also through the vapor pressure  $p_v$ .

Numerical solutions can, of course, be obtained. Typical performance curves would give the vapor temperature dependence on heat load, sink temperature, and reservoir temperature. Design aids for selecting a particular heat pipe geometry

to meet certain performance requirements are given in Chapter D, Design Procedures; and sample performance curves are given in Chapter P. The various heat pipe parameters, e.g., size of the storage reservoir and the properties of the working fluid, affect the control performance of the heat pipe are now evaluated.

The sensitivity of  $T_v$  with respect to changes in  $\dot{Q}$  and  $T_o$  can be assessed from Equation T-107 by forming the total differential of  $T_v$  as a function of  $d\dot{Q}$  and  $dT_o$ .

$$dT_o = 0 \quad ; \quad \frac{dT_v}{d\dot{Q}} = \left( \frac{1}{G_c} \right) \left( \frac{1}{1+S} \right) \quad T-109$$

$$d\dot{Q} = 0 \quad ; \quad \frac{dT_v}{dT_o} = (1) \left( \frac{1-S'}{1+S} \right) \quad T-110$$

where  $S$  and  $S'$  are defined as:

$$S \equiv \left( \frac{T_v - T_o}{G_c} \right) \frac{\partial G_c}{\partial T_v} > 0 \quad T-111$$

and

$$S' \equiv \left( \frac{T_v - T_o}{G_c} \right) \frac{\partial G_c}{\partial T_o} < 0 \quad T-112$$

If one examines Equations T-109 and T-110, it is seen that the term within the first bracket of each equation represents the temperature sensitivity for a fixed conductance heat pipe (see Equation T-107). In a self-controlled VCHP the sensitivity to variations of the heat load is attenuated by the factor  $(1/1 + S)$ . Effects of varying heat load are minimized if  $S$  is large.

The same requirements apply to minimizing the effects of sink temperature variations (Equation T-110). Again,  $S$  should be large. In this case, the attenuation is partially offset by the parameter  $S'$  which should be small in order to make the vapor temperature insensitive to the sink temperature. Unfortunately, the same design parameters which make  $S$  large also tend to increase  $S'$ . This is discussed in

more detail in the following sections where different types of self-controlled VCHP's are investigated more closely.

#### T.9.4.1 Self-Controlled VCHP with a Wicked, Uncontrolled Storage Reservoir

This is the simplest type of self-controlled VCHP and is shown schematically in Figure T-12. The wick extends past the condenser region into the storage reservoir. The temperature of the storage reservoir is allowed to float and will usually be equal to the sink temperature. A typical example is a heat pipe operating in the laboratory and rejecting its heat by either convection and/or radiation to the ambient. The inactive region of the condenser and the storage reservoir will be approximately at ambient temperature. Another example is a heat pipe which is part of a space radiator and has its storage reservoir thermally coupled to the radiator. The temperature of the inactive condenser region and of the storage reservoir will again closely follow the sink temperature.

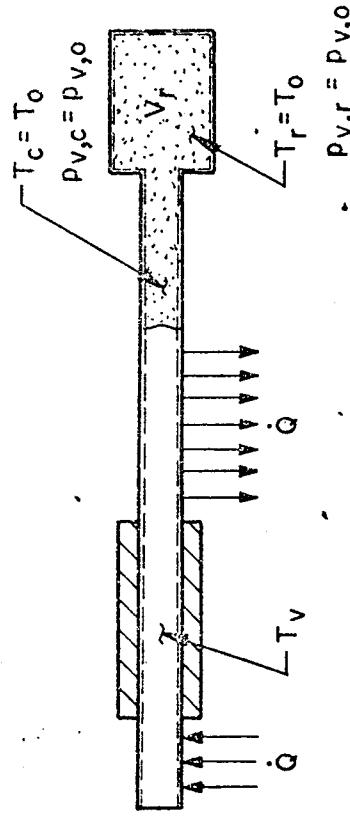


Figure T-12. Self-Controlled VCHP with a Wicked, Uncontrolled Reservoir

Since the storage reservoir is wicked, the partial pressure of the vapor within it is equal to the saturation pressure at the sink temperature. For this case we therefore have:

$$T_r = T_o \quad \text{and} \quad p_{v,r} = p_{v,o}$$

The normalized conductance of the condenser (Equation T-105) reduces to:

$$T-113$$

$$\frac{G_c}{(G_c)_{\max}} = 1 + \frac{V_r}{V_c} - \frac{m R T_o}{V_c (p_v - p_{v,o})} \quad T-114$$

The effects of variations of the heat load and sink temperature upon the vapor temperature can be examined by calculating the parameters  $S$  and  $S'$ .

$$S = (T_v - T_o) \left[ \frac{(G_c)_{\max}}{G_c} \left( \frac{V_r}{V_c} + 1 \right) - 1 \right] \frac{d \ln p_v}{dT_v} \quad T-115$$

$$S' = - (T_v - T_o) \left\{ \begin{aligned} & \left[ \frac{(G_c)_{\max}}{G_c} \left( \frac{V_r}{V_c} + 1 \right) - 1 \right] \\ & \left[ \frac{1}{T_o} + \frac{p_{v,o}}{p_v} \frac{d \ln p_{v,o}}{dT_o} \right] \end{aligned} \right\} \quad T-116$$

If we examine the last two equations we see that good control of the vapor temperature ( $S$  large) is achieved if:

- The ratio of storage-to-condenser volume ( $V_r/V_c$ ) is large.
- The relative slope of the vapor pressure curve of the working fluid ( $d \ln p_v/dT_v$ ) is steep.

As shown previously, a large value of  $S$  attenuates both the effects of heat load and sink temperature changes. However, the same design parameters which increase  $S$  also result in a large value for  $S'$  which, in turn, increases the sensitivity to sink temperature changes.\*

The sensitivity to changes of the sink temperature is the most severe disadvantage of the simple, self-controlled VCHP with wicked, uncontrolled storage reservoir. This constraint is largely removed by using a non-wicked reservoir to be

---

\* In Equation T-116, the dependence on the vapor pressure curve is not as pronounced as in Equation T-115 due to the attenuation of the slope of the vapor pressure by  $(p_{v,o}/p_v)$ . The two terms in the last bracket in Equation T-116 represent the effects of the sink temperature on the noncondensing gas and on the partial pressure of the vapor, respectively.

discussed in the next section.

#### T.9.4.2 Self-Controlled VCHP with a Non-Wicked Storage Reservoir

This configuration is shown schematically in Figure T-13. When the wick is removed from the reservoir, the partial pressure of the vapor no longer corresponds to the reservoir temperature since the reservoir contains no liquid. Instead, the equilibrium partial pressure of the vapor in the reservoir will be equal to that at the nearest location where saturation conditions exist. This location is near the end of the condenser at a place where the temperature is equal to the sink temperature. Thus we have:

$$p_{v,r} = p_{v,o} \quad T-117$$

The presence of working fluid vapor in the reservoir results from diffusion. In order to avoid vapor condensation in the reservoir and consequently in establishing a saturation vapor pressure, the reservoir temperature must be higher than the sink temperature. There are no other restrictions on the reservoir temperature. In practice, an elevated reservoir temperature is achieved by thermally coupling the reservoir to the evaporator as shown schematically in Figure T-14. The normalized condenser conductance becomes:

$$\frac{G_c}{(G_c)_{\max}} = 1 + \frac{T_o}{T_r} \cdot \frac{V_r}{V_c} - \frac{m R T_o}{V_c (p_{v,o} - p_{v,r})} \quad T-118$$

The two parameters  $S$  and  $S'$  are now:

$$S = (T_v - T_o) \left[ \frac{(G_c)_{\max}}{G_c} \left( \frac{T_o}{T_r} \cdot \frac{V_r}{V_c} + 1 \right)^{-1} \right] \frac{d \ln \frac{p_v}{p_{v,o}}}{dT_v} \quad T-119$$

$$S' = - (T_v - T_o) \left[ \frac{(G_c)_{\max}}{G_c} - 1 \right] \left[ \frac{1}{T_o} + \frac{p_{v,o}}{p_v} \frac{d \ln \frac{p_v}{p_{v,o}}}{dT_o} \right] \quad T-120$$

When comparing the parameters  $S$  and  $S'$  for the present case with those for the wicked

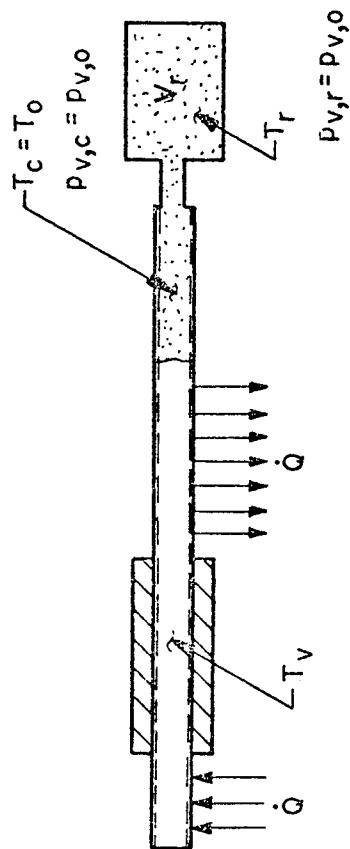


Figure T-13. Self-Controlled VCHP with a Non-Wicked Reservoir

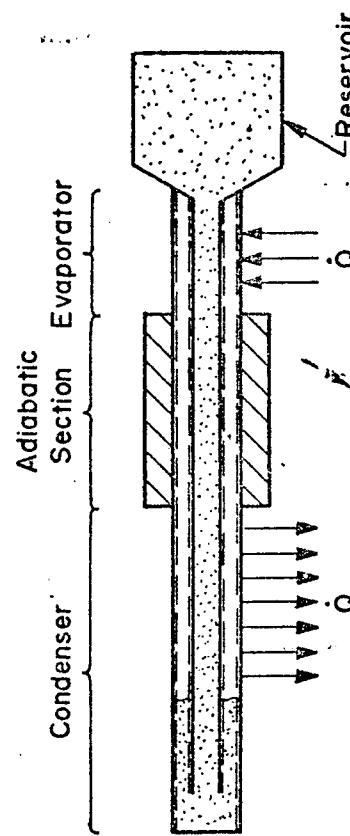


Figure T-14. VCHP with Reservoir Thermally Coupled to Evaporator

uncontrolled reservoir, one sees that the first parameter,  $S$ , is nearly unchanged. It is slightly smaller, however, since  $V_r/V_c$  is multiplied by the ratio  $T_o/T_r$  which is always less than unity. Thus, a self-controlled VCHP with a non-wick reservoir is slightly more sensitive to changes in the heat load (smaller  $S$ ) than one with a wicked reservoir.

This small disadvantage is more than offset by its much smaller sensitivity to changes of the sink temperature. When examining the parameter  $S'$  (Equation T-120) one sees that  $S'$  no longer contains the ratio  $V_r/V_c$ .  $S'$  is therefore significantly smaller than for a heat pipe with wicked reservoir. Since the magnitude of  $S'$  describes the sensitivity to sink variations, the non-wick reservoir heat pipe minimizes the influence of the sink temperature.

A non-wicked reservoir provides nearly the same control sensitivity with respect to changes of the heat load as the uncontrolled wicked reservoir, but it is much less sensitive to variations of the sink temperature. It is still a completely passive system in the sense that the reservoir temperature need not be controlled but need only be maintained above the sink temperature. A non-wicked reservoir heat pipe also has some serious disadvantages. It was already pointed out that the equilibrium vapor pressure in the reservoir is established by diffusion. Mass diffusion is a rather slow process, and this can lead to a slow response in the heat pipe's transient performance. A non-wicked reservoir heat pipe is also sensitive to accidental spillage of the liquid working fluid into the storage reservoir. This could easily occur either during handling prior to installation or during operation as a result of an unfavorable body force field. The presence of liquid in the reservoir would establish saturation conditions there which would negate the principle of a non-wicked reservoir. Generally, once liquid working fluid has leaked into the reservoir, the original equilibrium condition can only be restored by diffusion which could be an extremely slow process requiring days or weeks to complete. The analysis is also complicated by the phenomenon of thermal diffusion which tends to separate mixtures of gases at constant pressure due to a temperature gradient. But it was shown by Marcus (29) that thermal diffusion has only a small effect on the vapor pressure distribution in VCHP's.

T. 9.4.3 Self-Controlled VCHP with a Wicked, Temperature Controlled Storage Reservoir

This configuration combines the low sensitivity to sink variations of a non-wicked reservoir pipe with the practical advantage of having saturation conditions exist everywhere within the system. It is shown schematically in Figure T-15. The wick extends into the storage reservoir. Liquid working fluid is therefore present in the reservoir causing the partial pressure of its vapor to be in equilibrium with the reservoir temperature. The latter is maintained constant either by placing the reservoir in a constant temperature environment or by controlling it thermostatically.

The characteristic equation for the normalized condenser conductance is identical to Equation T-105. Since temperature and vapor pressure in the reservoir are independent of heat load and sink temperature, the parameters  $S$  and  $S'$  are the same as in the case of non-wicked reservoir (Equations T-119 and T-120). This system has the same response with regard to changes of the heat load and sink temperature as a non-wicked reservoir heat pipe.

However, there are two important restrictions on the reservoir temperature. First, it must be lower than the vapor temperature. If  $T_r$  becomes equal to  $T_v$ , the partial vapor pressure in the reservoir equals the total pressure in the system and the noncondensing gas is completely forced out of the reservoir. This condition usually leads to complete blockage of the condenser. If  $T_r > T_v$ , the heat pipe actually reverses and the reservoir not only cannot store gas but it becomes the evaporator. The second limit is a practical one -- the reservoir temperature will always be higher than the sink temperature since the sink temperature is usually the lowest one available.

If the reservoir can be located in a constant temperature environment, the requirement for a separate reservoir temperature control is eliminated. For those applications where a constant temperature environment is not available, a separate reservoir temperature control system is required. This added complication is usually not justified.

T. 9.5 Feedback Self-Controlled VCHP's

The passive, self-controlled VCHP is a fairly simple control device but its

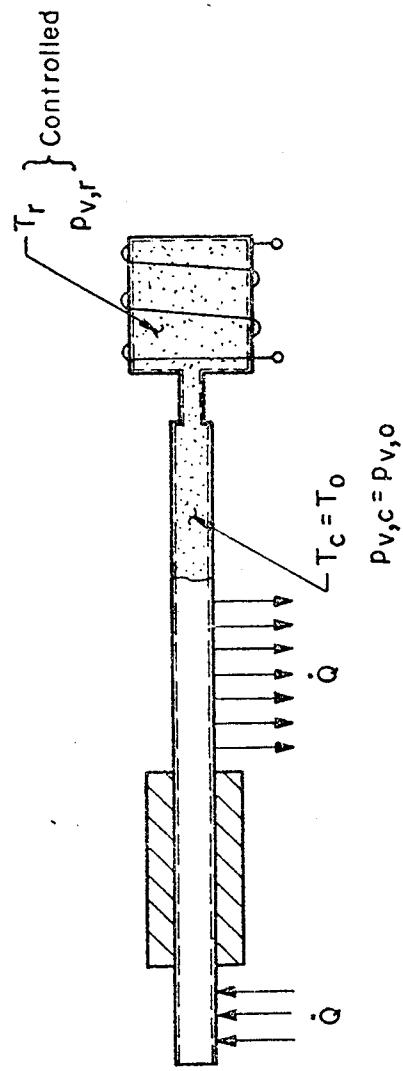


Figure T-15. Self-Controlled VCHP with a Wicked, Temperature Controlled Reservoir

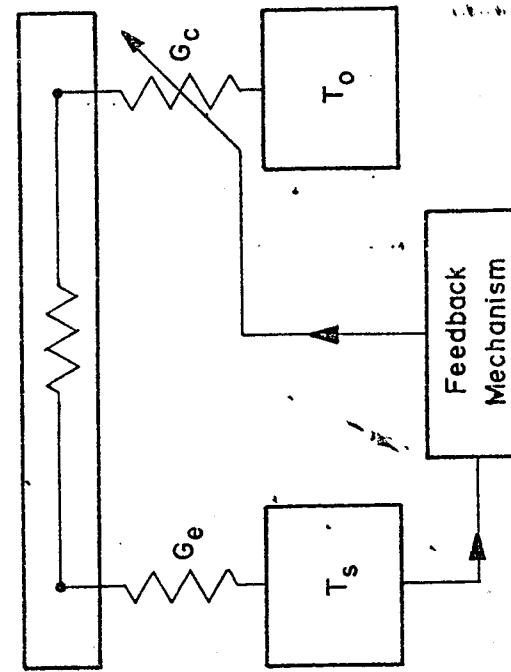


Figure T-16. Principle of Feedback System

temperature control capability is limited. From the preceding sections, it can be seen that absolute temperature control, with respect to changes in  $\dot{Q}$ , can only be approached if  $V_r/V_c \rightarrow \infty$  (Equations T-115 and T-119). Furthermore, regardless of the reservoir size, complete insensitivity to changes in the sink temperature is unattainable. An additional limitation of the passive, self-controlled heat pipe is the fact that it controls only the vapor temperature. The usual objective of using a VCHP is to control the temperature of the heat source and not the temperature of the vapor of the heat pipe. Heat source and vapor temperature are related in the following way:

$$T_s = T_v + \frac{1}{G_e} \dot{Q} \quad T-121$$

where  $G_e$  is the fixed conductance between heat source and the vapor of the VCHP. If a control system could be found which maintains the vapor temperature perfectly constant, the temperature of the heat source would still be affected by variations of the heat load. From Equation T-121, the following expression is obtained:

$$\frac{dT_s}{d\dot{Q}} = \frac{dT_v}{d\dot{Q}} + \frac{1}{G_e} \quad T-122$$

Thus for the extreme case of completely constant vapor temperature ( $dT_v/d\dot{Q} = 0$ ), the source temperature still varies in accordance with the heat load as:

$$\frac{dT_s}{d\dot{Q}} = \frac{1}{G_e} \quad \text{for} \quad \frac{dT_v}{d\dot{Q}} = 0 \quad T-123$$

In a feedback system, the source temperature is controlled rather than the vapor temperature. This approach eliminates the effect of the evaporator conductance on the temperature control of the heat source.

The principle of feedback temperature control is shown schematically in Figure T-16. As with the passive systems, control is attained by varying the condenser conductance  $G_c$ . But unlike the passive systems which were previously discussed, the condenser conductance is varied to meet the requirement of a constant source

temperature. This is achieved by monitoring the source temperature and then using a signal to adjust the condenser conductance accordingly. A feedback system can operate on any of the parameters which affect the condenser conductance. Referring to Section T. 9.3, feedback control could be achieved by varying either the effective size of the storage reservoir, its temperature, or the mass of the noncondensing gas.

Varying the mass of the noncondensing gas requires a rather complex system. Controlling the effective size of the storage reservoir and/or its temperature is more practical, and several methods have been proposed (5) (41) (36) and also implemented (5) (20) (4) (29).

#### T.9.5.1 Mechanical Feedback

A mechanical feedback system in which the size of the storage reservoir is adjusted in order to control the heat pipe's conductance is shown schematically in Figure T-17. Its theory of operation is given in detail in Reference (6). In principle, the mechanical feedback heat pipe functions as follows. The gas storage reservoir consists of a bellows and its effective volume is therefore determined by the displacement of the bellows. As shown earlier in Section T. 9.3, the heat pipe's conductance is increased if the volume of the reservoir increases. The reservoir volume is controlled by a smaller secondary bellows which contains an incompressible fluid. A capillary tube connects the secondary bellows with a temperature sensing bulb which is located at the component whose temperature is to be controlled (e.g., the heat source). If, for example, the temperature of the heat source increases, the incompressible fluid in the sensing bulb will expand and cause the secondary bellows to also expand. Since the two bellows are mechanically coupled, the volume of the storage reservoir will increase when the volume of the secondary bellows increases. Consequently, the condenser conductance increases since some of the noncondensing gas originally located in the condenser will recede into the enlarged reservoir. When the condenser conductance increases, the heat pipe can reject the operating heat load with a smaller  $\Delta T$  between the source and the sink. Finally, the source temperature will decrease and thus partly compensate for the initial increase which actuated the feedback mechanism. The initial rise in source temperature could have been caused by an increase in either the heat load or the sink temperature. Since the feedback system monitors the source

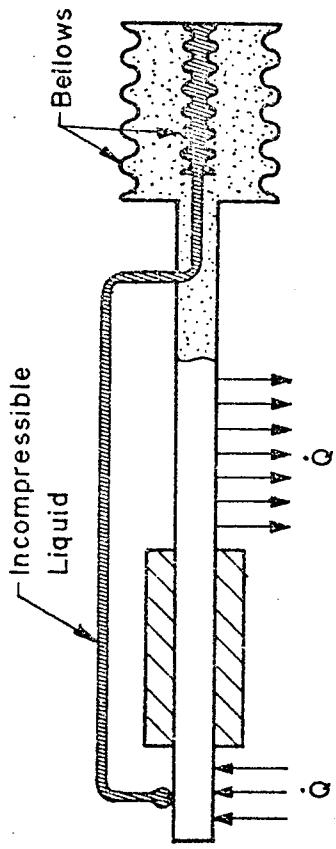


Figure T-17. Mechanical Feedback which Operates on  $V_r$

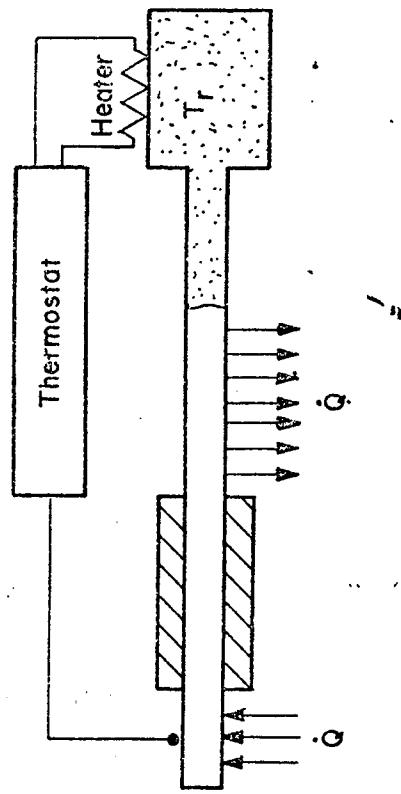


Figure T-18. Feedback which Operates on  $T_r$

temperature rather than the vapor temperature, its control capability is not affected by a low evaporator conductance. However, in order to maintain the source temperature nearly constant for appreciable changes in the heat load, the vapor temperature will actually decrease with increasing heat load and vice versa. This can be seen from Equation T-122 by setting  $dT_s/d\dot{Q}$  equal to zero. Since the evaporator conductance is always positive and assumed to be fixed,  $dT_v/d\dot{Q}$  must be negative in order to achieve a constant source temperature.

The major disadvantage of the mechanical feedback controlled VCHP is in its complexity. The design becomes rather difficult if good temperature control is required. Perfect temperature control is unachievable, although the system's performance is superior to that of a self-controlled VCHP.

#### T.9.5.2 Electrical Feedback

A more practical feedback controlled VCHP is the one shown schematically in Figure T-18. It has a fixed, wicked gas storage reservoir whose temperature is controlled by means of an auxiliary heater. There exists some commonality between this feedback system and the configuration of a self-controlled VCHP which was described in Section T.9.4.3. In both cases, the reservoir temperature is controlled. For the self-controlled VCHP it was sufficient to maintain the reservoir temperature constant. In the feedback system, the reservoir temperature is varied in order to control the source temperature while compensating for the effects of changing heat load and/or sink temperature. In fact, the self-controlled VCHP with constant reservoir temperature makes sense only if the reservoir can be coupled to a readily available constant temperature environment. If the reservoir temperature has to be thermostatically controlled, then the source temperature may just as well be monitored in order to get the benefit of a feedback system without incurring additional complexity.

The characteristic equation relating condenser conductance to reservoir temperature is identical to Equation T-105. If this equation is examined, it is observed that the reservoir temperature affects the conductance in two ways: through the equation of state of the noncondensing gas, and through the partial pressure of the working fluid vapor in the reservoir. The latter effect is usually the predominant one since the

pressure-temperature relationship of a saturated vapor is approximately exponential. Both mechanisms combine to vary the conductance of the condenser by changing the amount of gas which can be stored within the reservoir with the remaining gas flooding a portion of the condenser. If a non-wick reservoir were to be used, only the volume change of the gas would be available for controlling the condenser conductance. This would require unacceptably large variations of the reservoir temperature in order to achieve proper control. It is therefore important to use a wicked reservoir in which the saturated vapor of the working fluid exists.

The useful range of reservoir temperatures is bracketed by the sink temperature  $T_o$  as a lower practical limit and the vapor temperature  $T_v$  as the upper limit. Since the slope of the pressure-temperature relationship of a saturated vapor increases with increasing temperature, best control sensitivity is achieved when the reservoir is operated near the upper limit. Design procedures for feedback controlled VCHP's are presented in Chapter D of this Handbook.

Reservoir temperature control is achieved by using an electric heating element and simultaneously coupling the reservoir to the heat sink. The latter is important since it provides a necessary means for lowering the reservoir temperature. A temperature sensor (e.g., thermocouple, thermistor) is placed near the component whose temperature is to be controlled. The output signal is usually amplified, compared to a reference value, and the resulting error signal (if any) is used to control the input to the electric heating element.

Electric feedback control can provide nearly absolute temperature control since high-gain electronic amplifiers are readily available. It can eliminate the effects of varying sink temperature much more effectively than any self-controlled VCHP or even the mechanical feedback system discussed previously. An additional benefit is that, within limits, compensates for changes in the amount of noncondensing gas in the system. Generation of noncondensing gas (e.g., hydrogen) is one of the major problems in long-term heat pipe reliability. The feedback system will react to an increasing amount of noncondensing gas the same way it would react to a rising sink temperature. It will compensate by lowering the reservoir temperature thus making more storage space available for the gas.

These advantages must be weighed against the added complexity when compared with the simple, passive and self-controlled VCHP. In addition, the inclusion of a heater involves both a power requirement and the loss of inherent system reliability. The decision as to whether to use or not to use a feedback system involves a trade-off between performance requirements, system complexity, availability of control power, and economy.

#### T.9.6 Variable Set Point Heat Pipes

Applications for VCHP's are conceivable in which the temperature set point needs to be variable. The set point is defined as the nominal operating temperature around which the VCHP maintains control. With an electrical feedback system, this can easily be achieved by simply adjusting the reference signal. Self-controlled passive VCHP's maintain the operating temperature of the heat pipe around a set point determined by the gas inventory. Referring to the characteristic Equation T-108, it is seen that for a given geometry, heat load, and environment the vapor temperature (set point) depends on the amount or mass,  $m$ , of the noncondensing gas. Thus, the operating temperature can be raised or lowered by adding or removing gas. This approach would require a complex metering system to precisely control the gas inventory without, at the same time, affecting the working fluid inventory.

Another method of obtaining a variable set point is to keep the gas inventory constant and vary the reservoir volume or temperature. A concept in which the gas reservoir consists of a controllable bellow is shown in Figure T-19. Placing the variable reservoir inside the evaporator provides an easy method of obtaining a near zero pressure differential across the wall of the reservoir.

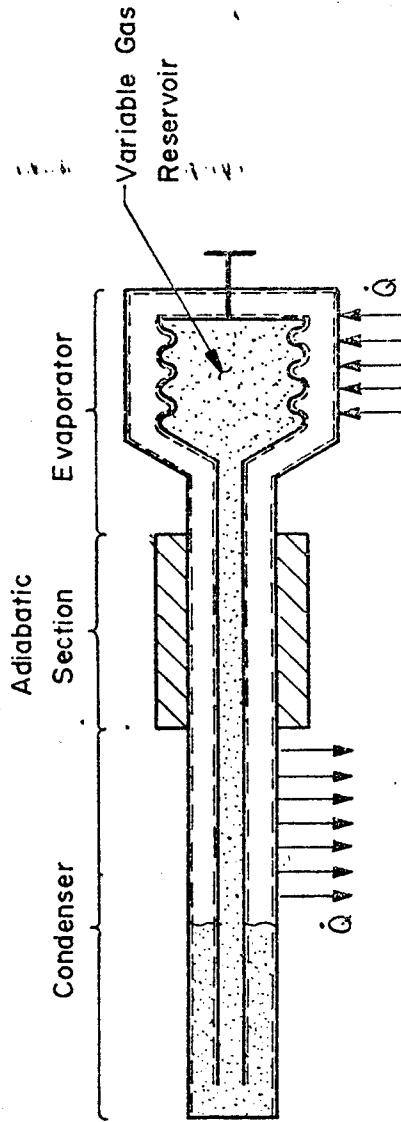


Figure T-19. Self-Controlled VCHP with Variable Set Point

If the characteristic Equation T-108 is examined for the control performance of a VCHP, it is seen that varying the reservoir volume also changes the control sensitivity of the pipe. It was previously shown that the sensitivity with respect to changes in heat load and sink temperature is improved if a large ratio of  $V_r/V_c$  is used. Increasing the set point requires a decrease of  $V_r$  and vice versa. But a decrease of  $V_r$  also reduces the control sensitivity. Thus, if the heat pipe is designed for adequate control sensitivity at the highest set point, a lowering of the set point (increase in  $V_r$ ) will improve the control sensitivity. However, if the set point is to be increased above the original design value, a serious loss in control sensitivity may result.

Varying the reservoir temperature represents another approach that may be employed to achieve set point control. If the reservoir is not wicked, control of the reservoir temperature provides set point control through variations of the gas temperature (see Equation T-118 in combination with Equation T-107). This has the same effect as varying the reservoir volume, since  $V_r$  and  $T_r$  appear in the same term in Equation T-118. The same comments regarding change of control sensitivity which were made when discussing volume control also apply here. In addition, in order to obtain a wide range in set point control, very large variations in gas temperature are required.

If the reservoir is wicked, set point control is provided through variations in both the gas temperature and the partial pressure of the vapor. This amplifies the set point sensitivity and reduces the variations in  $T_r$  necessary to affect changes in the nominal set point. The same comments concerning the change in control sensitivity also apply to the wicked reservoir -- that is, the heat pipe should be designed for adequate control at the highest set point.

From a practical point of view, the wicked system offers a substantially wider range of set point control for a reasonable range in reservoir temperature than does the non-wicked system. However, accurate temperature control of the reservoir usually requires the use of heaters and a thermostat; these are the same basic elements used in an electric feedback system. If the designer is willing to accept this system complexity, he should consider the use of a feedback system which not only offers set point control but also offers greatly improved control sensitivity.

### T.9.7 Active Variable Conductance Heat Pipes

Self-controlled VCHP's are designed to control their own vapor temperature and contain their own built-in control mechanism. Feedback controlled VCHP's also control their own system temperature but the control signal is generated external to the heat pipe. For example, in the electrical feedback system discussed in Section T.9.5, the source temperature is monitored electrically and an electrical input to the reservoir heater actuates the conductance control.

All VCHP's in which the conductance can be controlled by external means (e.g., bellows extension, auxiliary heater power) are not limited to only controlling their own system temperature. The control input can be generated by a number of sources to serve a variety of purposes. The control input can also be manually or automatically programmed to turn the heat pipe on or off at a specified time. The previous group of heat pipes are referred to as "Active VCHP's" since their conductance is subject to active, external control. In principle, any of the parameters listed in Table T-1 can be employed to vary the conductance in accordance with Equation T-105.

### T.9.8 Diffusion Effects

#### T.9.8.1 Flat Front Model

The theory of gas loaded VCHP's presented in the preceding sections is based on a sharp interface (flat front model) between active and inactive portions of the condenser. An ideal distribution does not exist in reality. The actual "front" is controlled by diffusion within the gas-vapor interface and by axial conduction in the wall. A typical diffuse front is shown in Figure T-20. It is seen that the "average" temperature in the inactive part of the condenser is somewhat higher than the sink temperature and that the average partial vapor pressure is higher than that corresponding to the sink temperature. This causes the temperature set point of the VCHP to be higher than predicted by theory for the particular gas inventory.

In non-wick reservoir heat pipes, this effect can be quite pronounced. The partial vapor pressure in a non-wick reservoir is theoretically equal to the partial pressure in the inactive condenser section (see Section T.9.4.2). If the

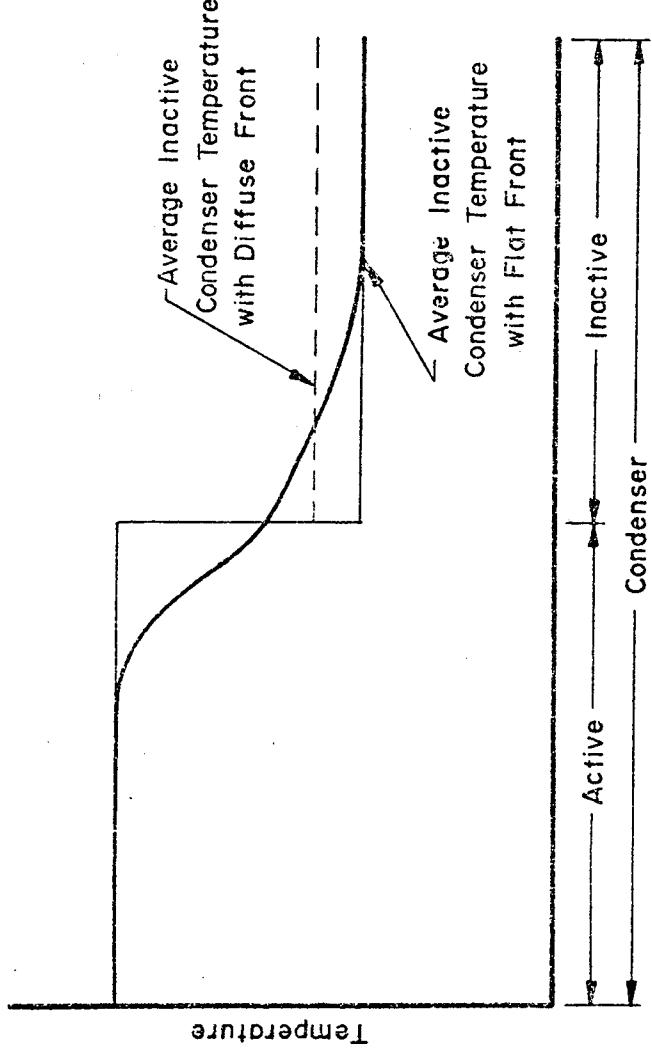


Figure T-20. Temperature Distribution in the Condenser for Flat Front and Diffuse Front Models

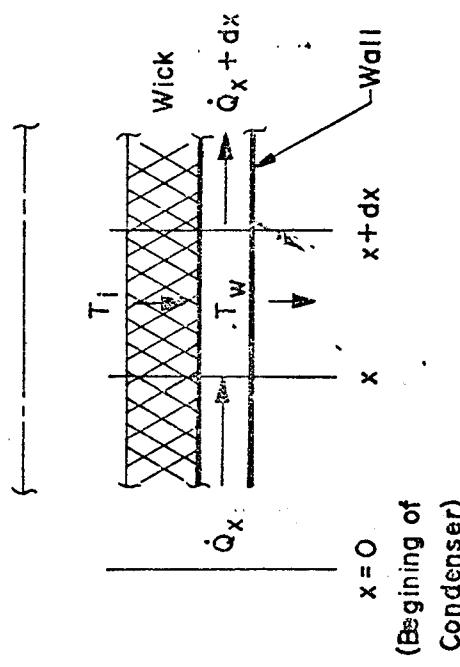


Figure T-21. Model for Derivation of Condenser Heat Balance

interface moves close to the end of the condenser ( $G_c \sim (G_c)_{\max}$ ), the tail of the diffuse front may extend into the reservoir and raise the vapor pressure in the reservoir. The deviation from prediction using the flat front model is more pronounced in a non-wick reservoir heat pipe since the effects of increased partial vapor pressure involve the entire reservoir. Marcus (31) conducted experiments to test the flat front theory. He instrumented a VCHP with an internal non-wick reservoir to measure the actual temperature profiles. Using a theoretical approach, similar to the one presented in Section T.9.3, he computed the vapor temperature as a function of active condenser length. In order to account for the diffuse temperature distribution he integrated the molar gas density along the inactive condenser section using the actually measured temperatures. The agreement between theory and experiment is very good, indicating that the flat front model does predict the control capability of the pipe accurately provided that realistic average temperatures for the inactive portion of the condenser and the reservoir are used.

#### T.9.8.2 Diffuse Front Model

A complete model of the diffuse interface in a gas-loaded heat pipe must include: (1) heat transfer between the condenser and environment; (2) axial conduction in the walls, wicks, and fins; (3) binary mass diffusion between the vapor and gas; and (4) radial wick resistance. The theory of a diffuse gas front is rather complicated, and therefore only the equations which define the model are given here. The method of solution as well as numerical results are given by Marcus (29).

The heat balance for a unit length condenser element is derived from the model shown in Figure T-21:

$$\dot{Q}_x + K(T_i - T_w) dx = \dot{Q}_{x+dx} + S(T_w - T_o) dx \quad T-124$$

$\dot{Q}_x$  is the axial conduction heat flow,  $K$  is the radial conductance through the wick, and  $S$  is the (linearized) conductance between the heat pipe wall and the environment.  $T_i$ ,  $T_w$ , and  $T_o$  are the temperatures of the vapor-wick interface, the wall, and the environment, respectively. The axial conduction heat flow  $\dot{Q}_x$  is related to the axial wall temperature gradient  $dT_w/dx$  through:

$$\dot{Q}_x = -C \frac{dT_w}{dx} \quad T-125$$

where  $C$  is the axial conductivity-area product for the condenser cross-section and includes contributions from the pipe wall, the wick, and any external fins. Equations T-124 and T-125 lead to the following heat balance on an element of the condenser:

$$C = \frac{d^2 T_w}{dx^2} + K (T_i - T_w) - S (T_w - T) = 0 \quad T-126$$

Fick's law of diffusion (7) for a binary mixture of gases yields the following equation for the noncondensing gas (g):

$$N_g = x_g (N_g + N_v) - c D_{g,v} \frac{dx}{dx} \quad T-127$$

where  $N_g$  and  $N_v$  are the molar fluxes of the gas and the vapor,  $x_g$  is the mole-fraction of the gas,  $c$  is the molar density of the mixture, and  $D_{g,v}$  is the mass diffusivity. The first term in Equation T-127 accounts for the flux associated with the bulk mass flow, while the second term represents the flux resulting from the diffusion superimposed on the bulk flow.

Conservation of mass of the noncondensing gas requires that:

$$N_g = 0 \quad T-128$$

The local mass flow rate of the vapor is related to its molar flux through:

$$\dot{m}_v = A_v M_v N_v \quad T-129$$

The molar density  $c$  can be found from the ideal gas law:

$$p_v = c R_o T_i \quad T-130$$

Where  $p_v$  is the total system pressure which is independent of the location  $x$ . Combining Equations T-127 through T-130 yields the following expression for the mass diffusion equilibrium:

$$\frac{p_v}{R_o T_i} D g_v A_v M_v \frac{d \ln x_g}{dx} = \dot{m}_v \quad T-131$$

Conservation of mass of the condensable vapor requires that the change in the mass flow rate  $\dot{m}_v$  is equal to the condensation rate which, in turn, is equal to the internal heat transfer rate divided by the heat of vaporization:

$$\frac{d \dot{m}_v}{dx} = K (T_i - T_w) / \lambda \quad T-132$$

Equations T-126, T-131, and T-132 form a set of three simultaneous differential equations in the three unknowns:  $T_w$ ,  $x_a$ , and  $\dot{m}_v$ . The internal temperature  $T_i$  is related to the partial pressure of the vapor  $(1 - x_g) p_v$  through the vapor pressure curve. Several assumptions were tacitly made in deriving the above equations:

- The partial pressure of the vapor is always in equilibrium with the temperature  $T_i$
- No radial gradients exist
- Energy transport due to the sensible heat is negligible
- The binary mixture obeys the Ideal Gas Law

The above equation may be solved using the appropriate boundary conditions. At the beginning of the condenser, the concentration of the noncondensing gas is zero.

$$x_g = 0 \quad \text{at} \quad x = 0 \quad T-133$$

The total heat rejected may serve as another boundary condition:

$$\dot{Q} = \int_0^{l_c} S (T_w - T_o) dx \quad T-134$$

Alternately, the fixed amount of noncondensing gas may be used as a boundary condition. Marcus (29) observes that theoretically two more conditions must be specified since Equation T-126 is of the second order. However, in the case of high radial wick conductance, several simplifying assumptions can be made and the two boundary conditions, Equations T-133 and T-134, suffice.

The preceding discussion indicates the general approach for analyzing a diffuse vapor-gas interface. The equations are sufficiently complex that closed form solutions are out of the question. Numerical solutions have been obtained which provide general information about several effects associated with a diffuse vapor-gas interface.

#### T.9.8.3 Numerical Analysis of Diffuse Vapor-Gas Front

Marcus (29) reports the results of a parametric study which evaluates the effects of wall conductivity, working fluid, and operating temperature on the vapor-gas interface. The computer program used in his analysis is based on a model similar to the one described in the preceding Section T.9.8.2.

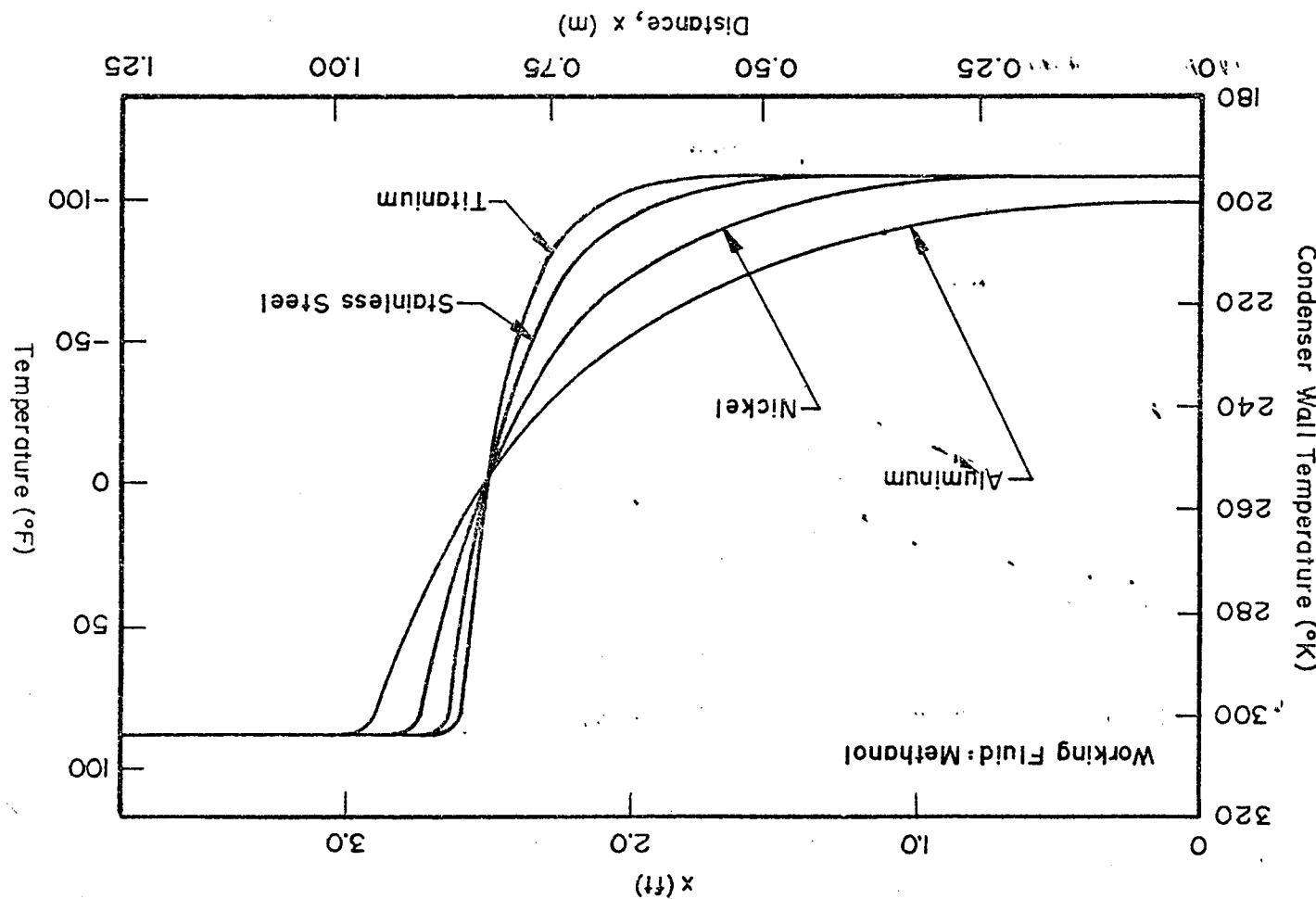
The results can be summarized as follows:

- Axial conduction in the pipe wall plays a substantial role in defining the vapor-gas interface. Typical temperature profiles along the condenser are shown in Figure T-22. One clearly sees that wall conductance tends to spread the front over the condenser.
- The effect of working fluid on the temperature profiles is insignificant (Figure T-23). This suggests that heat transport by mass diffusion is minimal and that axial conduction dominates.
- The operating temperature does not significantly alter the profile of the vapor-gas interface. Typical curves are shown in Figure T-24.

The above results are typical for heat pipes for spacecraft temperature control. There is no reason to believe that other gas controlled heat pipes would not exhibit the same qualitative behavior.

One important conclusion can be drawn from the numerical analysis. Since heat transport by mass diffusion appears to be insignificant when compared to axial conduction, the temperature profile in the vicinity of the interface is determined to

Figure T-22. Effect of Axial Wall Conduction on the Condenser Temperature Profile



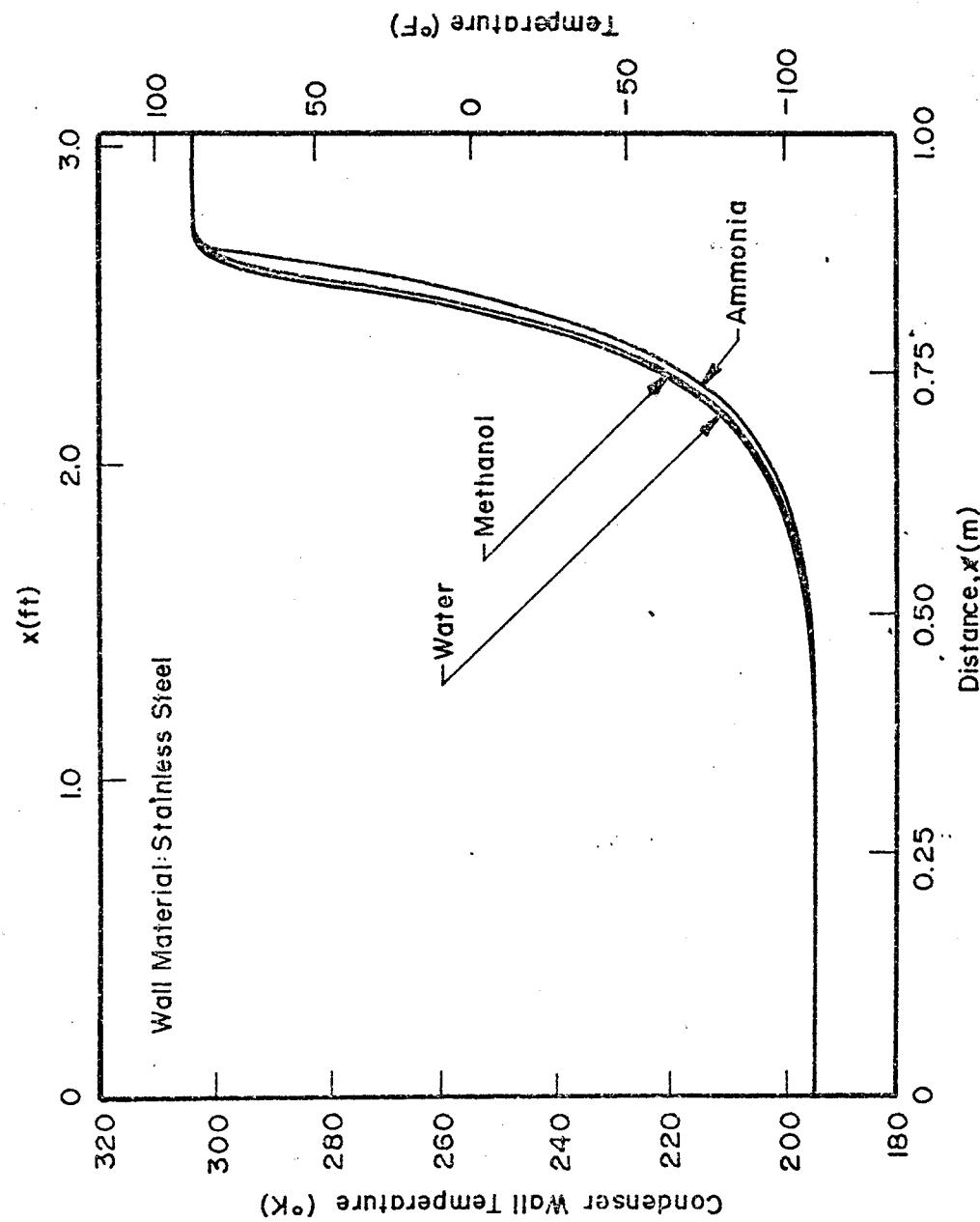


Figure T-23. Effect of Working Fluid on the Condenser Temperature Profile

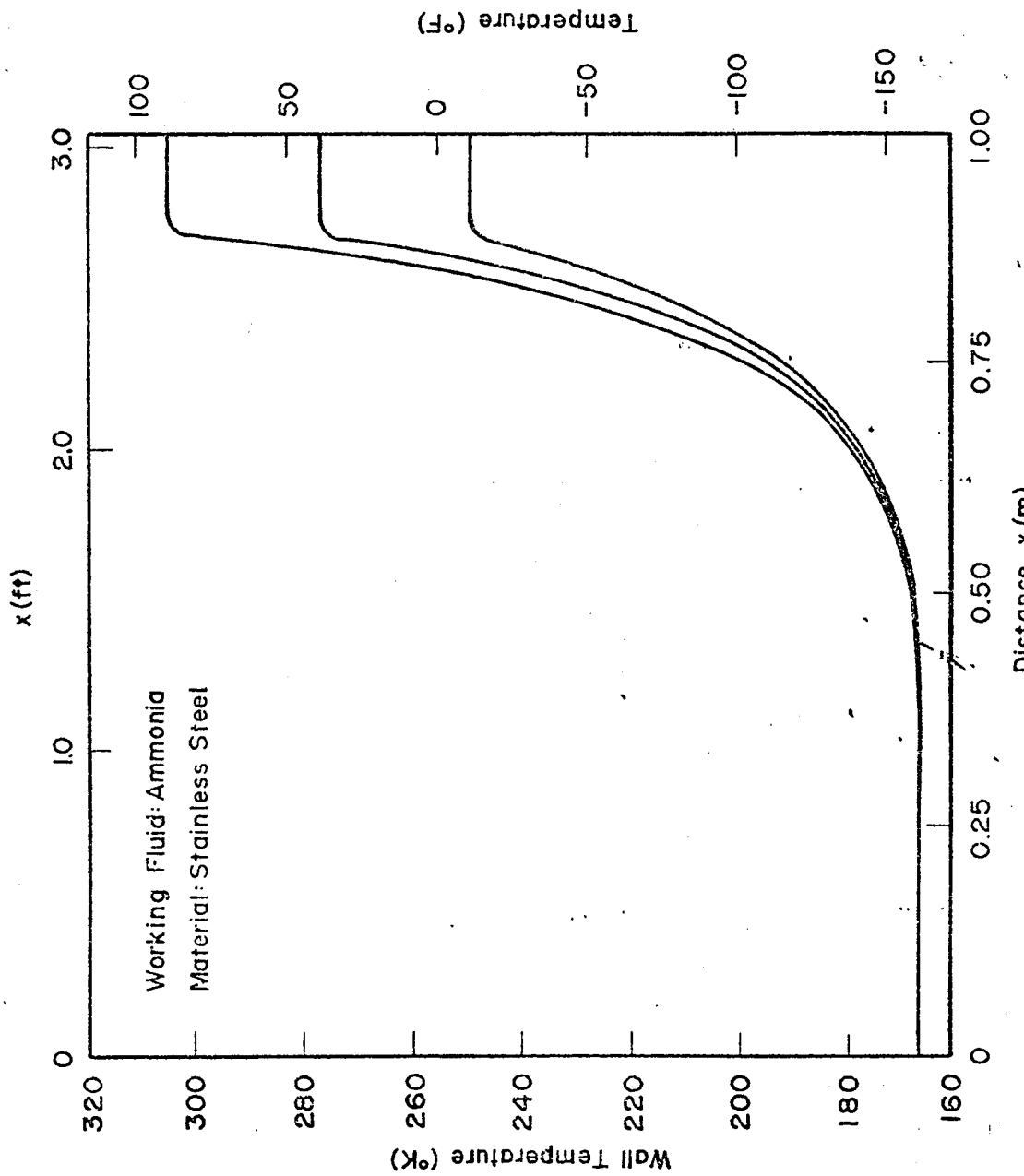


Figure T-24. Effect of Operating Temperature on the Condenser Temperature Profile

a first approximation by conduction and by heat transfer to the environment. Thus, a conventional "fin" equation (25) will, in most cases, adequately describe the temperature profile along the heat pipe.

The flat front model predicts the conductance of the heat pipe satisfactorily (Section T.9.8.1), in particular, if a realistic temperature profile is used to calculate the effective condenser temperature. Treating the inactive portions of the condenser as a fin provides an excellent approximation of the temperature profile and represents a first order refinement to the flat front model.

The detailed computer analysis provides information which cannot be obtained using the simple closed-form solution. An important example of this is the determination of the freeze-out rate of the working fluid. If the sink temperature is below the freezing point of the working fluid, a finite amount of vapor will continuously diffuse into that region and freeze there. Eventually this effect will result in a deficiency of working fluid and cause a hydrodynamic failure. The computer solution predicts the rate at which working fluid is lost.

#### T.9.8 Notes on Transients

The performance of heat pipes during transients is only partially understood at the present time. This is particularly true for VCHP's which represent control elements within a thermal system. A detailed discussion of transient behavior is beyond the scope of this Handbook but a summary of the salient points is presented.

The transient performance of conventional heat pipes has been discussed by several investigators (12) (13) (37) (22) (23). This work has been concerned primarily with the start-up dynamics at low temperatures and low vapor pressures. The results apply equally well to VCHP's, although here the problems associated with start-up are somewhat mitigated because the presence of a noncondensing gas does not permit the circulation of the working fluid at low pressures. Transient discussions of the various types of VCHP's can be divided into three groups -- that is, wicked reservoir, non-wicked reservoir, and feedback controlled VCHP's.

### T.9.9.1 Wicked Reservoir Heat Pipes

In wicked reservoir heat pipes, the partial pressure of the vapor everywhere in the system is in equilibrium with the local wick temperature. Diffusion effects may be neglected except for establishing the vapor-gas interface. The transient behavior of wicked reservoir VCHP's can therefore be adequately described by considering the sensible heat capacities of the various heat pipe elements and the conductances between them. The position of the vapor-gas interface is assumed to be in equilibrium at all times with the pressure and temperature distributions. Consequently, transient behavior can be predicted using ordinary thermal modeling techniques.

### T.9.9.2 Non-Wicked Reservoir Heat Pipes

In a non-wicked reservoir VCHP, the partial vapor pressure in the reservoir is established by diffusion. The length of the diffusion path between the nearest point of saturation, i. e., the end of the condenser and the reservoir, may be long and diffusion rates often dominate the transient response. The transient theory of non-wicked reservoir heat pipes is by no means fully developed. An excellent survey of the present state of development is given in Reference 29.

Another phenomenon which is peculiar to non-wicked reservoir VCHP's is the mechanism for removal of liquid working fluid from the reservoir. Ordinarily, the non-wicked reservoir contains only noncondensing gas and some working fluid vapor. Liquid may accidentally be spilled into the reservoir, as for example either as a result of handling or as a result of vibrations during launch. If the spillage occurs during handling, the bulk of the liquid can usually be removed by proper orientation. If this happens during launch and is then immediately followed by a zero "g" environment, no such removal mechanism exists. In either case, some liquid will remain in the reservoir. Under these conditions, when the heat pipe is started up, the vapor pressure in the reservoir will correspond to the saturation pressure of the liquid at the reservoir rather than the condenser temperature. Since the reservoir temperature is always higher than the condenser temperature, some of the gas will be forced out of the reservoir and the VCHP set point will be changed. In the extreme case, corresponding to a reservoir temperature equal to the evaporator temperature,

all of the gas will be forced out. Since the reservoir volume normally exceeds the condenser volume, the latter will be completely blocked and serious overheating of the heat source may result. These abnormal conditions will prevail until the liquid is evaporated from the reservoir and recaptured by the wick.

### T.9.9.3 Feedback Controlled VCHP's

Feedback systems exhibit a rather complex transient behavior. These systems contain all the elements of a typical control loop and are subject to the same performance characteristics. Unlike other VCHP's, feedback systems can possess unstable regimes in which oscillations may occur. Thermal feedback systems are more stable than are electrical feedback systems. There is no thermal equivalent to electrical inductance; and, unlike passive electrical systems, thermal systems suffer damping losses. The stability of feedback VCHP's should be established for each application.

Closely related to stability is the existence of "overshoot" and "undershoot" of the control parameter. A typical response for a feedback controlled VCHP, in which the source temperature is controlled, is shown in Figure T-25. Changes in the heat load and/or in the sink temperature cause the source temperature to temporarily deviate from the set point. As illustrated, the feedback system regains control and the set point is restored.

A lumped parameter model of a heat pipe feedback loop is presented in Reference 4 which shows that the response of the heat source is controlled by the following two time constants:

$$T_r = m_r C_{p,r} R_r \quad T-135$$

$$T_s = m_s C_{p,s} R_s \quad T-136$$

where  $m_r$  and  $C_{p,r}$  are the mass and the lumped specific heat of the reservoir, and  $m_s$  and  $C_{p,s}$  are the mass and the lumped specific heat of the heat source.  $R_r$  is the thermal resistance between the reservoir and the sink, and  $R_s$  is the thermal resistance between the heat source and the heat pipe evaporator. The response time is

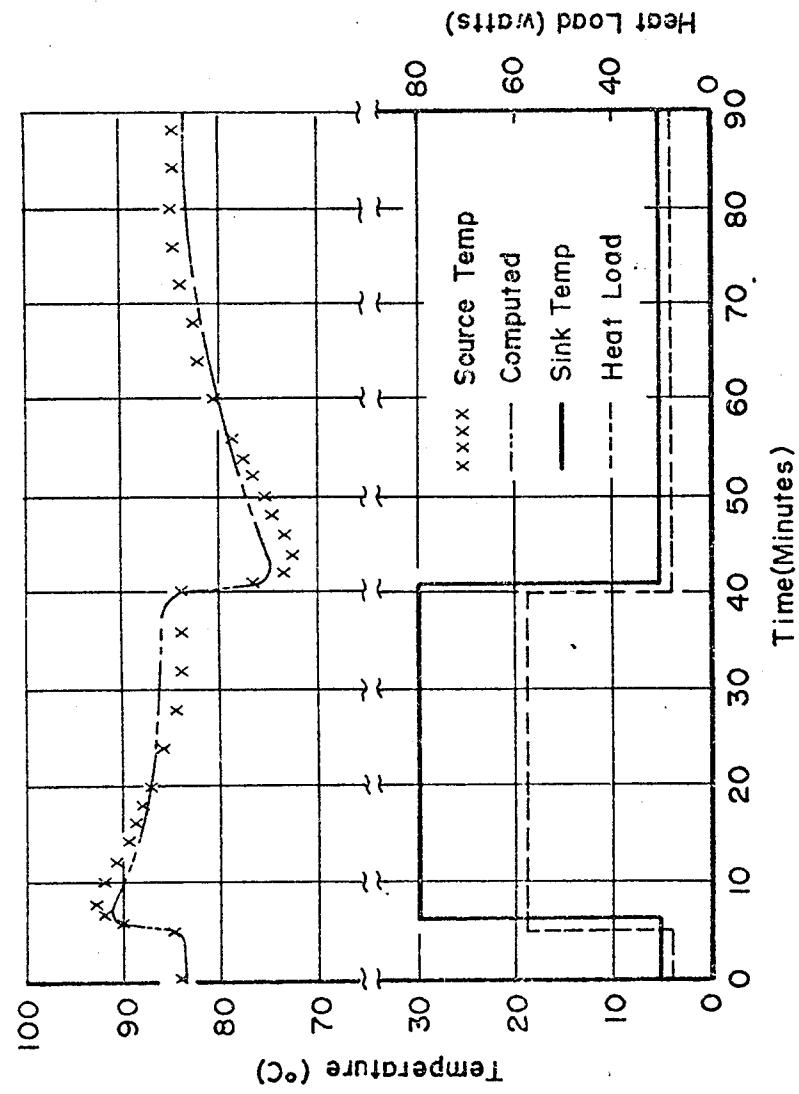


Figure T-25. Transient Response of Heat Source with Electrical Control

minimized if the ratio  $\tau_r / \tau_s$  is small. Since the time constant of the heat source is frequently determined by the application, the only available alternative is to make  $\tau_r$  as small as possible. The most desirable method of minimizing  $\tau_r$  is to minimize the heat capacity  $m_r$  of the reservoir. By closely coupling (thermally) the reservoir to the sink (small  $R_r$ ), a reduction in the reservoir time constant can be achieved but is generally undesirable since it increases the auxiliary power required to maintain the reservoir at the selected temperature during steady state operation.

#### T.9.10 Other Variable Conductance Techniques

Most of the investigative work on VCHP's has been concentrated on the technique of flooding the condenser with a noncondensing gas. This concentration is primarily due to the simplicity of such a VCHP. Many heat pipes which were never intended to be VCHP's inadvertently became variable as a result of the generation of noncondensing gas due to impurities or corrosion.

Other techniques for controlling a heat pipe's conductance have been proposed, but the theoretical and experimental work performed is limited. Every technique has its own unique control characteristics, and some requirements may be better met with one or more of the techniques discussed in the following sections.

##### T.9.10.1 Condenser Flooding with Liquid

This technique is closely related to noncondensing gas control. Variable conductance is achieved by inactivating part of the condenser by using an incompressible liquid. The most conveniently available liquid is the working fluid. The system is illustrated in Figure T-26.

Excess working fluid is contained in a reservoir which is located inside the heat pipe envelope. The effective volume of the reservoir is varied by means of a bellows which contains an auxiliary fluid in equilibrium with its vapor. Expansion of the bellows forces liquid working fluid out of the reservoir and into the condenser. This technique provides self-control of the source temperature; that is, increasing the heat load and/or the sink temperature causes the conductance to increase and this has the effect of minimizing the tendency for the source temperature to change.

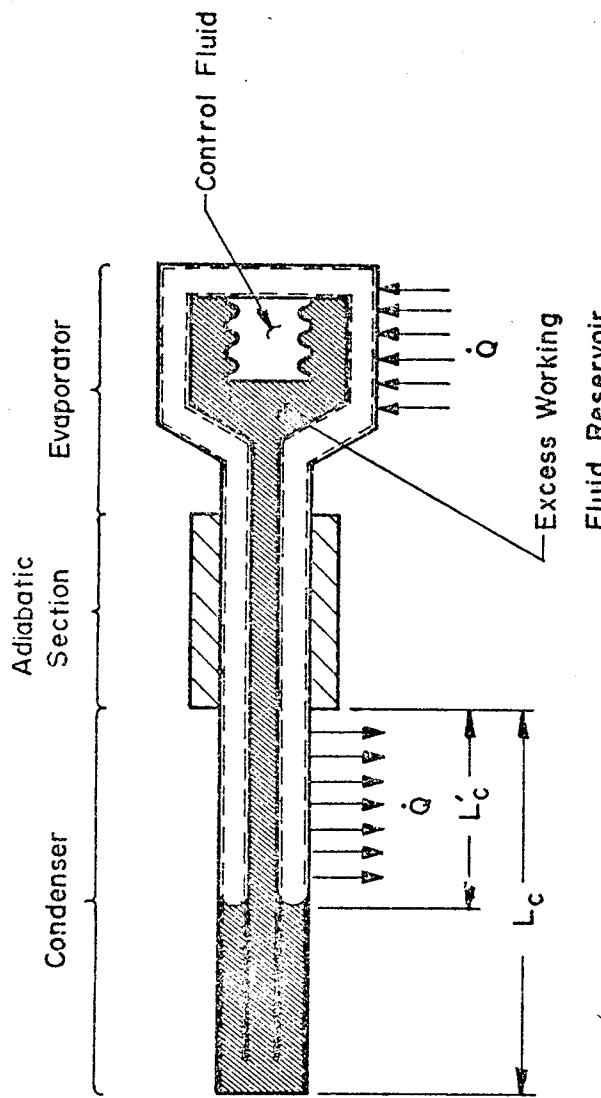


Figure T-26. Variable Conductance Through Condenser Flooding with Liquid

The control characteristics can be developed using a model similar to the one in Section T.9.4. Assuming that the fraction of the working fluid occupied by the wick and the vapor space is approximately constant (or negligible as in the case of the vapor), conservation of mass of the excess working fluid requires:

$$V_{ex} = V_r - V_b + A_c (L - L_c') \quad T-137$$

where  $V_r$  is the sum of the volumes of the reservoir and the capillary tube,  $V_b$  is the volume of the bellows containing the auxiliary control fluid, and  $V_{ex}$  is the volume of the excess fluid. Because the excess fluid is in the liquid state, conservation of mass corresponds to conservation of volumes. The volume occupied by the bellows ( $V_b$ ) is related to pressure difference between the working fluid and the auxiliary fluid through:

$$V_b = V_{bo} + \frac{A_b^2}{k} (p_a - p_v) \quad T-138$$

where  $V_{bo}$  is the equilibrium volume of the bellows,  $A_b$  is the bellows area, and  $k$  is the bellows spring rate.

Combining Equations T-137 and T-138 together with Equations T-98 and T-104 yields the following expression for the normalized condenser conductance:

$$\frac{G_c}{(G_c)_{\max}} = 1 - \frac{V_{ex} - V_r + V_{bo}}{V_c} + \frac{A_b^2}{k V_c} (p_v - p_a) \quad T-139$$

It is shown in Section T.9.4 that the sensitivity of the vapor temperature to the changes in  $\dot{Q}$  and  $T_o$  can be expressed in terms of two parameters,  $S$  and  $S'$ . The characteristic equations are:

$$\frac{dT_v}{d\dot{Q}} = \left( \frac{1}{G_c} \right) \frac{1}{1+S} \quad T-109$$

$$\frac{dT_v}{dT_o} = (1) \frac{1-S'}{1+S} \quad T-110$$

Using the definitions for  $S$  and  $S'$ , Equations T-111 and T-112 give for the present case:

$$S = \frac{T_v - T_o}{G_c} \frac{A_b^2}{k V_c} \left( \frac{\partial p_v}{\partial T_v} - \frac{\partial p_a}{\partial T_v} \right) \quad T-140$$

and

$$S' = 0 \quad T-141$$

According to Equations T-109 and T-110, condenser flooding with excess liquid thus attenuates fluctuations of  $\dot{Q}$  and  $T_o$  by the same amount. Because of the incompressibility of the liquid, the system is less sensitive to changes in the sink temperature as seen by the disappearance of the degrading parameter  $S'$ . Good control is achieved (large  $S$ ) if:

- The cross-sectional area of the bellows is large.
- The spring rate of the bellows is small.

- The slope of the vapor pressure curve of the working fluid is larger than that of the auxiliary fluid.

In addition to providing an insensitivity to changes in the sink temperature, temperature control using excess working fluid generally requires smaller storage reservoirs; and the interface between vapor and liquid is not subject to the diffusion effect as is the case in a gas-controlled heat pipe. These system advantages must be weighed against some disadvantages. Gravity tends to cause the excess fluid to puddle in the condenser rather than form a well-defined interface as shown in Figure T-26. In addition, the sink temperature must always be above the freezing point of the working fluid because the inactive part of the condenser will be approximately at sink temperature and freezing would form a solid plug preventing any further control. Finally, the excess liquid inventory may make the system heavier than a comparable gas-controlled VCHP.

#### T.9.10.2 Liquid Flow Control

Liquid flow control involves either interrupting or impeding the condensate return in the wick in order to partially dry out the evaporator (3). Because this technique invokes a partial hydrodynamic failure of the heat pipe, it is not a very desirable one. Furthermore, it is only applicable to temperature stable heat sources where the amount of heat removed by the heat pipe is controlled by the evaporator resistance. If this is not the case, a partial dry-out will cause the temperature along the dry evaporator section to continue to increase.

#### T.9.10.3 Vapor Flow Control

Interrupting the vapor flow between evaporator and condenser will result in a pressure difference in the vapor and, because of saturation conditions, a corresponding temperature difference. For a given axial heat flow rate, varying the temperature difference is equivalent to varying the heat pipe's conductance (Section T.8). The principle of this technique is shown schematically in Figure T-27. The vapor flow can be modulated by an external signal, e.g., the current of the electromagnet in Figure T-27; or the system can be self-controlled as shown in Figure T-28 (17).

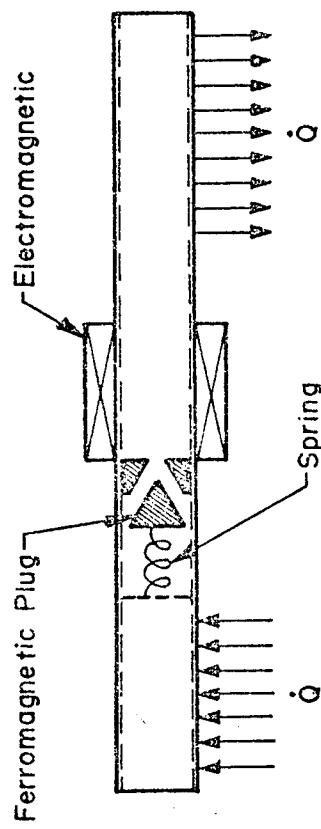


Figure T-27. Vapor Flow Control Using External Signal

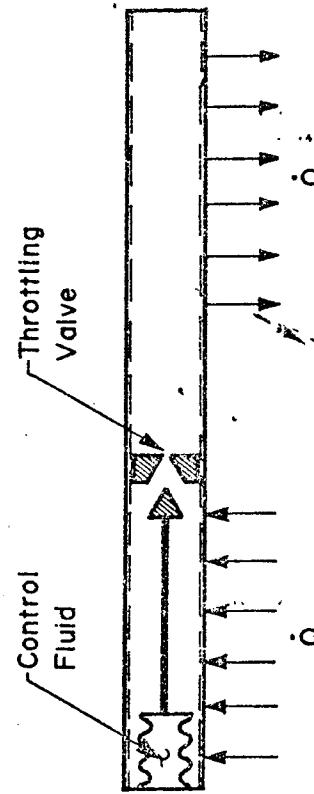


Figure T-28. Self-Controlled VCHP (Vapor Flow Control)

Vapor control represents a direct method of varying the axial conductance of the heat pipe. It does not, as all other techniques, render part of the condenser or evaporator ineffective. The entire evaporator and condenser are isothermal during all modes of operation since the pressure and temperature differential occurs across the throttle mechanism.

This obvious advantage is partially offset by the limited control range. The pressure difference created by the throttle must never exceed the capillary pressure of the wick. If the capillary pressure is exceeded, the vapor will "bubble" through the wick and around the throttle and the control capability will be lost. In a vapor flow-controlled heat pipe, the wick must be capable of providing sufficient capillary pressure to overcome the hydrodynamic losses and the pressure difference created for control purposes. From a hydrodynamic point of view, the wick must therefore be overdesigned.

The temperature difference which corresponds to a given pressure difference is obtained from the Clausius-Clapeyron equation (33).

$$\frac{\Delta T_v}{\Delta p_r} = -\frac{T}{\lambda \rho_v} \quad T-142$$

In order to achieve large temperature differences (large variations of the conductance) with small pressure differences, the vapor density of the working fluid should be low. Vapor control is most effective if a fluid is selected which has a low vapor pressure at the operating temperature.

D.1 Introduction

The theory of heat pipe operation developed in Chapter T.0 treats the various performance characteristics in general terms. Proper heat pipe design procedures dictate that the theory must be applied in accordance with established methodologies. The methodology of heat pipe design is summarized in Figure D-1. Prior to determining the best heat pipe design, the designer must assure himself that the heat pipe is, in fact, the best choice considering non-heat pipe design alternatives. In order to make this initial evaluation the designer must have a clear understanding of the limitations of heat pipes.

This chapter is subdivided into four parts. Problem Definition and Design Criteria describes the approach the designer uses in defining the application problem, and it discusses the design criteria for conventional and variable conductance heat pipes. Performance Limit Evaluation identifies those characteristics of heat pipes which have defined limits; these limits cannot fall within the specified design requirements of the selected heat pipe. Conventional Heat Pipe Design Procedures outlines the working fluid, wick design, container design, and fluid charge selection processes which are required in order to arrive at a reference design. Finally, Variable Conductance Heat Pipe Design addresses the problems peculiar to the gas-controlled heat pipe.

D.2 Problem Definition and Design Criteria

In order to take advantage of the unique properties of the heat pipe, several general criteria must be examined before proceeding with the detailed design of heat pipes for specific applications. The first objective of the designer should be to establish the relative advantages of the heat pipe as compared to other methods of heat transfer. Once the justification for the use of a heat pipe has been established, it is then necessary for the designer to establish, in detail, the thermal performance and design constraints for the heat pipe for the specific application.

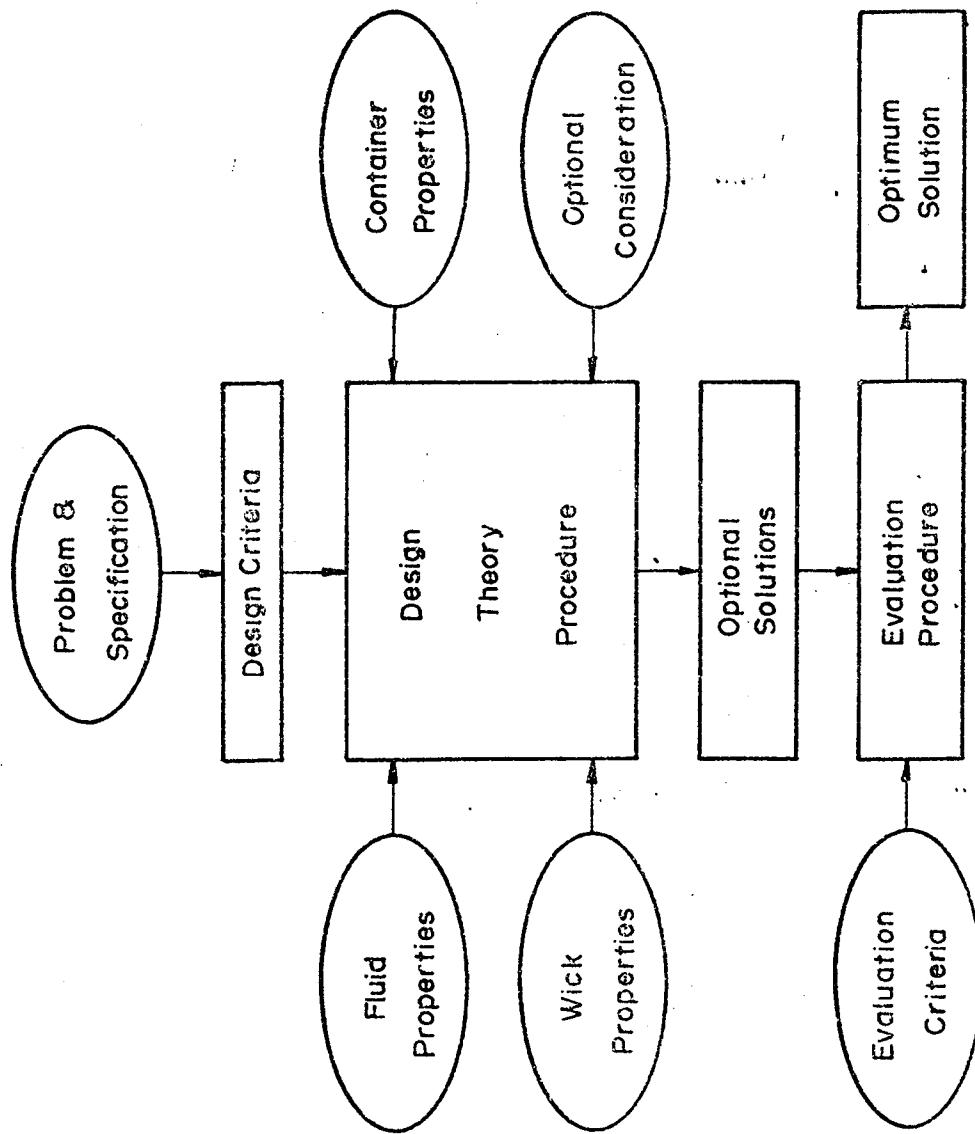


Figure D-1. Methodology of Heat Pipe Design

#### D.2.1 Problem Definition

The essential first step in the application and design of a heat pipe is to establish that the heat pipe is the best suited of the various alternatives for the particular heat transfer problem under consideration. While this may be an obvious statement, such a determination is not always easily discernible. Whatever the heat transfer problem may be, it is highly probable that a heat pipe can be designed to satisfy the requirements. However, the heat pipe may not be the only or the best design alternative.

Alternate design solutions generally fall into one of two categories: static systems (conductive, radiative, or convective heat transfer) or dynamic systems (forced-flow fluid heat transfer). While it is not the objective of this Handbook to discuss these alternatives, the designer should be aware of the merits and shortcomings of the heat pipe relative to other heat transfer systems which may be applied to his particular problem. To understand fully the advantages which may be gained and the penalties which must be paid with a heat pipe system requires a comprehensive knowledge of the capabilities of the heat pipe, an awareness of the alternatives available, and a basic understanding of the particular requirements of the application. As an aid toward developing this understanding, the pertinent properties of the heat pipe are listed in Table D-1. The following generalized discussion, in which are compared the relative merits of the heat pipe with respect to conductive heat transfer and forced-flow fluid heat transfer, provides examples of the types of trade-off studies required.

##### D.2.1.1 Heat Pipe vs. Conductive Heat Transfer

A statement which is often found in the literature is: "a heat pipe has an effective thermal conductance which is hundreds of times larger than that of a solid copper rod of identical cross-section and length." The designer must realize that this statement is true only where the heat transfer path is "sufficiently long". For example, consider the following problem:

Example D-1: Two highly temperature-sensitive electronic components, one located 2.54 cm (1 inch) and the other 15.24 cm (6 inches) from a heat sink, must be maintained as close as possible to the heat sink tem-

Table D-1. Summary of Conventional Heat Pipe Properties

- High Effective Thermal Conductance
- Nearly Isothermal Over Its Entire Length
- Capable of Variable Conductance
- Low Thermal Capacitance
- Lightweight
- External Pumping Power Not Required
- Mechanically Passive
- Reliable
- Noiseless
- Speed at Which Heat is Transported is Equal to the Velocity of the Vapor

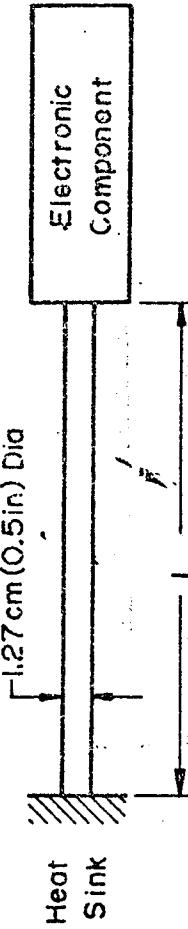


Figure D-2. Heat Transfer Model Considered in Example D-1

perature. Each component dissipates 10 watts of heat. Because of space limitations, the heat transfer path must not exceed 1.27 cm (1/2 inch) in diameter and the interfacing for heat transfer is limited to the circular ends of the tubular heat transfer element as illustrated in Figure D-2.

Weight is not a problem; therefore, either a heat pipe or a solid copper rod can be considered. The questions to be answered are: which design best meets the objective for the short heat transfer path, and which one best meets the objective for the longer heat transfer path?

Solution to Example D-1: The thermal conductivity of copper is approximately  $3.8 \text{ W/cm}^2\text{-K}$  ( $220 \text{ Btu/Hr-Ft}^2\text{-}^{\circ}\text{F}$ ). Typical heat pipes used in electronic cooling have evaporator and condenser film coefficients of  $.86 \text{ W/cm}^2\text{-K}$  ( $1500 \text{ Btu/Hr-Ft}^2\text{-}^{\circ}\text{F}$ ). The temperature drop in the vapor can usually be neglected. Based on the allowable 1.27 cm (1/2 inch) envelope diameter, the evaporator and condenser areas are both  $1.2 \text{ cm}^2$  ( $0.195 \text{ inch}^2$ ). For a heat load of 10 watts, the following temperature drops between the component and heat sink are calculated:

<u>Length of Heat Path (L)</u>	<u>Temperature Drop (<math>\Delta T</math>)</u>
2.54 cm (1 inch)	<u>Copper Rod</u> $5.2^{\circ}\text{C}$ ( $9.4^{\circ}\text{F}$ )
15.24 cm (6 inches)	<u>Heat Pipe</u> $31.3^{\circ}\text{C}$ ( $56.4^{\circ}\text{F}$ ) $8.6^{\circ}\text{C}$ ( $15.4^{\circ}\text{F}$ )

Therefore, the copper rod offers better performance for the electronic component located 2.54 cm ( $\frac{1}{2}$  inch) from the heat sink; whereas, the heat pipe is superior for the component located 15.2 cm (6 inches) from the heat sink.

The above example serves to illustrate one of a number of trade-off studies which must be made between heat pipes and thermal conductors. Other requirements which must often be considered in trade-off studies are weight, reliability, and cost. In general, the heat pipe will favor a lighter weight system but one which is more expensive and somewhat less reliable than a thermal conductor. Finally, depending on the requirements of the application, there are three heat pipe properties which must be considered:

1. The heat pipe is nearly isothermal (internally, the vapor temperature drop is negligible) and a thermal conductor is not. This feature of the heat pipe is often used to maintain the temperature uniformity between components and to increase the efficiency of heat transfer surfaces (radiative and convective).
2. By the introduction of a noncondensable gas, the heat pipe can be made to regulate component temperature under conditions of varying heat loads and/or sink temperatures.
3. The heat pipe represents a low thermal mass system which can be beneficial during periods of start-up, shut-down, and system transients.

#### D.2.1.2 Heat Pipe Vs. Forced Flow Systems

A generalized comparison of a forced flow system with a heat pipe is more restrictive than a comparison of a thermal conductor with a heat pipe. The designer should be aware, however, that major differences do exist between the heat pipe and a forced flow system. Both systems rely on the circulation of a fluid to transfer heat, but this is where their similarity stops. Pumping of the fluid in a heat pipe is achieved through capillary action which does not require moving parts or an external power supply. These features provide the heat pipe with a distinct advantage over a forced flow system for many applications (especially for spaceflight systems). Since electrical power supplies, bulky pumps, and accumulators are not required, the heat pipe represents a significantly lighter heat transport system. The simplicity of a heat pipe, heat transport system, combined with the ease with which system redundancy can be achieved, results in significant weight and reliability advantages.

While the simplicity of capillary pumping offers many advantages, the pumping power developed is very small. Therefore, the performance of the heat pipe is sensitive to its orientation in gravity and acceleration fields. These fields normally do not affect the performance of forced flow systems. Additionally, the heat pipe cannot transport as much heat over very long distances as can be transported by forced flow systems. This limitation, the Heat Transport Capability Factor ( $QL$ )<sub>max</sub> (see

Section T-6), is illustrated by the following example:

Example D-2: For a large spacecraft (e.g., Skylab) it is required to transfer 1000 watts of heat from a compartment on the sun side to a space radiator on the shade side. The vehicle diameter is approximately 9.1 meters (30 feet). The designer is asked to provide either a heat pipe or a forced flow system (independent of any existing system) to satisfy this requirement.

Solution to Example D-2: The designer has the option of using a heat pipe formed into a 9.1 meter (30 feet) diameter hoop as illustrated in Figure D-3a. Each half of the hoop must carry 500 watts over 1/2 the circumference -- a distance of approximately 14.3 meters (46.9 feet). Therefore, the required Heat Transport Factor  $\dot{Q}_L$  is  $7.15 \times 10^3$  watt-m ( $2.8 \times 10^5$  watt-in). Conventional heat pipes of 1.25 cm (1/2 inch) diameter (grooves or wire mesh) have Heat Transport Capability Factors ( $\dot{Q}_L$ )<sub>max</sub> in the order of 76 watt-m ( $3 \times 10^3$  watt-in). Therefore, 100 heat pipes of the conventional design are required. High performance heat pipes, such as those containing arteries, have potential Heat Transport Capability Factors in the order of  $2.5 \times 10^3$  watt-m ( $1.0 \times 10^5$  watt-in). Arterial heat pipes, although still developmental, would reduce the number of heat pipes required to three.

The non-heat pipe system alternative is to use a forced flow system. The required performance can be achieved using this system. The penalties attending the use of a forced flow system are those associated with dynamic systems, where each system element must have a high degree of reliability. Normally, the desired level of reliability in a dynamic system is obtained by providing redundancy; and this further complicates the system and increases its weight and cost. Redundancy in a heat pipe system can be provided either by over-designing the heat pipes to provide margin for single pipe failure or by providing additional heat pipes so that the failure of one or more heat pipes will not make the heat transport system unable to perform the heat removal function.

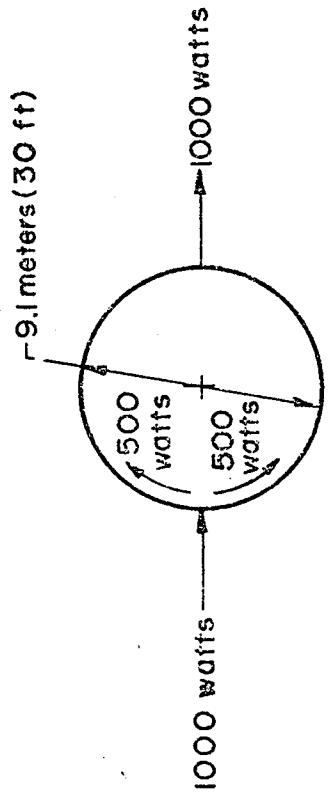


Figure D-3a. Heat Transfer Model for Example D-2

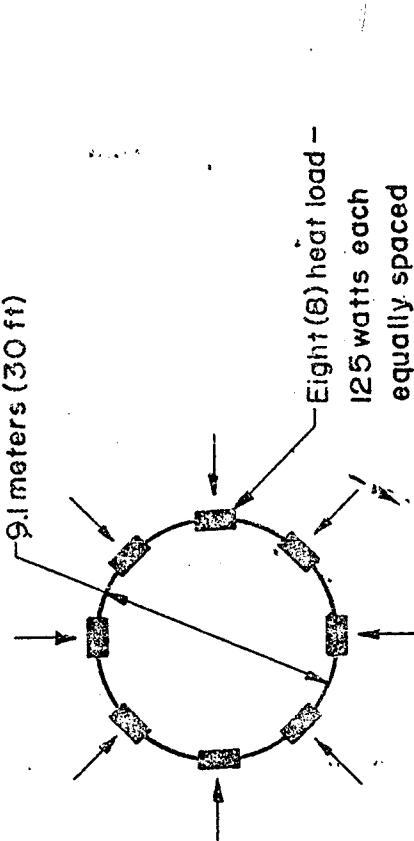


Figure D-3b. Heat Transfer Model for Example D-3

Example D-3: Consider another example--the case where the total heat specified in Example D-2 is divided into eight equal discrete loads (Figure D-3b). These loads are to be equally spaced over the circumference of the spacecraft. It is the objective, in this application, to uniformly spread the heat over the entire circumference in order to obtain efficient heat rejection to space.

Solution to Example D-3: In this case, the heat pipe must be capable of transporting 1/2 of each discrete load over 1/32 of the circumference. Therefore, the Heat Transport Factor  $\dot{Q}_L$  required is 56 watt-m ( $2.2 \times 10^3$  watt-in) (1/128 the requirement of Example D-2). As can be seen in this case, a single heat pipe would satisfy the requirement. Because of its simplicity, low weight, good reliability, and low cost, the heat pipe would, in this example, be the definite choice over a forced flow system.

#### D.2.1.3 Heat Pipe as a Temperature Control System

In addition to transporting heat, a variable conductance heat pipe can be used to provide temperature control. The choice of a variable conductance heat pipe over conventional thermal control methods (thermal coatings, louvers, forced fluid systems, etc.) depends on the requirements of the specific application. The choice of the type of variable conductance heat pipe which should be employed depends on the degree of temperature control required, the thermal environment, the heat load, the transient behavior, and the mode of operation (e.g., variable conductance, switch, or diode). The applicability of the various types of gas-controlled heat pipes as determined by their ability to control temperature is summarized in Table D-2. The mode of operation will very often influence the method used to achieve temperature control. As an example, liquid blockage can be used to accomplish rapid turn-down for diode operation.

#### D.2.2 Design Criteria

Once the heat pipe has been selected for a specific application, the basic performance parameters must be established before any design effort can be initiated. These parameters include operating temperature range, heat load requirements,  $\Delta T$

Variable Conductance Type	Applicability
Cold-Wickied Reservoir	Limited temperature control; useful for applications where heat load varies and where sink temperature is relatively constant.
Hot-Non-Wickied Reservoir	Good temperature control; useful for applications where relatively long start-up times can be tolerated.
Controlled Wickied Reservoir	Good temperature control; limited to applications where a relatively large reservoir can be tolerated or where the additional system complexity of auxillary heaters and a controller is acceptable.
Feedback Controlled	Absolute temperature control; limited to applications which require precise temperature control and which therefore justify the requirement for a controller.

Table D-2. Applicability of Gas-Controlled Heat Pipes

performance, heat load/heat sink interfacing requirements, and overall size, weight and geometry limitations. In addition to these basic performance requirements, design and operational constraints associated with testing, operational limits under gravitational or acceleration loads, mechanical interfacing, storage and operational lifetimes, pressure containment specifications, toxicity requirements, and provisions for structural support must also be established.

In order to organize and document these requirements, a specification should be prepared. This specification should be thorough and complete since it will be the document used for the design, development, and test efforts. A listing of the requirements which may be included in the heat pipe specification and the impact of these requirements on the heat pipe design are given in Table D-3. These requirements are treated in more detail in the following sections.

#### D.2.2.1 Operating Temperature Range

This requirement represents the primary constraint on the selection of the working fluid. Freezing point and critical temperature define the limits for the useable temperature range of a fluid; but, in practice, the useful temperature range must be well within these limits. For variable conductance heat pipes, the size of the reservoir and the system's response is determined by the selection of the operating temperature range for a particular fluid.

#### D.2.2.2 Thermal Load

To fully define this requirement it is necessary to specify the total thermal load to be handled and the number, magnitude, and location of discrete loads which make up the total load. This requirement in combination with the transport length determines the minimum size of the heat pipe and the type of wick design. The magnitude of the heat load and the required degree of temperature control determine the type, the size of the storage reservoir, and the response characteristics of the variable conductance heat pipe.

#### D.2.2.3 Transport Length

The transport length is the net distance over which the heat must be

Requirement	Impact on Heat Pipe Design
Operating Temperature Range	Choice of Working Fluid; Pressure Retention
Thermal Load	Heat pipe size, number of heat pipes, wick design, and choice of working fluid
Transport Length	Wick Design
Temperature Uniformity and Overall $\Delta T$	Evaporator and condenser design, conductive path length trade-off, heat pipe geometry
Physical Requirements	Size, Weight, and Geometry
Acceptance & Quality Testing	"One-G" environment operation and correlation with "Zero-G" operation
Ground Testing	Degrees of freedom in orientation, limits on operation during testing
Dynamic Environment	Operation under acceleration loads, structural integrity
Thermal Environment	Pressure retention during non-operating temperature cycles
Man Rating	Pressure Vessel Code; Fluid Toxicity
Mechanical Interfacing	Mounting provisions, provisions for thermal interfacing
Transient Behavior	Choice of working fluid, wick design, variable conductance type
Reliability	Leak tightness requirements, material compatibility, processing care and control, redundancy

Table D-3A. Summary of Design Criteria for a Conventional Heat Pipe

Requirement	Impact on Heat Pipe Design
Variation in Heat Load	
Variation in Heat Sink Condition	Choice of working fluid, size of reservoir, type of variable conductance heat pipe required
Control Sensitivity	

Table D-3B. Summary of Additional Criteria for Variable Conductance Heat Pipes

transported. This requirement in combination with the thermal load determined the capillary pumping requirements which, in turn, determine the wick design.

#### D.2.2.4 Temperature Uniformity and Overall $\Delta T$

The distribution of heat producing components, their power density, and the geometry of the ultimate heat sink will materially affect the degree of temperature uniformity which is achieved and the overall  $\Delta T$  of the heat pipe. The required temperature uniformity and the required overall  $\Delta T$  constrained by specifics of the application will be the determining factors in the selection of the evaporator and condenser designs. The power density of any single/multiple thermal load will determine the limit, if any, on boiling within the wick in the evaporator areas.

#### D.2.2.5 Physical Requirements

Size, weight, and geometry limitations specified by the application, when considered with the specified performance requirements, must be such that a practical heat pipe design can be obtained.

#### D.2.2.6 Acceptance and Qualification Testing

Thermal performance testing of the heat pipe is normally performed in a one "g" environment. It is necessary, therefore, to establish test criteria which will best simulate the actual in-service acceleration conditions. For heat pipes to be used in a zero "g" environment, test criteria must include the need to avoid excessive capillary pumping against gravity, minimization of contributions to the thermal performance due to "puddling", and the recognition that excess fluid will form a fluid slug in the condenser during zero "g" and detract from thermal performance.

#### D.2.2.7 Ground Testing

For space application, pre-launch operational verification is normally required. To achieve this, the orientation of the heat pipe within the spacecraft must be considered. A heat pipe designed with a minimum limitation on orientation is most desirable. This requirement must be traded off against overall thermal performance in a zero "g" environment.

## D.2.2.8 Dynamic Environment

Because capillary forces are relatively small, operation of a heat pipe under acceleration loads is limited. The frequency and nature of acceleration loads must be defined and imposed as operational constraints on the heat pipe if heat removal is required under these conditions. In addition, the heat pipe may be subjected to a dynamic environment; and the heat pipe must be designed to withstand these dynamic loads.

### D.2.2.9 Man Rating

For application to manned systems, heat pipes must be free of hazards. Toxicity of the working fluid, working fluid vapor pressure, and containment pressure retention capability are additional constraints which must be placed on the heat pipe design.

### D.2.2.10 Thermal Environment

In operation, the heat pipe will be subjected to a well-defined temperature range. In addition, throughout handling, storage, and system integration the heat pipe may be subjected to temperatures other than those occurring during normal operating conditions. Failure in the total system may result in excessive heat pipe temperatures. These potentially excessive temperature environments must be designed for. In the case of variable conductance heat pipes, the thermal environment will influence the reservoir size, the choice of working fluid, and the selection of the type of variable conductance heat pipe.

### D.2.2.11 Mechanical Interfacing

To achieve good thermal interfaces, it is first necessary to define the mechanical interfacing requirements. Surface flatness and finish of thermal interfaces have a strong influence on temperature gradients and on the evaporator and condenser performance. Interface filler materials improve the performance of mechanical interfaces; however, restrictions are often imposed on their use for space applications because of the outgassing associated with many of these materials.

#### D.2.2.12 Transient Behavior

Start-up is best accomplished by using a working fluid which is initially saturated. When this is not possible, as in the case of many cryogenic or liquid metal heat pipes, the wick should be designed to give good transport during the priming operation. When a variable conductance heat pipe is required, the transient behavior will depend to a large extent on the type employed and the choice of the working fluid.

#### D.2.2.13 Reliability

Two failure mechanisms impose limitations on the life of any heat pipe -- these are noncondensing gas generation and working fluid leakage. The life of the heat pipe is defined as the total time span from the time of final pinch-off of the heat pipe to the time at the end of mission life. This total time span determines the minimum leak-tightness requirement. Determination of the leak-tightness requirement is critical since heat pipes operate on a very small fluid inventory, and small leaks over the total time span can cause the heat pipe to become inoperable.

The working fluid must be compatible with the container and wick materials in order to avoid generation of noncondensable gases. For extended life requirements, even extremely small rates of noncondensable gas generation can be detrimental. This is especially true for heat pipes which have very small condenser regions. Noncondensable gases are swept from the evaporator to the condenser region; and, when sufficient gas is generated, condenser blockage can result.

#### D.2.2.14 Temperature Sensitivity

The degree of temperature control required will often determine the type of variable conductance technique which must be employed. Cold-wick reservoirs VCHP's can provide adequate temperature control for moderate heat load and sink temperature variations. A feedback controlled VCHP is capable of providing absolute temperature control for very severe variations of heat load and sink temperatures. For any variable conductance pipe, the required degree of temperature control will affect the choice of the working fluid and the reservoir size.

### D.3 Performance Limit Evaluation

Once the justification for using a heat pipe has been established and the performance requirements have been clearly defined, the designer must then select the design best suited to the application. At this time, the design effort can either take the form of evaluating existing designs to determine their suitability to the current application or of developing a new design specifically tailored to the requirements of the application.

The theory developed in Chapter T provides the background for performing evaluations and developing designs. The limits on heat pipe performance that were identified are:

- Capillary Pumping Limit
- Sonic Limit
- Entrainment Limit
- Heat Flux Limit

The capillary limit is the most commonly encountered limit; therefore, the designer will normally address most of his time to its evaluation. Generally, evaluation of the other three limits will not be necessary if:

- $M \lesssim 0.2$  (Sonic Limit - See Section T.7.1)\*
- $We < 1.0$  (Entrainment Limit - See Section T.7.2)

$$\bullet \frac{q t_w}{K_{\text{eff}}} = \frac{q}{h} < \Delta T_{\text{crit}} \quad (\text{Heat Flux Limit - See Section T.7.3})$$

Should any one of these conditions not be satisfied then that particular limit must be evaluated separately. If more than one limit exists for any particular case, then it must be determined which limit occurs first in order to be able to establish the maximum capability of the heat pipe. Application of the theory to determine these limits, consequences that may be expected when these limits are approached, and what can

---

\* If  $M < 0.2$  the computed error in pressure variations due to neglecting compressibility is less than one percent (12).

be done to the heat pipe design to avoid these limits are discussed in the following paragraphs.

### D.3.1 Capillary Heat Transport Limit

The Capillary Heat Transport Limit occurs when the hydrodynamic and hydrostatic losses in the heat pipe exceed the capillary pumping capability of the wick. Exceeding this limit results in local dryout of the wick in the heat input (evaporator) region and in a corresponding temperature rise of that region. In addition to permitting the heat source to rise in temperature beyond specifications, this temperature excursion can result in total heat pipe failure if temperatures are reached which are in excess of those which can be tolerated by the containment vessel material. If the temperature rise does not result in total heat pipe failure, the heat pipe will recover when the conditions causing inadequate capillary pumping are corrected. That is, this mode of failure of a heat pipe is reversible unless it results in a secondary failure which is non-reversible.

In most applications, temperature excursions which result from heat pipe failure cannot be tolerated because of the detrimental effects this has on system components. Therefore, the designer should incorporate adequate safety margins in the heat pipe design. To do this, it is first necessary for the designer to determine the Capillary Heat Transport Limit. To establish this limit, the designer may find it convenient to categorize the heat pipe in any one of the following three groups -- each with corresponding solutions which vary in complexity.

#### D.3.1.1 Category 1. General - One-Dimensional Heat Pipe

This is the broadest of the three categories. The relationships expressed here apply to any heat pipe design which has one-dimensional flow characteristics. The capillary pressure of the wick is given by:

$$\Delta P_{cap} = \frac{2 \sigma \cos \theta}{r_p} \quad D-1$$

The maximum permissible interfacial pressure difference (adjusted for the perpendicular

component of gravity) is:

$$(\Delta p_i)_{\max} \leq \frac{2 \sigma \cos \theta}{r_p} - \rho_1 g D \cos \beta \quad D-2$$

The local, axial heat flow rate is determined from:

$$\dot{Q}(x) = \int_0^x \dot{q}(x) dx \quad D-3$$

The axial pressure gradient in the liquid is given by:

$$\frac{dp_1}{dx} = \frac{\mu_1 \dot{Q}(x)}{K A_w \rho_1 \lambda} - \rho_1 g \sin \beta \quad D-4$$

The axial pressure gradient in the vapor for the various limits indicated is given by Equations D-5 through D-8:

$$\frac{dp_v}{dx} = - \frac{32 \mu_v \dot{Q}(x)}{D_{h,v} \frac{2}{A_v} \rho_v \lambda} \quad \text{for} \begin{cases} \bullet Re_r \approx 0 \\ \bullet \text{laminar vapor flow} \end{cases} \quad D-5$$

$$\frac{dp_v}{dx} = - \frac{32 \mu_v \dot{Q}(x)}{D_{h,v} \frac{2}{A_v} \rho_v \lambda} \left[ 1 + \frac{3}{4} Re_r - \dots \right] \quad \text{for} \begin{cases} \bullet Re_r < 1 \\ \bullet \text{laminar vapor flow} \end{cases} \quad D-6$$

$$\frac{dp_v}{dx} = - \frac{s \pi \dot{Q}(x)}{D_{h,v} \frac{2}{A_v} \rho_v \lambda^2} \quad \text{for} \begin{cases} \bullet Re_r \gg 1 \\ \bullet \text{laminar vapor flow} \end{cases} \quad D-7$$

$$\frac{dp_v}{dx} = - \frac{0.156 \mu_v^2}{D_{h,v} \frac{2}{A_v} \rho_v} Re^{7/4} \quad \text{for} \begin{cases} \bullet Re_r \approx 0 \\ \bullet \text{turbulent vapor flow} \end{cases} \quad D-8$$

The maximum interfacial pressure difference is:

$$(\Delta p_i)_{\max} = \int_{x'}^{x''} \left[ \frac{dp_v}{dx} - \frac{dp_1}{dx} \right] dx \quad D-9$$

The integration in Equation D-9 is extended between the points of minimum and maximum interfacial pressure difference. The step procedure for evaluating the Capillary Heat Transport Limit is as follows:

1. Calculate the net axial heat flow rate using Equation D-3.
2. Calculate the axial pressure gradients in the liquid and the vapor using Equations D-4 through D-8.
3. Determine the interfacial pressure difference  $\Delta p_i(x)$  using Equation D-10.

$$\Delta p_i(x) = \int_0^x \left[ \frac{dp_v}{dx} - \frac{dp_l}{dx} \right] dx + \text{Constant} \quad \text{D-10}$$

Find the axial location  $x'$  for the lowest value of  $\Delta p_i$  and the location  $x''$  for its highest value.

4. Compute  $(\Delta p_i)_{\max}$  from Equation D-9.
5. Use Equation D-2 to determine if the required  $(\Delta p_i)_{\max}$  is less than or exceeds the maximum permissible value for the particular wick.
- \* 6. If the inequality expressed by Equation D-2 is met, the wick design will provide the required capillary pumping. Otherwise a new wick design must be chosen and this procedure must be repeated.

#### D.3.1.2 Category 2. Special - One-Dimensional Heat Pipe

This category assumes that the wick properties are constant along the length of the heat pipe, that the vapor flow is laminar, that the vapor is incompressible, and that momentum effects are negligible. Many heat pipe design cases fall into this category. No limits are placed on the distribution of heat inputs and outputs,  $\dot{q}(x)$ ; and the heat pipe may have any number of bends and may be oriented arbitrarily with respect to any acceleration field.

---

\* As a minimum, the designer should add a safety factor of about 1.5 to the required capillary pumping in order to achieve a practical wick design.

The governing Equations D-1, D-2, and D-3 apply to this category. The maximum interfacial pressure difference assumes the following simplified form:

$$(\Delta p_i)_{\max} = -C \int_{x'}^{x''} \dot{Q}(x) dx + \int_{x'}^{x''} \rho_1 g \sin \beta dx \quad D-11$$

where the constant C is defined as:

$$C = \frac{32 \mu_v}{\rho_v A_v D_{h,v} \lambda} + \frac{\mu_1}{K A_w \rho_1 \lambda} \quad D-12$$

The following step procedure can be used to evaluate the Capillary Heat Transport Limit of heat pipes which fall into this category:

1. Establish that the one-dimensional model applies and that the wick and the heat pipe properties are constant along the entire length of the heat pipe.
2. Verify that momentum changes due to evaporation and condensation are negligible. This will be true if:

$$Re_r = \frac{\dot{q}_{\max}}{2 \pi \mu_v \lambda} \ll 1 \quad D-13$$

where  $\dot{q}_{\max}$  is the largest heat input or output.

3. Calculate the net axial heat flow rate  $\dot{Q}(x)$  using Equation D-3. Obtain maximum value of  $\dot{Q}(x)$  and verify that the vapor flow is laminar ( $Re \ll 2200$ ) and incompressible ( $M < 0.2$ ).
4. Determine the interfacial pressure difference  $\Delta p_i(x)$  as follows:

$$\Delta p_i(x) = -C \int_0^x \dot{Q}(x) dx + \int_0^x \rho_1 g \sin \beta dx \quad D-14$$

Find the axial location  $x'$  for the lowest value of  $\Delta p_i$  and the location  $x''$  for its highest value.

5. Compute  $(\Delta p_i)_{\max}$  from Equation D-11.

6. Continue as in Category 1 (Steps 5 and 6).

The following general comments may aid the designer in performing the above evaluation. The first problem is that of evaluating the heat pipe where the overall size is established but the ratio of vapor-to-liquid space must be determined. As a starting point for computing the Mach and the Reynolds numbers, the vapor area  $A_v$  can be assumed to be one-half of the total internal cross-sectional area of the heat pipe. Once the final size of the wick is established and if in the process the vapor area was further reduced then the Mach and Reynolds numbers should be rechecked.

Another time saving step is to perform a quick check to determine whether the wick will be able to satisfy the body forces. If the elevation of the highest heat pipe point (with respect to the acceleration field) is greater than the static capillary pumping height of the wick, then the capillary pumping limit will be exceeded irrespective of any heat input. The static capillary pumping height is defined as:

$$h_{\max} = \frac{2\sigma \cos \theta}{r_p \rho_1 g} \quad D-15$$

In order to accurately determine the Capillary Heat Transport Limit for practical heat pipe designs in specific applications a computer analysis must be performed. This is because the magnitudes and locations of heat sources/heat sinks and the effects of acceleration influence the locations of the maximum and the minimum interfacial pressure differences. The following example problem is an illustration of how the designer can determine the Capillary Heat Transport Limit of a heat pipe which has a non-standard geometry.

Example D-4: Consider the heat pipe design shown in Figure D-4. It consists of a U-shaped tube having two vertical legs and one horizontal leg.

Solution to Example D-4: In order to simplify the analysis, assume that evaporator and condenser sections are located near the very end of the two legs (corresponding to a situation where heat is applied and removed through the end caps). Assume that the three legs are of equal

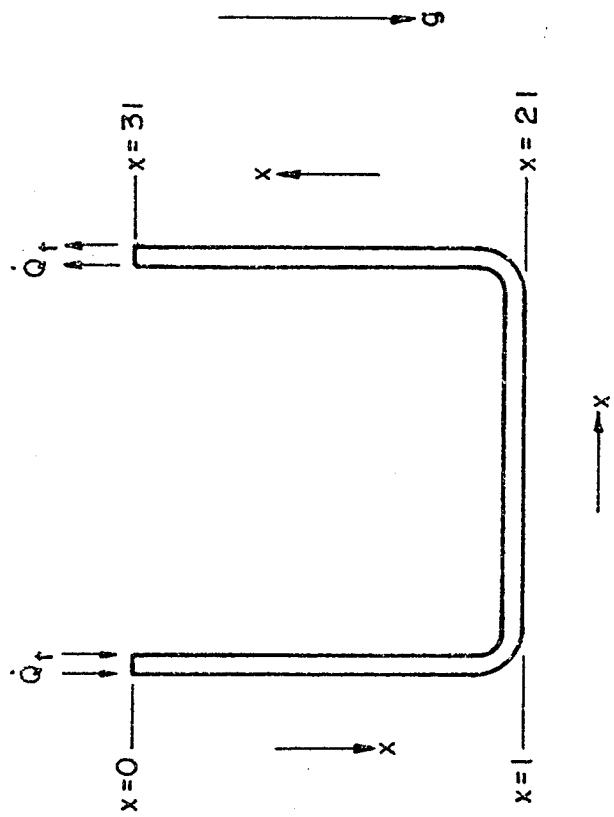


Figure D-4. Schematic Representation of U-Shaped Heat Pipe

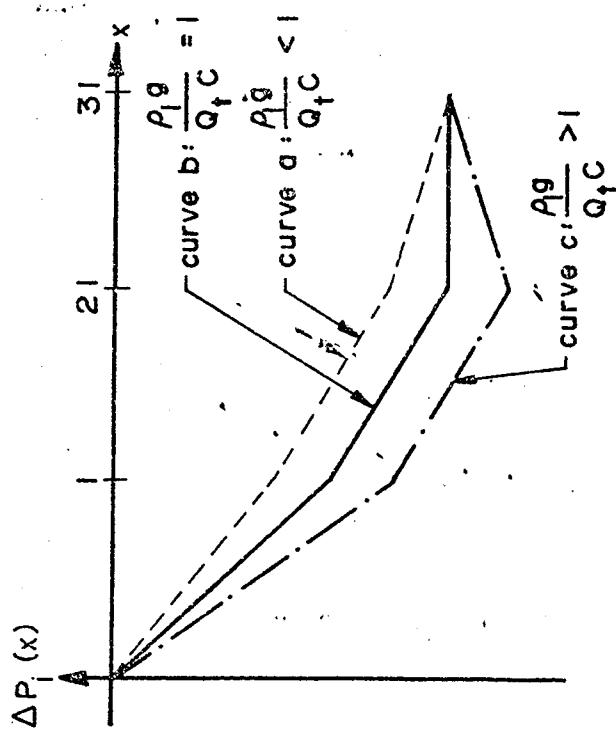


Figure D-5. Variations of  $\Delta P_i$  in U-Shaped Heat Pipe

length. The  $x$  coordinate is located as shown. The axial heat flow rate  $\dot{Q}(x)$  and the orientation  $\beta(x)$  are then as follows:

$$\begin{aligned}
 \text{Left Leg} &: 0 < x < 1 & \dot{Q}(x) &= \dot{Q}_t & \sin \beta &= -1 \\
 \text{Center Leg} &: 1 < x < 2 & \dot{Q}(x) &= \dot{Q}_t & \sin \beta &= 0 \\
 \text{Right Leg} &: 2 & 1 < x < 3 & 1 & \dot{Q}(x) &= \dot{Q}_t & \sin \beta &= +1
 \end{aligned}
 \quad \text{D-14}$$

The interfacial pressure difference  $\Delta p_i(x)$  may be calculated from Equation D-14.

$$\begin{aligned}
 \text{Left Leg} &: \Delta p_i(x) = -C \dot{Q}_t x - \rho_1 g x & 0 < x < 1 & & & \\
 \text{Center Leg} &: \Delta p_i(x) = -C \dot{Q}_t x - \rho_1 g 1 & 1 < x < 2 & 1 & & \text{D-17} \\
 \text{Right Leg} &: \Delta p_i(x) = -C \dot{Q}_t x + \rho_1 g (x - 3) & 2 & 1 < x < 3 & 1 & \text{D-18}
 \end{aligned}$$

The next step is to locate the points of maximum and minimum interfacial pressure difference. In the left and center leg, the slope of  $\Delta p_i(x)$  versus  $x$  is everywhere negative. In the right leg, it is negative, zero, or positive depending on whether the ratio  $\rho_1 g / C \dot{Q}_t$  is less than, equal to, or larger than one. The variation of  $\Delta p_i$  with respect to  $x$  is shown schematically in Figure D-5. It is seen that the highest value of  $\Delta p_i$  is always located at  $x = 0$ . The location of the lowest value of  $\Delta p_i$  depends on the relative magnitude of body force  $\rho_1 g$  and viscous flow losses  $C \dot{Q}_t$ . The maximum interfacial pressure difference  $(\Delta p_i)_{\max}$  can now be found for each of the three regimes:

$$\left. \begin{aligned}
 \frac{\rho_1 g}{C \dot{Q}_t} &< 1 & x' = 3 & 1, x'' = 0 & (\Delta p_i)_{\max} &= 3 & 1 C \dot{Q}_t \\
 \frac{\rho_1 g}{C \dot{Q}_t} &= 1 & x' \text{ undetermined, } x'' = 0 & & (\Delta p_i)_{\max} &= 3 & 1 C \dot{Q}_t \\
 \frac{\rho_1 g}{C \dot{Q}_t} &> 1 & x' = 2 & 1, x'' = 0 & (\Delta p_i)_{\max} &= 2 & 1 C \dot{Q}_t \\
 & & & & & & + \rho_1 g 1
 \end{aligned} \right\} \quad \text{D-19}$$

After  $(\Delta p_i)_{\max}$  has been found the remaining parts of the design procedure are straightforward.

The important point demonstrated by this example is that the locations of the minimum and the maximum interfacial pressures may depend on the relative magnitude of gravity and viscous forces. If gravity is very small,  $\Delta p_i(x)$  decreases steadily from one end of the heat pipe to the other. For this case, the contribution of gravity in the two legs cancel each other and the maximum value of  $\Delta p_i$  is exactly what it would be without gravity.

If gravity is large, the point of minimum  $\Delta p_i$  shifts to  $x = 2L$ . The right leg of the heat pipe now acts as a refluxer. In the intermediate case where  $\rho_1 g = C \dot{Q}_t$ , the interfacial pressure difference in the right leg is constant since gravity and viscous losses exactly cancel each other.

#### D.3.1.3 Category 3. Special - Closed Form Solutions

Closed form solutions for the Capillary Heat Transport Limit could not be determined for heat pipes in the previous two categories because the locations of the maximum and the minimum interfacial pressures were dependent on the combined effects of the heat flow rate  $\dot{Q}(x)$  and the body forces. Closed form solutions may be found for special cases where the conditions imposed on Category 2 obtain and where:

- Gravitational forces are absent
- Or, where the limits of integration  $x'$  and  $x''$  are independent of  $\dot{Q}(x)$

Two special cases -- a heat pipe operated in zero gravity (Case #1) and a straight heat pipe operated in a gravity field with one evaporator and one condenser each located at opposite ends and which is operated with the evaporator elevated above the condenser (Case #2) -- are of special interest because a large majority of all heat pipes are covered by these two cases.

For the cases for which closed form solutions may be found, it is convenient to define two useful parameters.

- $\dot{Q}L =$  Heat Transport Factor which is determined by the requirements of the application.

- $(\dot{Q}L)_{\max} = \text{Heat Transport Capability Factor which is determined by the design of the heat pipe and represents its maximum heat transport capability.}$

Both parameters have the dimension of heat flow rate  $\dot{Q}$  (watts) times a length (meter or inch) and are given in watt-meters or in watt-inches. Thus, any heat pipe design which has a Heat Transport Capability Factor greater than that required for the application will operate satisfactorily.

#### D.3.1.3.1 Case #1. Heat Pipe Operating in Zero Gravity Fields

For this case, consider heat pipes operating in zero gravity fields with no restrictions placed either on the shapes of the heat pipes or on the distribution of their evaporators and their condensers. The conditions imposed on Category 2 heat pipes, however, must be met. The Heat Transport Factor for this case is:

$$\dot{Q}L = \int_{x''}^{x'} \dot{Q}(x) dx \quad D-20$$

The limits of integration ( $x'$  and  $x''$ ) are found by evaluating the integral between 0 and  $x$  and then finding lowest and highest value of the resulting function. The lowest value corresponds to a location of  $x = x'$  and the highest value to a location of  $x = x''$ . The Heat Transport Capability Factor is given by:

$$(\dot{Q}L)_{\max} = \frac{\Delta P_{cap}}{C} = \frac{2 \sigma \cos \theta}{\frac{r_p}{\rho_v A_v D_{h,v} \lambda} + \frac{\mu_1}{K A_w A_1 \lambda}} \quad D-21$$

This equation can also be written in a more convenient form as follows:

$$(\dot{Q}L)_{\max} = \frac{2 K A_w \cos \theta F_1}{r_p} N_1 \quad D-22$$

The parameter  $F_1$  represents the ratio of the flow pressure drop in the liquid to the sum of the flow pressure drops in liquid and vapor.

$$F_1 = \frac{\Delta P_1}{\Delta P_1 + \Delta P_V} = \frac{1}{1 + \frac{\nu_v}{\nu_1} \frac{32 K}{D_{h,v}^2} \frac{A_w}{A_v}} \quad D-23$$

The Liquid Transport Factor  $N_1$  is a property of the working fluid and is defined as:

$$N_1 = \frac{\rho_1 \sigma_\lambda}{u_1} \quad D-24$$

D.3.1.3.2 Case #2. Conventional Heat Pipes Operating in Gravity Fields

A closed form solution can also be determined for a straight heat pipe with one evaporator and one condenser and which is operating in the heat pipe mode (evaporator elevated above condenser with respect to gravity). The conditions imposed on Category 2 heat pipes also apply for this case. The Heat Transport Factor for this case is:

$$\dot{Q}L = \dot{Q}_t L_{\text{eff}} \quad D-25$$

where  $\dot{Q}_t$  is the total heat to be transferred by the heat pipe and where  $L_{\text{eff}}$  is defined by the expression:

$$L_{\text{eff}} = \frac{1}{2} L_e + L_a + \frac{1}{2} L_c \quad D-26$$

The Heat Transport Capability Factor is given by:

$$(\dot{Q}L)_{\text{max}} = \frac{2 K A_w (1 + \eta) \cos \theta F_1}{r_p p} N_1 \quad D-27$$

where the terms  $F_1$  and  $N_1$  have been defined previously and where the parameter  $\eta$  is defined as the ratio of the sum of all pressure differences due to body forces to the available capillary pressure; i.e.,

$$\eta = - \frac{r_p D \cos \beta}{2 H \cos \theta} + \frac{r_p L \sin \beta}{2 H \cos \theta} \quad D-28$$

where  $H$ , the wicking height factor, is a property of the working fluid only and is defined as:

$$H = \frac{\sigma}{\rho_1 g} \quad D-29$$

The above expression for the Heat Transport Capability Factor (Equation D-27) applies for any location of the evaporator and the condenser (provided the evaporator is elevated above the condenser). However, the length  $L$ , which must be used in Equation D-28, is the total length of the heat pipe and not the distance between the location of the evaporator and the location of the condenser.

In the preceding paragraphs, methods that may be used to determine the Capillary Heat Transport Limit were outlined. Should the designer be faced with the situation that this limit is exceeded by the requirements, he then must take the necessary steps to modify the design. The designer, therefore, must be able to determine what corrective design actions are required.

In order to take corrective design action it is first important to determine the proportion of hydrodynamic losses to hydrostatic losses. If the heat pipe is in zero "g", then only the hydrodynamic losses exist. If the heat pipe is in a gravity field, the proportion of hydrostatic losses to hydrodynamic losses can be determined. The maximum wicking height is given by Equation D-15. If the actual elevation  $h$  of the highest point with respect to the lowest point on the system is more than one-half  $h_{max}$ , then the larger portion of the capillary pumping capability must be used to overcome body forces. If  $h$  is less than one-half  $h_{max}$ , hydrodynamic losses predominate. To overcome excessive hydrodynamic or hydrostatic losses, the designer has the choice of changing the working fluid, the wick design, or the size (geometry) of the heat pipe.

The parameters which will affect the capability of the heat pipe to overcome the hydrostatic losses are:

- The Wicking Height Factor ( $H$  in Equation D-29) which is a property of the working fluid.
- The effective pore radius,  $r_p$ .

This suggests that the methods by which the effect of the hydrostatic losses on heat pipe performance can be minimized are to select a fluid with a high Wicking Height Factor  $H$  and/or a wick design with small effective pore radius  $r_p$ .

The parameters which affect the capability of the heat pipe to overcome hydrodynamic losses are:

- The Liquid Transport Factor  $N_1$  (in Equation D-24) which is a property of the working fluid.
- The wick properties which include the permeability  $K$ , the cross-sectional area  $A_w$ , and the effective pore radius  $r_p$ .
- The parameter  $F_1$  (in Equation D-23) which is the ratio of the flow pressure drop in the liquid to the total pressure drop in the heat pipe.

If  $F_1 < 0.5$ , then a major part of the hydrodynamic losses are in the vapor phase.

Should this be the case, an increase in the vapor cross-sectional flow area  $A_v$ , which will also normally result in a corresponding increase in  $D_{h,v}$ , is the simplest method by which hydrodynamic losses in the vapor phase can be minimized. In most design cases, however,  $F_1 \simeq 1$  which means that most of the hydrodynamic losses occur in the wick. In this event, the designer has a number of options. He may choose a fluid with a higher Liquid Transport Factor  $N_1$ , increase the permeability  $K$  of the wick, or increase the fluid cross-sectional flow area  $A_w$ .

In varying the various parameters to achieve the desired effect, the designer should keep in mind that certain parameters are interdependent. For example, changing the fluid parameter  $H$  to achieve better hydrostatic properties also means that the Liquid Transport Factor  $N_1$  will also change thus affecting the hydrodynamic properties of the heat pipe. Fortunately, most fluids which exhibit a high value for one factor also exhibit a high value for the other. In other cases, changing one parameter will improve one aspect of performance at the expense of another. For all wick designs, with the notable exception of composite wicks (see Section W. 3), a decrease in the effective pore radius  $r_p$  will result in a corresponding decrease in the permeability

K of that wick. A decrease in the effective pore radius of the wick will improve the hydrostatic performance but will increase the hydrodynamic losses. The converse is also true. It is apparent that trade-off studies must be conducted in order to optimize the performance of a heat pipe.

#### D.3.2 Sonic Limit

As was noted previously, compressibility effects are not included in the development of the theory for the Capillary Heat Transport Limit. If the vapor flow in the heat pipe is in the range  $0.2 < M < 1.0$ , compressibility effects cannot be neglected. At the fundamental limit of  $M = 1.0$ , the axial heat flux limit is given by the equation:

$$\frac{\dot{Q}_s}{A_v} = \frac{\rho_v \lambda \sqrt{\gamma \frac{R_o}{M} T}}{\sqrt{2(\gamma + 1)}} = \frac{\rho_v \lambda v_s}{\sqrt{2(\gamma + 1)}} \quad D-30$$

where  $\dot{Q}_s$  is defined as the maximum axial flow rate at any location in the heat pipe and  $A_v$  is the vapor cross-sectional area at that location. The vapor density  $\rho_v$  and the sonic velocity  $v_s$  are evaluated at the stagnation temperature at the stagnation point in the evaporator section. Thus, if the capillary limit of any heat pipe results in a heat flow rate  $\dot{Q}$  which exceeds the limit expressed in Equation D-30, capillary pumping will no longer determine the maximum heat transport capability. Instead, the Sonic Limit will define this upper bound. For a heat pipe operating in the range  $0.2 < M < 1.0$ , the Capillary Heat Transport Limit of the heat pipe must be reduced to account for compressibility effects. Unfortunately, the theory of compressibility effects in a heat pipe is not as yet fully developed. Therefore, the designer is forced to employ judgement and available empirical data to design a heat pipe for operation in this vapor flow region. Under these conditions, the ability to predict heat pipe performance is poor and therefore vapor velocities of  $M > 0.2$  should be avoided. This can be done by selecting the working fluid such that operation at low vapor pressures is not required. For those cases where this is unavoidable, the vapor space  $A_v$  should be made as large as possible. A typical unavoidable situation occurs in the start-up transient of liquid metal heat pipes. In this case, the designer

should limit  $\dot{Q}$  during the start-up to avoid the Sonic Limit and/or compressibility effects.

#### D.3.3 Entrainment Limit

Entrainment in a heat pipe occurs whenever the relative velocity of the liquid and vapor phase are such that liquid droplets are torn from the wick and "entrained" in the vapor. Since the quantity of liquid entrained does not pass through the evaporation/condensation process, the heat pipe's transport capability is reduced by an amount proportional to the quantity of liquid entrainment. Experimental data indicate that the onset of entrainment corresponds to:

$$We = \frac{s_v \left( \frac{\dot{Q}}{A_v} \right)^2}{\sigma / z} = 1 \quad D-31$$

where the parameter  $z$  is set approximately equal to the mesh size of the wick. The corresponding axial heat flux limit is given by:

$$\left( \frac{\dot{Q}}{A_v} \right)_{\max} = \left[ \frac{\rho_v \sigma \lambda^2}{z} \right]^{1/2} \quad D-32$$

The entrainment limit is probably the least severe of all the heat pipe limitations. If a heat pipe is operating in a range where entrainment may be a consideration, the effects of entrainment can be eliminated by employing a small pore size wick at the liquid/vapor interface and/or by increasing the vapor space cross-sectional area.

#### D.3.4 Heat Flux Limit

The Heat Flux Limit in any heat pipe is reached when critical boiling heat fluxes in the evaporator are exceeded. Exceeding the heat flux limit is characterized by an excessive rise in heat pipe evaporator  $\Delta T$ . A general model for predicting the evaporator Heat Flux Limit is not presently available. Attempts to specify the Heat Flux Limit by using the appropriate working fluid properties have not, as yet, proved reliable for heat pipe design.

Typical evaporator heat fluxes which have been reported in the literature are given in Table D-4 for several fluids and wicks. These values are not intended to represent the fundamental Heat Flux Limit. The heat pipe designer may, however, use these reported values, in combination with the indicated wick designs, as a guide for specifying the evaporator heat flux.

#### D.4 Conventional Heat Pipe Design Procedures

Once the specifications for a heat pipe application are defined, the design can be established by following a basic design procedure. Among the many aspects of heat pipe design, the following are considered basic:

- Selection of the proper working fluid
- Determination of the wick design
- Selection of container design
- Determination of the proper fluid charge

##### D.4.1 Selection of Working Fluid

A variety of physical, chemical, and thermodynamic properties of a particular working fluid must be evaluated to determine whether or not that fluid is suitable for the specific heat pipe application. The general considerations on which the selection of candidate fluids must be based are:

- Operating temperature
- Fluid operating pressure
- Liquid transport factor
- Wicking capability in body-force field
- Heat transfer capability
- Fluid compatibility and stability

###### D.4.1.1 Operating Temperature

Since a heat pipe cannot function below the freezing point temperature or above the thermodynamic critical point temperature of its working fluid, the operating

Temperature °K	°F	Fluid	Wick	Evaporator Heat Flux		Reference
				W/cm <sup>2</sup>	Btu/Hr-Ft <sup>2</sup> x 10 <sup>-3</sup>	
80	-315	N <sub>2</sub>	Circumferential Grooves (19 Grooves/cm)	0.5	1.6	3
300	80	NH <sub>3</sub>	Axial Grooves	7.5	24	4
300	80	NH <sub>3</sub>	Circumferential Grooves (59 Grooves/cm)	8.0	25	6
453	355	H <sub>2</sub> O	5 Layers of 100 Mesh Screen	30	95	5
453	355	H <sub>2</sub> O	Circumferential Grooves (50 Grooves/cm)	150	476	5
1100	1538	Na	5 Layers of 65 Mesh Screen	50	159	11
1100	1538	Na	11 Layers of 330 Mesh Screen	320	1010	11
1000	1340	Na	Porous Metal Powder	805	2550	13

Table D-4. Experimental Evaporator Heat Fluxes

temperatures must lie within this temperature range. The application will specify that the heat pipe must operate in the cryogenic, ambient, or high temperature ranges. The designer has a choice of a number of working fluids for each of these temperature ranges. Figure I-2 presents a bar diagram which groups these fluids according to operating temperature range and relative order of heat transport capability. In general, a working fluid should be selected such that the operating temperature range avoids adverse vapor dynamics (sonic limit, entrainment limit, or simply excessive  $\Delta P_v$ ) due to low vapor densities and corresponding high vapor velocities.

#### D.4.1.2 Operating Pressure

The maximum operating temperature is frequently established by the ability to design satisfactory heat pipe containers within the weight restrictions established by the application. The vapor pressures at various temperatures for some working fluids are shown in Figure D-6. When screening the available working fluids for a given operating temperature range, the designer should keep in mind the general "rule of thumb" which establishes that at the lowest temperature the vapor pressure should be greater than 0.1 atmosphere and at the highest temperature the vapor pressure should be less than 10 atmospheres. Adequate attention must be given to evaluating the heat pipe design for all possible temperature environments to which the heat pipe may be subjected. The heat pipe may be subjected to high temperature conditions which may result in substantially higher internal pressure than those experienced during normal operating conditions; e. g., storage of a cryogenic heat pipe at ambient conditions.

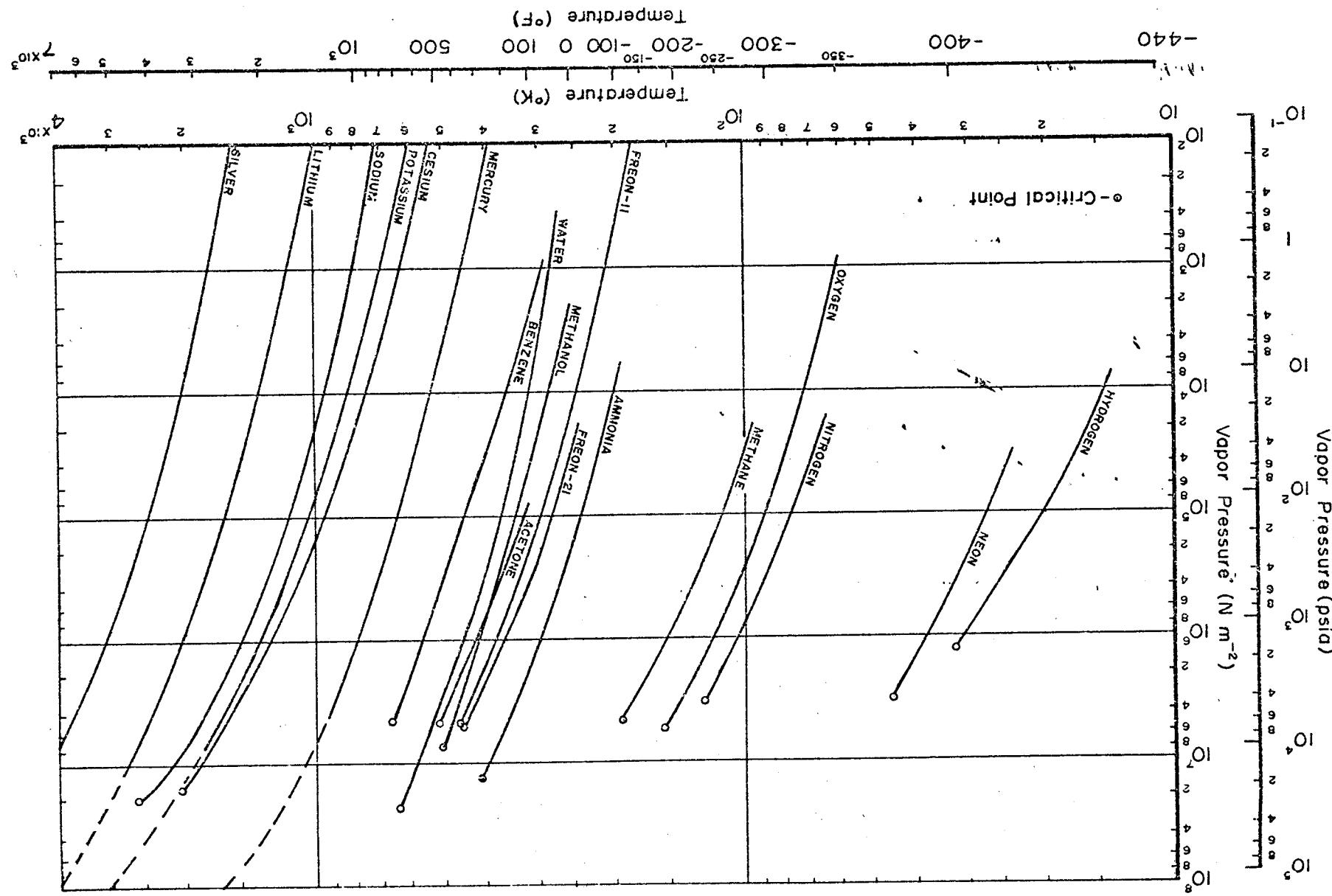
If the critical point of the fluid is exceeded, the designer can calculate an approximate pressure by using the simple equation of state for an ideal gas.

$$pV = nRT$$

D-33

This equation holds, with a fair degree of accuracy, for highly superheated vapors. In order to calculate internal pressures, which are fairly accurate throughout the entire superheated vapor region, more complex equations of state (developed from empirical data) must be utilized. One of the best known and most useful such equations

Figure D-6. Comparison of Vapor Pressures of Various Working Fluids



is the Beattie-Bridgeman equation of state. This equation is:

$$P = \frac{RT}{V^2} \left( 1 - \frac{\epsilon'}{V} \right) (V + B) - \frac{A}{V^2} \quad D-34$$

where

$$A = A_0 \left( 1 - \frac{a}{V} \right)$$

$$B = B_0 \left( 1 - \frac{b}{V} \right)$$

$$\epsilon' = \frac{c}{VT^3}$$

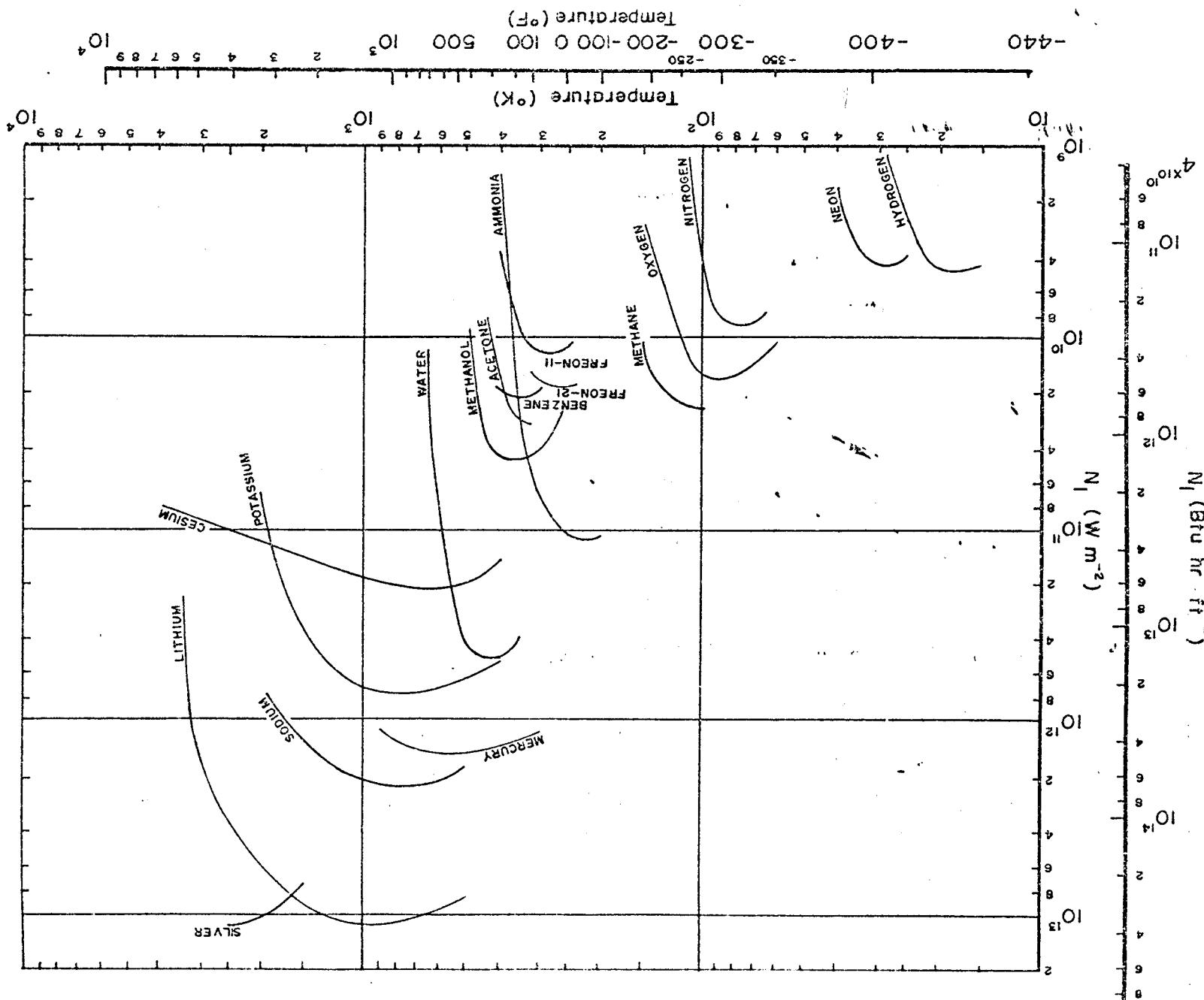
$A_0$ , a,  $B_0$ , b, and c are constants that must be determined experimentally for each fluid. If the constants are not available for a particular fluid, it is suggested that the ideal gas equation be used and a safety factor of 2.5 to 3 be applied to the working stress of the heat pipe container material.

#### D.4.1.3 Liquid Transport Factor

The capillary pumping ability of the working fluid is best described by the Liquid Transport Factor  $N_1$  defined in Section D-3. This factor states that the highest performance of a heat pipe is obtained with a fluid which has a high surface tension, high liquid density, high latent heat of vaporization, and a low viscosity. In Figure D-7, the Liquid Transport Factor is plotted versus temperature for selected fluids in the three basic operating temperature regions (cryogenic, ambient, and liquid metals). Notice that each curve contains a rather broad maximum near the normal boiling point of the particular fluid. The decrease in the Liquid Transport Factor on the low temperature side of the boiling point is primarily due to the increase in liquid viscosity. On the high temperature side of the boiling point, the decrease in this factor occurs because the liquid latent heat, liquid density, and liquid surface tension all decrease more rapidly than the liquid viscosity. The  $N_1$  decreases to zero at the critical temperature because the latent heat and surface tension become zero.

For heat pipes operating in the absence of bcdy forces and for conditions where the vapor pressure drop is negligible, the capillary pumping limit is directly

Figure D-7: Comparison of Liquid Transport Factors for Several Working Fluids



proportional to the Liquid Transport Factor. However, in the general design case, there is no simple grouping of fluid properties which serves as an exact basis for selection. Therefore, the  $N_1$  factor can only serve as a figure of merit for candidate heat pipe working fluids. To finalize the choice of fluid, a parametric evaluation must be conducted to include the Liquid Transport Factor, the expected body-force field, and the wick configuration (using the generalized heat pipe equation).

#### D.4.1.4 Fluid Wicking Capability in Body-Force Field

As indicated in the previous section, the presence of body forces can influence the relative performance of various heat pipe working fluids because:

- The body-force head is subtracted from the maximum capillary head in determining the capillary pumping available to overcome flow losses.
- The body-force head must be overcome by surface tension effects in order to prime the wick configuration.

Since in both cases the problem is one of surface tension forces working against body forces, the ratio of these forces represents a basis of fluid comparison. In terms of fluid properties, this ratio is proportional to the "Wicking Height Factor".

$$H = \frac{\sigma}{\rho_1 g} \quad D-35$$

Thus, to minimize adverse body-force effects, the designer should select a working fluid which has a high value for this parameter. For purpose of comparison, the Wicking Height Factor is given in Chapter F for various working fluids as a function of temperature.

#### D.4.1.5 Heat Transfer Capability

Besides the fluid hydrodynamic and hydrostatic properties, the designer must also consider the radial heat transfer in the evaporator, especially if boiling would seriously degrade hydrodynamic performance. The criteria for nucleation has

been discussed in Section T.7.3. Assuming the critical radius in Equation T-81 for the critical superheat is equal to the wick pore size, the pertinent fluid property grouping for superheat tolerance is  $\sigma / \lambda \rho_v$ . Based on Equation T-80, this grouping, multiplied by the liquid thermal conductivity, yields a measure of the fluid's radial heat transfer tolerance with respect to nucleation. This parameter, called the Nucleation Tolerance Factor  $K_1 \sigma / \lambda \rho_v$ , is plotted versus operating temperature for selected working fluids in Figure D-8. For high heat flux applications, the designer should consider candidate fluids with a high value for this parameter.

Although the heat pipe has been frequently considered an isothermal heat transfer device, a thermal gradient must always exist between the heat input and output regions during operation. This gradient is determined by the radial heat flux and the thermal conductance of the heat pipe wall and the wick material saturated with the working fluid. The effective conductance of the wick will be discussed more fully in Section D.4.2. As far as the selection of the working fluid is concerned, it is always best to choose the fluid with the highest thermal conductivity.

#### D.4.1.6 Fluid Compatibility and Stability

A major factor in the selection of a working fluid is its stability and compatibility with other materials in the heat pipe system. In contrast to most corrosion problems, the structural integrity of the tube wall is not the primary consideration. Critical to the performance of a heat pipe is the noncondensable gas that is generated because of chemical reactions. This gas collects in the condensing region and causes condenser blockage. An example of this is the hydrolysis of water which occurs in aluminum-water heat pipes.

Corrosion and erosion of the container and wick can also result in a change in the wetting angle of the working fluid as well as in the permeability, porosity, or capillary pore size of the wick. Solid precipitates resulting from corrosion and erosion are transported by the working fluid to the evaporator region where they are deposited when the liquid vaporizes. This leads to an increased resistance to fluid flow in the evaporator which results in lowering the Heat Flux Limit in the evaporator.

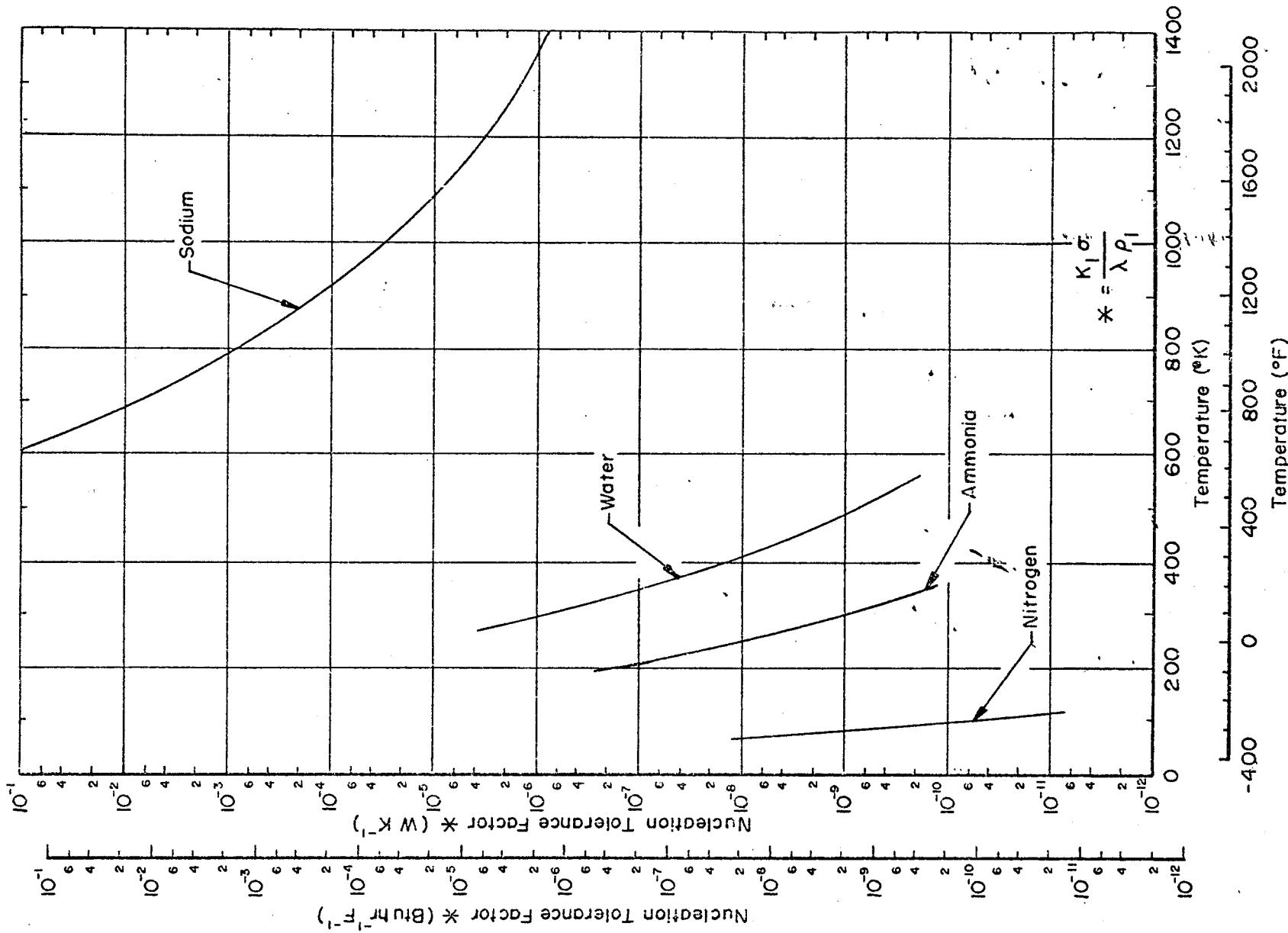


Figure D-8. Nucleation Tolerance Factors of Several Commonly Used Working Fluids

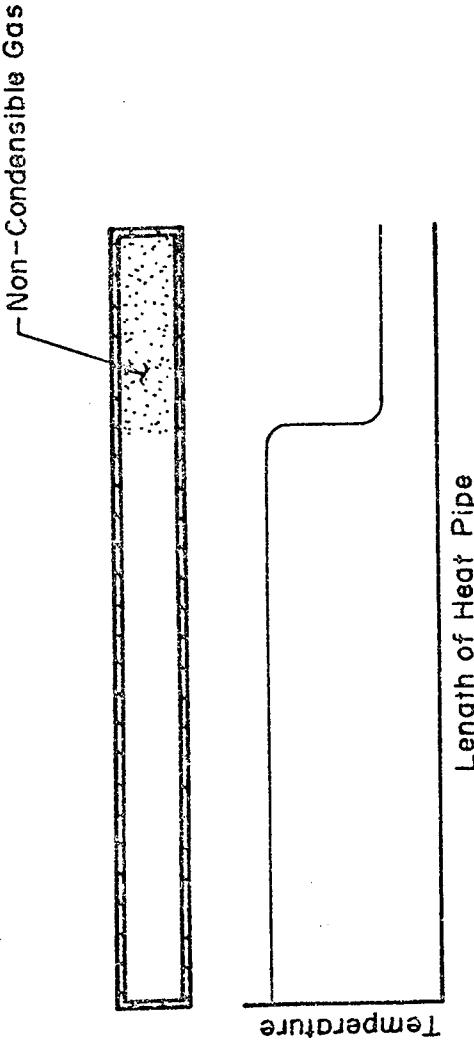


Figure D-9. Effect of Gas Build-Up on Temperature Uniformity of Heat Pipe

The compatibility and stability of the combination of working fluids and heat pipe materials at intended operating temperatures must be established by testing. A widely used approach to compatibility testing is to employ the actual heat pipe hardware and monitor the rate of gas generation. As mentioned previously, noncondensable gas generated within a heat pipe collects at the end of the condenser, blocking vapor flow and causing a local temperature drop (see Figure D-9). Thus, by monitoring the temperature distribution along a heat pipe operating at constant temperature the rate of gas generation can be determined. Several such compatibility tests have been performed by many different experimenters and laboratories. The designer is referred to Chapter M for a compilation of reported data.

#### D.4.2 Wick Design

The purpose of the wick is to provide the necessary flow area for liquid return from the condenser to the evaporator and to provide the pores required to develop capillary pumping. The properties of the wick are characterized by the permeability  $K$  and the effective pumping radius  $r_p$ . The permeability, the effective radius, and the wick cross-sectional area  $A_w$  determine the ability of the heat pipe to overcome hydrodynamic losses. The effective pumping radius is the only wick

parameter which determines the ability of the heat pipe to overcome hydrostatic forces.

The wick design should be capable of providing a high capillary pressure; that is, it should have a small effective pore radius. At the same time, it should have a high permeability  $K$  to minimize resistance to flow, which in turn requires large flow channels or pores. These conflicting requirements which exist in "conventional wick" designs have led to the development of non-isotropic "composite wicks" in which capillary pumping and permeability can be independently optimized. Unfortunately, the high performance "composite wicks" are somewhat sensitive to priming and therefore are less reliable than conventional wicks.

At this stage of heat pipe technology, the choice between conventional and composite wicks is often subjective. Conventional wick designs are in more advanced stages of development; and, therefore, a considerable amount of design and performance data is available. Composite wicks, on the other hand, are less developed and therefore less is known about the details of their behavior. Composite wicks are capable of high performance; and, if the requirements of a specific application are such that they cannot be satisfied with a conventional wick, the designer is forced to consider a composite wick.

#### D.4.2.1 Conventional Wick Design

The first step in the design of a wick is the selection of the type of wick most suitable for the application. This selection is not always easy and will frequently require an iteration. It was noted earlier that no single wick is suitable for all applications. Conversely, the requirements of a particular application can usually be satisfied with several wick designs. In selecting the type of wick, the following primary criteria should be considered:

- Permeability
- Capillary pumping
- Thermal conductance
- Complexity (cost)

In addition to these primary criteria, other requirements must also be considered. Fundamentally, the wick material must be compatible with the working fluid and the container material. The reader is referred to Chapter M for information about compatibility between different wick materials and working fluids. Another requirement for a wick is that it must have mechanical stability when exposed to dynamic forces. The most severe environment is frequently encountered during the launch of space vehicles. Experience has shown, however, that even the more sophisticated wick structures withstand simulated launch environments remarkably well. Nevertheless, dynamic forces must be considered in wick design. Different wick designs require different amounts of liquid for the same heat transport capability. As a rule of thumb, the required fluid inventory must be increased as the permeability of the wick is decreased. For many applications, the amount of working fluid is not critical; but, in some applications, the fluid inventory must be minimized, as for example:

- The working fluid is very expensive (e.g., cesium).
- The working fluid is dangerous when exposed to the environment in the event of a heat pipe failure (e.g., alkali metals and toxic fluids).
- The heat pipe has to be exposed to temperatures above the critical point of the working fluid. The internal pressure then becomes proportional to the fluid inventory.
- Excess working fluid may form a slug or puddle which impairs the heat pipe's conductance.

Table D-5 presents a "rating" of some of the more commonly used wicks in terms of the primary criteria. The wicks are shown schematically in Figure D-10. The rating G represents the best permeability of the wick designs listed when it appears in the permeability column for a wick. The rating P represents the poorest permeability for these same conditions. The rating M represents an average between G and P.

Permeability and capillary pumping determine the hydrodynamic heat transport capability of a wick. On examination of Equation D-27 for the Heat

Wick Type	Comments			
	Permeability	Capillary Pumping	Thermal Conductance	Complexity
a. Circumferential Screen	P-M	G	P	G
b. Circumferential Sintered	P-M	G	M	M
c. Slab Wick	P-M	G	G	With Screw Thread or Single Layer Screen as Circumf. Wick
d. Axial Grooves	M-G	P	G	Not Available in All Heat Pipe Materials
e. Open Annulus	G	P	P	M
f. Open Artery	G	P	G	M
g. Closed Artery	G	G	P	Pedestal, Spiral, or Tunnel Arteries
h. Circumferential Composite	M	G	M-P	Conductance Rating Depends on Whether Wick Sintered
i. Composite Slab	M	G	G	Not Very Sensitive to "Perfect" Closure of Pumping Wick
j. Closed Annulus	G	G	P	M-P
k. Grooves Covered by Screen	M-G	G	G	M-P
l. Spiral Artery	M-G	G	G	P

Table D-5. Wick Selection Criteria

Transport Capability Factor  $(\dot{Q}L)_{\max}$ , it is seen that  $(\dot{Q}L)_{\max}$  depends on the wick properties as follows:

$$(\dot{Q}L)_{\max} \propto A_w \frac{K}{r_p} (1 - \alpha r_p) \quad D-36$$

where  $\alpha$  is defined as  $-\eta/r_p$ , a proportionality constant containing the fluid properties, and the acceleration component (gravity).

From Equation D-36 it is seen that  $(\dot{Q}L)_{\max}$  is proportional to  $K/r_p$ . Large permeability and small capillary radius are two desirable wick characteristics. The ratio of  $K/r_p$  is frequently used as a parameter for describing the wick's hydrodynamic capability. In conventional wicks,  $K$  and  $r_p$  are related by the following approximation:

$$K \sim r_p^2 \quad D-37$$

This relationship indicates that  $K/r_p$  will grow with increasing pore size. In the absence of gravity ( $\alpha = 0$ ), the wick with the largest practicable pore size will yield the best heat transport capability. In a gravity field, this simple criterion is no longer true. As can be seen from Equation D-36, the pore size must be kept reasonably small in order that the term  $(1 - \alpha r_p)$  does not become too small. Using the approximation Equation T-39, it is noted that  $(\dot{Q}L)_{\max}$  becomes a quadratic function of  $r_p$  and an optimum pore size can be found with a corresponding maximum  $(\dot{Q}L)_{\max}$ . The use of this optimization for sizing the wick is not recommended since the approximation Equation D-37 does not hold for many wicks. Instead, the designer should select a wick with a static head at least twice as high as the maximum elevation between any two points in the heat pipe for the given application. Next, the designer can use the performance curve in Chapter P to check as to whether the performance of the selected wick falls in the range of the requirements. These performance curves are not intended for detailed design of a wick but for initial screening of the various wick candidates. Following this initial selection, the wick can then be sized using either the computer code HPAD (Chapter C) or by hand calculations using equations from Chapter W (Wick Properties), Chapter T (Heat Pipe Theory), and Section 3 of this chapter.

Ranges of physical pore sizes, capillary radii, and permeabilities for some typical wicks are given in Table D-6. Also listed in this table are the maximum static wicking heights for water.

The third column in Table D-5 rates the various wicks in terms of thermal conductance. The primary concern is the heat transfer at the evaporator and condenser since the temperature drop within the vapor is usually negligible. The thermal conductance is not only a property of the wick but also depends, to a great extent, on the thermal conductivity of the working fluid. With respect to their conductivity, all fluids can be divided into two groups -- nonconducting fluids and liquid metals. The range of thermal conductivities for both groups is:

- Nonconducting Fluids : 0.1 - 0.7 W/m<sup>0</sup>K (0.06 - 0.40 Btu/Hr-Ft-<sup>0</sup>F)
- Liquid Metals : 10 - 200 W/m<sup>0</sup>K (5.8 - 11.5 Btu/Hr-Ft-<sup>0</sup>F)

Because the difference in thermal conductivities between nonconducting fluids and liquid metals is more than an order of magnitude, different considerations apply to the two groups. In liquid metal heat pipes, one is seldom concerned with the conductance of the wick itself since the high conductivity of the fluid provides for high heat transfer coefficients even for fairly thick layers of wick. But for heat pipe containing nonconducting fluids, the effective conductance is strongly dependent on the wick design.

A simplified model for the heat transfer process at the evaporator and the condenser assumes that heat is conducted through the heat pipe wall and through the wick-liquid matrix to the liquid-vapor interface where evaporation occurs. More complex models, such as the recession of the liquid-vapor interface into the wick and/or nucleate boiling within the wick, have been proposed but are not sufficiently refined to be used for design purposes. These models are briefly discussed in Chapter T.

The conduction model yields for the effective heat transfer coefficient at evaporator and condenser (excluding the contribution of the wall):

$$h_{int} = \frac{k_{eff}}{t}$$

D-38

Table D-6. Properties of Typical Conventional Wicks

Wick Type	Characteristic	Dimension	Effective Capillary Radius	Max. Wicking Height with $H_2O$ at $100^{\circ}C$	Permeability	$m \times 10^{-3}$	$in \times 10^{-3}$	$m \times 10^{-3}$	$in \times 10^{-3}$	$m \times 10^{-3}$	$inches$	$m^2 \times 10^{-10}$	$ft^2 \times 10^{-12}$	
30 Mesh Screen	0.50	20	0.43	16.9	29	1.14	25	25	25	25	2.69			
100 Mesh Screen	0.14	5.5	0.12	4.7	104	4.1	1.8	1.8	1.8	1.8	0.19			
200 Mesh Screen	0.07	2.75	0.063	2.5	197	7.75	0.55	0.55	0.55	0.55	0.059			
Shirted Fibers/ Powders	-	-	0.01-0.1	0.4-4.0	1250-125	50-5	0.1-10	0.1-10	0.1-10	0.1-10	0.01-1			
Axial Grooves	0.25- $\frac{3}{4}$ -5	10-60	0.25-1.5	10-60	50-8	2-0.3	35-1250	3.8-135						
Open Annulus	0.25-1.5	10-60	0.25-1.5	10-60	50-8	2-0.3	50-2000	5.4-215						
Open Artery	1-3	40-120	0.50-1.5	20-60	25-8	1-0.3	300-3000	32-320						

where  $k_{eff}$  is the effective thermal conductivity of the wick-liquid matrix and "t" is its thickness. From Equation D-38, it is evident that high conductance can only be achieved if the thickness of the wick adjacent to the evaporation and condensation surfaces is kept at a minimum. This requirement has led to the development of "high conductance" wick structures in which the main transport wick is removed from the wall and only a thin secondary wick is used for circumferential distribution of the working fluid. Examples of such high conductance wicks are: the porous slab and the arterial wick, in both the conventional and the composite configuration.

The effective thermal conductivity of the wick-liquid matrix is bracketed by the series and the parallel path conduction model (Equation T-90) which is repeated here for easy reference:

$$\frac{k_s k_1}{\epsilon k_s + (1 - \epsilon) k_1} \leq k_w \leq (1 - \epsilon) k_s + \epsilon k_1$$

D-39

(parallel)

(series)

The performance curves in Chapter P give the overall conductance of typical heat pipes for the two extreme cases; i. e., using the series or the parallel path conduction model. As a general rule, the series path conduction model will apply for wicks which are only in mechanical contact; e. g., wraps of screen, packed particles, fibres, or spheres. Sintered wicks, on the other hand, will have an effective conductivity which is better approximated using the parallel path model. Typical heat transfer coefficients for heat pipes containing nonconducting working fluids are summarized in Table D-7.

The effective conductance of grooves, which are integral parts of the heat pipe envelope, are not described by either of the above models. At the present time, no satisfactory model for the heat transfer from a grooved surface is available. The designer will have to rely on empirical data.

The final primary criterion (last column, Table D-5) for selecting a wick is its complexity and the corresponding cost to manufacture. This criterion is highly subjective since its importance depends a great deal on the application. For example,

Wall Material/Type	Heat Transfer Coefficients		Comments
	W/m <sup>2</sup> -°K	Btu/Hr-Ft <sup>2</sup> -°F	
Aluminum	173,000	100,000	$0.89 \times 10^{-3}$ m (0.035 in) wall
Copper	440,000	250,000	$0.89 \times 10^{-3}$ m (0.035 in) wall
Stainless 316	24,000	14,000	$0.89 \times 10^{-3}$ m (0.035 in) wall
Molybdenum	154,000	89,000	$0.89 \times 10^{-3}$ m (0.035 in) wall
Multilayer Screen	600-1060	100-170	$10^{-3}$ m (0.040 in) Thick SST Wick - Non-Conducting Fluid
Sintered Wick	4700-6700	830-1180	$2.25 \times 10^{-3}$ m (0.09 in) Circular Wick - Water (10)
Secondary Wick (Single Layer)	3000-9000	350-1600	200 Mesh Screen Non-Conducting Fluid
Grooves	3000-15,000	500-2500	Aluminum Wall 20-200 Grooves/inch

Table D-7. Typical Heat Transfer Coefficient for Heat Pipes

in a heat pipe which is intended for protecting a vital component of an expensive space craft, cost will be of secondary importance when judged against performance and reliability. On the other hand, heat pipes which are designed for mass production must contain wicks which can be manufactured at low cost.

As a general rule, those wicks which are simple to install and do not require precise process control to manufacture are usually the least expensive. Multi-wraps of screen, layers of fibrous material, or slabs of porous material fall into this category. Fabricated wicks, such as arteries, annuli, etc., are high cost wicks. Sintered wicks are medium cost wicks, and their cost will depend to a large extent on the available process; they are expensive in small quantities but can be potentially cheap when mass produced. The cost of grooved tubing is determined by the material. Grooves can be extruded or swaged rather inexpensively in copper and other ductile materials. Grooved aluminum tubing is moderately expensive in small quantities because of prorated die costs, while in large quantities it promises to be relatively inexpensive.

#### D.4.2.2 Composite Wick Design

Composite wicks consist of two separate structures which might be labeled "transport wick" and "pumping wick". The term transport wick is used to describe the wick configuration which is responsible for the axial transport of the working fluid. It basically corresponds to the equivalent non-composite wick of the same geometry. In the case of a composite wick consisting of fine and coarse screen it applies to the coarse screen. In the case of an artery or annulus it applies to the open artery or annulus. For screen covered grooves, the transport wick corresponds to the open grooves. The pumping wick consists of a small pore structure (usually a fine mesh screen) which is responsible for the capillary pumping but which has a minor contribution to the effective axial flow path.

Most of the considerations which are important for conventional wicks also apply to composite wicks. Typical ranges for capillary pumping capability and permeabilities can be obtained from Table D-6. The effective capillary radius is that of the pumping wick, and the effective permeability is that of the transport wick.

In case of a composite wick formed from fine and coarse mesh screen (e.g., composite circumferential and composite slab) the permeability of the coarser screen should be used. In case of an artery, annulus, or screen covered grooves, the values of  $K + \gamma_p$  for the corresponding non-composite configurations also apply for the composite counterparts.

The heat transfer considerations for composite wicks are the same as for conventional wicks. The effective heat transfer coefficient is controlled by the thickness of the wick adjacent to the heat input/output surface. Composite wicks differ, however, in one important aspect from conventional wicks -- they must be primed. The priming process encompasses the saturating of the wick with working fluid either during initial start-up of the heat pipe or after a burn-out. The requirements for priming are:

- The static wicking height of the transport wick is sufficient to fill the wick with working fluid at the particular orientation of the heat pipe.
- The heat load during priming does not exceed the heat transport capability of the transport wick, without the benefit of the capillary pumping of the small pore screen.

The self-priming requirement establishes an upper limit for the "openness" of the transport wick and the diameter of any artery. In zero "g", the composite wick will always prime as long as the second condition is not violated. But in a one "g" environment, the transport wick must have a pumping head at least equal to the height of the wick structure. Otherwise, self-priming is impossible in any orientation.

For an annular type composite wick (Figure D-10j) this requirement translates to:

$$\frac{2 \sigma \cos \theta}{\delta_{\max}} = \rho_1 g D_i$$

where  $\delta_{\max}$  is the maximum permissible gas and  $D_i$  the internal heat pipe diameter.

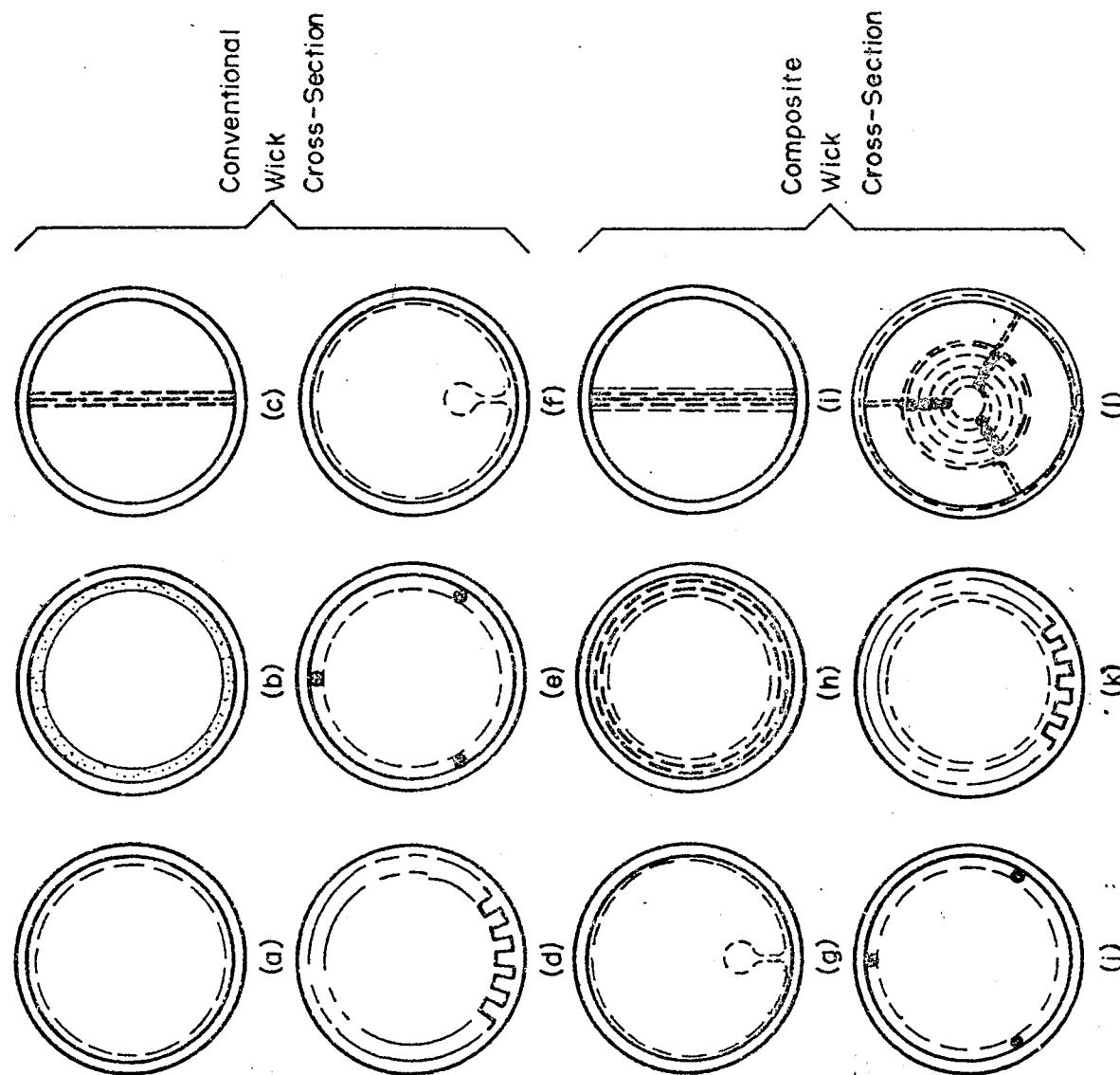


Figure D-10. Some Wick Types

For a pedestal artery (Figure D-10g) the maximum artery diameter is given by (2):

$$D_{\max} = \frac{1}{2} \left( \sqrt{h^2 + \frac{8\sigma}{\rho_1 g}} - h \right) \quad D-41$$

where  $h$  is the height of the pedestal. The self-priming requirement is included in the HPAD computer code. The program will alert the user if a wick is used which is not self-priming or, in the case of an artery or annulus, it will limit the optimization to sizes which will prime.

The maximum theoretical pumping capability of a composite wick can only be realized if the wick is completely filled with liquid. During a partial fill condition, a liquid-vapor interface is located inside the transport wick. The capillary pumping is thus reduced to a value which corresponds to the effective pore radius of the transport wick. This effect is illustrated in Figure D-11 for an arterial wick. In Figure D-11a the artery is completely filled, the liquid-vapor interface is located in the fine screen, and the maximum capillary pumping corresponds to the pore radius of the screen. In Figure D-11b the artery is filled except for a small bubble. The effective pumping radius is now the radius of the bubble. In Figure D-11c the bubble has reached its maximum diameter and the effective pumping radius is that of the artery.

It should be emphasized that the effect of incomplete filling (bubbles) in a composite wick is much more severe than in a conventional wick. In the latter, internal voids simply reduce the available liquid flow area but do not affect the capillary pumping. In the composite wick, voids or bubbles will reduce the capillary pumping to a value equal to that of the transport wick. Incomplete filling can be the result of:

- Insufficient amount of working fluid
- Nucleation within the composite wick due to excessive local heat flux
- Entrapment of noncondensing gas

The formation and stability of voids in composite wicks is not fully understood. Experience has shown that wicks consisting of different mesh-size screen are less

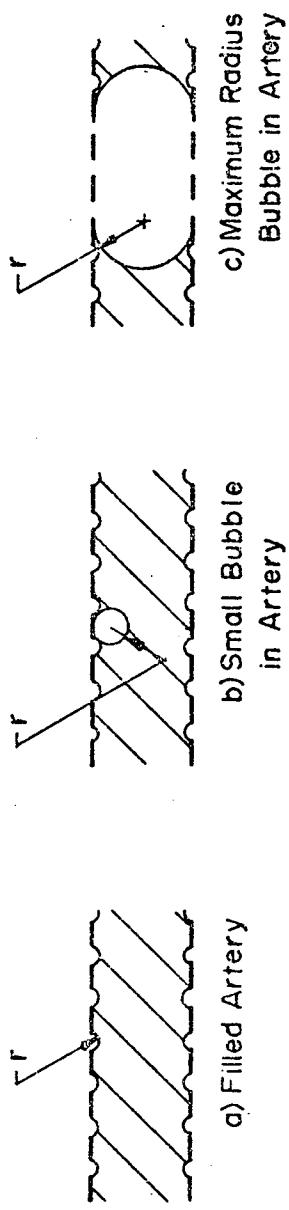


Figure D-11. Liquid Vapor Interface in Arteries

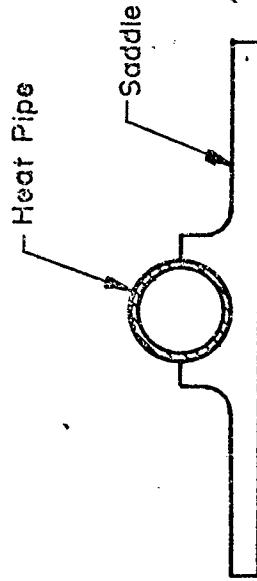


Figure D-12. Saddle Interfacing with Round Heat Pipe

susceptible to the formation of voids than those with wide open flow channels such as arteries and annuli.

Imperfections in the pumping wick have the same general effect as incomplete filling. The maximum interfacial pressure which the wick can sustain is determined by the largest opening in the pumping wick. Since the maximum interfacial pressure difference exists at the evaporator, imperfections in that region are most damaging to the performance. Close quality control during fabrication of composite wick heat pipes is therefore very important and adds to their cost. Whenever possible, a hydrostatic pressure test should be conducted on the completed wick in order to locate and repair any imperfections.

#### D.4.3 Container Design

Design of a heat pipe container includes the following:

- Container material selection
- Selection of a configuration including size and shape
- Structural consideration

##### D.4.3.1 Material Selection

Any material selected for the construction of the heat pipe container must be compatible with the working fluid (see Chapter C). In addition, the material must provide sufficient strength for the retention of the vapor pressure in the operating range as well as any anticipated temperature cycles during processing and nonoperating periods. Normally, conductance through a heat pipe container wall is negligible even if low conductivity materials are used because the conductance path (wall thickness) is often very small. However, if thick walls are required for pressure retention and if the application consists of concentrated local heat loads, a high thermal conductivity material may be preferred. Finally, fabricability of the container must be considered. Joining (welding, brazing, etc.), machining, forming, extruding, and sintering are processing methods which may be appropriate for the container. It must be emphasized that joining is an important consideration if the required leak tightness is to be achieved.

#### 4.3.2 Configuration Selection

The container configuration will depend on the requirement for the wick and the vapor space area and the shape best suited for pressure retention and for interfacing with the heat source and the heat sink. In addition to providing the minimum required cross-sectional area, the size of the container will also be determined by the heat transfer area required for evaporation and condensation. The requirement for heat transfer area is influenced by boiling heat flux limits in the evaporator and the required thermal conductance of the heat pipe.

For pressure retention, the cylindrical shape is the most efficient configuration; and materials are most commonly available in this shape (tubes and pipes). For interfacing purposes, however, a square shape which provides flat interfacing surfaces is desirable. In most heat pipe designs, this problem is resolved by using a round tube design and a saddle interface (see Figure D-12). The advantage of the saddle is that optimum interfacing, axial and radial heat transfer, thermal conductance, and pressure retention can be achieved simultaneously. Attachment of saddles must be carefully considered, especially if the saddle material, selected on the basis of weight and thermal conductivity, differs from the tube material.

#### D.4.3.3 Structural Consideration

The primary structural consideration which must be evaluated in the heat pipe container design is its ability to withstand internal pressure. The factors which must be considered in this evaluation are:

- Internal pressure which is a function in the working fluid and the highest anticipated temperature.
- Material strength which is determined by the container material and the highest anticipated temperature.
- Container geometry as discussed previously.
- Effect of any fabrication processes on the strength of the material (e.g., effects of welding on the heat treat condition of materials such as aluminum).

- Long-term effect of elevated temperature on the strength of the material.

Minimum requirements for container wall thickness, joint design and joining processes, and end cap design are determined on the basis of these factors.

In addition to pressure retention, the designer must consider effects of dynamic loads on the integrity of the heat pipe. This usually consists of designing the proper external mounting supports for the heat pipe. In addition, if the selected wick design is not sufficiently rigid to be self-supporting under dynamic loading, supports must be provided in the container to restrain the wick.

Finally, end caps and fill tubes must be provided to complete the container design. Considerations in end caps design include the joining process and pressure retention (and sometimes wick or artery closure). The joint design between the end cap and the container must be such that sufficient leak-tightness is reliably achieved. The joint must also be such that it will be capable of withstanding internal pressure and dynamic loads which may be induced during the life of the heat pipe. Considerations in fill tube design include pressure retention, interfacing with fluid charging apparatus, and final pinch-off. Final pinch-off is the single most important step in the design of a fill tube. The pinch-off must usually be performed with a net pressure differential between the inside and the outside of the heat pipe. Furthermore, for most heat pipe fluids, there is no convenient method of determining leak-tightness after the final pinch-off. Therefore, the designer should consider carefully the pinch-off procedure to be used and design the fill tube accordingly.

#### D.4.4 Fluid Inventory

The full potential of a heat pipe can only be achieved if it is properly filled with the working fluid. An underfill will result in degradation of performance. An overfill can result in condenser blockage (or overpressure in supercritical cases). This is especially true in zero "g" environments where there are no body forces to "spread" the excess fluid and where a "slug" is formed in the condenser. If the slug is large enough the condenser can be partially or fully blocked thus reducing the overall

thermal conductance of the heat pipe. Unfortunately, an accurate determination of the fluid inventory for most types of wicks is not possible for the following reasons:

- Variation of Liquid Density: Even if a 100% fill were accurately determined for one temperature, the variation of the liquid density will cause an underfill or overfill at other temperatures.
- Wick Nonuniformity: Wick cross-sectional area and porosity may vary along the length of the heat pipe.
- Meniscus Recession: If the wick is fully saturated under no-load conditions, liquid will be expelled when a heat load is applied because the meniscus of the vapor-liquid interface recedes. This effect is especially pronounced in axial grooves having a small aspect ratio.

If all of the above factors are included in the fill determination, the calculated fluid inventory will consist of a range of values between a maximum and a minimum. If overfill can be tolerated, the maximum value should be used and maximum wick performance will be achieved. If the condenser is sensitive to slug formation, the minimum value should be used and the wick size increased to offset the loss in performance. An alternative to the last case is to include, as part of the wick, an excess fluid reservoir. Such a reservoir can be "wicking" material with pores larger than those of the "primary" wick, and any excess will be collected in the reservoir.

D.5.1 General

The design of variable conductance heat pipes (VCHP's) includes all of the elements that affect conventional heat pipe design along with those factors which relate to the variable conductance mode of operation. This section presents a design procedure which is applicable to the various types of gas-controlled variable conductance heat pipes. Variable conductance methods such as liquid blockage, liquid or vapor flow control, etc., are still in the development stages and their design procedures are not well defined at this time.

The general parameters which influence the design of gas-controlled heat pipes have been discussed in the preceding sections. Basically, the designer must first determine a satisfactory conventional heat pipe design which meets the hydrodynamic and heat transfer requirements. Particular attention must be paid to those parameters (namely, wick design and working fluid) which also affect the variable conductance mode. Once the basic heat pipe design is defined, flat-front theory (see Section T.9.3) should be used to establish the type of gas-controlled heat pipe required, the necessary reservoir size, and the gas charge.

The different types of variable conductance heat pipes can be classified into two general categories -- wicked and non-wicked reservoir systems. Both active and passive control can be used with either reservoir type; however, because of the diffusion-controlled transient phenomena associated with non-wicked reservoirs, general practice has been to apply active control to only the wicked reservoir systems.

The general assumptions associated with Flat-Front analysis of either wicked or non-wicked reservoir systems are as follows:

- Thermal conduction and diffusion effects are negligible.
- The entire length is active at the maximum condition (maximum heat load at the highest sink temperature).
- The inactive part of the condenser is at the sink temperature.

- The noncondensable gas obeys the Ideal Gas Law.

Using these assumptions the following equations apply:

- Conservation of Mass

$$m_g = m_{g,r} + m_{g,c} \quad D-42$$

- Law of Additive Partial Pressures

$$\left. \begin{aligned} p_v &= p_{v,0} + p_{g,0} && \text{(Inactive Condenser)} \\ p_v &= p_{v,r} + p_{g,r} && \text{(Reservoir)} \end{aligned} \right\} \quad D-43$$

- Ideal Gas Equation of State

$$(pV)_g = (mRT)_g \quad D-44$$

Thus, at the maximum condition (maximum heat load at the highest sink temperature):

$$m_g = \left( \frac{p_v - p_{v,r}}{R_g T_r} \right)_{\max} V_r \quad D-45$$

and at the minimum condition (minimum heat load at the lowest sink temperature):

$$m_g = \left( \frac{p_v - p_{v,0}}{R_g T_0} \right)'_{\min} V'_{v,c} + \left( \frac{p_v - p_{v,r}}{R_g T_r} \right)_{\min} V_r \quad D-46$$

where  $V'_{v,c}$  is defined as the volume of the vapor space in the inactive condenser at the minimum condition. For the purposes of simplification and clarification, the following two terms are defined:

$$\Psi_0 \equiv \frac{p_v - p_{v,0}}{T_0} \quad ; \quad \Psi_r \equiv \frac{p_v - p_{v,r}}{T_r} \quad D-47$$

These terms are proportional to the gas densities in the condenser or the reservoir at the various conditions specified. For example,  $\Psi_{r, \max}$  is the gas density in the reservoir (at the maximum condition) multiplied by the Gas Constant  $R_g$ . The storage volume and gas charge required for a gas-controlled heat pipe can be determined (in terms of Equations D-47) by solving Equations D-45 and D-46:

$$\frac{V_r}{V_{v,c}} = \frac{\Psi_{o,min}}{\Psi_{r,max} - \Psi_{r,min}} \quad D-48$$

$$\frac{(mR)_g}{V'_{v,c}} = \frac{V_r}{V'_{v,c}} \Psi_{r,max} \quad D-49$$

That is, the gas charge is obtained by multiplying the storage volume by  $\Psi_{r,max}$ .

These equations apply, in general, to gas-controlled heat pipes. Before proceeding to the application of these equations to the specific types of gas-controlled heat pipes, it is important to understand how they relate to temperature control.

The most important parameter in a thermal control system is the temperature control required (i. e., control sensitivity). This parameter is essentially the allowable variation in heat source temperature ( $\Delta T_s$ ) which in turn relates to the reliability of the heat source. Once the required heat source temperature control has been defined, the corresponding maximum and minimum heat pipe vapor temperatures are determined from:

$$T_v = T_s - R_s \dot{Q} \quad D-50$$

For a constant resistance  $R_s$  between heat source and heat pipe, Equation D-50 defines the permitted variations of  $T_v$  for a specified  $\Delta T_s$  and  $\Delta \dot{Q}$ .

The vapor pressures ( $p_{v,max}$  and  $p_{v,min}$ ) corresponding to the required vapor temperature limits are then determined from saturation conditions for the working fluid. Thus, while the temperature control required does not appear explicitly in the equations defining the storage requirements, it does enter implicitly through the heat pipe vapor pressures.

One final comment which applies to gas-controlled heat pipes is that the tighter the control required the larger the reservoir size. For a specific type of VCHP and fixed reservoir end conditions, as  $p_v, \min$  approaches  $p_v, \max$  ( $\Psi_r, \min$  approaches  $\Psi_r, \max$ ), the denominator of Equation D-48 decreases and the required storage increases. When the denominator of Equation D-48 becomes zero or negative, no further improvement in temperature control can be obtained with the type of VCHP being investigated.

#### D.5.1.1 Wicked Reservoir Systems

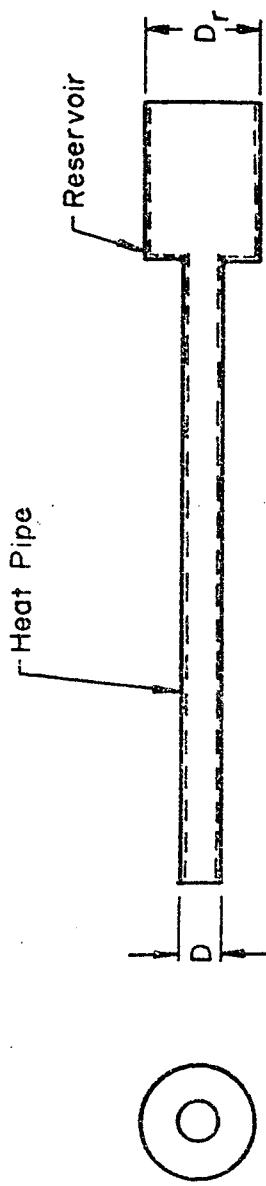
A reservoir wick is used to provide a return path for any liquid that collects in the reservoir either through diffusion and condensation of the vapor or through accidental spillage of working fluid. The presence of a wick saturated with liquid also establishes a saturation partial vapor pressure of the working fluid which is in equilibrium with the reservoir temperature.

The reservoir wick may be an extension of the heat pipe wick or it may be an entirely different type of wick. Since the reservoir wick does not have to satisfy any heat transfer requirements, a very simple design such as multiple layers of screen attached to the reservoir wall is sufficient. The only requirements for the reservoir wick are that it be integrated with the condenser wick and that it provides sufficient wicking height in a gravity field. The latter requirement can also affect the mechanical design or the integration of the reservoir. The reservoir geometry and its integration must be compatible with the requirement of capillary pumping against at least the perpendicular component of gravity. As an example, consider the two cases illustrated in Figure D-13. In the first case, where the heat pipe is concentric with the cylindrical reservoir, the effective required pumping height is:

$$h = \frac{D_r + D}{2} \quad D-51$$

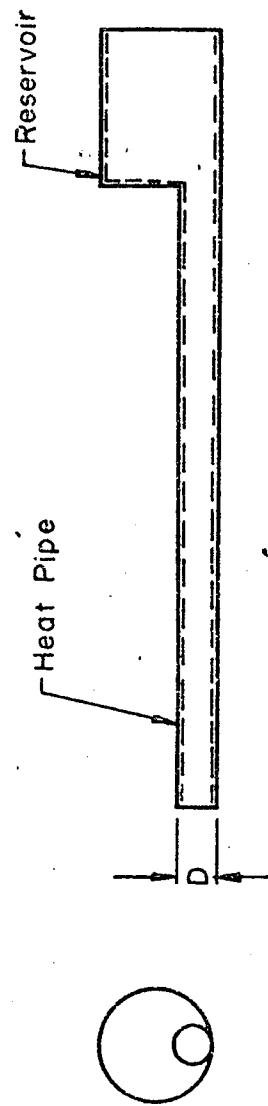
In the second case, the requirement is substantially less, being equal to:

$$h = D$$



$$h = \frac{D_r + D}{2}$$

Case 1 Heat Pipe with Concentric Reservoir



$$h = D$$

Case 2 Heat Pipe with Off-Set Reservoir

Figure D-13. Wicking Height Requirements for Wicked Reservoir Systems

The presence of a wick in a closed system guarantees that saturation conditions exist provided, of course, that the temperature is not above the critical point of the fluid. The saturated vapor in the reservoir is in equilibrium at the reservoir temperature. At the maximum condition, the vapor in the reservoir reduces the volume available for gas storage. However, at the minimum condition, the saturated vapor reduces the amount of gas required to fill the reservoir and therefore reduces the storage requirements.

#### D.5.1.1.1 Cold Reservoir

The simplest variable conductance heat pipe is commonly referred to as a "cold reservoir" type. As shown in Figure T-12, its reservoir is in thermal equilibrium with the sink condition (i.e.,  $T_r = T_o$ ). The storage volume requirement for a cold reservoir system is:

$$\frac{V_r}{V_{v,c}} = \frac{\Psi_{o,min}}{\Psi_{o,max} - \Psi_{o,min}} \quad D-53$$

and the gas charge requirement is:

$$\frac{(mR)_g}{V_{v,c}} = \frac{V_r}{V_{v,c}} \Psi_{o,max} \quad D-54$$

The "cold reservoir" VCHP is generally the easiest one to fabricate and integrate with another system and therefore the least expensive. However, because the reservoir has a wick and is in equilibrium with the sink temperature, its control capability is limited. In particular, unless relatively coarse temperature control is satisfactory, the cold reservoir type is suited for those applications where the maximum sink temperature is substantially less than the operating temperature and only moderate variations in sink temperature occur.

#### D.5.1.1.2 Reservoir at Constant Temperature

A relatively simple extension of the cold reservoir system is one in which

the reservoir is interfaced with some other component, structural member, etc., whose temperature is relatively insensitive to variations in the sink condition (i. e.,  $T_r = \text{constant}$ ). This system is capable of far greater control than an equivalent cold reservoir type. Its storage volume requirement can be determined from:

$$\frac{V_r}{V_{v,c}} = \frac{\Psi_{o,\min}}{\Psi_{r,\max} - \Psi_{r,\min}} \quad \text{D-55}$$

and its gas charge requirement is:

$$\frac{(mR)_g}{V_{v,c}} = \frac{V_r}{V_{v,c}} \quad \Psi_{r,\max} \quad \text{D-56}$$

A VCHP with a temperature controlled, wicked storage reservoir is far less sensitive to variations in the sink temperature than one whose reservoir is coupled to the sink temperature. Conversely, for a specified control sensitivity and sink temperature range, the VCHP with a temperature controlled reservoir will require a much smaller reservoir size. The only restriction with a controlled reservoir system is that the reservoir temperature must be less than the minimum vapor temperature.

When passive methods cannot be used to maintain the reservoir at a constant temperature, a reservoir heater can be employed. This is a type of active control wherein a feedback controller is used to regulate a reservoir heater such that the reservoir temperature is kept constant under varying sink conditions. Minimum heater power requirements result if the reservoir is maintained at a temperature just slightly above the maximum sink temperature. The equations defining the storage requirements are identical to those for the passive system.

#### D.5.1.3 Feedback VCHP

Each of the preceding systems require an infinite storage volume in order to provide absolute control of the heat pipe temperature (i. e.,  $\Delta T_V = 0$ ). Even if nearly absolute control of the vapor temperature could be obtained practically, this

would not guarantee that the heat source temperature (which is really the parameter of interest) would be maintained constant. As indicated by Equation D-52, there is always a finite thermal impedance between the heat source and the heat pipe vapor temperature. Consequently, even though the vapor temperature is kept constant, unacceptable heat source temperature fluctuations could result from variations in the heat load, since:

$$\Delta T_s = \Delta T_v + R_s \Delta \dot{Q} \quad D-57$$

Under these circumstances, or when the desired control cannot be obtained with practical reservoir sizes, an active feedback system can be employed. In the feedback system, the vapor temperature decreases with increasing heat load or vice versa, thereby permitting absolute control (i.e.,  $\Delta T_s = 0$ ,  $T_v = -R_s \Delta \dot{Q}$ ) of the heat source. The active feedback system is essentially the same as the heated reservoir system discussed previously, except that, instead of monitoring reservoir temperature and maintaining it constant, a controller senses the heat source temperature and regulates the reservoir temperature to derive the desired control.

In order to minimize the reservoir size, the auxiliary heater should keep the reservoir near the vapor temperature at the condition of minimum heat load and lowest sink temperature. This results in larger power requirements for the feedback system than for the heated reservoir type. However, the auxiliary power required is generally relatively small; its magnitude being associated primarily with the transient requirements. At the condition of maximum heat load and highest sink temperature, in order to achieve full utilization of the reservoir for gas storage, the reservoir temperature should approach the sink temperature. Thus, in the feedback system the reservoir temperature will vary between the maximum sink temperature and the minimum vapor temperature as the system varies between maximum and minimum conditions. The storage requirements for a feedback system are defined by the general Equations D-48 and D-49.

#### D.5.1.2 Non-Wickcd Reservoirs

One other type of gas-controlled heat pipe is the "hot reservoir" system.

This design utilizes a non-wick reservoir which is thermally coupled to either the heat pipe evaporator or the heat source as shown in Figure T-14. The reservoir is non-wick to avoid saturation conditions at temperatures equal to or greater than the heat pipe vapor temperature. Saturation conditions would, of course, prevent gas storage in the reservoir. Because there is no interconnection between the heat pipe wick and the reservoir, any fluid from the heat pipe that is accumulated in the reservoir, due to spillage or diffusion, must diffuse back out during start-up. This can result in relatively long start-up times (e.g., several hours) for this type of system.

Under normal operating conditions, vaporized working fluid which has diffused from the condenser will exist within the reservoir. As Marcus (9) points out, the partial pressure of this vapor will not correspond to the reservoir temperature but to the temperature at the mouth of the reservoir where the wick ends. Generally, a feeder tube which is in equilibrium with the sink condition is employed between the reservoir and the condenser section. Consequently, under the assumptions of the flat front model, the partial pressure of vapor in the reservoir corresponds to the sink temperature. The storage volume requirement for a "hot reservoir" system is therefore:

$$\frac{V_r}{V'_{v,c}} = \frac{\Psi_{o,min}}{\left(\frac{T_o}{T_r} \Psi_o\right)_{max} - \left(\frac{T_o}{T_r} \Psi_o\right)_{min}} \quad D-58$$

and the gas charge requirement is:

$$\frac{(mR)_E}{V'_{v,c}} = \frac{V_r}{V'_{v,c}} \left(\frac{T_o}{T_r} \Psi_o\right)_{max} \quad D-59$$

where the reservoir temperature is equal to the heat source or heat pipe evaporator temperature.

#### D.5.2 Design Considerations

Once the flat-front analysis has been performed, the gas-front analysis of

Marcus (9) may be employed to evaluate conduction and diffusion effects and their impact on the design. More specifically, the gas-front analysis should be used to evaluate diffusion freeze-out rates whenever the minimum equivalent sink temperature is below the melting temperature of the working fluid. Also, the gas-front analysis allows one to account for conduction as it affects the required active length of the condenser and the reservoir temperature and therefore its size. As pointed out in the theory section, the simple fin-equation can also be used to evaluate conduction effects.

Until now, nothing has been said about the choice of noncondensable gas.

The following general considerations apply:

1. The noncondensable gas should have a critical temperature well below the minimum sink temperature. This is necessary to avoid real gas effects which are not very accurately predicted and also to guarantee that inaccuracies in predicting the minimum condition do not lead to a two-fluid heat pipe system whose control characteristics are substantially different.
2. When high diffusion rates are desired, as in the case of start-up with hot non-wick reservoir types, a gas with a low molecular weight should be employed. If diffusion freeze-out is a potential problem, a gas with a high molecular weight should be used. In general, the diffusion rate is inversely proportional to the molecular weight of the gas.
3. Gases, such as helium, with very low molecular weights have a tendency to stratify across the diameter of the heat pipe tube. This results in only partial blockage of the circumference of the condenser and could result in a significant change in the heat pipe's conductance. This is particularly true with large diameter heat pipes.

### D.5.3 Design Procedure

#### VCHP.

The following procedure is recommended for the design of a gas-controlled VCHP.

1. Establish the nominal source temperature and its allowable variation (i.e.,  $T_s, \text{max}$  and  $T_s, \text{min}$ ). Special attention should be paid to establishing these limits, since the tighter the control temperature the larger the reservoir and/or the more complicated the VCHP type required.
2. Calculate the heat pipe's operating temperature limits (i.e.,  $T_v, \text{max}$  and  $T_v, \text{min}$ ) from Equation D-50.
3. Establish the sink temperature extremes ( $T_o, \text{min}$  and  $T_o, \text{max}$ ).
4. Determine the basic heat pipe design (hydrodynamics and heat transfer) using the procedure outlined in Section D.4. The following considerations which affect the variable conductance aspects of the system should be taken into account.
  - Wick Design: The operation of composite wicks, particularly the arterial types, is very susceptible to the presence of noncondensable gas. Efforts are currently underway to develop arterial variable conductance heat pipes (6); however, they have met with limited success. If a composite wick design is required to satisfy transport requirements, a multi-layered slab type geometry is recommended. (It has a higher self-priming capability and is not subject to catastrophic performance degradation as a result of bubble formation. However, it does not have the maximum transport capability of the open artery design.) Also, a non-condensable which has a low degree of solubility in the working fluid should be used. The low solubility minimizes the tendency of the gas to go into solution in the condenser and

minimizes the tendency of forming a bubble if this gas comes out of solution in the warmer evaporator section. Also, since the required reservoir volume is directly proportional to the condenser vapor volume, a wick design which minimizes vapor space in the condenser may be desirable. Trade-offs affecting the wick design such as weight, fluid inventory, and containment should also be evaluated.

- Working Fluid: Very often, the choice of working fluid will be dictated entirely by the transport requirements and the nominal operating temperature range. Where trade-offs are available, a working fluid should be selected whose freezing temperature is above the minimum sink condition. When this is not possible, diffusion freeze-out rates should be calculated for candidate working fluid/gas combinations.

Containment should also be considered when choosing the working fluid. Since the required reservoir volume will be approximately an order of magnitude larger than the condenser volume, containment of a high pressure fluid could pose a problem, particularly if weight is a prime consideration. Fluids which have moderate to low operating vapor pressures are generally recommended. Finally, the working fluid should have a high ratio of  $(p_v/p_{v,0})_{\text{max}}$  in order to maximize the effective storage capacity of the reservoir at the maximum condition.

5. Select the VCHP Type: The kind of VCHP required for a particular application will depend on the following factors:
  - The degree of temperature control required.
  - The magnitude of the variations in heat load and/or sink condition.

- The magnitude of the maximum sink temperature relative to the nominal operating condition.
- Specific system requirements or constraints (e.g., Will start-up requirements be compatible with a hot reservoir system? Can auxiliary power be made available for feedback control, etc.?)

As a general rule, the tighter the control, or the larger the variations in heat load or sink conditions, the more sophisticated will be the required system. This also applies as the sink temperature approaches the heat pipe operating temperature.

The flat-front analysis presented earlier should be used to determine whether a particular VCHP type can provide acceptable control for the conditions established in Steps 2 and 3. As noted previously, acceptable VCHP designs are those for which the ratio  $V_r^t/V_{v,c}^t$  is positive and within practical upper limits. When the desired control cannot be obtained with a particular VCHP type, the designer must be willing to decrease the degree of control, select a more complicated VCHP, or select a different thermal control system. For convenience, the equations required to calculate storage volume and gas charge requirements for the different types of VCHP's are listed in Table D-8.

In the case of feedback controlled heat pipes (FCHP), parameters such as overshoot and response time which are associated with its transient behavior should also be considered. The best response characteristics are obtained by minimizing the ratio  $\tau_r/\tau_s$  where  $\tau_r$  and  $\tau_s$  are the time constants of the reservoir and heat source respectively (1). The time constant is defined as:

$$\tau = m C_p R$$

D-60

D-70

Since the time constant of the heat source generally is a fixed system

Table D-8. Storage and Gas Charge Requirements for Variable Conduction Heat Pipes

VCHP Type	Storage Volume Requirements Multiply $V_x/V_c$ By Gas Charge Requirements	$\frac{V_x/V_c}{V_o, \text{min}} - \frac{V_o, \text{max}}{V_x, \text{min}}$	Cold Reservoir
Wicked Reservoir	$\frac{V_x, \text{max}}{V_o, \text{min}} - \frac{V_o, \text{max}}{V_x, \text{min}}$	$\frac{V_x, \text{max}}{V_o, \text{min}}$	Constant Temperature
FCHP	$\frac{V_x, \text{max}}{V_o, \text{min}} - \frac{V_o, \text{max}}{V_x, \text{min}}$	$\frac{V_x, \text{max}}{V_o, \text{min}}$	Wicked Reservoir
Hot Reservoir	$\left( \frac{T_x}{T_o} \Psi_o \right)_{\text{min}} - \left( \frac{T_x}{T_o} \Psi_o \right)_{\text{max}}$	$\left( \frac{T_x}{T_o} \Psi_o \right)_{\text{max}}$	FCHP

parameter, the transient behavior is optimized by minimizing  $T_r$ . This requires minimizing the heat capacitance of the reservoir.

The auxiliary heater power required to control the reservoir is:

$$Q_a = R_r (T_r - T_o) \quad D-61$$

and therefore the reservoir's resistance should be adjusted to be consistent with the available auxiliary power.

One final consideration with regard to the design of an FCHP is the choice of working fluid. Working fluids whose saturated vapor pressure has a steep slope in the operating reservoir temperature range will give the best transient performance. The slope of the vapor pressure curve is defined as:

$$\alpha = \frac{1}{p_v} \frac{dp_v}{dT} \quad D-62$$

Therefore, for a given reservoir temperature change, the steeper the slope the larger the fractional change in pressure. Consequently, the effective storage volume changes more rapidly and the response of the overall system is improved.

6. Determine the Gas Charge: Once the type of VCHP has been determined along with the required reservoir size, a noncondensable gas should be selected and the necessary charge calculated using the appropriate equation from Table D-8. Except for potential stratification phenomena, helium is recommended for use as the noncondensable. In addition to being inert, its low critical temperature eliminates the possibility of real gas effects in almost all applications. Also, its solubility is relatively low; and, with the exception of hydrogen, it gives the fastest mass diffusion rates.
7. Perform Gas Front Analysis: In those applications where diffusion freeze-out is a potential problem or where thermal isolation of the

reservoir from the condenser section cannot be accomplished, the Gas-Front Analysis of Marcus should be performed.

8. Establish Reservoir Design: Once the reservoir has been sized, the reservoir's mechanical and thermal design and system integration can be defined. The final design must be consistent with requirements such as containment, self-priming, the variable conductance type, and overall system constraints as well as fabrication and cost considerations. Where possible, cylindrical reservoirs are recommended since they are easiest to fabricate and can provide good containment.

As in the case of all system design, a final design will be arrived at after a series of iterations involving the different steps of the design procedure. The number of iterations may be minimized if a good definition of the application is available and if the designer has a good understanding of the various steps and factors which affect the design. When designing a VCHP, particular attention should be paid to the degree of temperature control required and the magnitude of the sink temperature relative to the operating temperature. These parameters generally have the greatest impact on the type of VCHP that will be required. Once the VCHP type has been established, most other design considerations follow.

## P.0 PERFORMANCE CURVES

This section contains a compilation of performance curves for typical heat pipes. The data from which the graphs were plotted were obtained from the "Heat Pipe Analysis and Design" (HPAD) code and the "Variable Conductance Heat Pipe Analysis" (VCHPA) code.

The purpose of this section is to provide the designers with a quick graphical reference for the approximate performance of a selected design. The graphs are not intended to replace detailed design and analysis but are intended to help in the initial screening of the various available options. Of course, it has not been possible to include all combinations of wicks, heat pipe geometries, fluids and temperatures; however, an effort was made to select the most representative combinations. With some practice, the designers should be able to extrapolate to other combinations which are not too far removed from the given examples.

### P.1 Conventional Heat Pipes

Performance parameters are presented for a total of 24 combinations of temperatures, wicks, and heat pipe diameters. These combinations are shown in Table P-1. For each of the four selected temperatures, one particular fluid/material

Table P-1. Combinations of Temperatures, Wicks, and Heat Pipe Diameters

Temperature (°K)	Type of Wick	Heat Pipe Diameter (cm)	(inches)
77	-320	Circumferential Screen	1.27
273	32	Slab Wick	2.54
373	212	Axial Grooves	1
1100	2011		

combination was chosen which is representative for heat pipes to be operated about this temperature level. The selected working fluids and materials are listed in Table P-2.

Table P-2. Combinations of Working Fluids, Wicks, and Heat Pipe Materials

Temperature (°K)	Working Fluid	Container Material	Wick Material		
			Slab	Circumferential Screen	Grooves
77	N <sub>2</sub>	Al	SS	SS	Al
273	NH <sub>3</sub>	Al	SS	SS	Al
373	H <sub>2</sub> O	Cu	Cu	Cu	Cu
1100	N <sub>2</sub>	SS	SS	SS	SS

All performance parameters are calculated for a standard heat pipe length of 1.10 m (44 inches) and with an evaporator and condenser length of 0.1 m (4 inches) each. This particular length was chosen because it represents a corresponding effective transport length of 1.0 m (40 inches). The calculated values for  $\dot{Q}_{\max}$  have, therefore, the same numerical value as  $(\dot{Q}_L)_{\max}$ , and the two parameters are interchangeable. Uniform heat input and output was assumed, and the wall thickness of the heat pipe was 0.89 mm (0.035 inches). The properties of the porous screen wick ( $r_p$  and  $K$ ) were calculated using Equations W-8 and W-17 of Chapter W. The porosity of the porous wick was assumed to be 70%.

Three (3) types of performance curves are given for each of the 24 combinations of temperatures, wick types, and heat pipe diameters shown in Table P-1. Performance curves of the type A give the maximum heat transport capability as a function of several wick parameters for a "zero g" environment. In the case of the circumfer-

ential screen and the porous slab wick, the independent parameter is the wick thickness. Results are given for five mesh sizes; i.e., 20, 30, 50, 100 and 200. All curves show an initial increase in the heat transport capability with increasing wick thickness, followed by a decrease which is caused by the decrease in vapor flow area. Also indicated on the curves is the range of wick thickness over which the vapor flow is laminar (solid lines). Within this range, the results can be expressed in terms of the Heat Transport Capability Factor  $(\dot{Q}L)_{\max}$  and are applicable to other heat pipe lengths. When the vapor flow is turbulent (dashed part of the curves) the plotted  $\dot{Q}_{\max}$  is only applicable for the particular length of 1.1m.

For the case of axial grooves, the data represent the result of an optimization and the plotted  $\dot{Q}$  (or  $(\dot{Q}L)_{\max}$ ) is the maximum attainable at each aspect ratio. A permissible range of groove and land widths was specified, and the code selected the optimum value which yields the highest  $\dot{Q}$ . The range of widths was .25 mm to 1.0 mm (0.010 inch to 0.040 inch) for the 1.27 cm (1/2 inch) pipes and .25 mm to 2.0 mm (0.010 inch to 0.080 inch) for the 1 inch pipes. The type A curves for the grooved heat pipes give the maximum  $\dot{Q}$  (or  $(\dot{Q}L)_{\max}$ ) in addition to the optimum groove width and number of grooves for each aspect ratio.

Type B curves give the maximum static head in a "one g" environment. The perpendicular component of gravity has been accounted for; thus, the curves give the maximum height to which one end of the heat pipe may be elevated without drying out the wick. For the two porous wick types, the static head is plotted as a function of mesh size and for the grooved heat pipe as a function of groove width. For the latter one, the static head is independent of heat pipe diameter since each groove is assumed to be independent of the others.

Type B curves provide qualitative information regarding the heat pipe's performance in a "one g" environment. Once a wick has been selected from the type A curves, the designer can estimate the degradation which will be experienced at a given evaporator elevation. The maximum heat transport capability decreases approximately linearly with evaporator elevation. The heat transport capability is a maximum at "zero g" and zero at an elevation equal to the static head. Thus, at an elevation equal to 50% of the static head the performance obtained is equal to 50% of that in

"zero g". Similarly, at 80% of the static head the performance would be only 20% of the "zero g" value. This relationship is only an approximation. It holds best when the static head is large compared to the heat pipe diameter and when the vapor flow is laminar.

Type C curves provide information about the heat pipe's conductance. For each one of the 24 combinations of temperature, wick, and heat pipe diameter, the conductance is given in dependence of wick thickness or, in the case of grooves, in dependence of the aspect ratio. Thus, for every wick design defined by a type A performance curve, a corresponding conductance is given by a type C curve.

Unfortunately, conductances are much less amenable to theoretical predictions than heat transport capability and static head. The following approach has therefore been used. The overall conductance was calculated as the reciprocal of the sum of 5 thermal resistances; namely, the evaporator wall, evaporator wick, vapor temperature drop, condenser wick, and condenser wall.

The greatest uncertainty exists for the two wick resistances. In case of the circumferential screen wick, the conductance is given for the two extreme cases of effective wick conductivity; i. e., that corresponding to the series and parallel conduction model (see Equation D-39). For the porous slab wick and for the axial grooves, the overall conductance is given for three different internal heat transfer coefficients which are indicated on the respective curves. The ranges chosen will most likely bracket the actual conditions existing in practical heat pipes.

For most wick designs, the temperature drops through the walls and wicks are dominating and the temperature drop along the vapor is small. The range for which the latter is less than 1% of the total temperature drop is indicated by a solid line; the remaining range is indicated by a dotted line. Within the range covered by a solid line, the designer can easily scale the overall conductance for different evaporator and condenser lengths. For example, if the evaporator length is increased from 0.1 m to 0.2 m (4 inches to 8 inches), the overall conductance will increase by a factor of  $(0.2 + 0.1)/(0.1 + 0.1) = 1.5$ .

The performance curves for conventional heat pipes are arranged as follows:

(1)	Circumferential Screen Wick	(Pages P-7 to P-11)
	77 <sup>0</sup> K	Type A and C Page P-7
	273 <sup>0</sup> K	Type A and C Page P-8
	373 <sup>0</sup> K	Type A and C Page P-9
	1100 <sup>0</sup> K	Type A and C Page P-10

Static Wicking Height (Type B): 77, 273, 373, 1100<sup>0</sup>K - Page P-11

(2)	Slab Wick	(Pages P-12 to P-15)
	77 <sup>0</sup> K	Type A and C Page P-12
	273 <sup>0</sup> K	Type A and C Page P-13
	373 <sup>0</sup> K	Type A and C Page P-14
	1100 <sup>0</sup> K	Type A and C Page P-15

The Static Wicking Height of the slab wick is identical to that of the circumferential screen wick for the same mesh size screen.

(3)	Grooved Wick	(Pages P-16 to P-20)
	77 <sup>0</sup> K	Type A and C Page P-16
	273 <sup>0</sup> K	Type A and C Page P-17
	373 <sup>0</sup> K	Type A and C Page P-18
	1100 <sup>0</sup> K	Type A and C Page P-19

Static Wicking Height (Type B): 77, 273, 373, 1100<sup>0</sup>K - Page P-20

## P.2 Variable Conductance Heat Pipes

Performance curves for Variable Conductance Heat Pipes (VCHP) are presented for two (2) nominal operating temperatures -- 318<sup>0</sup>K and 1100<sup>0</sup>K. The first

temperature is typical for electronic equipment; the second one for high temperature radioisotope heat sources. Ammonia was chosen for the low temperature case and sodium for the high temperature.

The curves are applicable for VCHP's with cold, wicked reservoirs. They can be used for sizing the reservoir when the range of sink temperatures is specified (type D curves). In addition, a performance analysis is provided for a specified heat pipe design (type E curves).

In the type D curves, the ratio of reservoir-to-(inactive) condenser volume is plotted as a function of allowable vapor temperature  $\Delta T$ . Each curve represents a different range of sink temperature variations. These curves are to be used to find the required reservoir size once the allowable  $\Delta T$  of the vapor temperature and the maximum and minimum sink temperatures have been specified. One sees that for a given range of sink temperatures a lower limit for the vapor  $\Delta T$  exists; better control is not possible regardless of the reservoir size.

Once the reservoir has been sized for the extreme conditions, the type E curves give the control performance within this range. The vapor temperature is plotted as a function of heat load with the sink temperature as parameter.

Unlike the performance curves for conventional heat pipes, the curves for VCHP cannot easily be extrapolated to other cases. They are presented as examples of the performance of VCHP's with cold wicked reservoir. The data plotted are a direct output of the VCHPA code and can be used as a guide in using this program.

The performance curves for VCHP's are arranged as follows:

(1) Nominal vapor temperature  $318^{\circ}\text{K}$

Type D

Page P-21

Type E

Page P-22

(2) Nominal vapor temperature  $1100^{\circ}\text{K}$

Type D

Page P-23

Type E

Page P-24

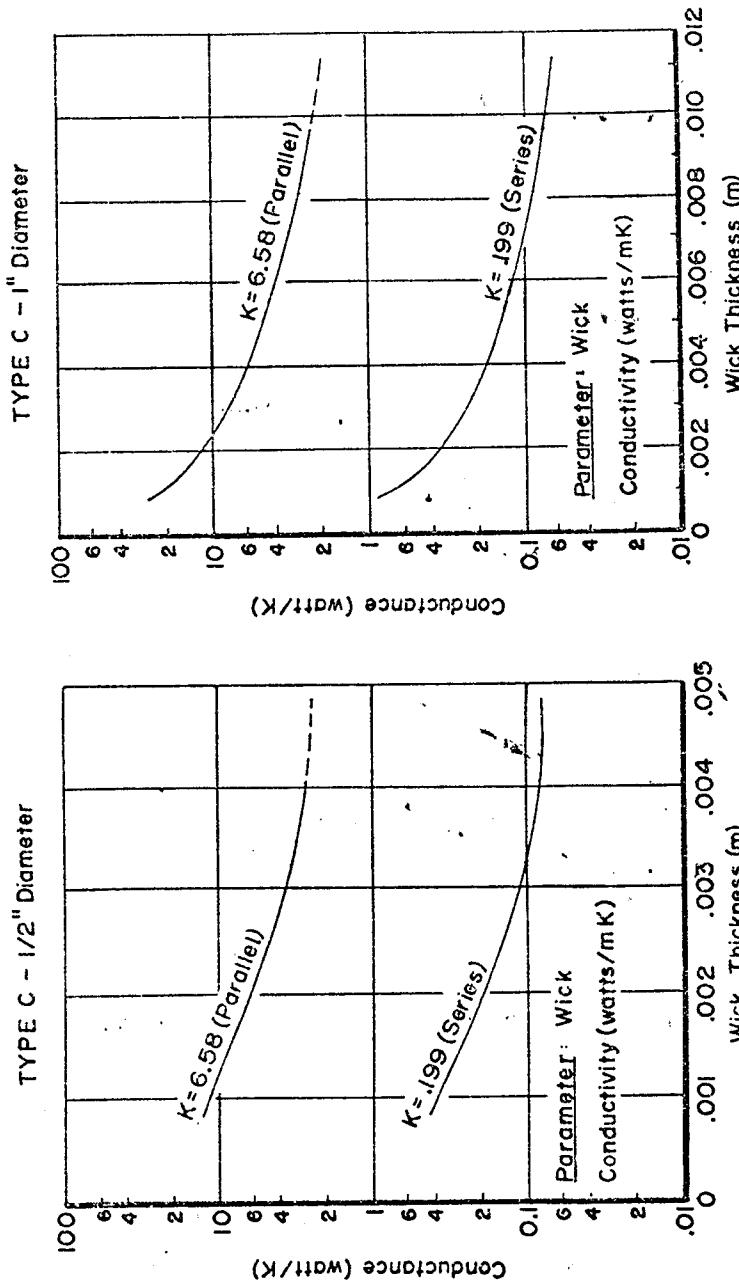
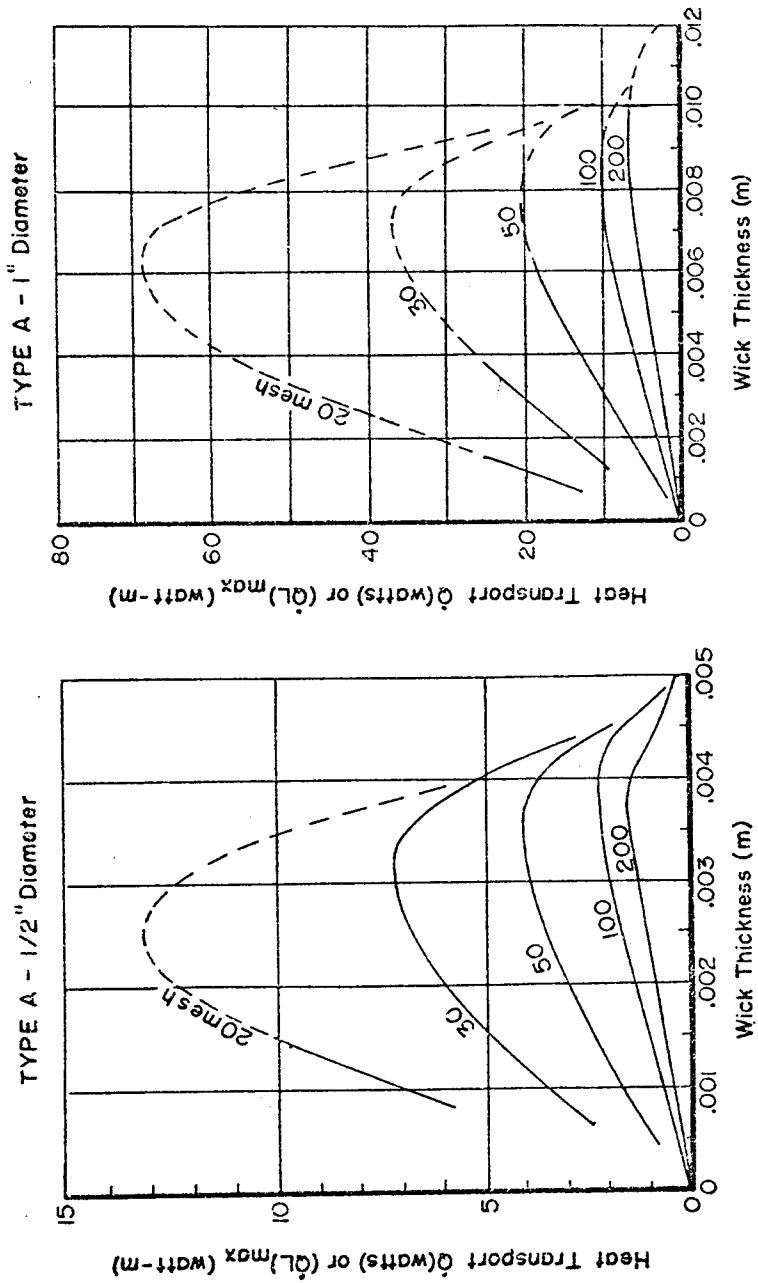


Figure P-1. Circumferential Wick

Axial Heat Transport (Type A) and Heat Pipe Conductance (Type C)

Temperature:  $77^{\circ}\text{K}$  ( $-320^{\circ}\text{F}$ )

Container Material: Aluminum

Working Fluid: Nitrogen

Wick Material: Stainless Steel

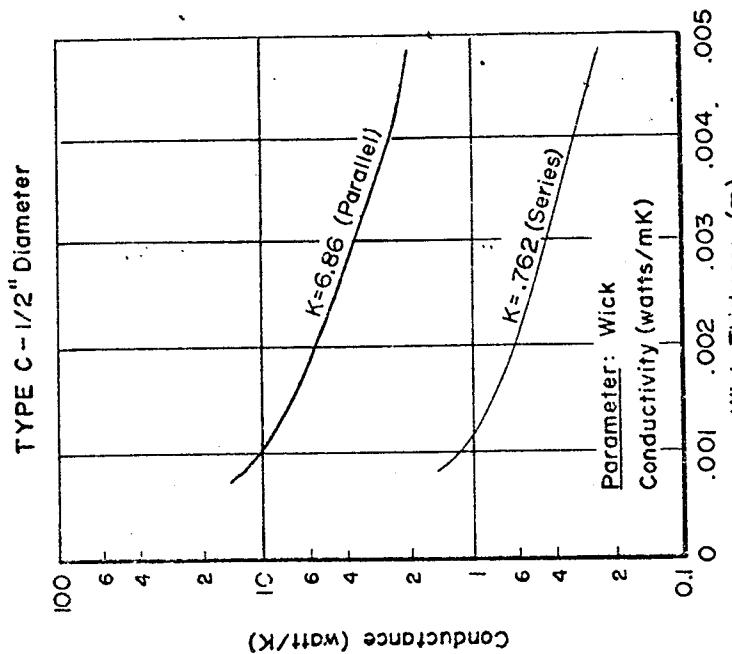
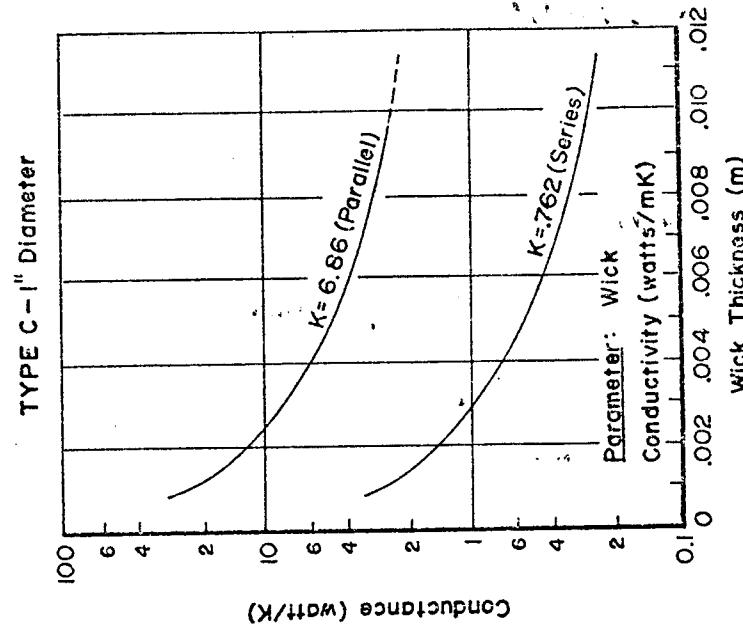
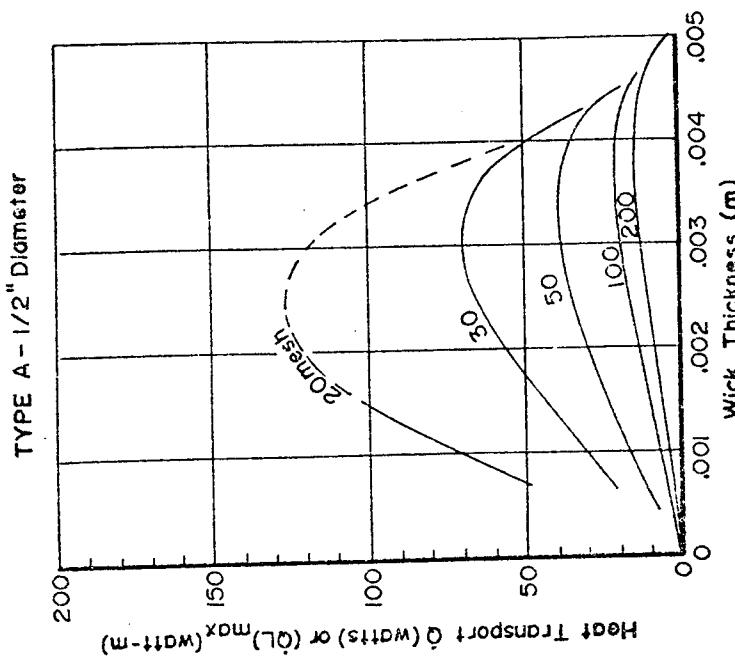
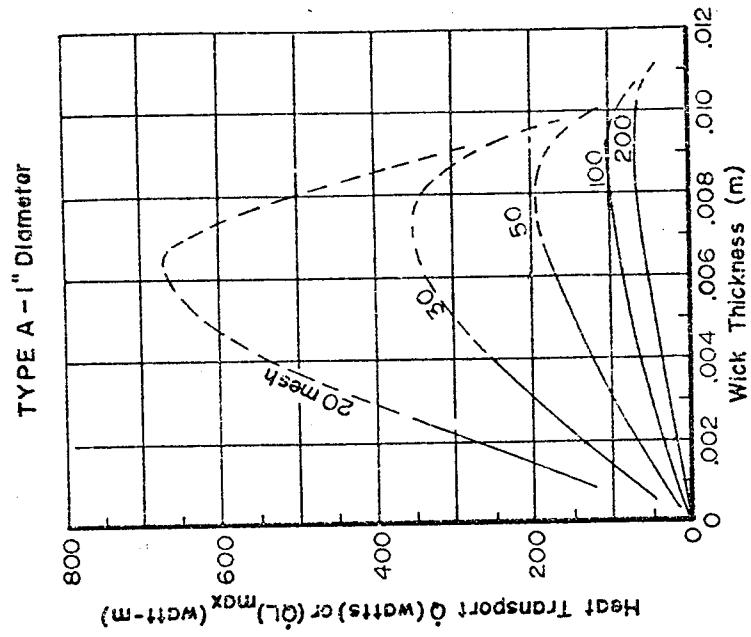


Figure P-2. Circumferential Wick

Axial Heat Transport (Type A) and Heat Pipe Conductance (Type C)

Temperature: 273°K (32°F)  
Container Material: Aluminum  
Working Fluid: Ammonia  
Wick Material: Stainless Steel

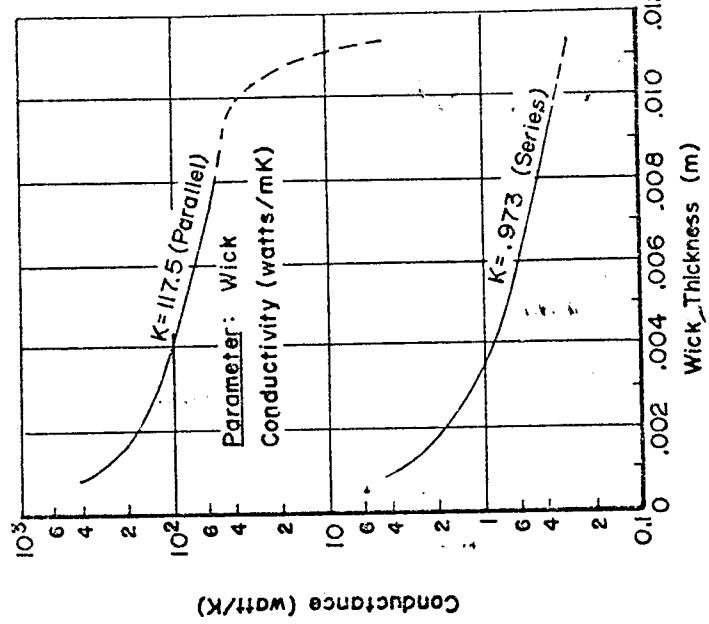
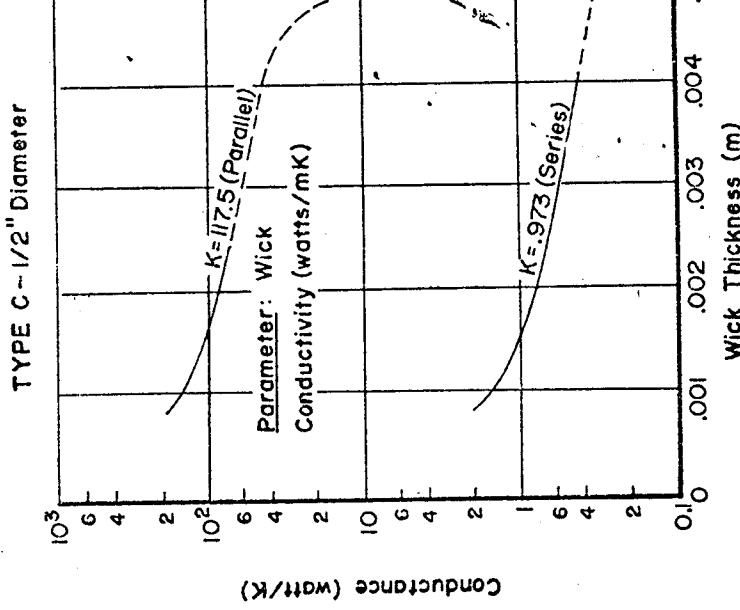
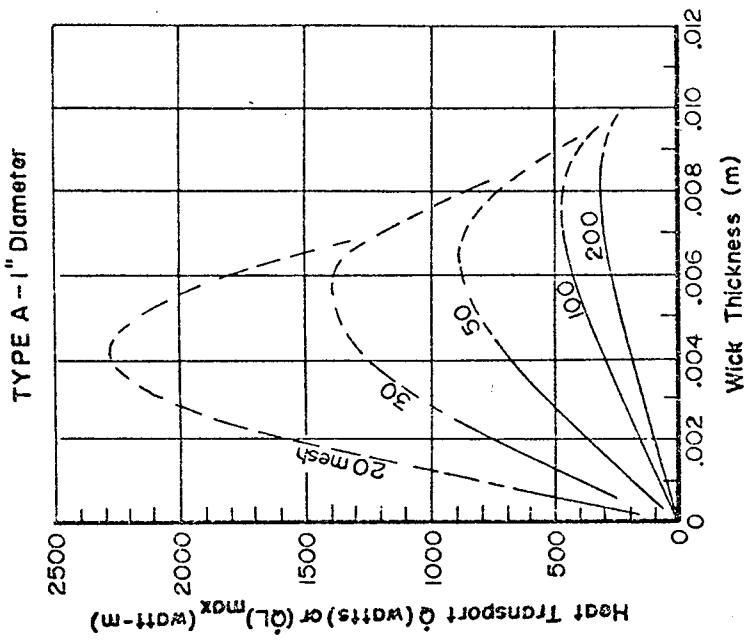
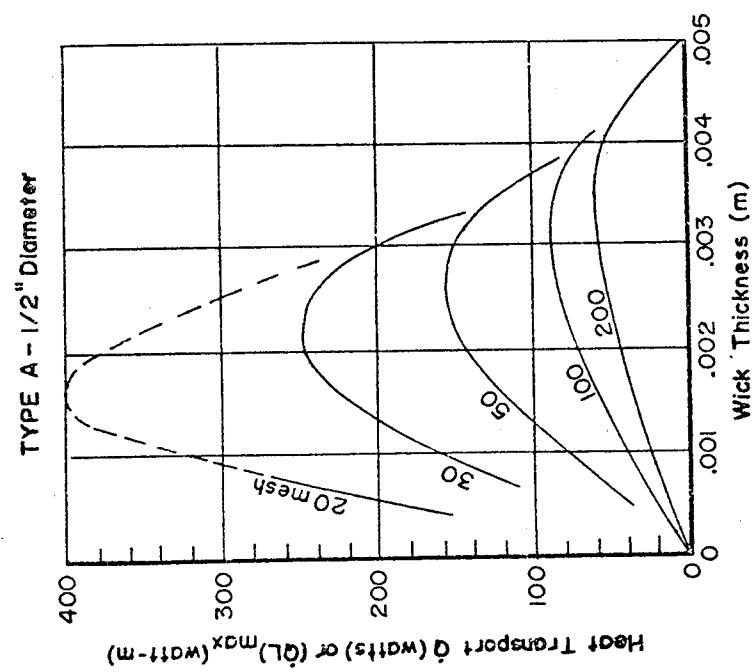


Figure P-3. Circumferential Screen Wick

~ Axial Heat Transport (Type A) and Heat Pipe Conductance (Type C)  
 Temperature: 373°K (212°F)  
 Working Fluid: Water  
 Container Material: Copper  
 Wick Material: Copper

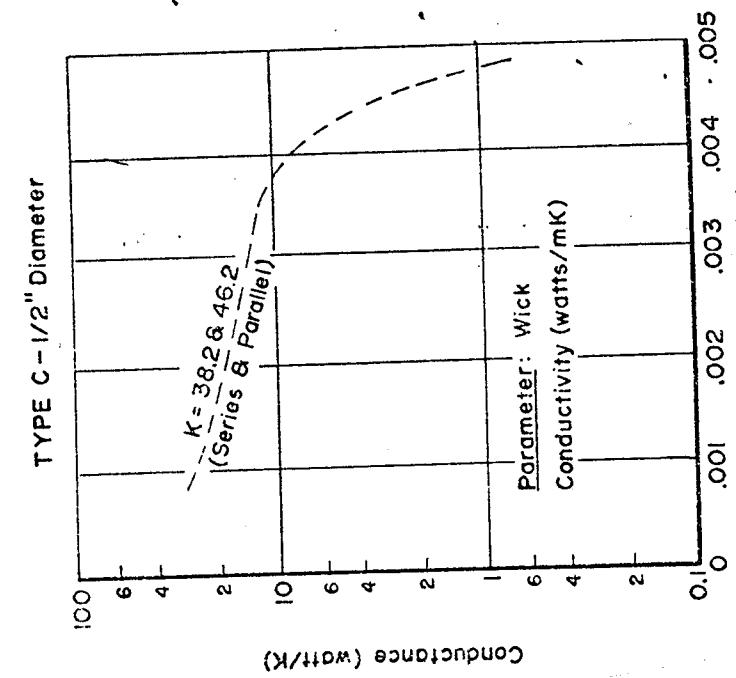
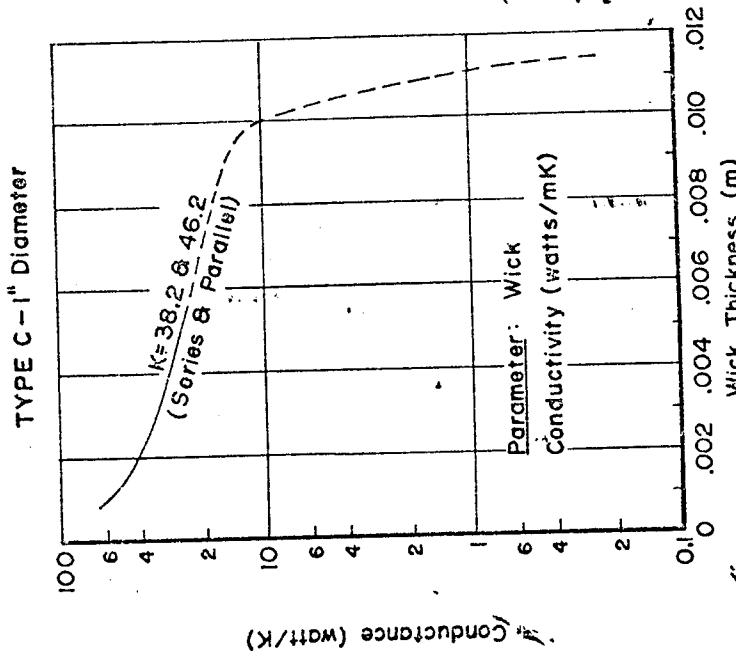
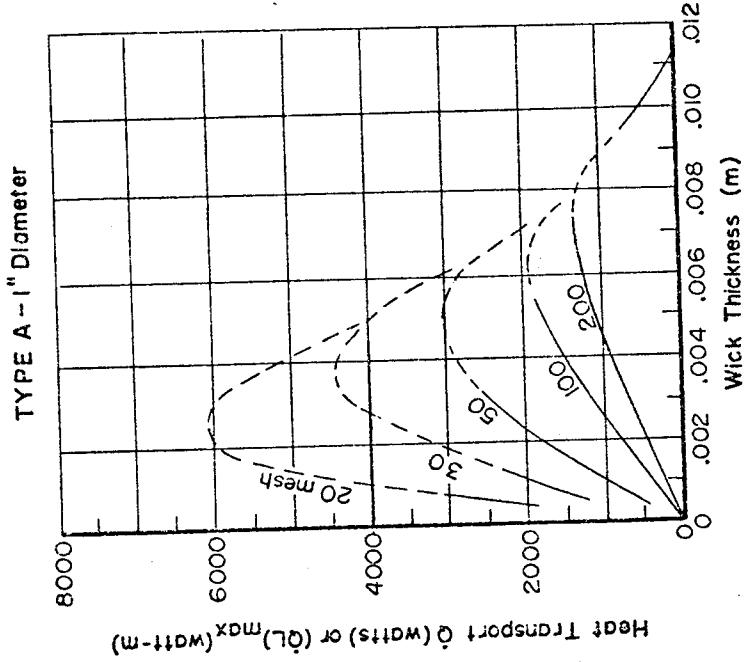


Figure P-4. Circumferential Screen Wick

Axial Heat Transport (Type A) and Heat Pipe Conductance (Type C)

Temperature:  $1100^{\circ}\text{K}$  ( $2011^{\circ}\text{F}$ )

Container Material: Stainless Steel

Working Fluid: Sodium

Wick Material: Stainless Steel

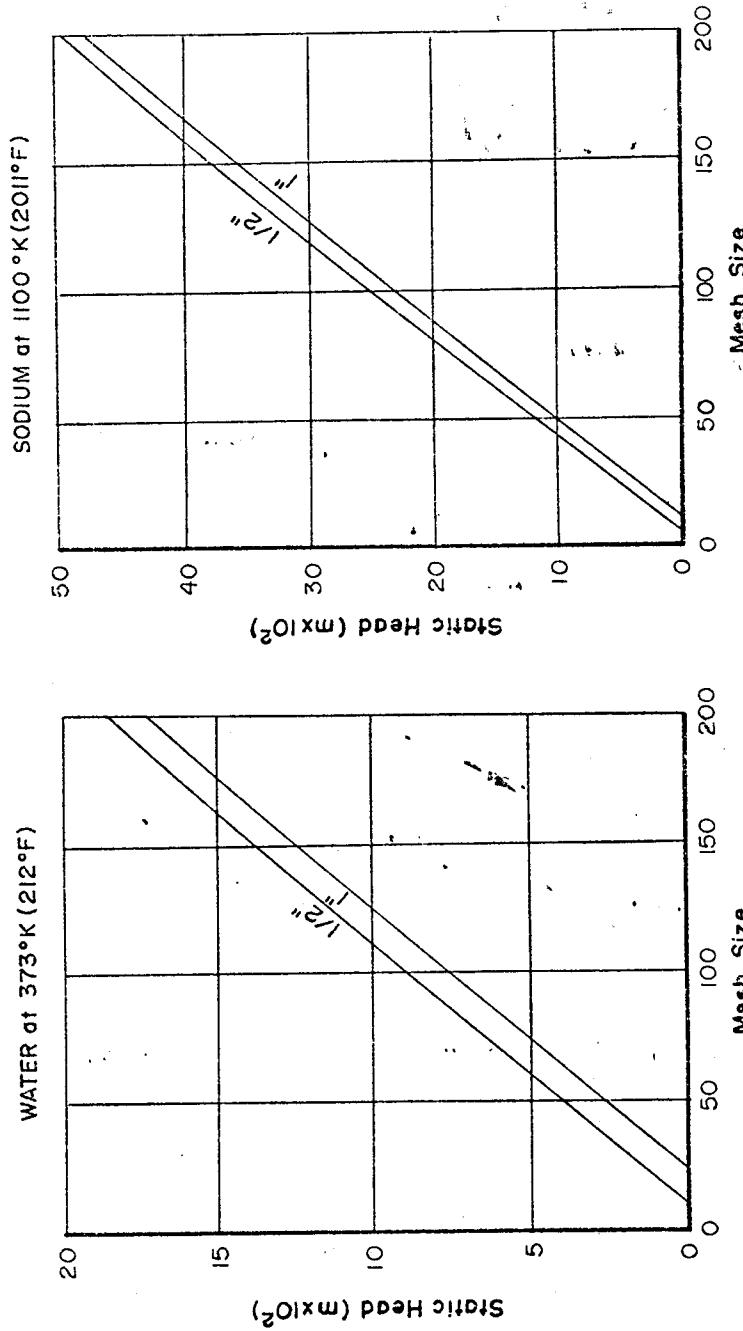
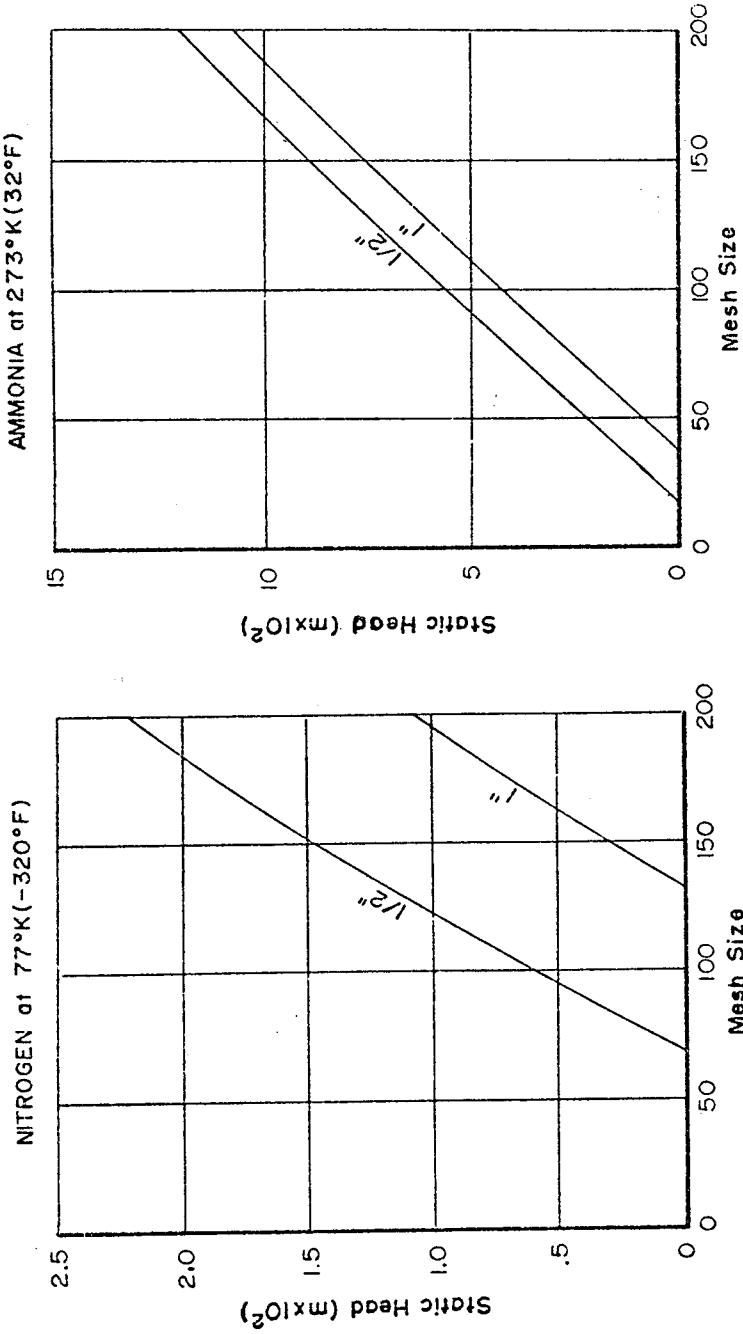
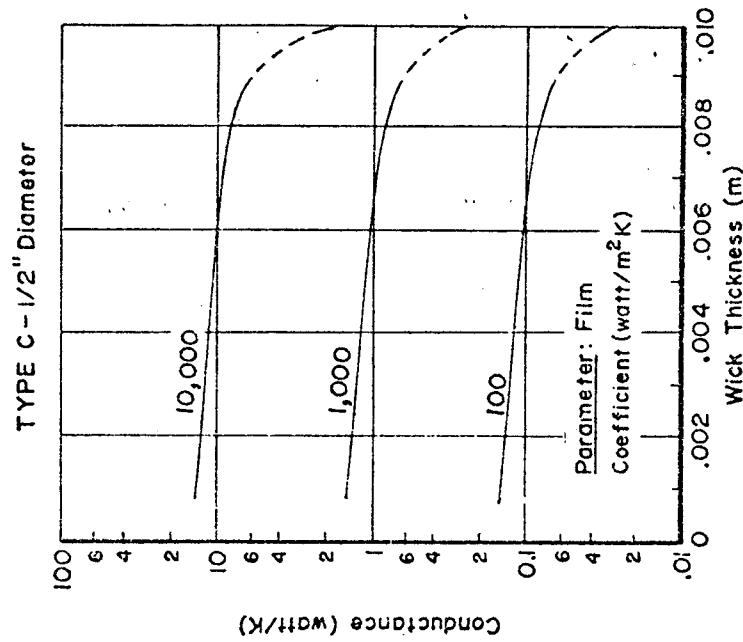
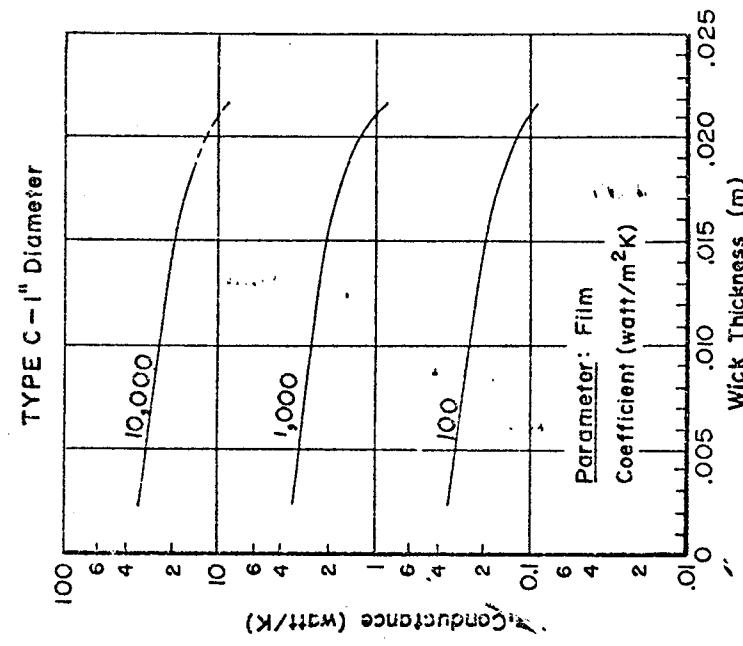
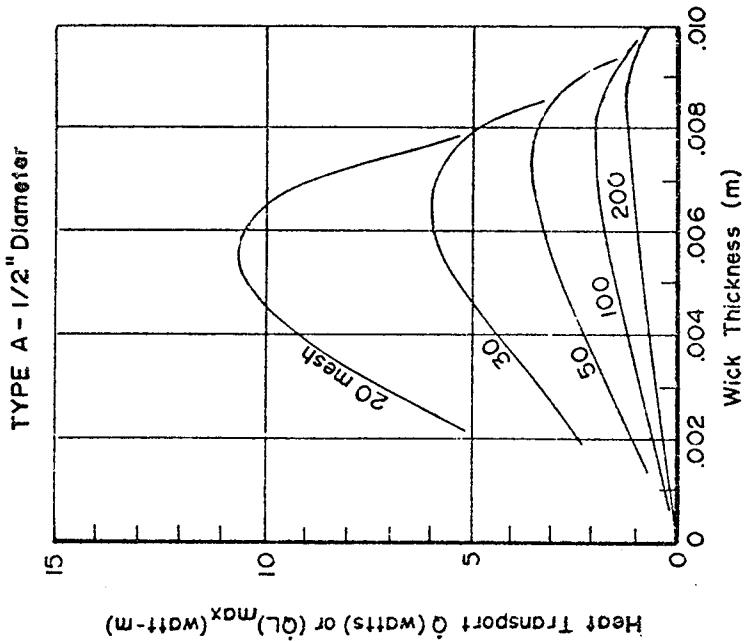
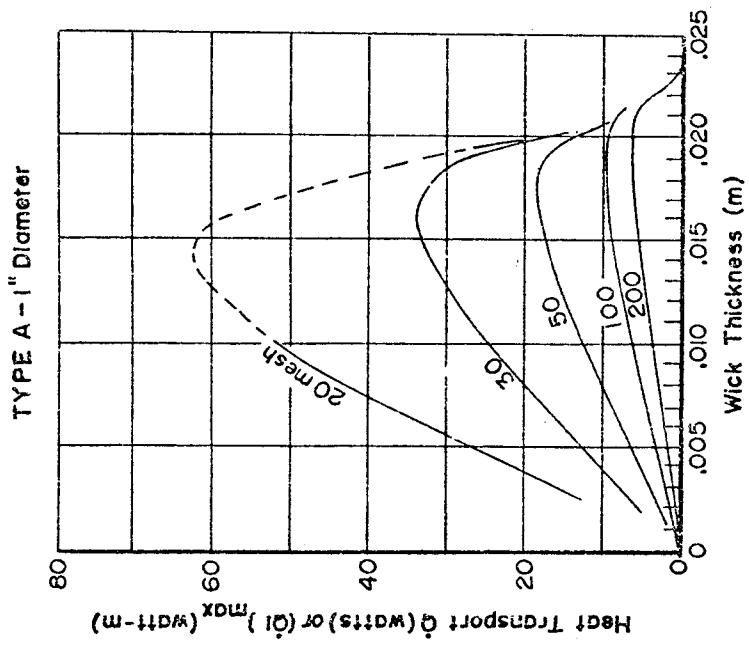


Figure P-5. Circumferential Screen Wick  
Static Wicking Height (Type B) 1.27 cm (1/2") and 2.54 cm (1") Heat Pipe Diameter



**Figure P-6. Porous Slab Wick**

**Axial Heat Transport (Type A) and Heat Pipe Conductance (Type C)**

Temperature: 77°K (-320°F)  
Container Material: Aluminum

Working Fluid: Nitrogen  
Wick Material: Stainless Steel

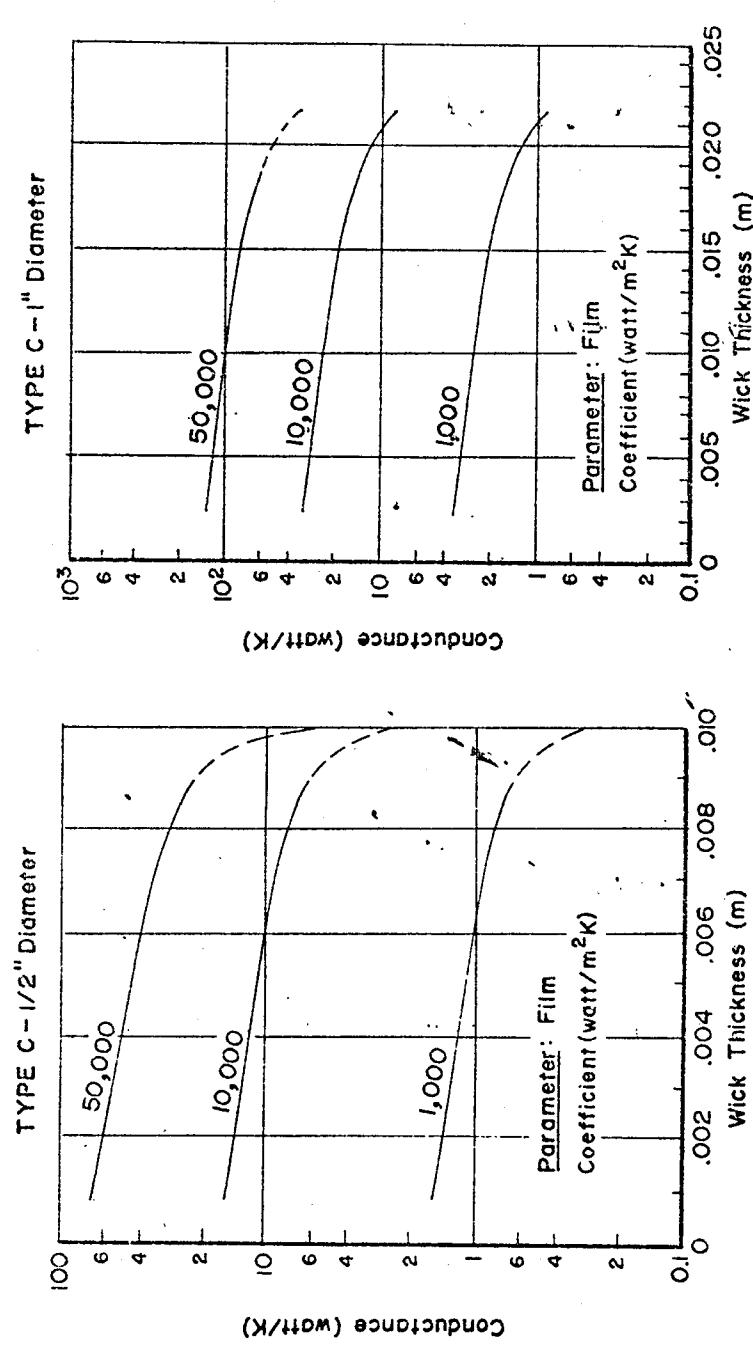
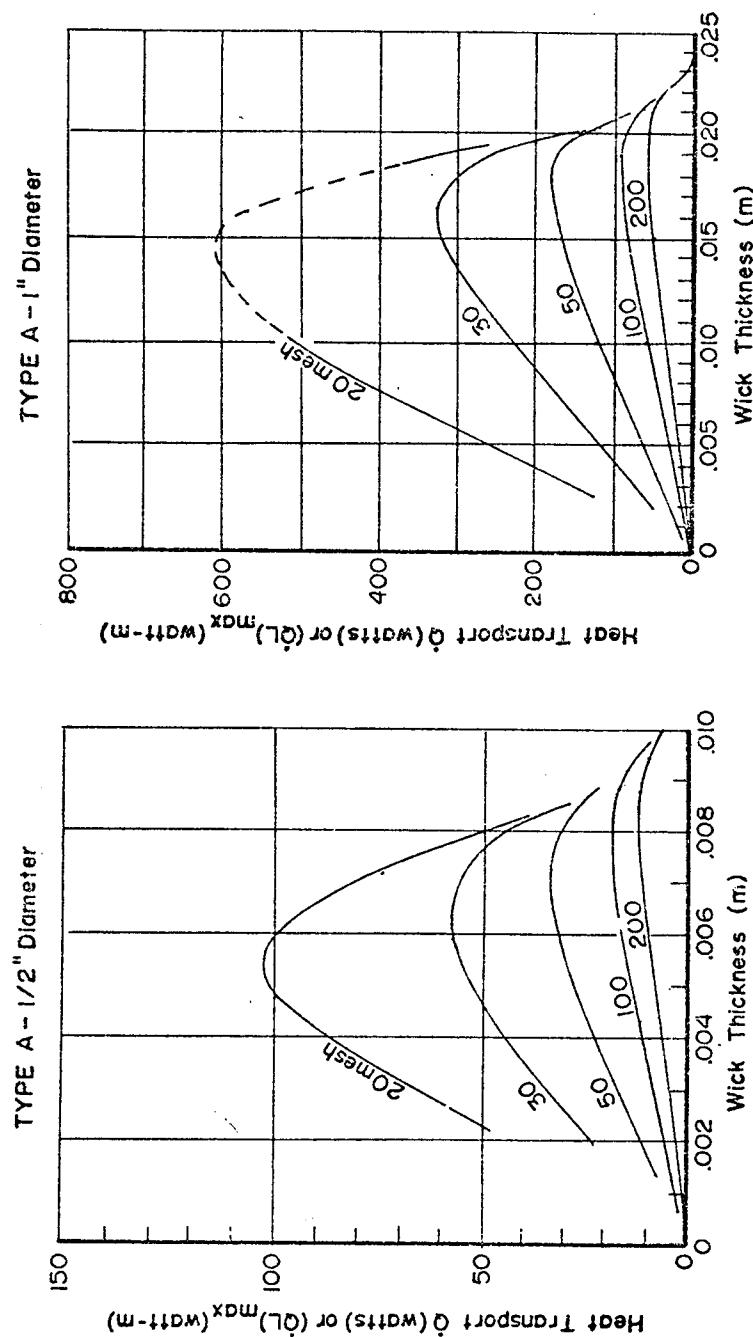


Figure P-7. Porous Slab Wick

Axial Heat Transport (Type A) and Heat Pipe Conductance (Type C)

Temperature: 273°K (32°F)

Container Material: Aluminum

Working Fluid: Ammonia

Wick Material: Stainless Steel

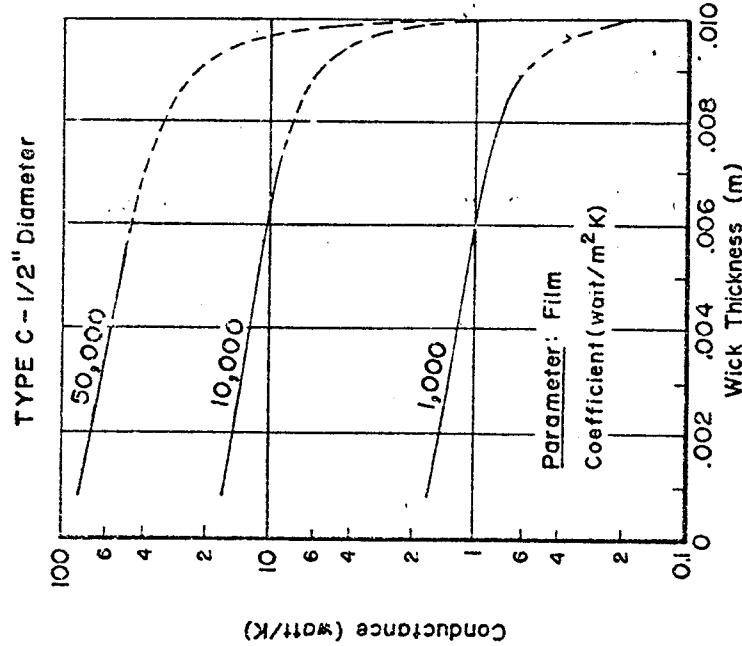
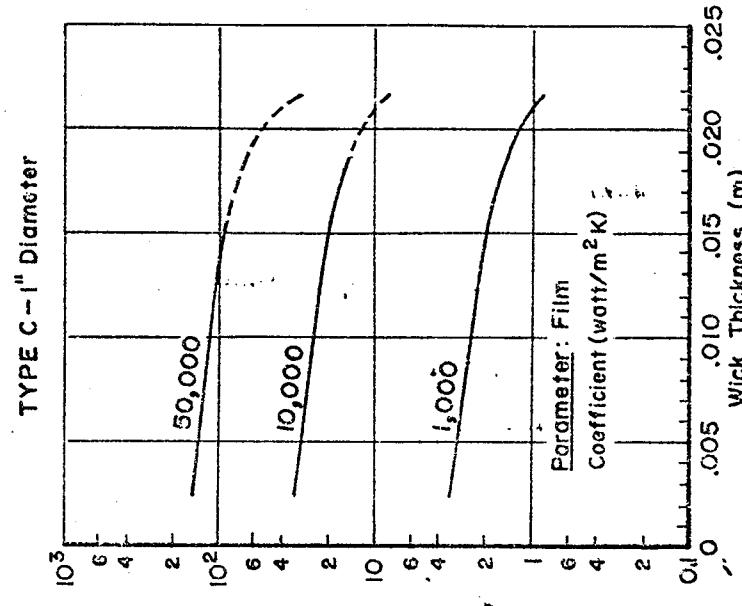
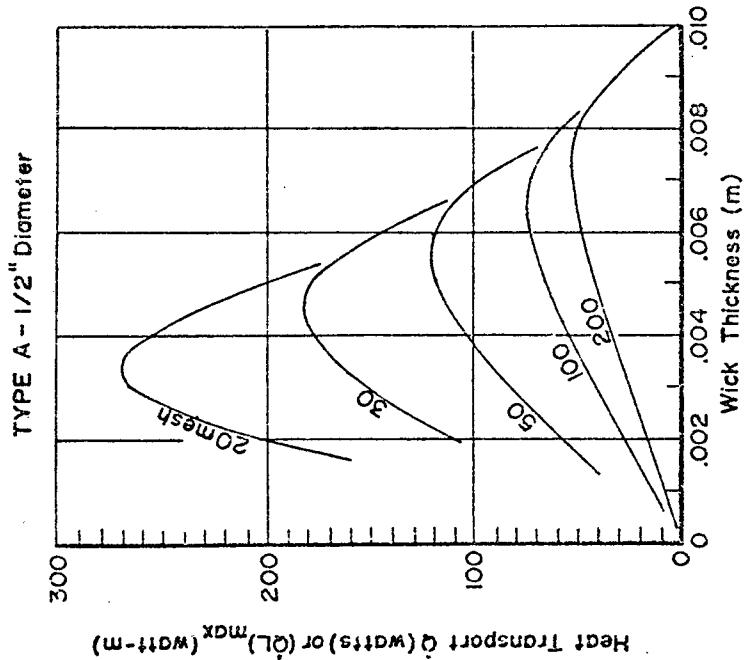
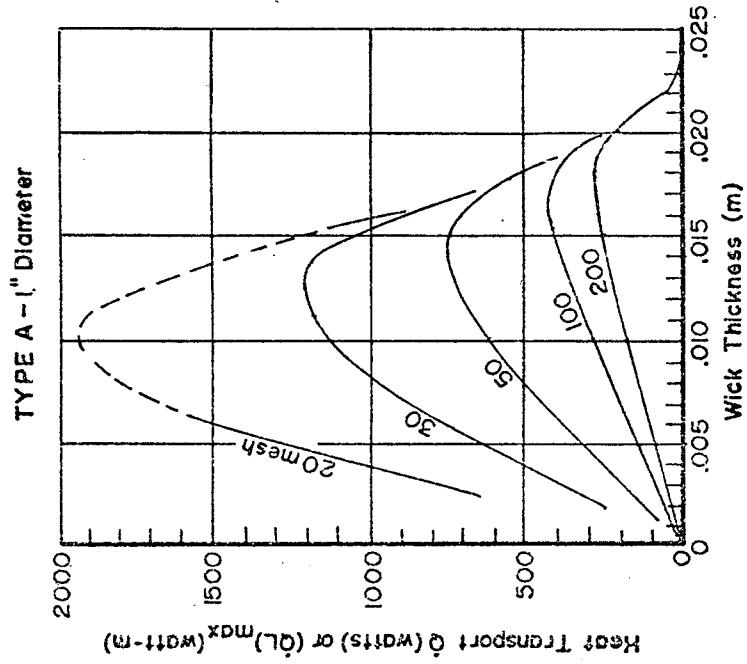


Figure P-8. Porous Slab Wick  
 Axial Heat Transport (Type A) and Heat Pipe Conductance (Type C)  
 Temperature: 373°K (212°F)  
 Container Material: Copper  
 Working Fluid: Water  
 Wick Material: Copper

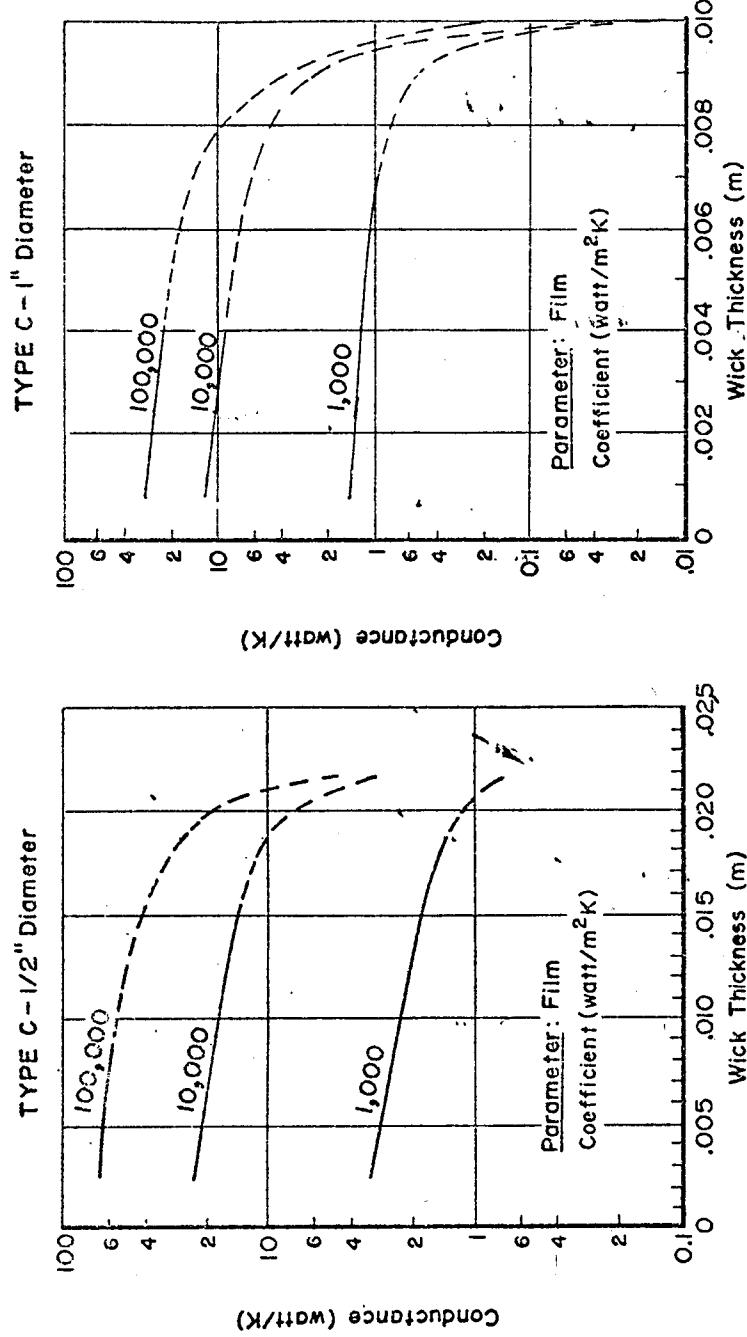
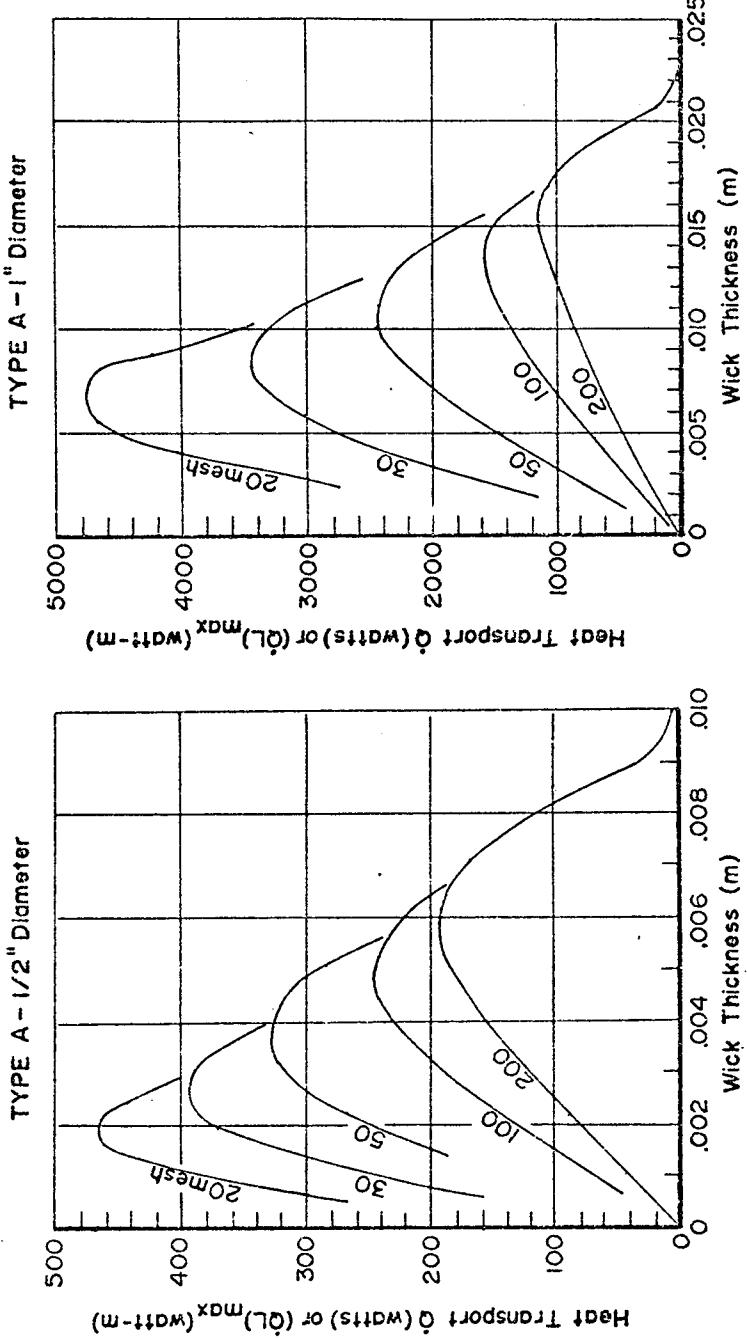


Figure P-9. Porous Slab Wick

Axial Heat Transport (Type A) and Heat Pipe Conductance (Type C)

Temperature:  $1100^{\circ}\text{K}$  ( $2011^{\circ}\text{F}$ )

Working Fluid: Sodium

Container Material: Stainless Steel

Wick Material: Stainless Steel

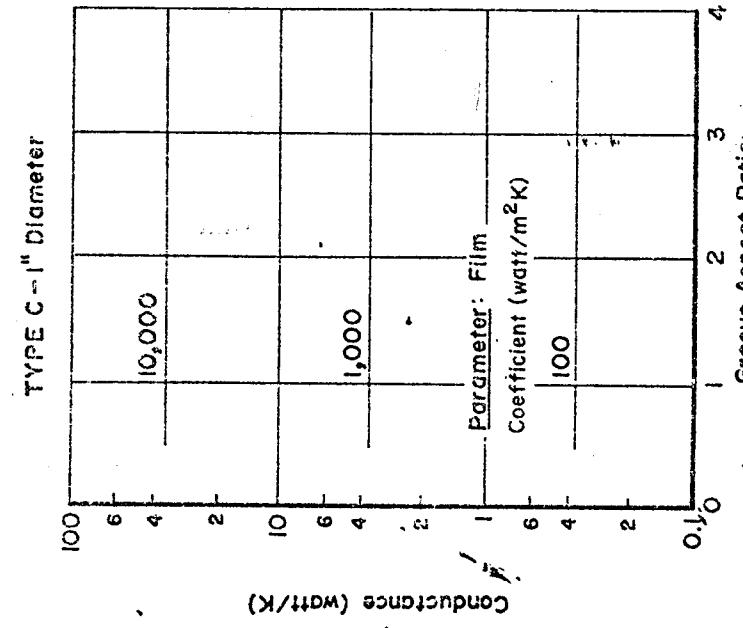
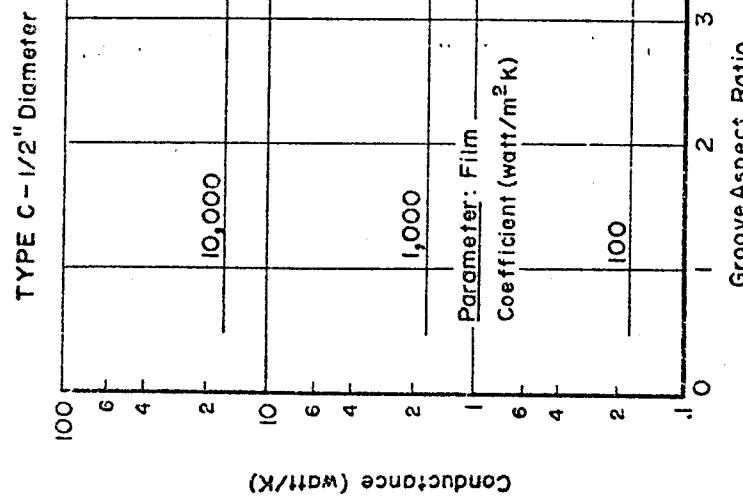
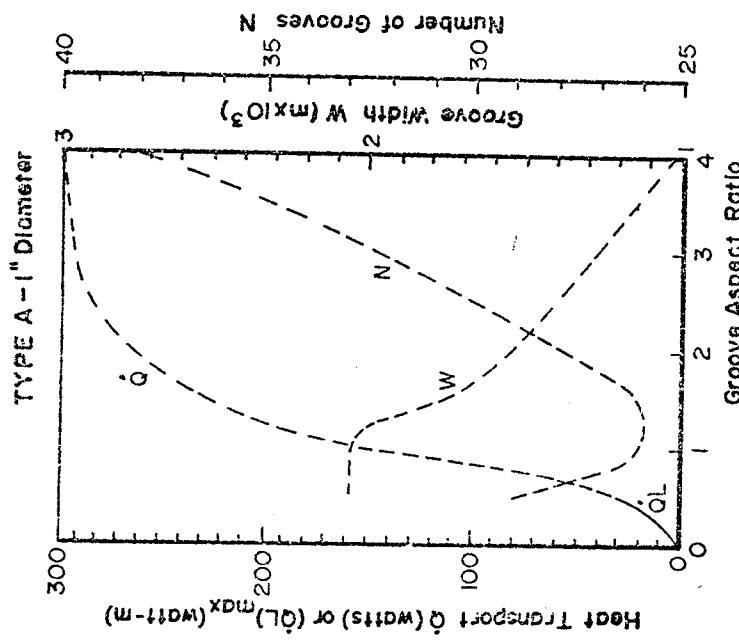
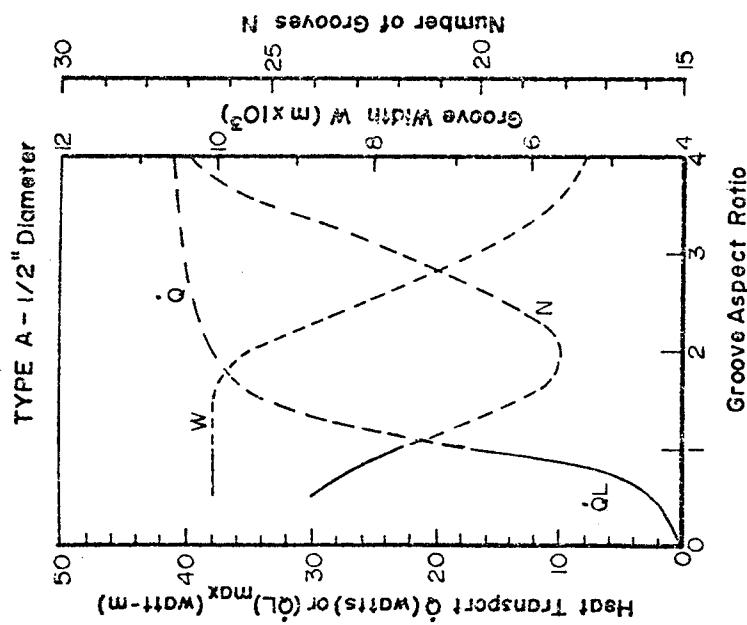


Figure P-10. Axially Grooved Heat Pipe

Axial Heat Transport, Groove Width and Number of Grooves (Type A)

and Heat Pipe Conductance (Type C)

Temperature: 770K (-320°F) Working Fluid: Nitrogen Container Material: Aluminum

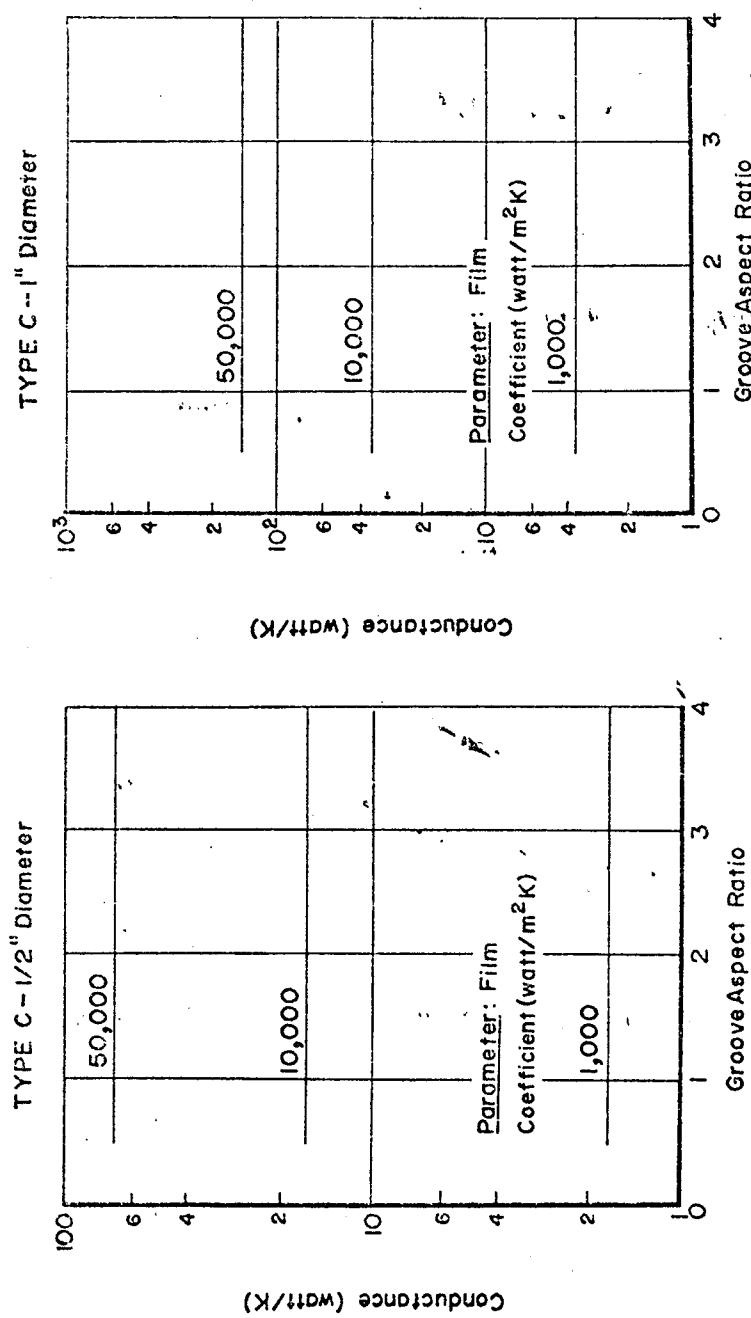
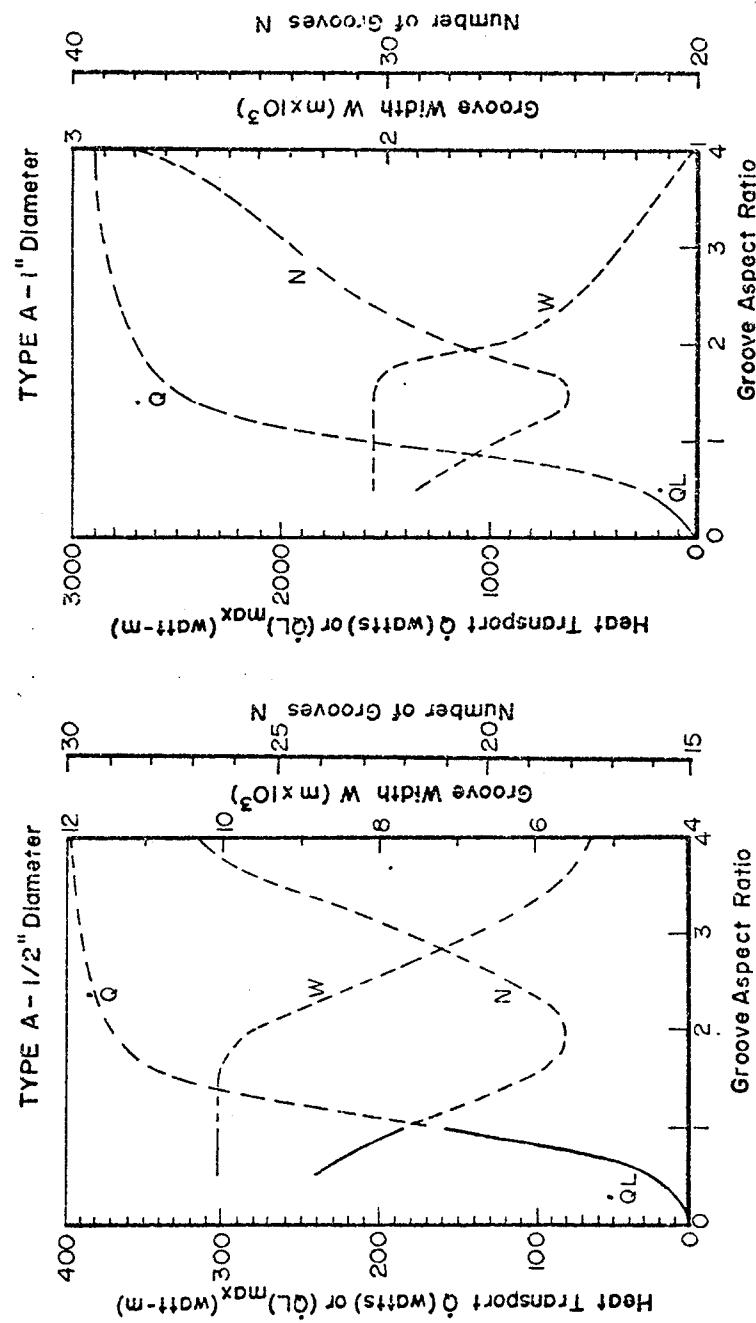


Figure P-11. Axially Grooved Heat Pipe  
Axial Heat Transport, Groove Width and Number of Grooves (Type A)  
and Heat Pipe Conductance (Type C)  
Temperature: 77°K (320°F) Working Fluid: Ammonia Container Material: Aluminum

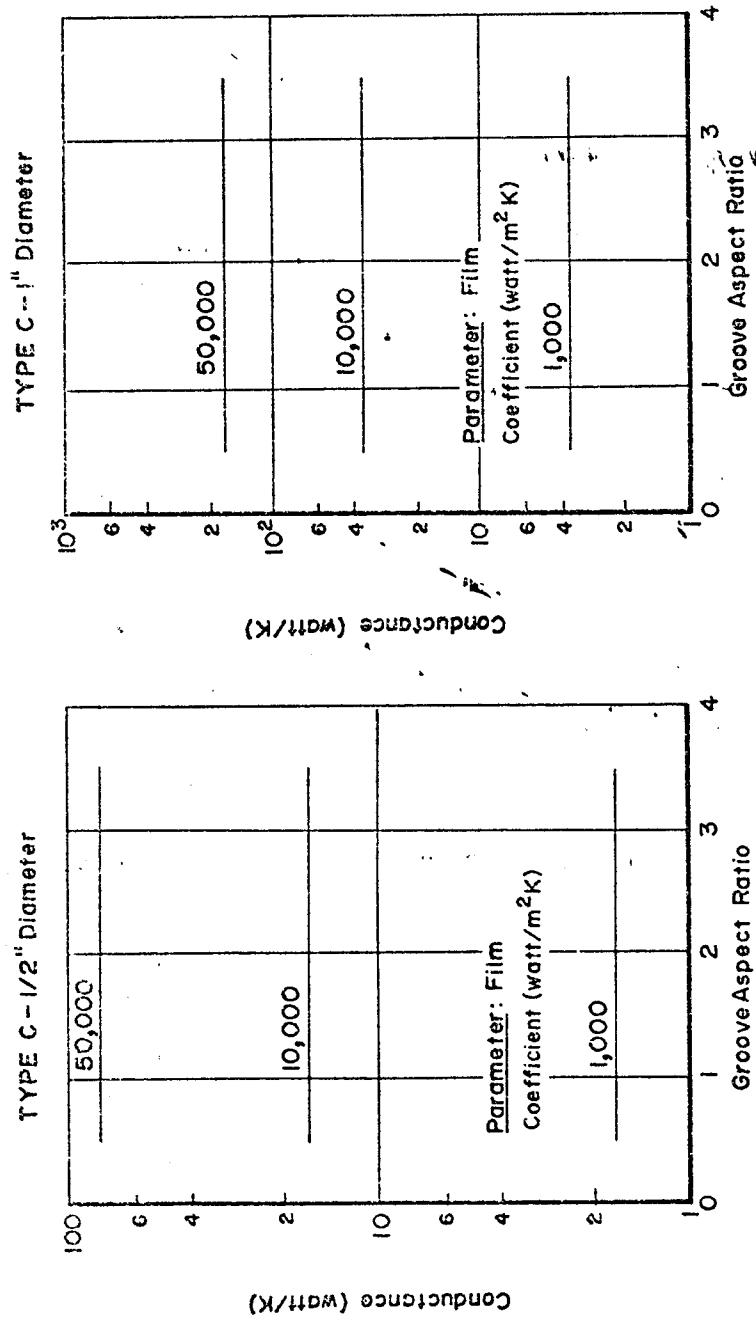
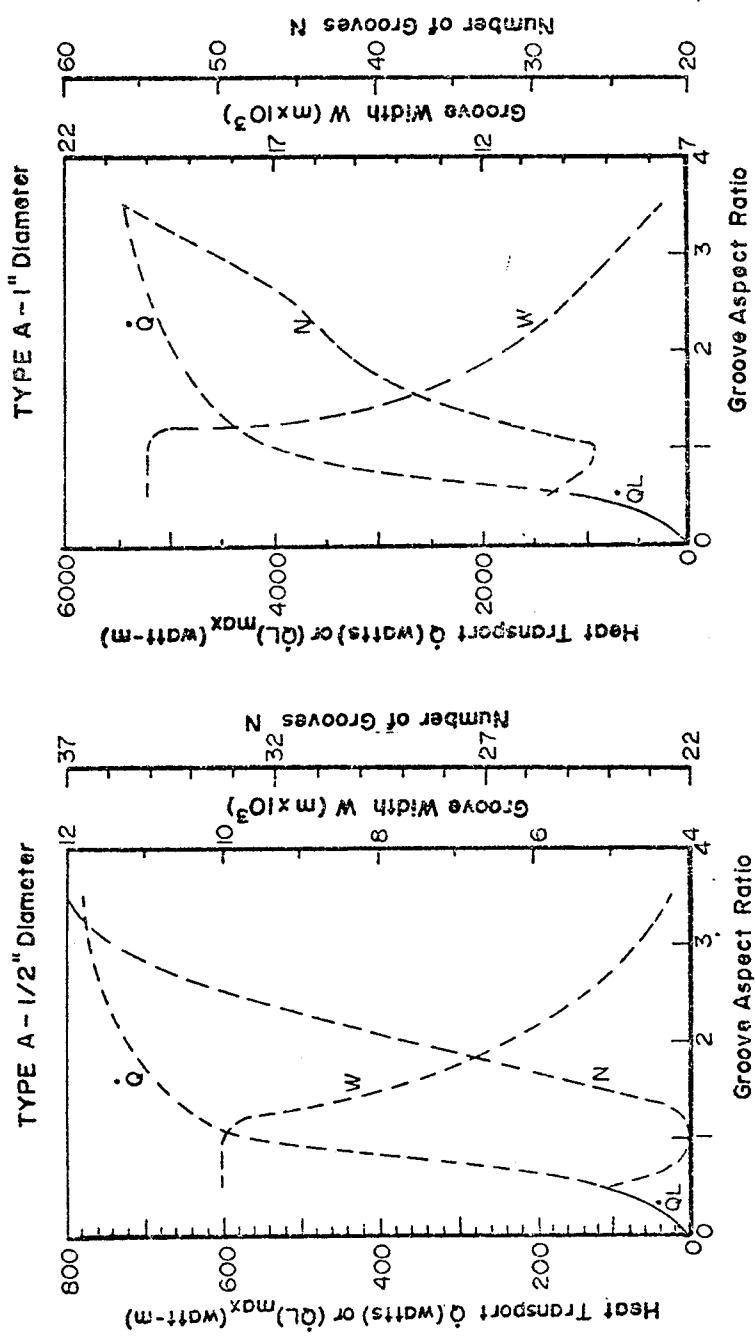


Figure P-12. Axially Grooved Heat Pipe  
Axial Heat Transport, Groove Width and Number of Grooves (Type A)  
and Heat Pipe Conductance (Type C)  
Temperature: 373OK (212°F) Working Fluid: Water Container Material: Copper

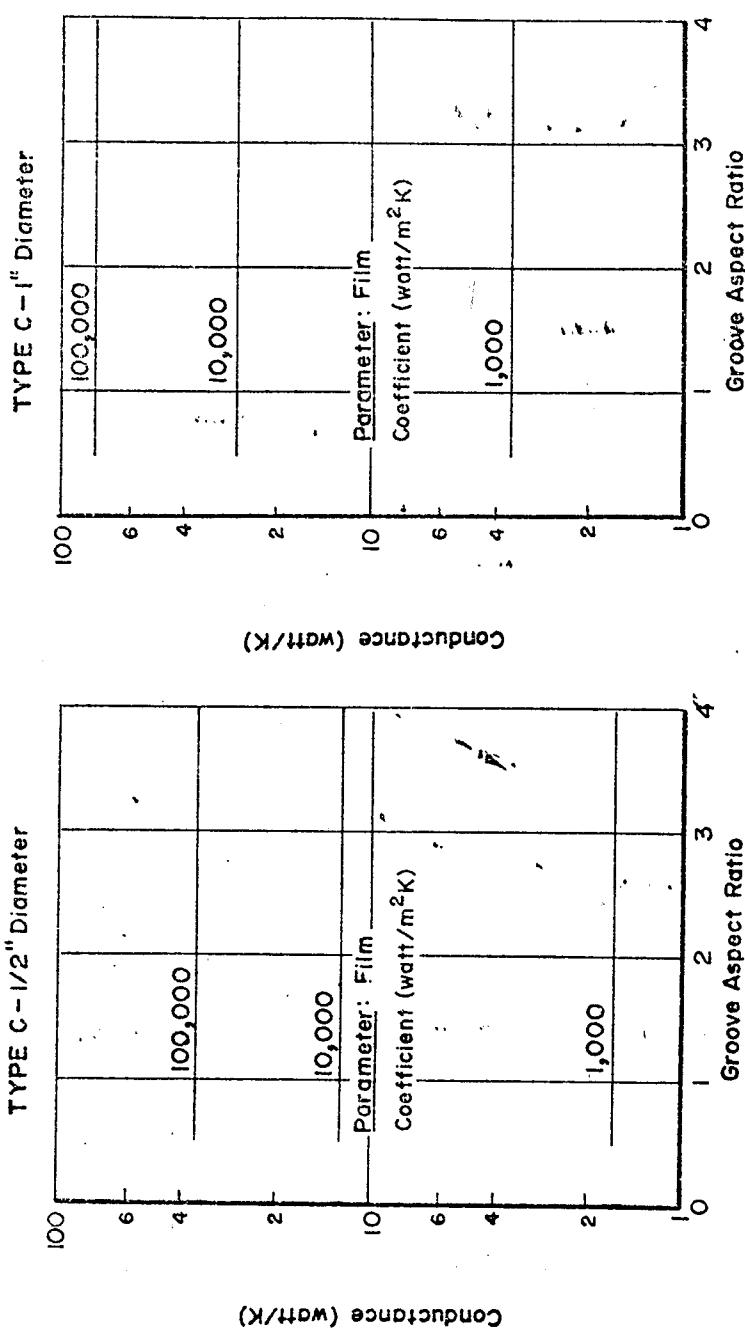
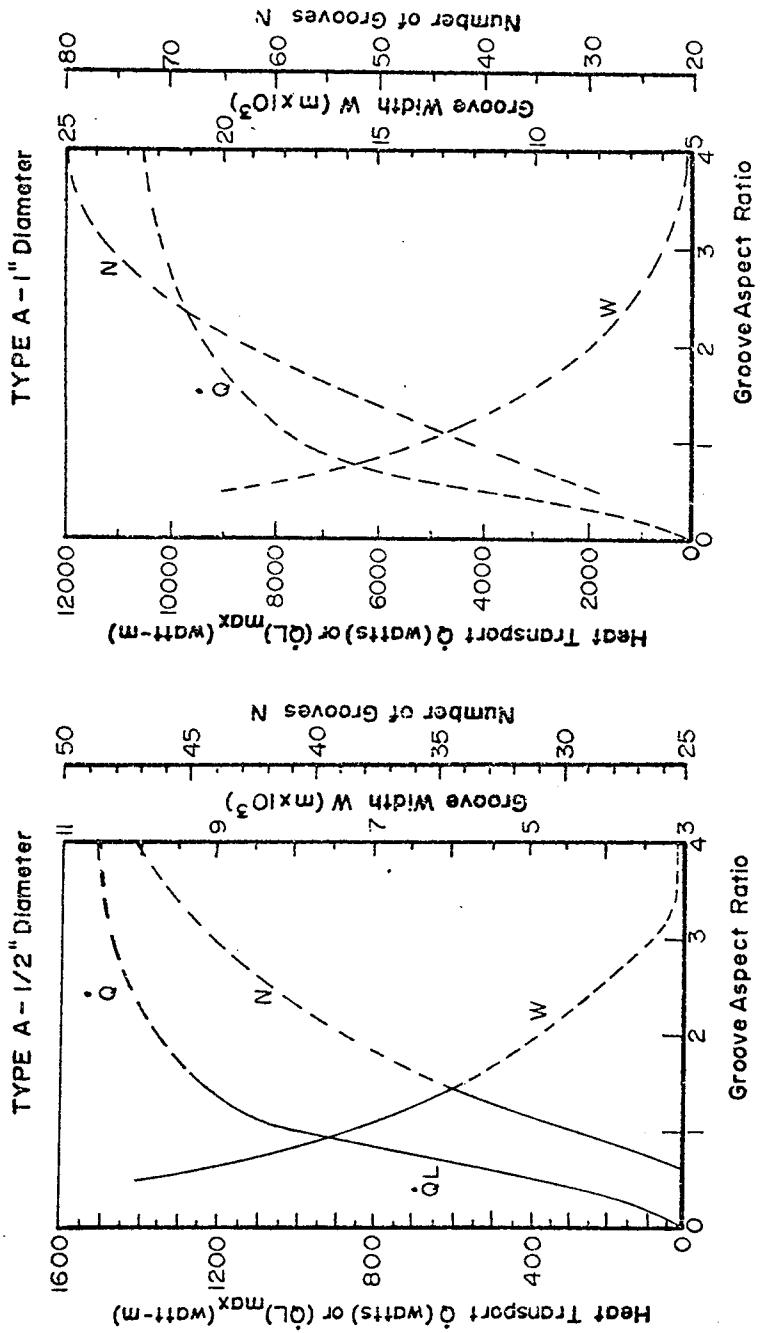


Figure P-13. Axially Grooved Heat Pipe

Axial Heat Transport, Groove Width and Number of Grooves (Type A) and Heat Pipe Conductance (Type C)

Temperature: 1100°K (2011°F) Working Fluid: Sodium Container Material: Stainless Steel

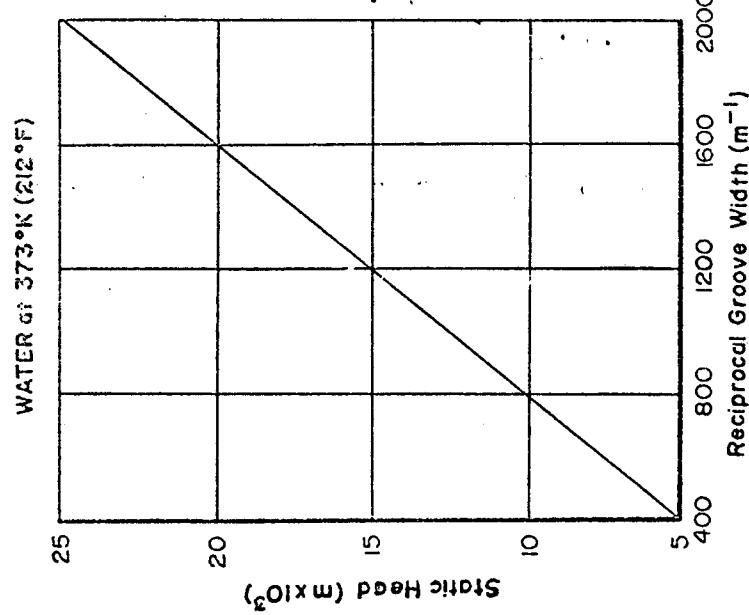
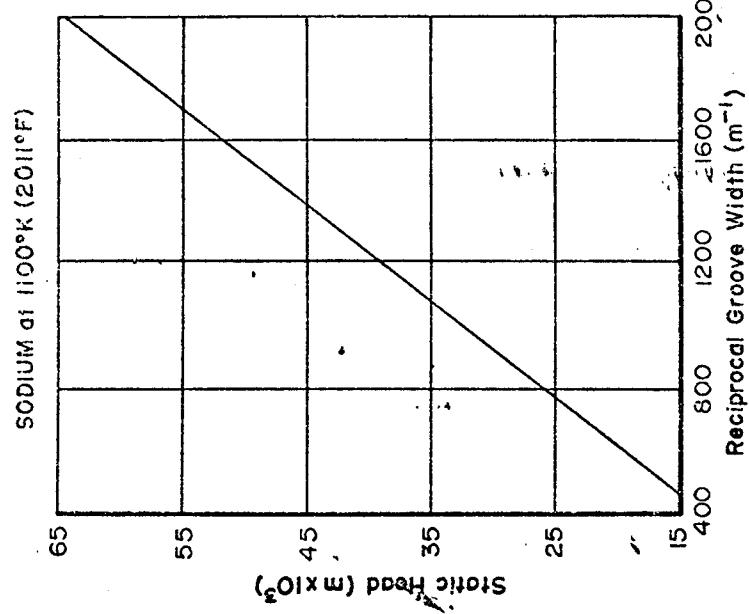
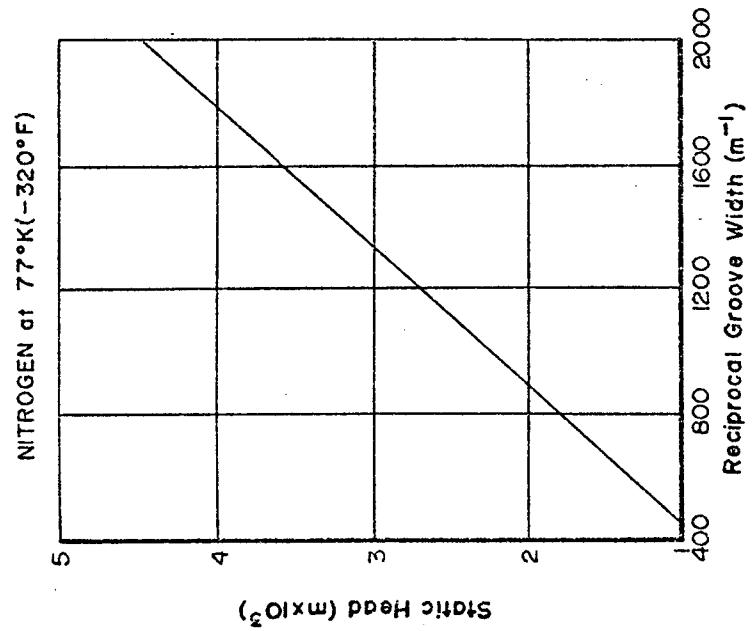
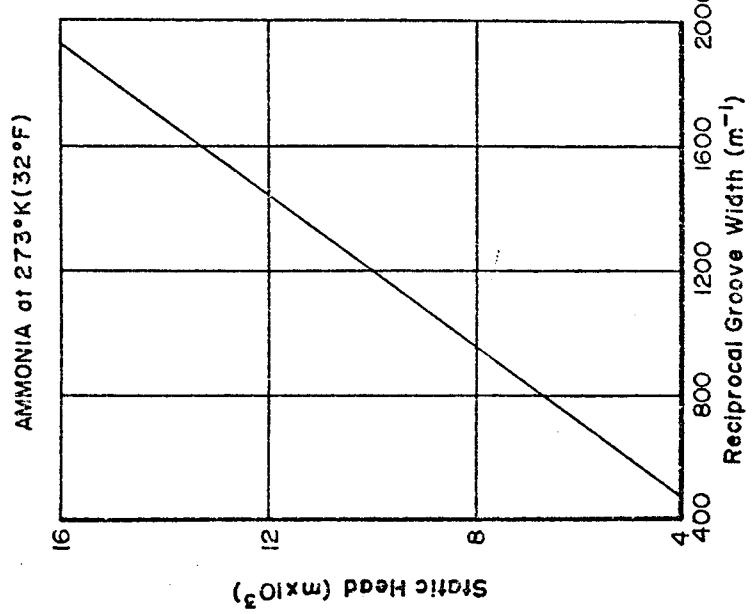


Figure P-14. Axially Grooved Heat Pipe

Static Wicking Height (Type B) (Independent of Heat Pipe Diameter)

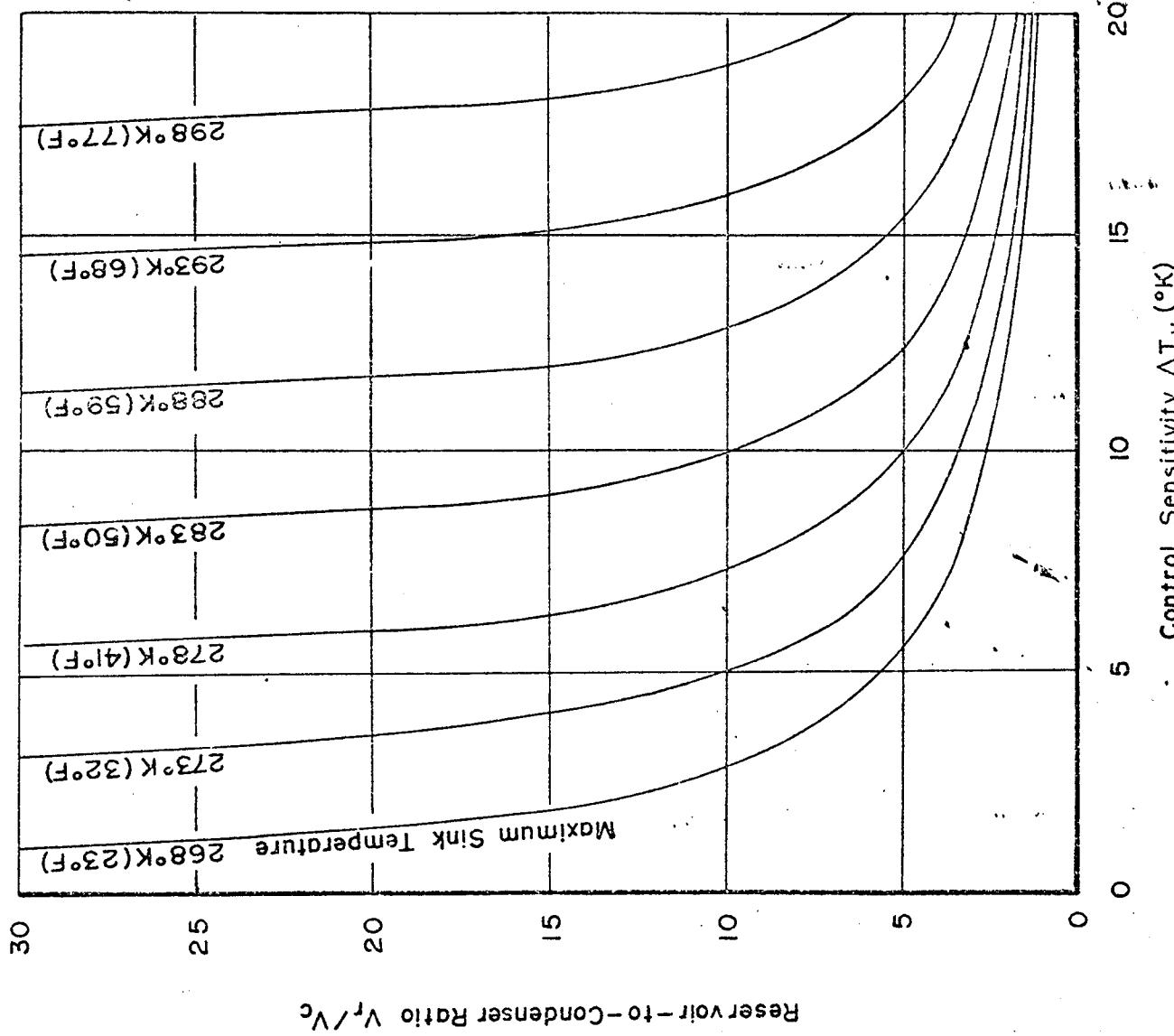


Figure P-15. Reservoir Sizing for VCHP with Cold-Wicked Reservoir (Type D)

Nominal Vapor Temperature: 318°K (113°F)  
 Minimum Sink Temperature: 268°K (23°F)  
 Working Fluid: Ammonia

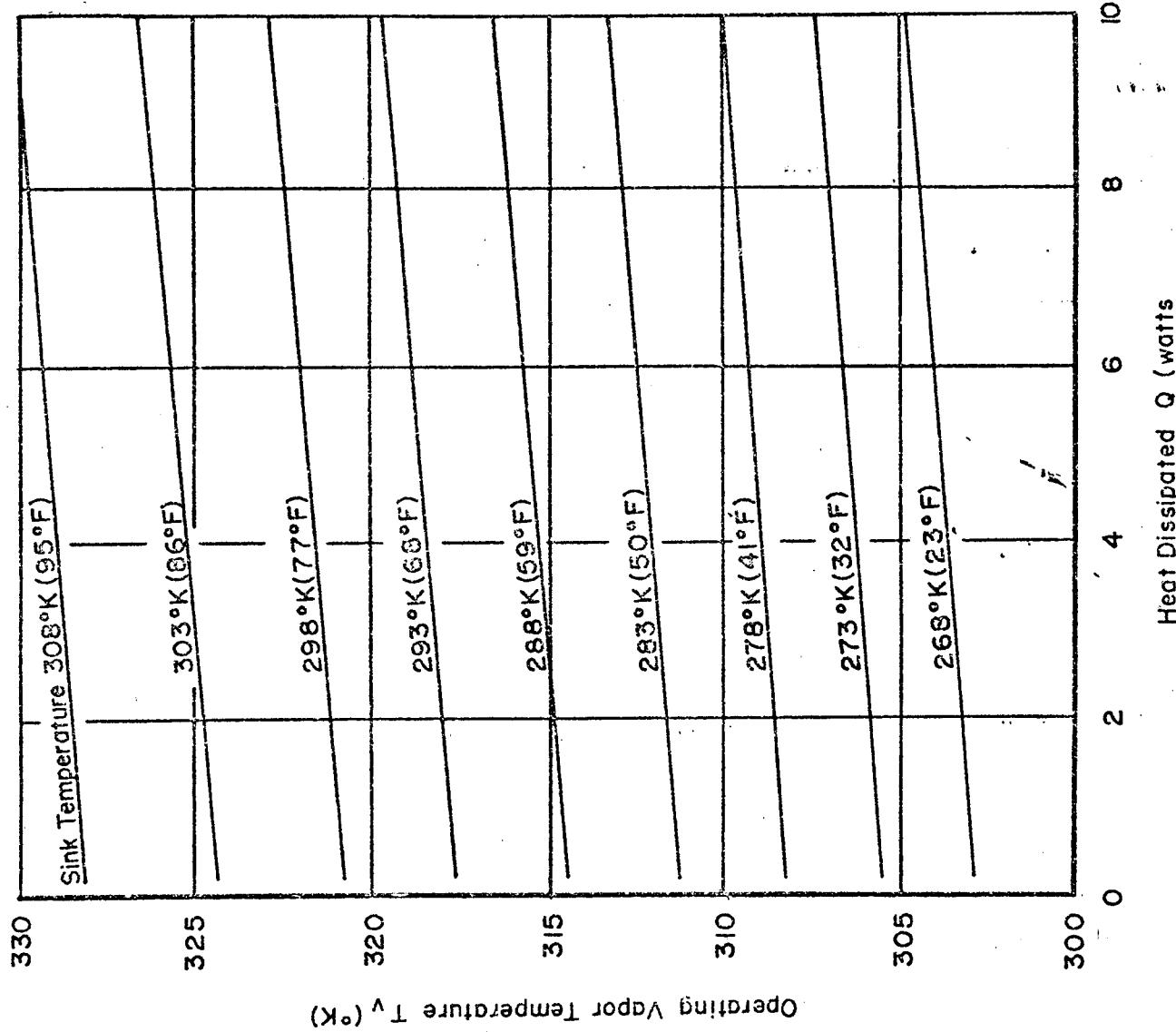


Figure P-16. Performance of VCEP with Cold Wicked Reservoir

Vapor Temperature versus Heat Load (Type E)

Nominal Vapor Temperature: 318°K (113°F)

Range of Sink Temperatures: 268° to 308°K (23° to 95°F)

Working Fluid: Ammonia

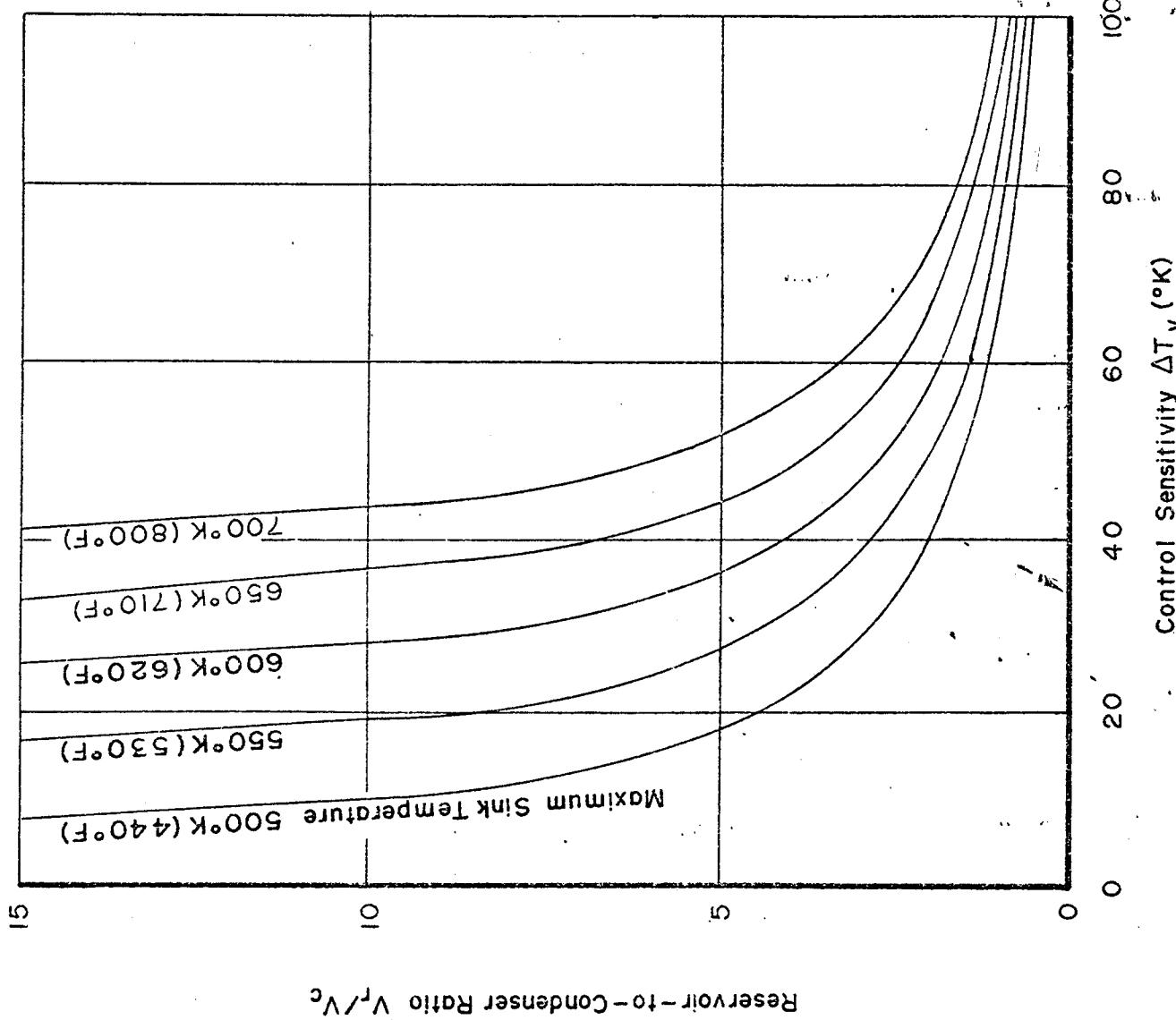


Figure P-17. Reservoir Sizing for VCHP with Cold Wicked Reservoir (Type D)

Nominal Vapor Temperature: 1100K (2011°F)  
 Minimum Sink Temperature: 500K (440°F)  
 Working Fluid: Sodium

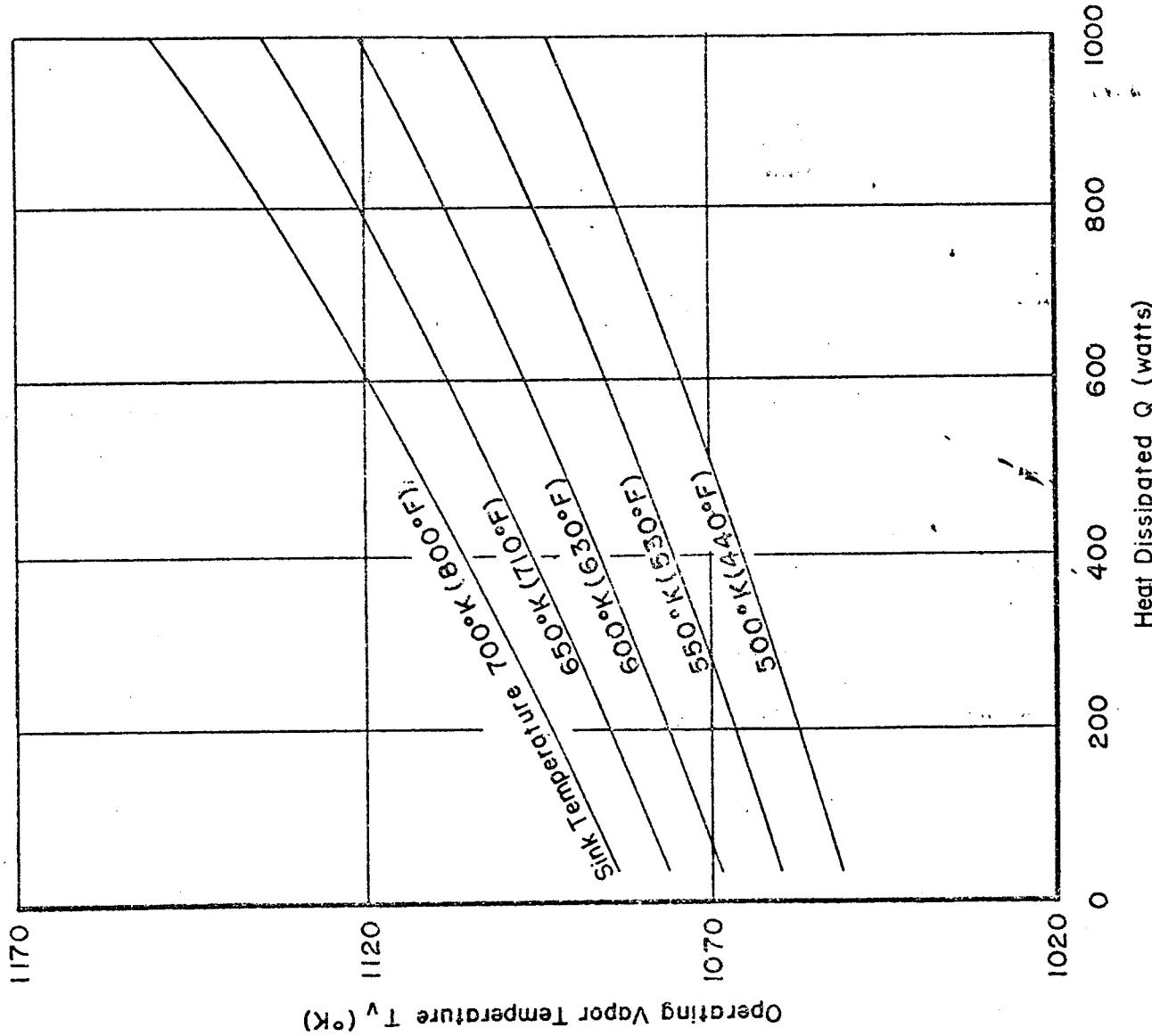


Figure P-18. Performance of VCHP with Cold Wicked Reservoir

Vapor Temperature versus Heat Load (Type E)

Nominal Vapor Temperature: 1100°K (2011°F)  
 Range of Sink Temperatures: 500° to 700°K (440° to 800°F)  
 Working Fluid: Sodium

W.1 Basic Properties

The choice of a wick design for a specific heat pipe application is determined by the proper trade-off between several important parameters. First, the wick should be capable of providing a high capillary pressure which is equivalent to possessing a small effective pore radius. Secondly, it should be capable of supporting high flow rates which means the wick should have a high permeability and therefore a large effective pore radius. These conflicting requirements have led to the development of non-isotropic "composite wicks" for which capillary pumping and permeability can be independently optimized. Finally, in many designs, the wick is directly in the heat flow path and therefore its thermal conductivity is an important consideration. The wick thermal conductivity is a function both of the wick material and the wick porosity.

W.2 Prediction of Properties

As was discussed in the Theory Chapter, often the only way to obtain accurate values for the various properties of wicks is by experimental measurements. However, reasonable estimates for preliminary evaluations can be made for several configurations.

W.2.1 Effective Pore Radius

The effective pore radius of a wick is defined in the Theory Chapter in terms of the maximum capillary pressure that the wick can sustain. The applicable Equation T-9 is repeated here:

$$\Delta P_{cap} = \frac{2 \sigma \cos \theta}{r_p}$$

W-1

For a few well-defined cases (see Figure W.1) the effective pore radius can be estimated with reasonable accuracy.

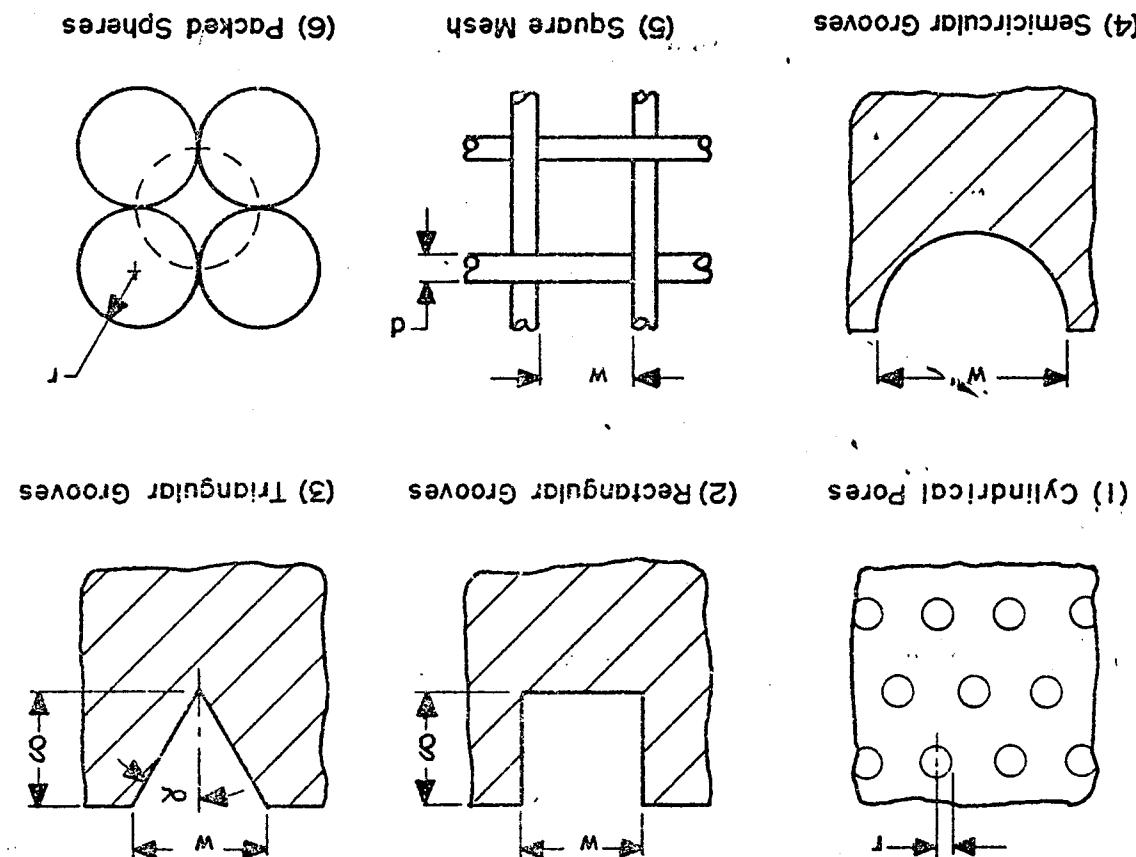
1. Cylindrical pores:

$$r_p = r$$

W-2

W-1

Figure W-1. Cases for Which the Effective Pore Radius can be Estimated



2. Rectangular grooves:

$$r_p = w$$

W-3

3. Triangular grooves: In the Theory Chapter, an analytical expression for the maximum capillary pressure in triangular grooves is given:

$$\Delta p_{cap} = \frac{\sigma \cos(\alpha + \theta)}{w/2} \quad W-4$$

In comparing Equation W-4 with Equation W-1, the difficulty of calculating a value for  $r_p$  independent of the wetting angle  $\theta$  becomes obvious since  $\cos(\alpha + \theta)$  cannot be resolved into factors containing just  $\alpha$  and  $\theta$ . For zero wetting angle, Equations W-1 and W-4 may be solved for the effective pore radius:

$$r_p = \frac{w}{\cos \alpha} \quad (\theta = 0) \quad W-5$$

R. G. Bressler and P. W. Wyatt (3) performed a numerical evaluation of the effective pore radius of triangular, semicircular, and square grooves. Their analytical results agreed well with capillary rise experiments. For triangular grooves they obtained:

$$r_p = \frac{w \cos \alpha}{1 - \sin \alpha} \quad W-6$$

In the limits for either very small  $\alpha$ 's (nearly rectangular grooves) or for  $\alpha \rightarrow \pi/2$ , Equations W-5 and W-6 give identical results. Some discrepancy exists for intermediate values of the groove half-angle.

4. Semicircular grooves: Reference 3 gives the following expression for the capillary radius:

$$r_p = \frac{1}{2} \frac{\pi w}{(\pi - 2)} \quad W-7$$

W-3

5. Wire mesh: For a square mesh weave and zero wetting angle, Reference 4 gives the following relation:

$$r_p = \frac{w + d}{2} \quad W-8$$

When the wire diameter and spacing are approximately equal, Equation W-8 reduces to:

$$r_p \approx w \approx d \quad W-9$$

Equations W-8 and W-9 are applicable only to single layers of screen. It is noteworthy that the last two equations predict an effective pore radius which is approximately equal to the mesh opening. It would be expected that the effective radius would be closer to one-half the opening; however, experimental evidence verifies the validity of Equations W-8 and W-9. For multilayer screens, no generally applicable relationship is known. The effect of intermeshing is to reduce the effective pore radius; therefore, Equation W-8 yields a conservative estimate for multilayer screens.

6. Randomly packed spheres: Analysis of the packing of spheres reveals that for any one mode of packing, the porosity is independent of sphere size; i. e., the ratio of pore-to-sphere volume is a constant. Thus, the pore radius is a definite fraction of the sphere radius. Assuming a cubic packing mode for the spheres, References 8 and 17 give the following relation:

$$r_p = 0.41 r \quad W-10$$

where  $r$  is the average sphere radius. The average sphere radius is often a difficult quantity to determine; Scheidegger (21) discusses this in detail and the reader is referred to his discussion. Equation W-10 is also a good approximation for sintered particle wicks.

7. Fibrous wicks (21):

$$r_p = \frac{d + \sqrt{32 K/\epsilon}}{2}$$

W-11

where  $d$  is the fiber diameter. This relation can also be used for felt metals.

The above equations offer only approximate estimates for the effective pore radius in various "well defined" wick structures. Generally, precise design values can only be determined by experimental measurements. Literature values for experimental determinations are relatively sparse. Table W-2 summarizes much of the available data.

W.2.2 Permeability of Various Wicks

Working estimates for the value of the permeability can only be found for certain well-defined wick geometries. The analytical expressions are summarized below and the experimental results are given in Table W-2.

1. Parallel cylindrical capillaries of circular cross-section (13):

$$K = \frac{\epsilon D^2}{32}$$

W-12

The porosity,  $\epsilon$ , is defined here as the fraction of the volume of the capillaries to the total volume. This term often causes confusion when irregular porous materials are encountered. Scheidegger (21) discusses this and the concept of permeability in detail. Equation W-12 applies also for a single capillary tube if  $\epsilon = 1$  is used.

2. Closed rectangular channels (9):

$$K \approx \frac{D_h^2}{2 (f \cdot Re)}$$

W-13

Equation W-13 was obtained by rearranging the expressions from

Reference 13 into parameters which are consistent with the nomenclature of this Handbook. The hydraulic diameter used in Equation W-13 is defined as:

$$D_h = \frac{4 \times \text{Flow Area}}{\text{Wetted Perimeter}} \quad \text{W-14}$$

According to Equation W-13, the permeability of rectangular channels is a function of the parameter  $f \cdot Re$ , which is the product of the Fanning friction factor and the Reynolds number. For laminar flow, which always exists in the liquid phase of a heat pipe, the product of  $f \cdot Re$  is a constant and independent of the flow rate (13) and is only a function of the aspect ratio of the flow channel. This relationship is plotted in Figure W-2. For the special case of cylindrical channels,  $f \cdot Re$  equals 16 and the permeability given by Equation W-13 becomes identical for that of a single capillary tube (Equation W-12 with  $\epsilon = 1$ ).

3. Concentric Annuli: The expression for the permeability is identical to Equation W-13. The hydraulic diameter  $D_h$  must be evaluated using Equation W-14, and the product ( $f \cdot Re$ ) is given in Figure W-3 for various ratios ( $D_i/D_o$ ) of inner-to-outer diameter.
4. Open, rectangular channels (grooves): Equation W-13 also applies for open grooves. However, in calculating the hydraulic diameter  $D_h$  from Equation W-14, it is observed that only a part of the perimeter is wetted and that the groove may not be completely filled. The hydraulic diameter of a rectangular groove, accounting for the effect of the meniscus (see Figure W-4), is given by:

$$D_h = \frac{4 \delta w - A_{\text{seg}}}{w + 2\delta} \quad \text{W-15}$$

The area of the segment  $A_{\text{seg}}$  is a function of the radius of curvature  $R$ :

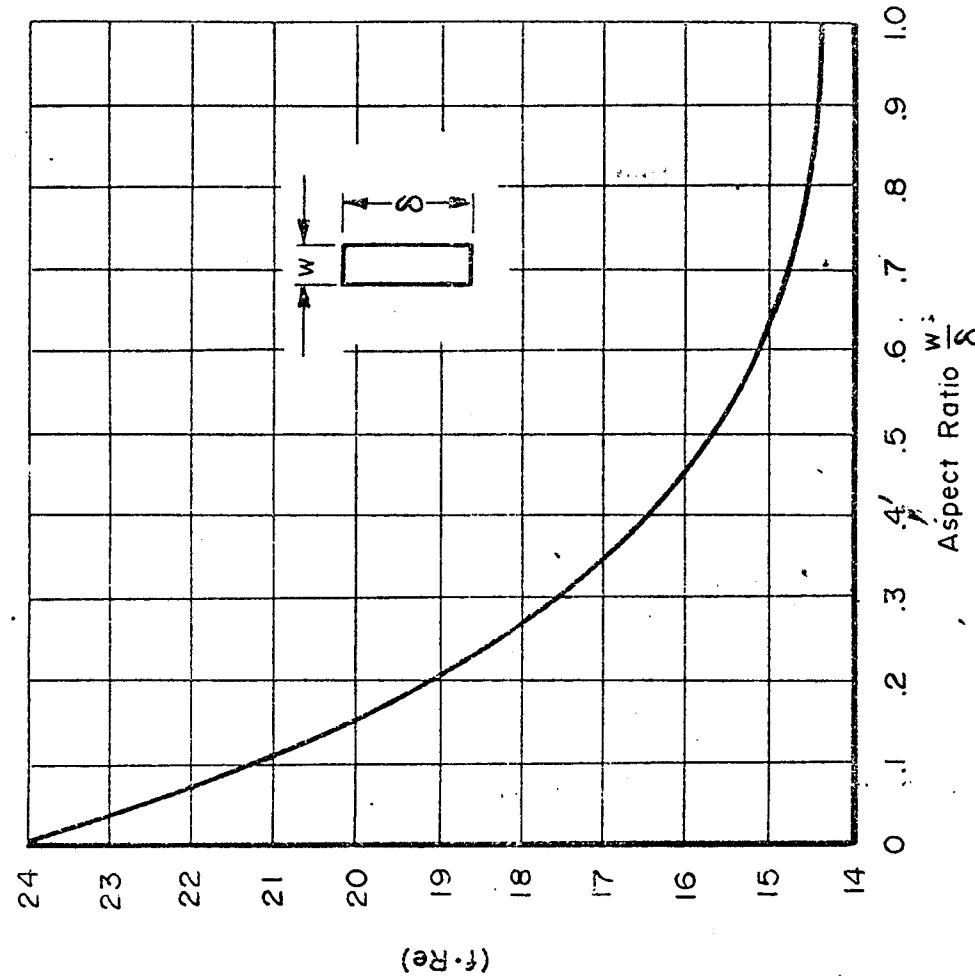


Figure W-2.  $(f/Re)$  vs. Aspect Ratio for Fully Developed Laminar Flow in Rectangular Tubes

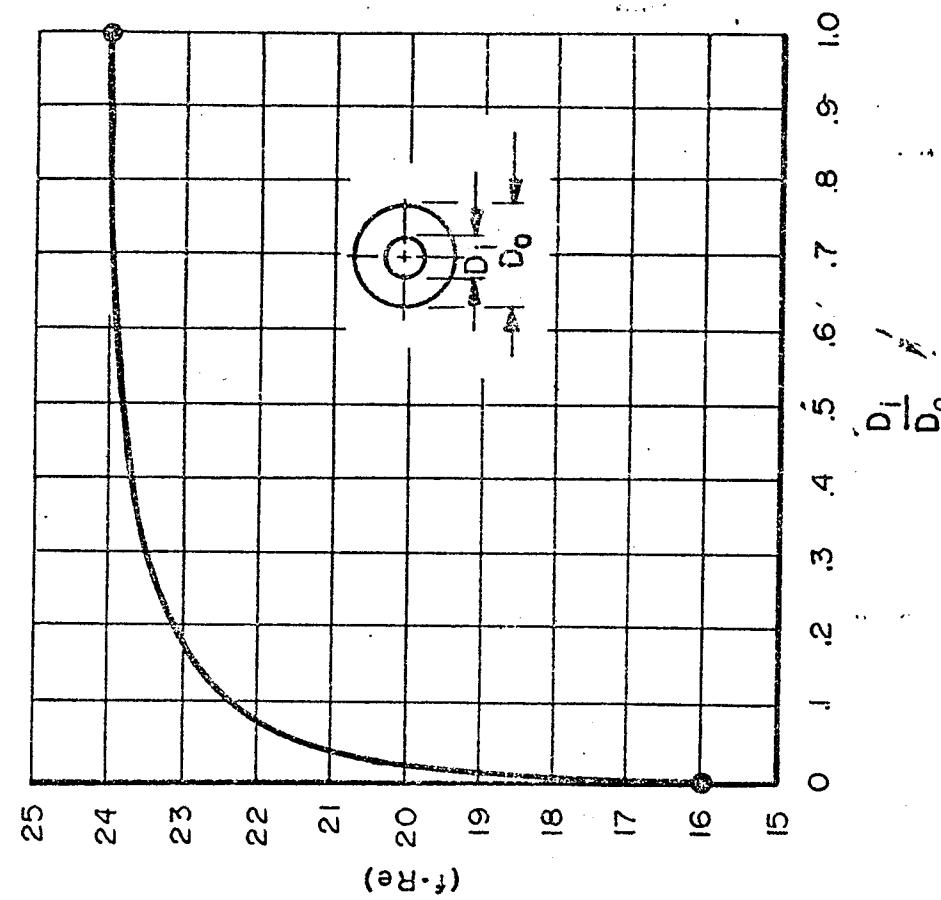


Figure W-3. (F·Re) for Fully Developed Laminar Flow in Circular Annuli

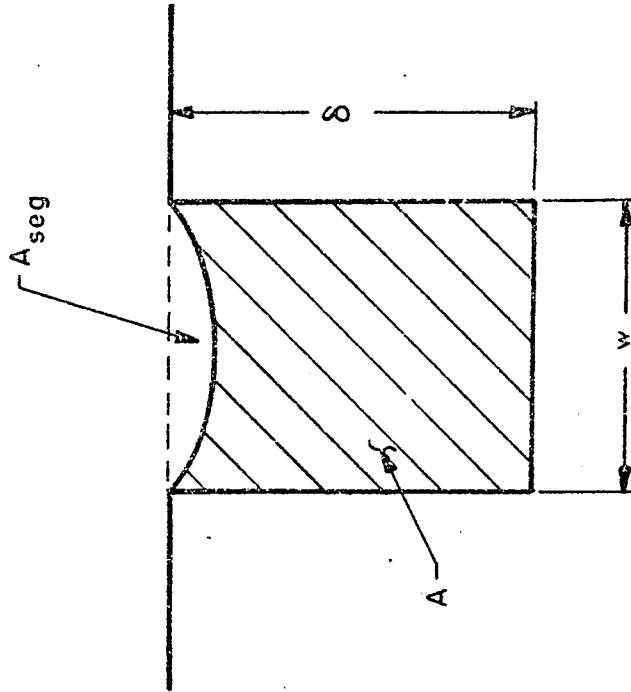


Figure W-4. Rectangular Groove with Meniscus Segment

$$A_{\text{seg}} = R^2 \sin^{-1} \left( \frac{w/2}{R} \right) - \frac{w}{2} \sqrt{R^2 - \left( \frac{w}{2} \right)^2} \quad \text{W-16}$$

At the condenser end,  $R$  approaches infinity and  $A_{\text{seg}}$  equals zero. At the evaporator end,  $R$  attains its minimum value which is equal to  $w/2$  if the heat pipe is operating at its capillary limit and the wetting angle is zero. Thus, the area of the segment and the effective hydraulic diameter of the grooves vary along the length of the heat pipe. Partially filled grooves can be treated with the same basic Equations -- W-13, W-15, and W-16. However, they are of no practical value in heat pipes since they have only one, fixed meniscus ( $R = w/2 \cos \theta$ ). The pressure balance in a heat pipe requires that the interfacial pressure, and therefore the radius of the meniscus varies in accordance with the pressure gradients in the liquid and the vapor. Since partially filled grooves do not permit this axial variation of  $R$  they represent an unstable operating condition.

5. Wire mesh (22) (19):

$$K = \frac{d^2 \epsilon^3}{122 (1 - \epsilon)^2}$$

W-17

The porosity  $\epsilon$  may either be determined experimentally or estimated from screen manufacturers' data sheets. Marcus (18) gives an analytical expression for the porosity which neglects intermeshing of the wires:

$$\epsilon = 1 - \frac{\pi S N d}{4}$$

W-18

The dimensionless empirical "Crimping Factor,  $S'$ " is normally of the order of unity ( $\sim 1.05$ ). If intermeshing of tightly wound screens is accounted for (5), the Crimping Factor,  $S$ , may be as large as 1.3. Equation W-17 is plotted in Figure W-5 and the agreement with several experimental studies is indicated. For quick reference, the predicted permeabilities of several standard mesh screens are also shown.

6. Packed spheres:

$$K = \frac{(2r)^2 \epsilon^3}{150 (1 - \epsilon)^2}$$

W-19

where  $r$  is the average sphere radius. This is the Blake-Kozeny equation (2) which, except for the empirical constant, is equivalent to the equation for screens.

W. 3 Composite Wicks

Conventional wicks, such as multilayer screens, grooves, fibrous wicks, etc., suffer from the conflicting requirement of high capillary pumping (which is obtained with small pores) and good permeability (which is obtained with large pores). The concept of "composite wicks" circumvents this conflict because the capillary

W-10

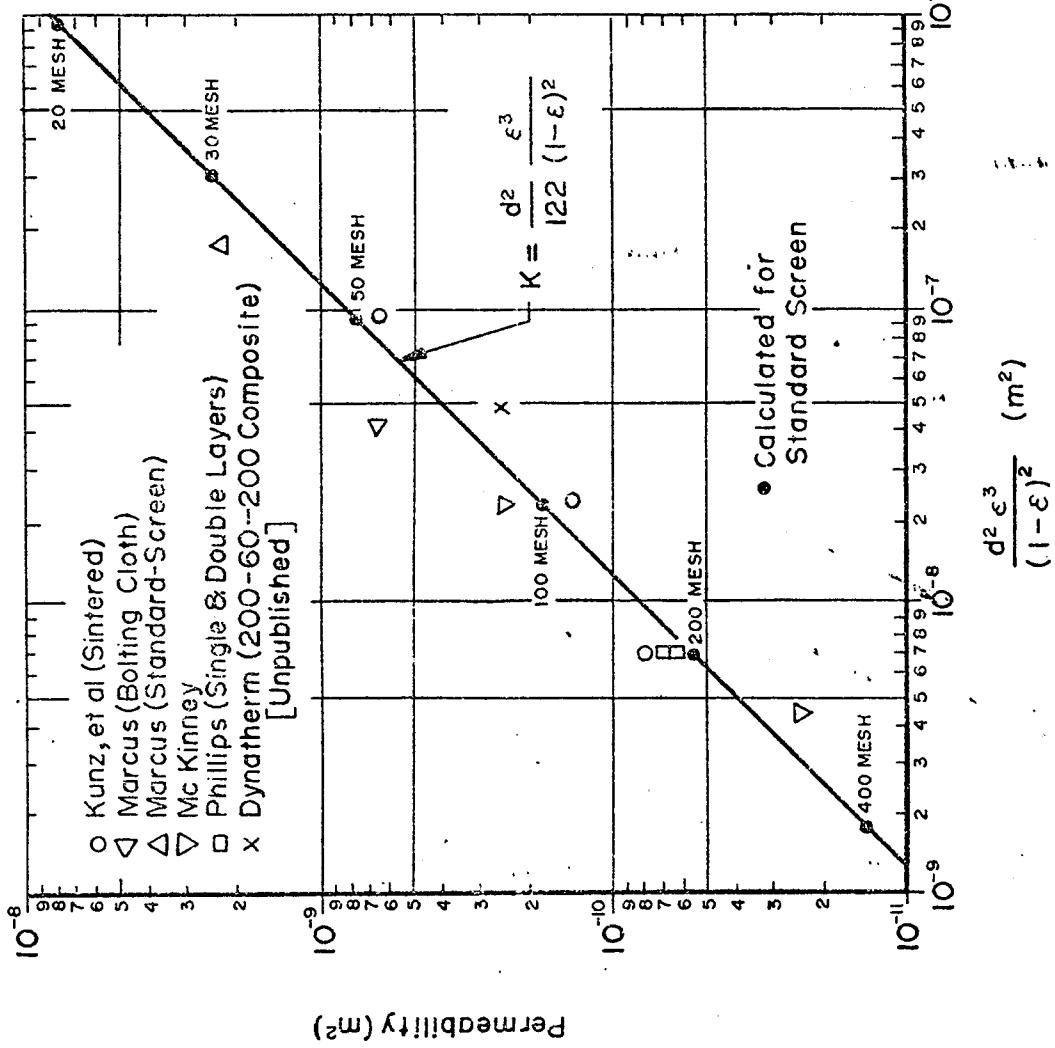


Figure W-5. Permeability of Screen Wicks  
(Modified Blake-Kozeny Equation)

pumping function is separated from the transport function of the wick. Typical configurations of composite wicks are shown in Figure W-6, and the corresponding permeabilities and wick areas are given in Table W-1. In each of these configurations, the liquid-vapor interface is located in the wick having the small pores and this provides the high capillary pumping. The bulk of the liquid flows through the wick with the larger pores, and this provides the high permeability which results in a low frictional pressure drop.

In order to realize the high capillary pumping capability of the small pore wick, the following two conditions must prevail:

1. The liquid-vapor interface must be located within the wick with the small pores.
2. No vapor or gas bubbles which are larger than the pore size of the outer wick can exist within the coarse, inner wick.

The first condition stipulates that the wick must be fully saturated; that is, sufficient working fluid must be present to fill the entire wick. The second condition is more difficult to achieve. Vapor bubbles may be generated as a result of nucleate boiling. Noncondensing gas bubbles may either be generated as a result of gas coming out of solution or may simply be trapped in the wick during the initial priming of the wick (1). Generally, the more open the flow passages of the coarser wick, the more sensitive the wick is to failures associated with vapor or gas bubbles. Thus, the arterial wicks (4, 5, 6 and 7 shown in Figure W-6) are more difficult to maintain primed than are composite wicks (2 and 3 shown in Figure W-6) consisting of different mesh size screen.

Several mechanisms are available for priming the wick prior to start-up of the heat pipe. In a zero "g" environment, priming will occur automatically as a result of surface tension forces since the liquid will seek the state of lowest-free energy which is attained when the wick is completely filled. In a one "g" environment, priming of the wick is usually accomplished as a result of surface tension forces, but the presence of gravity opposes the filling of the wick since filling generally increases the potential energy of the system. As a general rule of thumb, a composite wick will be self-priming if the capillary pressure of the coarser wick exceeds the gravity head

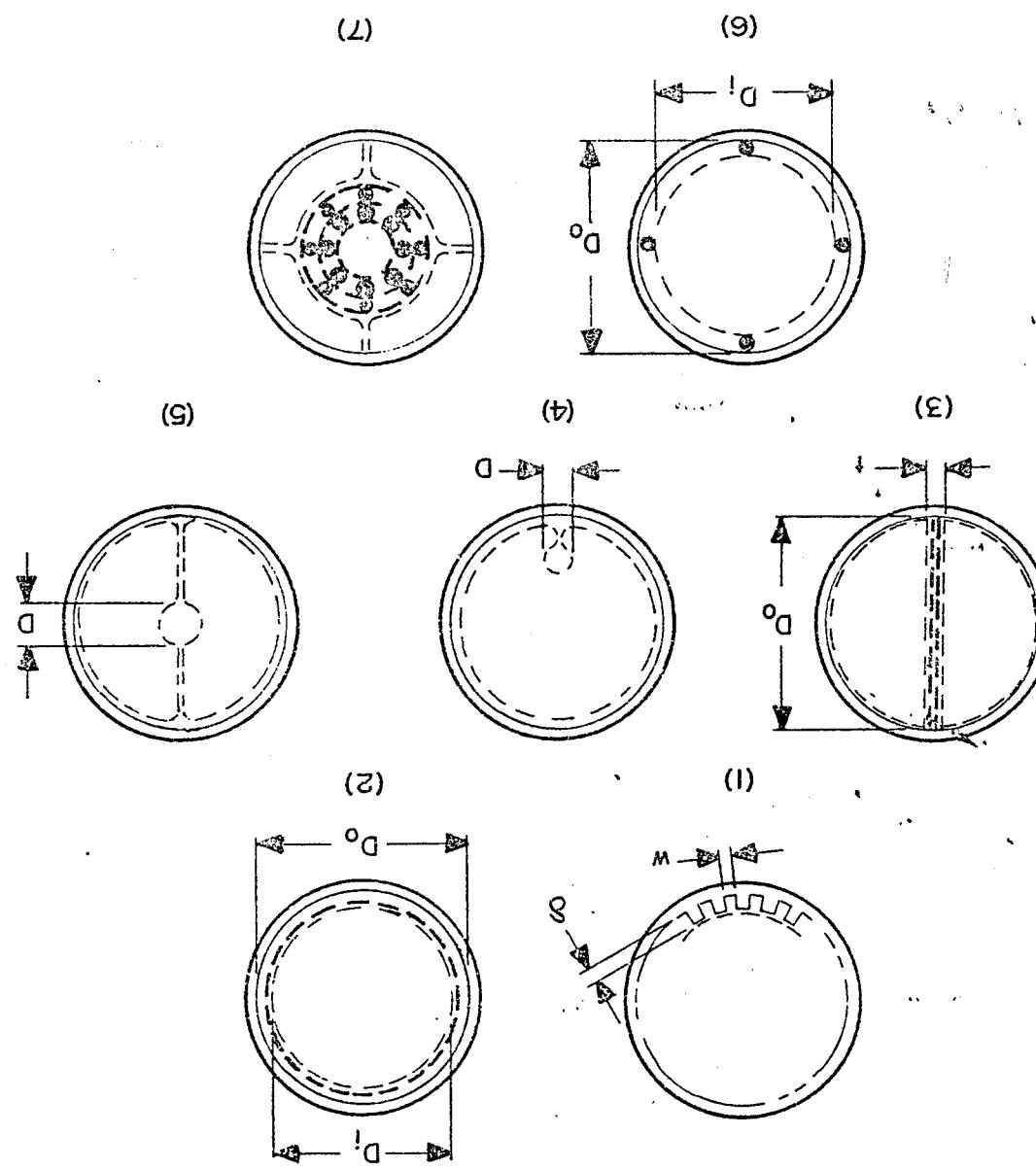


Figure W-6. Selected Composite Wick Geometries

Table W-1. Properties of Selected Composite Wicks

No.	Wick Type	Permeability	Wick Area	Comments
1	Screen Covered Axial Grooves	$2 \frac{6}{5} \frac{w}{2}$ $(f \cdot Re) (6 + w)^2$	$N^6 w$	$N =$ number of grooves $(f \cdot Re)$ from Figure W-2
2	Multilayer Screen with Smaller Mesh Screen Adjacent to Vapor Space	$d^2 \frac{e^3}{3}$	$\frac{122 (1 - e)^2}{4 (D_o^2 - D_i^2)}$	$D_o =$ Inner diameter of wall $D_i =$ Vapor Core Diameter $e$ and $d$ apply to coarse screen
3	Composite Slab	$d^2 \frac{e^3}{3}$	$t D_o$	$t$ and $e$ apply to coarse screen
4	Closed Artery	$\frac{D^2}{32}$	$\frac{\pi}{4} D^2$	$D =$ Diameter artery
5	Closed Annulus	$\frac{1}{4} (D_o^2 - D_i^2)$	$\frac{2 (f \cdot Re)}{\pi} (D_o - D_i)$	$D_o =$ Inner diameter of wall $D_i =$ Vapor Core Diameter $f \cdot Re$ from Figure W-3 $e$ and $t$ apply to coarse screen Effect of spacer wires neglected
6	Spiral Artery	$\frac{t^2}{12}$	$t l$	$t =$ spacing b/w spiral layers $l =$ unrolled spiral length $e$ and $t$ apply to coarse screen Effect of spacer wires neglected

associated with the largest dimension  $h$  as measured in the direction of the gravity field:

$$\frac{2\sigma \cos \theta}{(r_p)_{\text{coarse}}} \geq \rho_1 g h \quad W-20$$

For the case of an arterial wick, a more detailed equation is given in Reference 1.

A different priming mechanism, which does not rely on surface tension forces, is described in Reference 15. It has been referred to as "pressure" or "Clapeyron" priming. It utilizes a pressure difference between the outside and the inside of the composite wick to force fluid into the wick. The pressure difference is due to a corresponding temperature difference in the liquid. Relatively small temperature differences can result in large pressure differences if the saturation pressure is not too low. Pressure priming can provide a stronger driving force than surface tension alone. It is therefore less sensitive to gravity, and wicks with much wider flow passages can be primed in a gravity field. For details of the technique, the reader is referred to Reference 15.

#### W.4 Experimental Values

Very little experimental data for wick materials suitable for use in heat pipes has been reported in the literature. Much of the available data is summarized in Table W-2. Investigators have utilized various techniques for determining the effective pumping radius and the permeability of the wicks. It has been observed that the results are influenced by the test methods so that care must always be exercised when the experimental data is used.

##### W.4.1 Effective Pore Radius

Several investigators (16) (14) (10) (7) have used the technique of measuring the maximum height  $h$  to which a liquid will rise in a wick material when the bottom of the material is immersed in the liquid. The effective pore radius can then be determined using:

$$r_p = \frac{2\sigma \cos \theta}{\rho_1 g h} \quad W-21$$

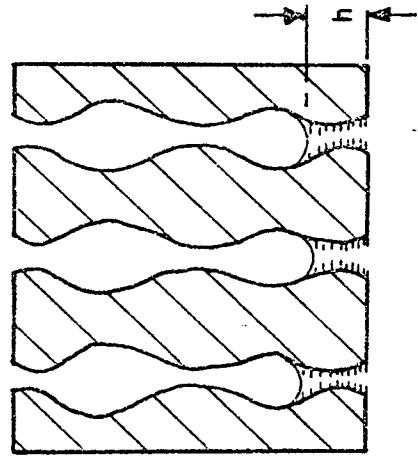
This method measures the smallest pore size present and thus tends to predict higher capillary pressures than will be representative of a nonhomogeneous wick having varying pore sizes.

Variation of up to 25% has been found (14) between the maximum heights attained with rising liquid levels in a dry wick and falling liquid levels in a saturated wick. This effect has been attributed to the existence of unevenly sized passages in the wick (sections of predominantly "large" passages interspersed with other sections of predominantly "small" passages, as illustrated in Figure W-7). The rising maximum height is reached when a section of "large" passages is encountered. However, the falling liquid in a saturated wick can form menisci with smaller radii at a higher height and thereby maintain a liquid column at this height even though a section of "too large" pores exists at a lower height. Thus, two measurements of the maximum wicking height on the same wick sample can yield very different values for the effective capillary radius, and care must be exercised before applying the data to the design of heat pipes. The conservative approach is to use the effective pore radius corresponding to the rising liquid level.

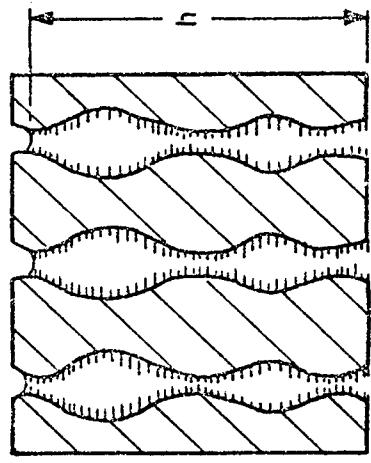
It is also important when making these measurements to enclose the wick material in a saturated atmosphere to avoid attaining too low a maximum height which can result from evaporation. A modification of this technique has been used by several investigators (20) (19). This involves fastening a thin section of wick material over the end of a nonporous tube and then filling the tube with test liquid and either raising the tube or lowering a reservoir to a level at which the wick can no longer support the column of liquid. Equation W-21 is then used to obtain the effective pore radius. The maximum height can be obtained in a much shorter time than with the previous technique (which may require a period of more than one week).

Another measurement technique used employs a section of wick over the end of a tube in contact with a column of test liquid. But instead of measuring the height of the column of liquid which can be supported, the overpressure,  $p_o$  required to force a bubble of air through the wick is determined (20) (19) and then the following relationship is applied:

$$r_p = \frac{2\sigma \cos \theta}{p}$$



Rising Meniscus (Dry Wick)



Falling Meniscus (Saturated Wick)

Figure W-7. Variations in Measured Wicking Height as a Function of Measurement Technique in Non-Uniform Wick Material

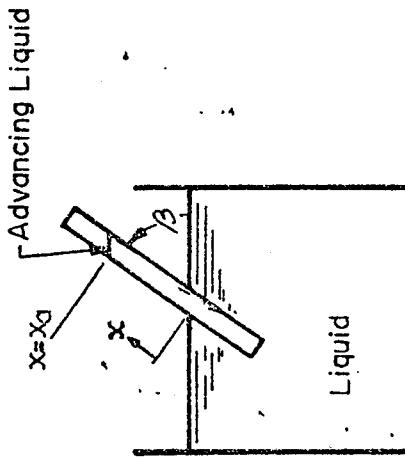


Figure W-8. Advancing Liquid Front Test Setup for Determination of  $r_p$  and  $K_p$

This technique also gives the value for the largest pore size present in the wick. It has been reported (20) that this technique gives essentially the same result as the previous method. However, the test used to establish this equivalence utilized a 200-mesh stainless steel screen (which has very little variation in pore size); thus, both test methods would be expected to yield similar values for  $r_p$ .

The rate of rise of liquid in the wick can be used to determine the effective capillary radius and also the permeability (7) (10) (11). This technique is discussed to illustrate the application of the equations developed in the Theory Chapter. If one end of the test wick is placed in the fluid, as indicated in Figure W-8, then the rate  $dx_a/dt$  of the advancing front is related to the massflow of the liquid through:

$$\dot{m}(x) = \epsilon \rho_1 A_w \frac{dx}{dt} \quad W-23$$

Combining Equation W-23 with the equations for the pressure gradients (T-4, T-15 and T-22) gives:

$$\frac{dp_1}{dx} = - \frac{\epsilon \mu_1 dx_a/dt}{K} - \rho_1 g \sin \beta \quad W-24$$

Integration along the column of liquid yields the pressure at the advancing interface:

$$p_1(x_a) = \int_0^{x_a} \frac{dp_1}{dx} dx + p_1(0) \quad W-25$$

The capillary pressure developed at the advancing interface is given by:

$$\Delta p_{cap} = \Delta p_1(x_a) = \frac{2 \sigma \cos \theta}{r_p} = p_v(x_a) - p_1(x_a) \quad W-26$$

But since this system is open to the atmosphere:

$$p_v(x_a) = p_y(0) = p_1(0) \quad W-27$$

Combining Equations W-24, W-25 and W-27 with W-26 gives:

$$\frac{2 \sigma \cos \theta}{r_p} = p_1(0) - \int_0^{x_a} \left( -\frac{\epsilon \mu_1 dx_a / dt}{K} - \rho_1 g \sin \beta \right) dx - p_1(0) \quad W-28$$

Integrating and rearranging yields:

$$\frac{dx_a}{dt} = \frac{K}{\epsilon \mu_1} \frac{2 \sigma \cos \theta}{r_p} \frac{1}{x_a} - \frac{K}{\epsilon \mu_1} \rho_1 g \sin \beta \quad W-29$$

Thus, a plot of  $dx_a / dt$  vs.  $1/x_a$  is a straight line and the permeability is determined from the intercept and  $r_p$  is determined from the slope. In the horizontal (minimum g) case, Equation W-29 reduces to the simple form:

$$\frac{2 \sigma \cos \theta}{r_p} = \frac{\epsilon \mu_1 x_a}{K} \frac{dx_a}{dt} \quad W-30$$

which integrates to:

$$t_a = \frac{r_p \mu_1 \epsilon}{4 K \sigma \cos \theta} x_a^2 \quad W-31$$

where  $t_a$  is the time required for the front to reach an axial location  $x_a$ . This has been verified experimentally with twenty inch lengths of  $\text{SiO}_2$  fabric wicks (7).

It is difficult to obtain reproducible data with this approach due to the difficulty in making precise measurements of the motion of the liquid front; this is especially true during the early rise above the surface of the reservoir. Much of this difficulty is associated with the ability to see the actual leading edge of the liquid. The addition of coloring and/or fluorescing agents has been considered, but the fluid properties may be changed and the results thereby invalidated. Other techniques suggested include the placement of indicating papers (such as litmus) at intervals along the wick or the insertion of wire electrodes (in nonmetallic wicks) at intervals along the wick. Any such external indicators suffer from the problem that they are discontinuous and that they bias the time of liquid front passage by the indicator reaction time. Thus, all of the rise time experiments show only approximate adherence to the above formulas.

As with the determination of effective pumping radii, several techniques of varying complexity are available for the determination of the permeability of wick materials. All methods involve the measurement of the pressure gradient along the wick concurrently with a determination of the flow rate of the test fluid.

The simplest technique (generally only applicable to fairly thick wick samples) involves the clamping of the test specimen in a chamber of dimensions such that all surfaces are in tight contact in order to prevent the fluid from bypassing the sample.

A fluid flow under a constant pressure head is then maintained until a constant pressure profile is established across the sample. The pressure profile is measured using a series of pressure probes as indicated in Figure W-9. The equilibrium flow rate is determined by weighing the amount of fluid collected over a specific period of time.

The permeability can then be calculated from Equation W-32:

$$K = \frac{L}{\Delta p_1} \frac{\dot{m}_1}{A_w \rho_1} \quad W-32$$

where  $L$  is the length of the sample and  $\Delta p_1$  is the pressure drop as measured along this length. Equation W-32 follows directly by integration of Darcy's law (Equation T-15). The data obtained using this experimental method are usually reproducible. Unfortunately, this technique does not duplicate the condition inside a heat pipe where one surface of the wick is free to permit the formation of menisci of various shapes. Katzoff (14) has suggested that this can reduce the apparent permeability of the wick since the effective flow area is reduced.

A modification of the above technique has been used to obtain permeability measurements under conditions more closely resembling those in a heat pipe (20). In this case, the pressure probe taps are placed under the wick and a vapor space is left in the test chamber above the wick. The test fixture is tilted in such a manner that gravity aids the liquid flow. The tilt is adjusted so that the pressure due to viscous drag is exactly balanced by the gravity pressure gradient (Figure W-10). For these test conditions, Equations T-4, T-15 and T-22 yield the following relation:

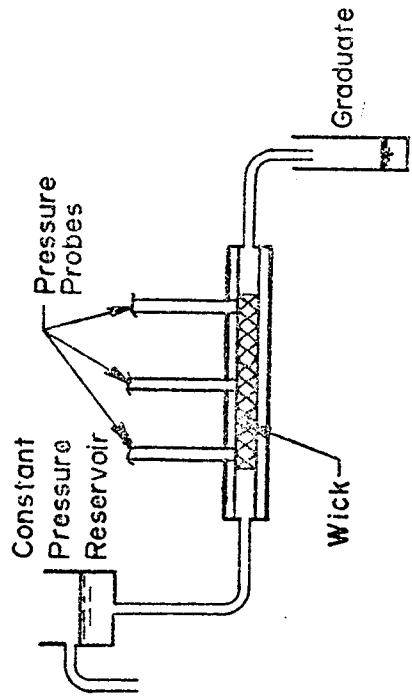


Figure W-9. Forced Flow  $K$  Measurement Apparatus

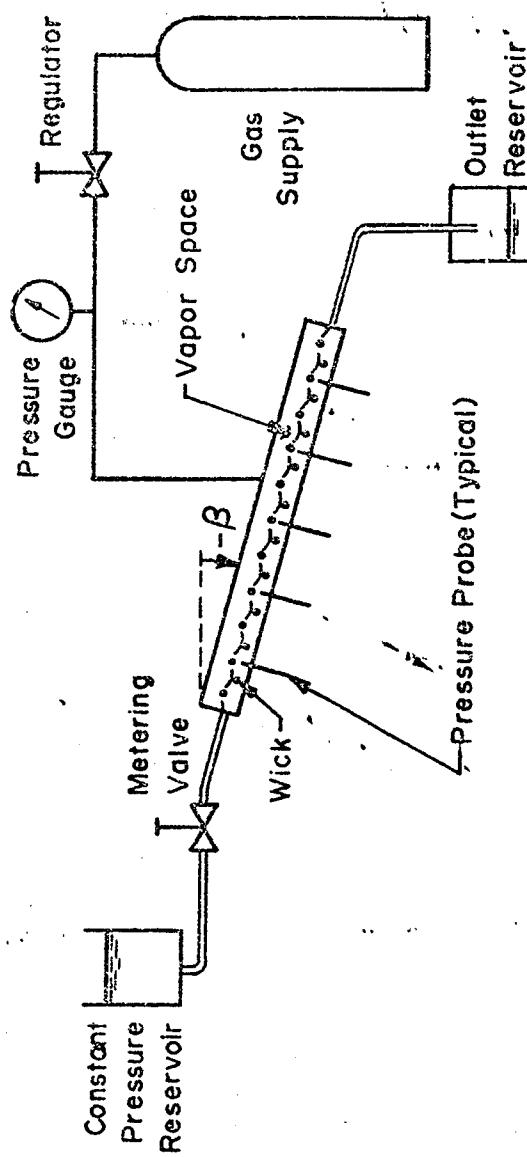


Figure W-10. Test Setup for Determination of  $K$  by Gravity Flow

$$-\frac{\mu_1 \dot{m}_1}{K A_w \rho_1} - \rho_1 g \sin \beta = 0$$

W-33

and

$$K = \frac{\mu_1 \dot{m}_1}{A_w \rho_1^2 g \sin \beta} \quad (\beta < 0)$$

The effective radius  $r_{\text{eff}}$  of the meniscus between liquid and vapor can be determined from:

$$\frac{2 \sigma \cos \theta}{r_{\text{eff}}} = p_v - p_l \quad W-35$$

where  $p_v$  and  $p_l$  are the pressures in the vapor and the liquid phases, respectively. This effective meniscus may be varied by adjusting the pressure in the vapor space above the wick. The recession of the meniscus into the wick modifies the flow pattern and reduces the cross-sectional area available for liquid flow. Both of these effects reduce permeability over that of a completely filled wick. This technique, although it provides useful information, has proved difficult to control experimentally. As a result, most experimenters have utilized the forced flow method.

Measurements have also been made of pressure gradients in actual operating heat pipes. Presumably, these tests should yield the most representative data. However, serious problems with vapor bubbles in the pressure probes have severely limited the reproducibility of data from such tests (20).

W. 5 Suppliers of Wick Materials

Metal Foams

Astro Met Associates Inc.  
95 Barron Drive  
Cincinnati, Ohio 45215

General Electric Co.  
Metallurgical Products Dept.  
Box 237, General Post Office  
Detroit, Michigan 48238

W-22

W-34

Gould, Inc.  
Gould Laboratories  
540 East 105th Street  
Cleveland, Ohio 44108

Union Carbide Corporation  
12900 Snow Road  
Parma, Ohio

Metal Felts

Astro Met Associates, Inc.  
95 Barron Drive  
Cincinnati, Ohio 45215

Brunswick Corporation \*  
Technical Division  
1 Brunswick Place  
Skokie, Illinois

Screen

Cambridge Wire Cloth  
P. O. Box 399  
Cambridge, Maryland 21613

Michigan Wire Cloth Company, Inc.  
2100 Howard Street  
Detroit, Michigan 48216

Newark Wire Cloth Company  
351 Vernon Avenue  
Newark, New Jersey 07104

Tobler, Ernst & Traver, Inc.  
420 Saw Mill River Road  
Elmsford, New York 10523

Composite Screen

Aircraft Porous Media, Inc.  
32 Sea Cliff Avenue  
Glen Cove, New York 11542

\* Formerly Huyck Metals Company

Finned Tubing

Noranda Metal Industries, Inc.  
French Tube Division  
P. O. Box 558  
Newtown, Connecticut 06470

Porous Metals

Union Carbide Corporation  
Stellite Division  
1020 W. Park Avenue  
Kokomo, Indiana 46901

No.	Wick Type and Description	Test Liquid	$r_p \times 10^6$ m	Porosity	$K \times 10^2$ m <sup>2</sup>	Method	D
1	Screen, SST, 120 mesh	$H_2O$	281	R1	3.02	D	
2	Screen, SST, 120 mesh, oxidized at 600°C	$H_2O$	190.9	R1	1.73	D	
3	Screen, SST, 200 mesh	$H_2O$	.733	58	R4	.52	B
4	Screen, SST, 200 mesh	$C_6H_6$	.733	57	R4		B
5	Screen, SST, 200 mesh	$CH_3OH$	.733	56	R4		B
6	Screen, SST, 400 mesh	$H_2O$		29	R3		C
7	Screen, SST, 400 mesh	$C_2H_5OH$		30	R3		C
8	Screen, SST, 80 x 700, Double Dutch Twill	$(CH_3)_2CHOH$	<40	R4	.075	J	
9	Screen, SST, 165 x 1400, Double Dutch Twill	$(CH_3)_2CHOH$	<18	R4	.044	J	
10	Screen, SST, 200 x 1400, Double Dutch Twill	$(CH_3)_2CHOH$	<14	R4	.024	J	
11	Screen, SST, 250 x 1400, Double Dutch Twill	$(CH_3)_2CHOH$	<12	R4	.011	J	
12	Screen, SST, 325 x 2300, Double Dutch Twill	$(CH_3)_2CHOH$	<10	R4	.006	J	
13	Screen, SST, 375 x 2300, Double Dutch Twill	$(CH_3)_2CHOH$	<8	R4	.006	J	
14	Screen, SST, 450 x 2750, Double Dutch Twill	$(CH_3)_2CHOH$	<7	R4	.006	J	
15	Screen, SST, 670 x 120, Reverse Dutch Twill	$(CH_3)_2CHOH$	<27	R4		J	
16	Screen, SST, 720 x 140, Reverse Dutch Twill	$(CH_3)_2CHOH$	<21	R4		J	
17	Screen, SST, 850 x 155, Reverse Dutch Twill	$(CH_3)_2CHOH$	<20	R4		J	
18	Screen, Nickel, 50 mesh	$H_2O$	1813	R1	5.81	D	

No.	Wick Type and Description	Test Liquid	$r_p \times 10^6$ m	Porosity	$K \times 10^2$ m <sup>2</sup>	Method	Reference	Table W-2. Experimentally Determined Wick Properties (Continued)				
								W-26	W-26	W-26	W-26	W-26
19	Screen, Nickel, 50 mesh, oxid @ 600°C	$H_2O$	580.2	R1	6.47	D						
20	Screen, Nickel, 50 mesh, sintered	$H_2O$	.625	R1	6.63	A						
21	Screen, Nickel, 100 mesh, sintered	$H_2O$	.679	<131	R1	1.52	A					
22	Screen, Nickel, 100 mesh, sintered	$H_2O$	.678	84	R1		A					
23	Screen, Nickel, 200 mesh, sintered	$H_2O$	.676	64	R1	.77	A					
24	Screen, Nickel, 500 mesh	$H_2O$	.60	12.5	R4		J					
25	Screen, Nickel, 1000 mesh	$H_2O$	.48	10.6	R4		J					
26	Screen, Nickel, 1000 mesh	$CH_3OH$	.48	10.6	R4		J					
27	Screen, Nickel, 1500 mesh	$H_2O$	.36	6.7	R4		J					
28	Screen, Nickel, 2000 mesh	$H_2O$	.22	6.1	R4		H					
29	Screen, Nickel, 2000 mesh	$CH_3OH$	.22	5.3	R4		H					
30	Screen, Copper, 60 mesh	$H_2O$	481	R1	4.20	D						
31	Screen, Copper, 60 mesh, oxidized	$H_2O$	298	R1	2.38	D						
32	Screen, Phosphor Bronze, 120 mesh	$C_2H_5OH$	102	R3		C						
33	Screen, Phosphor Bronze, 120 mesh	$H_2O$	105	R3		C						
34	Screen, Phosphor Bronze, 200 mesh	$C_2H_5OH$	54	R3		C						
35	Screen, Phosphor Bronze, 200 mesh	$H_2O$	60	R3		C						
36	Screen, Phosphor Bronze, 250 mesh	$C_2H_5OH$	51	R3		C						

Table W-2. Experimentally Determined Wick Properties (Continued)

No.	Wick Type and Description	Test Liquid	Porosity $\times 10^6$ m	Method $K \times 10^2$ m <sup>2</sup>	Reference
37	Screen, Phosphor Bronze, 250 mesh	H <sub>2</sub> O	48	R3	C
38	Screen, Phosphor Bronze, 270 mesh	C <sub>2</sub> H <sub>5</sub> OH	41	R3	C
39	Screen, Phosphor Bronze, 270 mesh	H <sub>2</sub> O	43	R3	C
40	Screen, Phosphor Bronze, 325 mesh	C <sub>2</sub> H <sub>5</sub> OH	32	R3	C
41	Screen, Phosphor Bronze, 325 mesh	H <sub>2</sub> O	33	R3	C
42	Screen, Sintered, SST	H <sub>2</sub> O	.822	110	R1
43	Screen, Sintered, SST	H <sub>2</sub> O	.916	94	R1
44	Screen, Sintered, SST	H <sub>2</sub> O	.808	65	R1
45	Felt, 347 SST, C38 (FM 134)	H <sub>2</sub> O	.35	49	R1
46	Felt, 347 SST, C38 (FM 123)	H <sub>2</sub> O	.35	42.5	R1
47	Felt, SST, A-8 (FM 1101, 1101)	H <sub>2</sub> O	.90	26.5	R1
48	Felt, SST, A-8 (FM 1102, 1107, 1112)	H <sub>2</sub> O	.80	13.5	R1
49	Felt, SST, A-8 (FM 1103, 1108)	H <sub>2</sub> O	.70	7.5	R1
50	Felt, SST, A-8 (FM 1104, 1109)	H <sub>2</sub> O	.60	5	R1
51	Felt, SST, A-8 (FM 1105, 1110)	H <sub>2</sub> O	.40	2.3	R1
52	Felt, 430 SST, B-62 (FM 1305, 1309)	H <sub>2</sub> O	.95	260	R1
53	Felt, 430 SST, B-62 (FM 1302, 1306, 1310)	H <sub>2</sub> O	.90	191	R1
54	Felt, 430 SST, B-62 (FM 1303, 1307, 1311)	H <sub>2</sub> O	.80	120	R1



Table W-2. Experimentally Determined Wick Properties (Continued)

No.	Wick Type and Description	Test Liquid	Porosity $r_p \times 10^6 \text{ m}$	Method $K \times 10^2 \text{ m}^2$	Reference
55	Felt, 430 SST, B-62 (FM 1304, 1308, 1312)	$\text{H}_2\text{O}$	.60	50 R1	.80 L
56	Felt, Nickel	$\text{H}_2\text{O}$	.891	155 R4	5.17 B
57	Felt, Nickel, A30	$\text{H}_2\text{O}$	.815	120 R1	.306 D
58	Felt, Nickel, A30 (FM 415)	$\text{CH}_3\text{OH}$	55.9	R1	.48 K
59	Felt, Nickel, A-16 (FM 1201, 1205, 1209)	$\text{H}_2\text{O}$	.85	40 R1	.88 L
60	Felt, Nickel, A-16 (FM 1205)	$\text{H}_2\text{O}$		37.9 R1	1.27 D
61	Felt, Sintered, Nickel	$\text{H}_2\text{O}$	.828	< 38 R1	A
62	Felt, Sintered, Nickel	$\text{H}_2\text{O}$	.868	< 37 R1	.397 A
63	Felt, Sintered, Nickel	$\text{H}_2\text{O}$	.825	< 37 R1	.337 A
64	Felt, Sintered, Nickel	$\text{H}_2\text{O}$	.689	< 37 R1	.151 A
65	Felt, Sintered, Nickel	$\text{H}_2\text{O}$	.628	< 37 R1	A
66	Felt, Sintered, Nickel	$\text{H}_2\text{O}$	.880	< 37 R1	.308 A
67	Felt, Sintered, Nickel, A30 (FM 315, 415)	$\text{H}_2\text{O}$	.85	37 R1	1.75 L
68	Felt, Sintered, Nickel	$\text{H}_2\text{O}$	.709	< 36 R1	A
69	Felt, Sintered, Nickel	$\text{H}_2\text{O}$	.626	< 35 R1	A
70	Felt, Sintered, Nickel	$\text{H}_2\text{O}$	.820	< 32 R1	A
71	Felt, Nickel, A30, oxid @ 600°C	$\text{H}_2\text{O}$		32.5 R1	D
72	Felt, Nickel, A16 (FM 1202, 1206, 1210)	$\text{H}_2\text{O}$			L .48

Table W-2. Experimentally Determined Wick Properties (Continued)

No.	Wick Type and Description	Test Liquid	$r_p \times 10^6$ m	Porosity	$K \times 10^2$ m <sup>2</sup>	Method	Reference
73	Felt, Nickel, A30 (FM 320, 420)	$H_2O$	.80	25.5	R1	.80	I
74	Felt, Nickel, A16 (FM 1203, 1207, 1211)	$H_2O$	.70	17	R1	.116	I
75	Felt, Nickel, A16 (FM 1204, 1208, 1212)	$H_2O$	.60	10.5	R1	.042	I
76	Felt, 347 SS, A30 (FM 627)	$H_2O$	.55	7	R1	.016	I
77	Felt, Copper	$CH_3OH$	.895	279	R3		B
78	Felt, Copper	$H_2O$	.895	229	R4	12.4	B
79	Felt, Copper	$C_6H_6$	.895	216	R4		B
80	Felt, Copper, FM 1006	$H_2O$	.80	144	R1	.778	D
81	Felt, Copper, FM 1006, oxid @ 300°C	$H_2O$	.80	40.6	R1		D
82	Felt, OFHC Copper, A40 (FM 1006)	$H_2O$	.80	23	R1	.37	I
83	Foam, Nickel, AmPorNik 220-5	$CH_3OH$	.960	267	R3		B
84	Foam, Nickel, AmPorNik, 220-5	$H_2O$	.960	229	R4	37.2	B
85	Foam, Nickel, AmPorNik, 220-5	$C_6H_6$	.960	216	R4		B
86	Foam, Nickel, AmPorNik, 210-5	$H_2O$	.944	229	R4	27.3	B
87	Foam, Copper, AmPorCOP, 210-5	$CH_3OH$	.945	229	R3		B
88	Foam, Copper, AmPorCOP, 210-5	$C_6H_6$	.945	229	R4		B
89	Foam, Copper, AmPorCOP, 210-5	$H_2O$	.945	216	R4	20.2	B
90	Foam, Copper, AmPorCOP, 220-5	$H_2O$	.912	241	R4	23.2	B

Table W-2. Experimentally Determined Wick Properties (Continued)

No.	Wick Type and Description	Test Liquid	Porosity $\times 10^6$	$K \times 10^{10} \text{ m}^2$	Method	Reference
91	Powder, Sintered, Nickel	$\text{H}_2\text{O}$	.696	82	R1	A
92	Powder, Sintered, Nickel	$\text{H}_2\text{O}$	.691	69	R1	A
93	Powder, Sintered, Nickel	$\text{H}_2\text{O}$	.658	61	R1	2.73
94	Powder, Sintered, Nickel	$\text{H}_2\text{O}$	.597	58	R1	A
95	Powder, Sintered, Nickel	$\text{H}_2\text{O}$	.477	< 31	R1	A
96	Powder, Sintered, Nickel	$\text{H}_2\text{O}$	.540	< 36	R1	.808
97	Powder, Sintered, Nickel	$\text{H}_2\text{O}$	.52	9.39	R1	.009
98	Powder, Sintered, Cu	$\text{H}_2\text{O}$	.51			
99	Deposited Cu	$\text{H}_2\text{O}$	.60			
100	Deposited Cu, Bonded	$\text{H}_2\text{O}$	175	R1	1.11	K
101	Beads, Cu, 20-30 mesh, Sintered	$\text{H}_2\text{O}$				
102	Beads, Monel, 20-30 mesh	$\text{H}_2\text{O}$	.40	352	R2	E
103	Beads, Monel, 30-40 mesh	$\text{H}_2\text{O}$	.40	252	R2	E
104	Beads, Monel, 40-50 mesh	$\text{H}_2\text{O}$	.40	179	R2	E
105	Beads, Monel, 50-70 mesh	$\text{H}_2\text{O}$	.40	126	R2	1.25
106	Beads, Monel, 70-80 mesh	$\text{H}_2\text{O}$	.40	96.9	R2	.775
107	Beads, Monel, 80-100 mesh	$\text{H}_2\text{O}$	.40	81.5	R2	.559
108	Beads, Monel, 100-140 mesh	$\text{H}_2\text{O}$	.40	63.4	R2	.328

Table W-2. Experimentally Determined Wick Properties (Continued)

No.	Wick Type and Description	Test Liquid	$\epsilon_p \times 10^6$	Porosity	$K \times 10^2$	$m$	Method	Reference
109	Beads, Monel, 140-200 mesh	$H_2O$	.40	44.5	R2	.110	E	
110	$SiO_2$ Fabric (Refrasil), horizontal	$H_2O$	16.3	R1	2.37	b	F	
111	$SiO_2$ Fabric (Refrasil), elevated	$H_2O$	14.6	R1	.0160	b	F	
112	Membrane, Nuclepore, 8 $\mu$ , Polyacarbonate	$H_2O$	7.4	R4			H	
113	Membrane, Nuclepore, 8 $\mu$ , Polyacarbonate	$CH_3OH$	5.0	R4			H	
114	Membrane, Nuclepore, 1 $\mu$ , Polyacarbonate	$CH_3OH$	0.9	R4			H	

## Notes for Table W-2

Investigators	Ref. No.	Investigators	Ref. No.
A Kunz	16	G Gould Laboratories	12
B Phillips	20	H Dynametherm Corporation	19
C Katzoff	14	J Kressilik	24
D Freeggens	10	K Marcus	18
E Ferrell	8	L Huycik Metals Company	23
F Farraam	7		

## Effective Pore Radius Measurement Techniques

A Kunz	16	G Gould Laboratories	12
B Phillips	20	H Dynametherm Corporation	19
C Katzoff	14	J Kressilik	24
D Freeggens	10	K Marcus	18
E Ferrell	8	L Huycik Metals Company	23
F Farraam	7		

Permeability was determined by forced flow technique except where noted:

a Gravity flow technique  
 b Plot of  $\frac{dx^2}{dt}$  vs.  $\frac{1}{x}$

## F.0 FLUID PROPERTIES

In this section, selected physical properties and calculated parameters useful in heat pipe calculations are summarized for the majority of "good" working fluids. Eighteen fluids are treated -- six useful for cryogenic temperatures, six useful for low temperatures, and six useful for high temperatures. These fluids are listed in Table F-1 and are presented in this section in the order of their increasing boiling temperatures; the one exception is ammonia which is commonly considered a low temperature working fluid, and therefore it has been incorporated in the second group of working fluids.

Table F-1 lists the following invariable properties of these eighteen working fluids in both International Scientific (SI) units and in British Engineering units:

- Chemical Formula
- Boiling Temperature
- Molecular Weight
- Critical Temperature
- Melting Temperature
- Critical Pressure

The graphs that follow Figure F-1 present separately the temperature dependent physical properties and the calculated heat pipe design parameters. These properties are given in SI units for the more commonly used fluids. Conversion tables between cgs, British Engineering, and SI units are given in the Introduction, I.O.

The following eight temperature dependent physical properties are given in the first chart for each of the selected fluids:

- Vapor Pressure
- Liquid Density
- Surface Tension
- Vapor Density
- Latent Heat of Vaporization
- Liquid Viscosity
- Liquid Thermal Conductivity
- Vapor Viscosity

The data were obtained from several sources for each of the fluids, and no attempt was made to indicate the accuracy of each curve. The majority of the data were obtained from the underlined references listed below:

Temperature Range

References

Cryogenic	1, 2, <u>5</u> , 10, <u>12</u> , 18, 20
Low	1, <u>5</u> , <u>7</u> , 8, <u>10</u> , 13, 14, 15, <u>17</u> , 18, 20, 24
High	3, <u>4</u> , 6, 7, 9, 10, 11, 15, <u>16</u> , <u>19</u> , 21, 22, 23

The temperature range covered is from the melting point to the critical point. Uncertain or extrapolated data are indicated by a dashed line. In order to both conserve space and to make all of the data for a given fluid readily accessible, all of the properties are plotted against a common scale and the conversion factors are indicated on the individual curves. Thus, the surface tension of water at 400°K is plotted as 535. The legend on the curve indicates that the plotted quantity is the surface tension in N/m multiplied by  $10^4$ . Therefore, the actual surface tension is  $535 \times 10^{-4}$  N/m or 0.0535 N/m.

The second chart for each fluid presents the following calculated parameters which are useful in heat pipe calculations:

$$\text{Liquid Transport Factor} : N_1 = \frac{\lambda \rho_1 \sigma_1}{\mu_1} = \frac{\lambda \sigma_1}{\nu_1}$$

$$\text{Wicking Height Factor} : H = \frac{\sigma}{\rho_1 g}$$

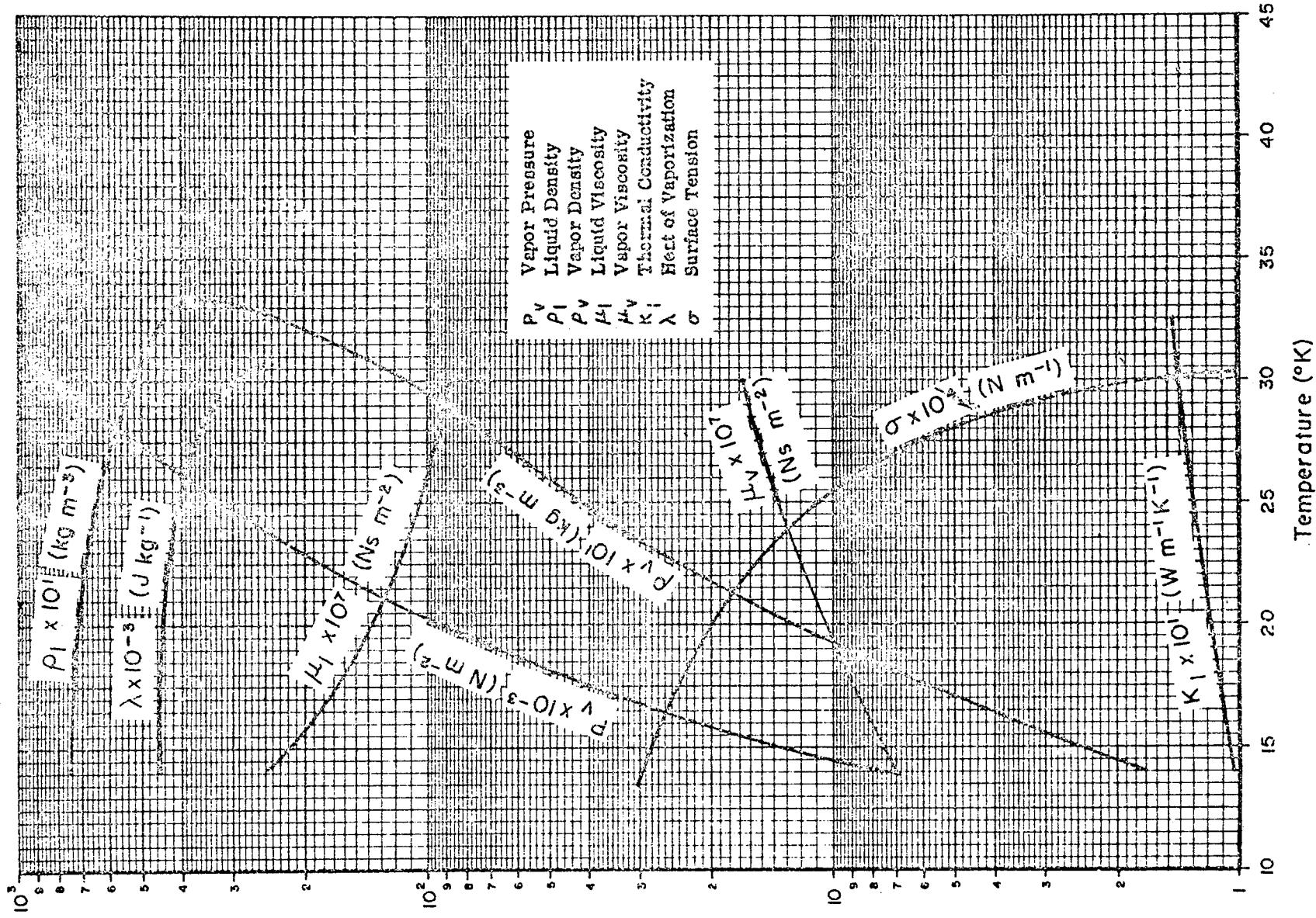
$$\text{Ratio of Kinematic Viscosities} : \frac{\nu_v}{\nu_1} = \frac{\mu_v \rho_1}{\mu_1 \rho_v}$$

$$\text{Sonic Limit} : \left( \frac{\dot{Q}}{A_v} \right)_{s, \text{max}} = \frac{\rho_v \lambda v_{\text{stag}}}{\sqrt{2(\gamma+1)}}$$

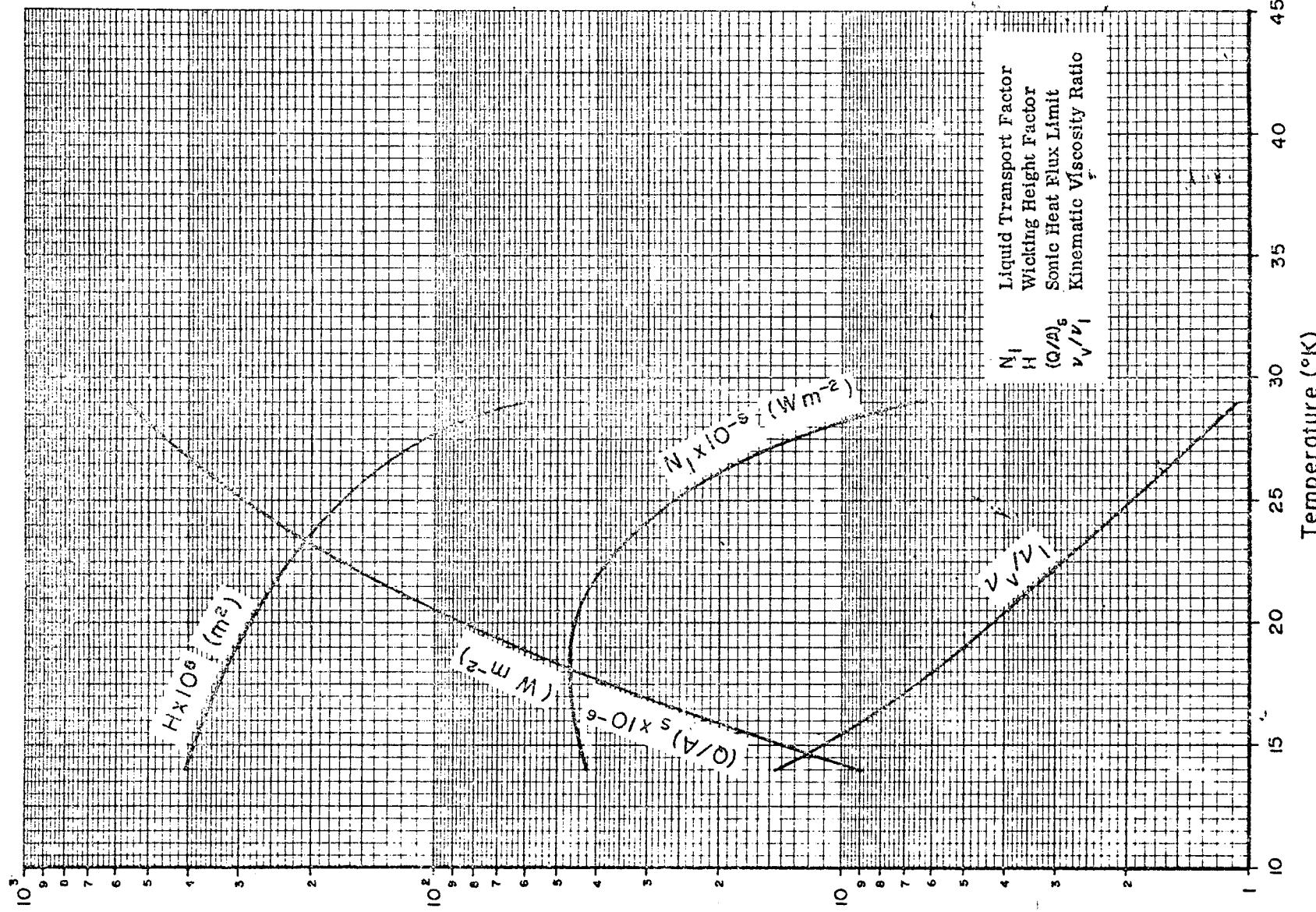
No.	Fluid	Chemical Formula	Molecular Weight	Temperature				Pressure N/m <sup>2</sup> x 10 <sup>-5</sup>	Psia		
				°K	°F	°K	°F				
1	Hydrogen	H <sub>2</sub>	2.016	14.0	-434.5	20.3	-423.2	32.9	-400.5	13.15	187
2	Neon	Ne	20.183	24.6	-415.4	27.2	-410.7	44.4	-379.8	27.22	394.7
3	Nitrogen	N <sub>2</sub>	28.013	63.1	-346.1	77.3	-320.6	126.0	-232.9	33.95	492.5
4	Oxygen	O <sub>2</sub>	31.999	54.8	-361.1	90.2	-297.3	154.7	-181.2	50.76	736
5	Methane	CH <sub>4</sub>	16.043	88.7	-300	111.7	-258.6	191.1	-115.7	46.4	673
6	Freon-21	CHCl <sub>2</sub> F	102.924	138.2	-211.0	282.1	48.1	451.7	353.3	51.7	750
7	Ammonia	NH <sub>3</sub>	17.031	195	-108.7	239.7	-28.2	405.3	269.8	112.8	1635.7
8	Freon-11	CCl <sub>3</sub> F	137.369	162.2	-168	297.0	74.9	471.2	388.4	44.08	639.5
9	Acetone	(CH <sub>3</sub> ) <sub>2</sub> CO	58.082	178.5	-138.4	329.7	133.7	509.5	457.4	47.83	693.5
10	Methanol	CH <sub>3</sub> OH	32.042	175.3	-142.0	337.8	148.4	513.1	463.8	79.77	1156.9
11	Benzene	C <sub>6</sub> H <sub>6</sub>	78.115	278.6	41.8	353.3	176.2	562.1	552.1	49.23	714
12	Water	H <sub>2</sub> O	18.015	273.2	32.0	373.2	212	647.3	705.4	221.1	3206.2
13	Mercury	Hg	200.59	234.3	421.7	629.8	673.9	1735	2663	1050	15,225
14	Cesium	Cs	132.91	302	84	939	1230	2050	3230	172.3	2500
15	Potassium	K	39.102	336.6	146.2	1049	1428	2440	3932		
16	Sodium	Na	22.990	370.8	667.4	1156	1621	2600	4220	4580	
17	Lithium	Li	6.939	453	815	1613	2440	4100	6938	5912	
18	Silver	Ag	107.870	1234	1761	2450	3950	7500	13,040		

Table F-1. Selected Properties of Some Heat Pipe Working Fluids

Fluid Properties of Hydrogen (SI Units)

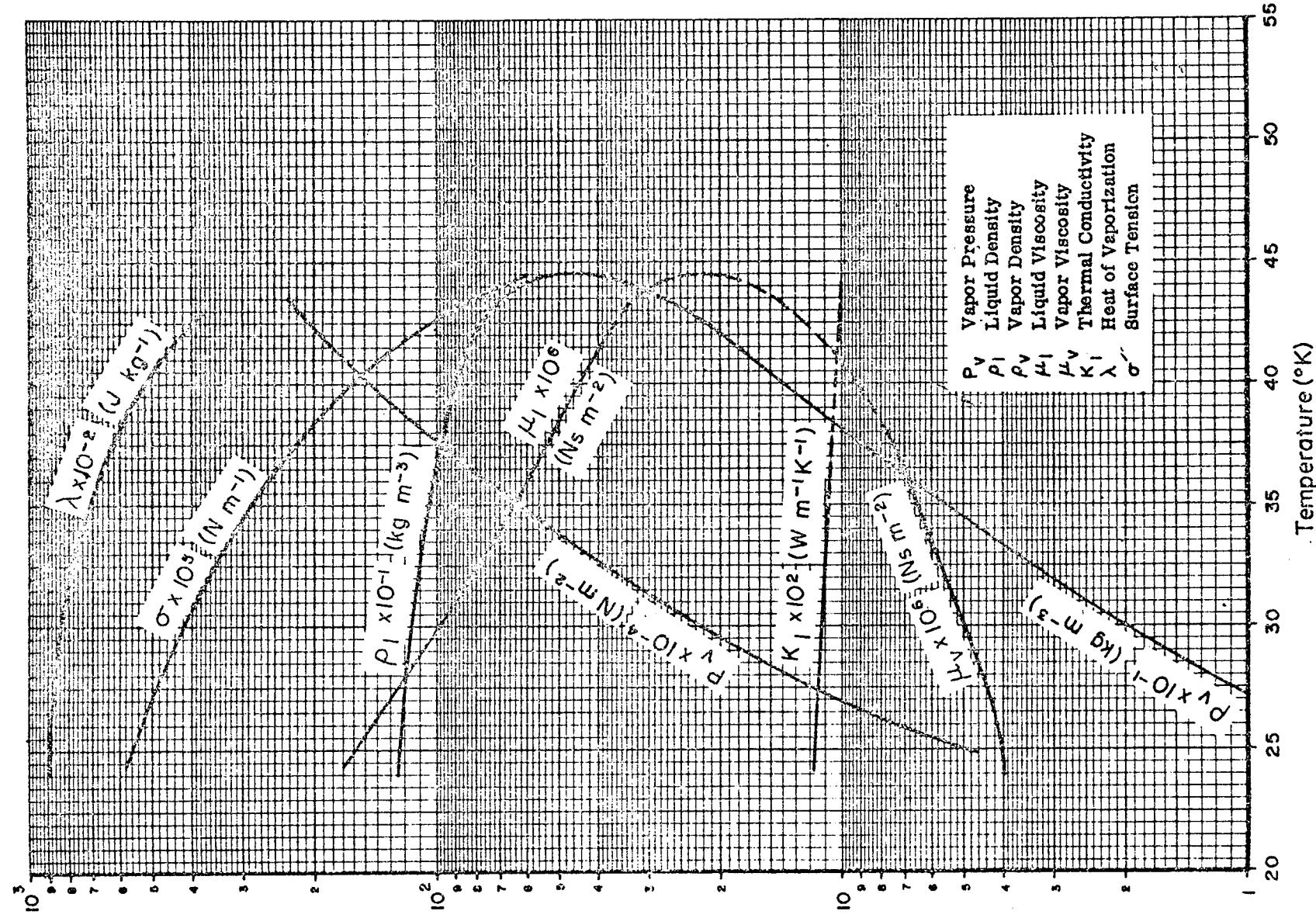


Heat Pipe Design Parameters of Hydrogen (SI Units)

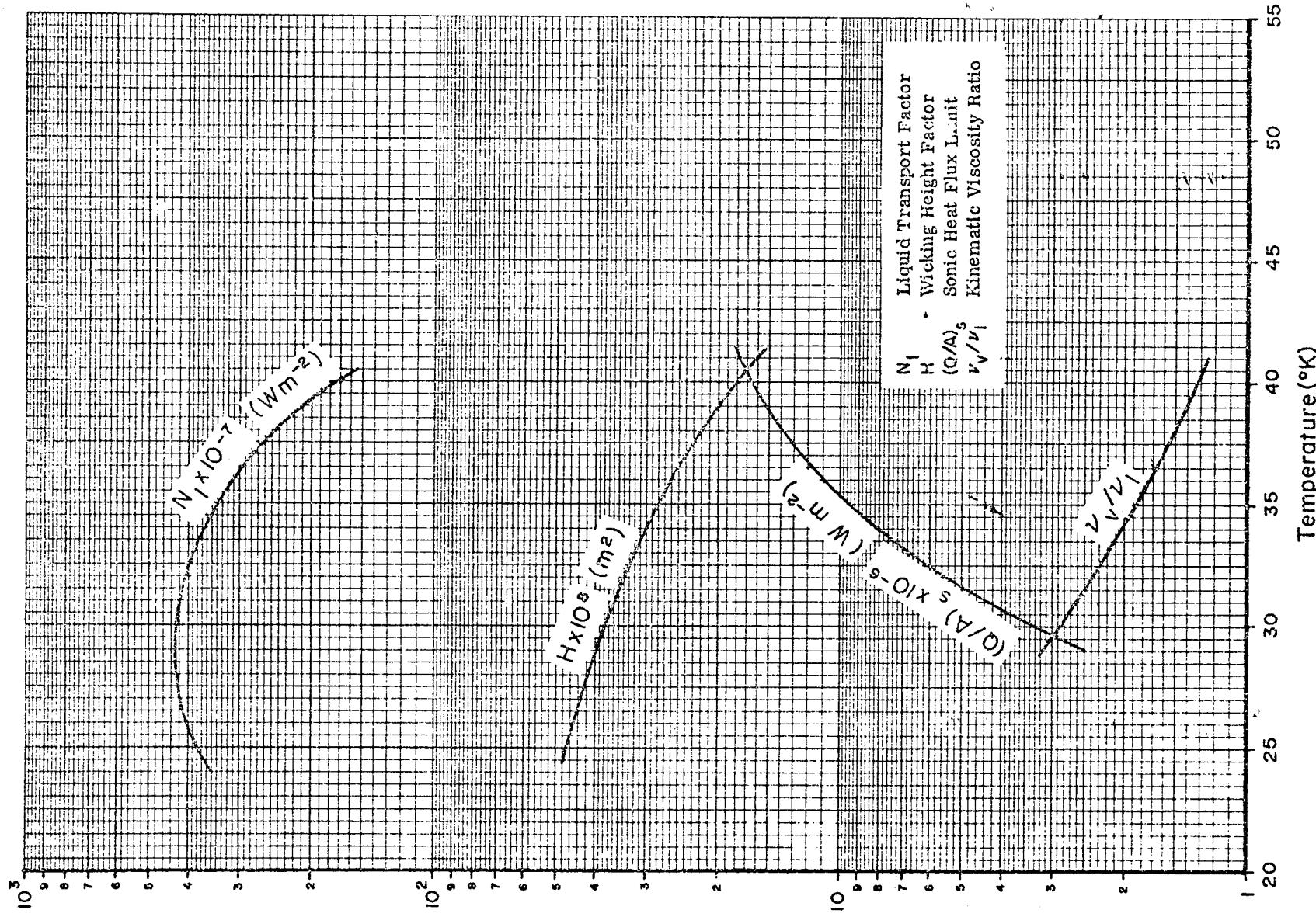


F-5

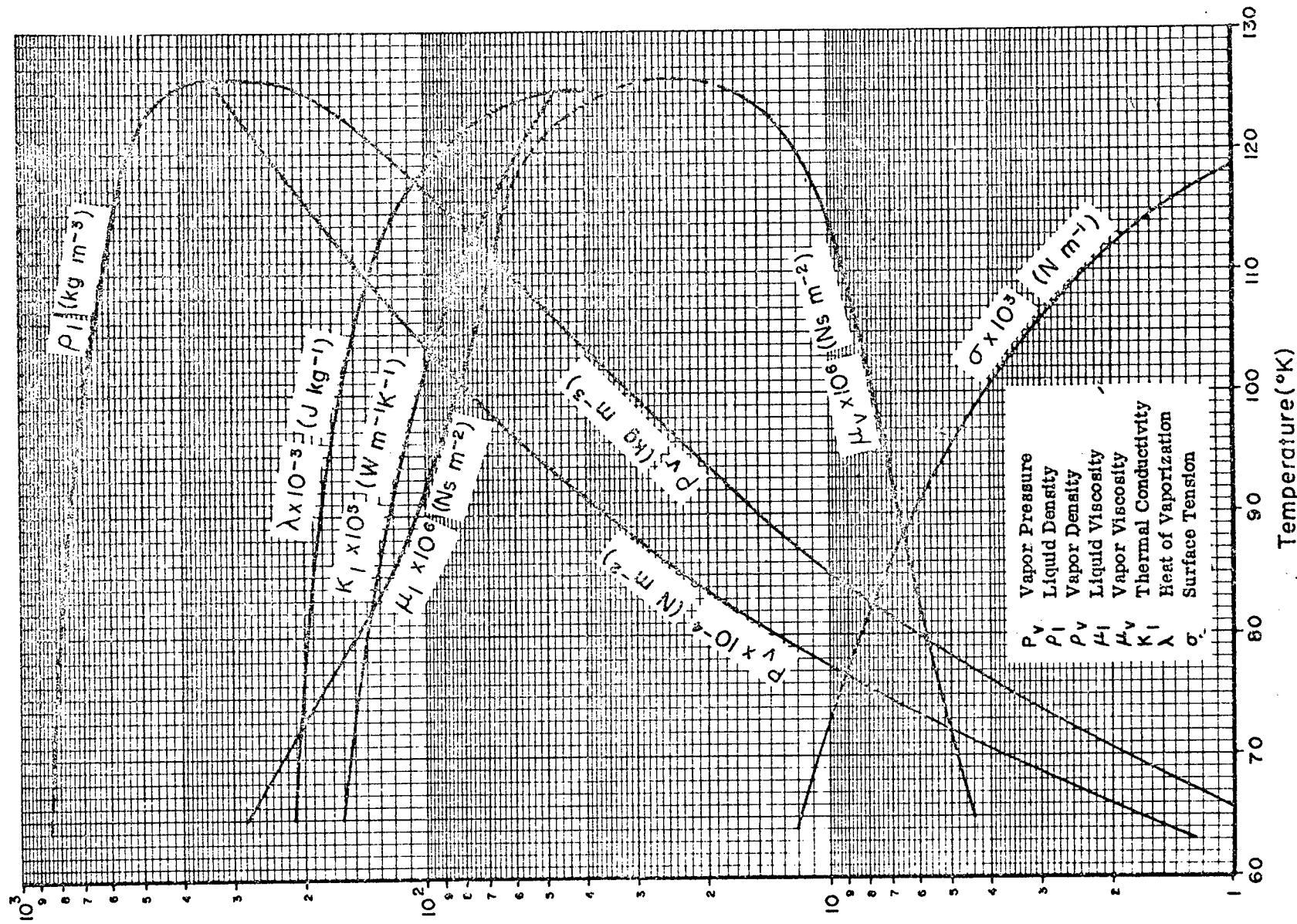
### Fluid Properties of Neon (SI Units)



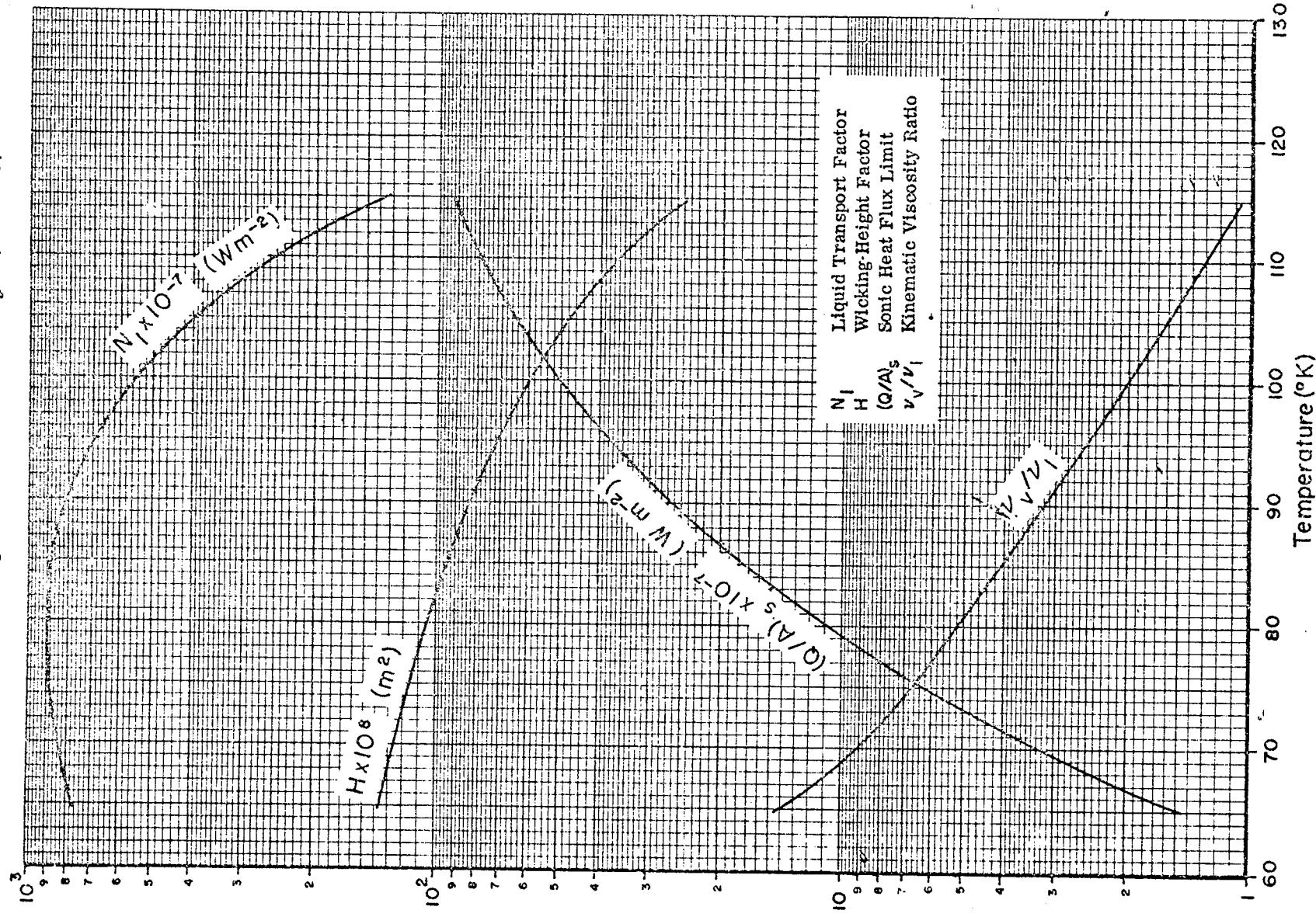
Heat Pipe Design Parameters of Neon (SI Units)



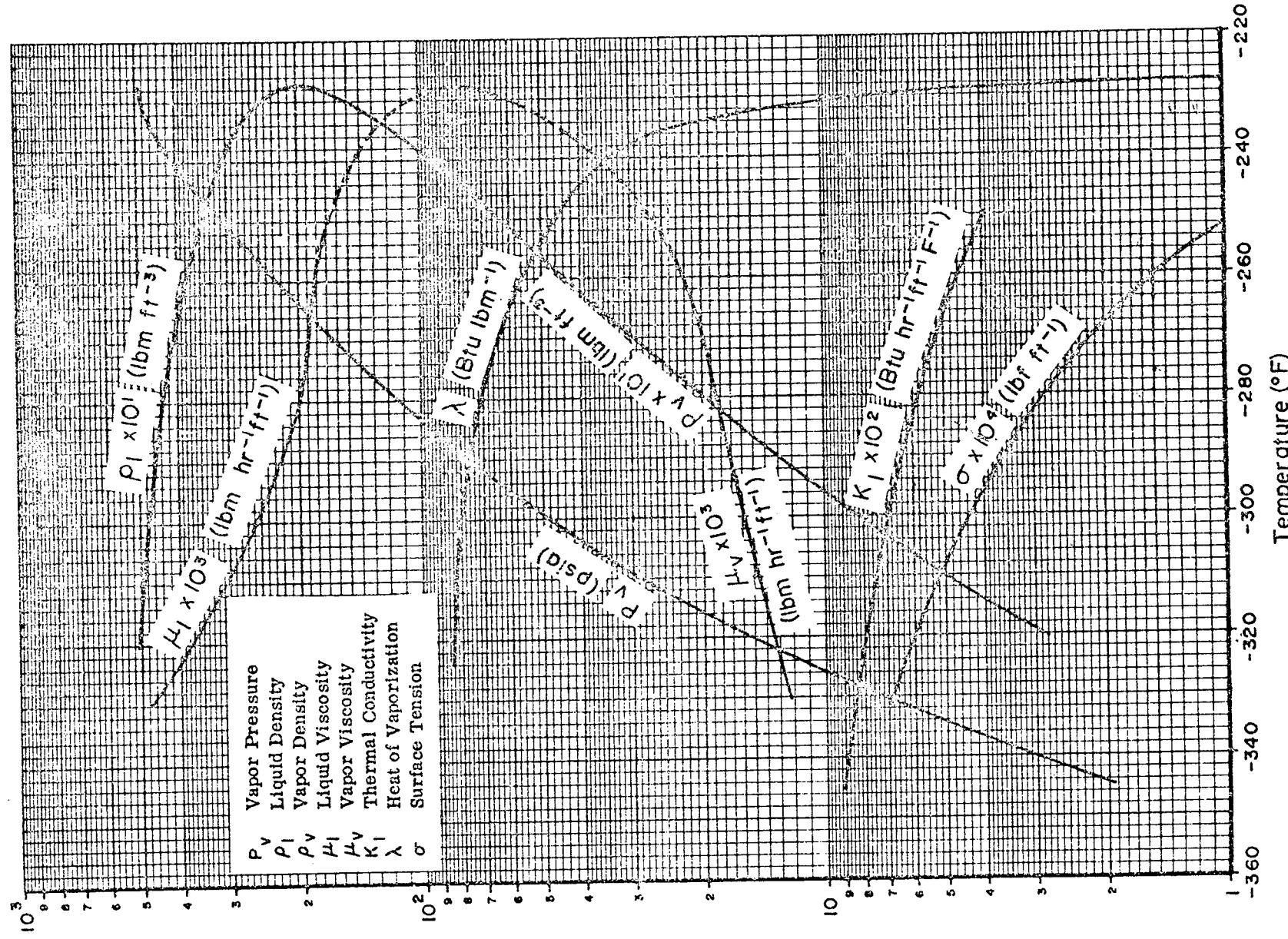
### Fluid Properties of Nitrogen (SI Units)



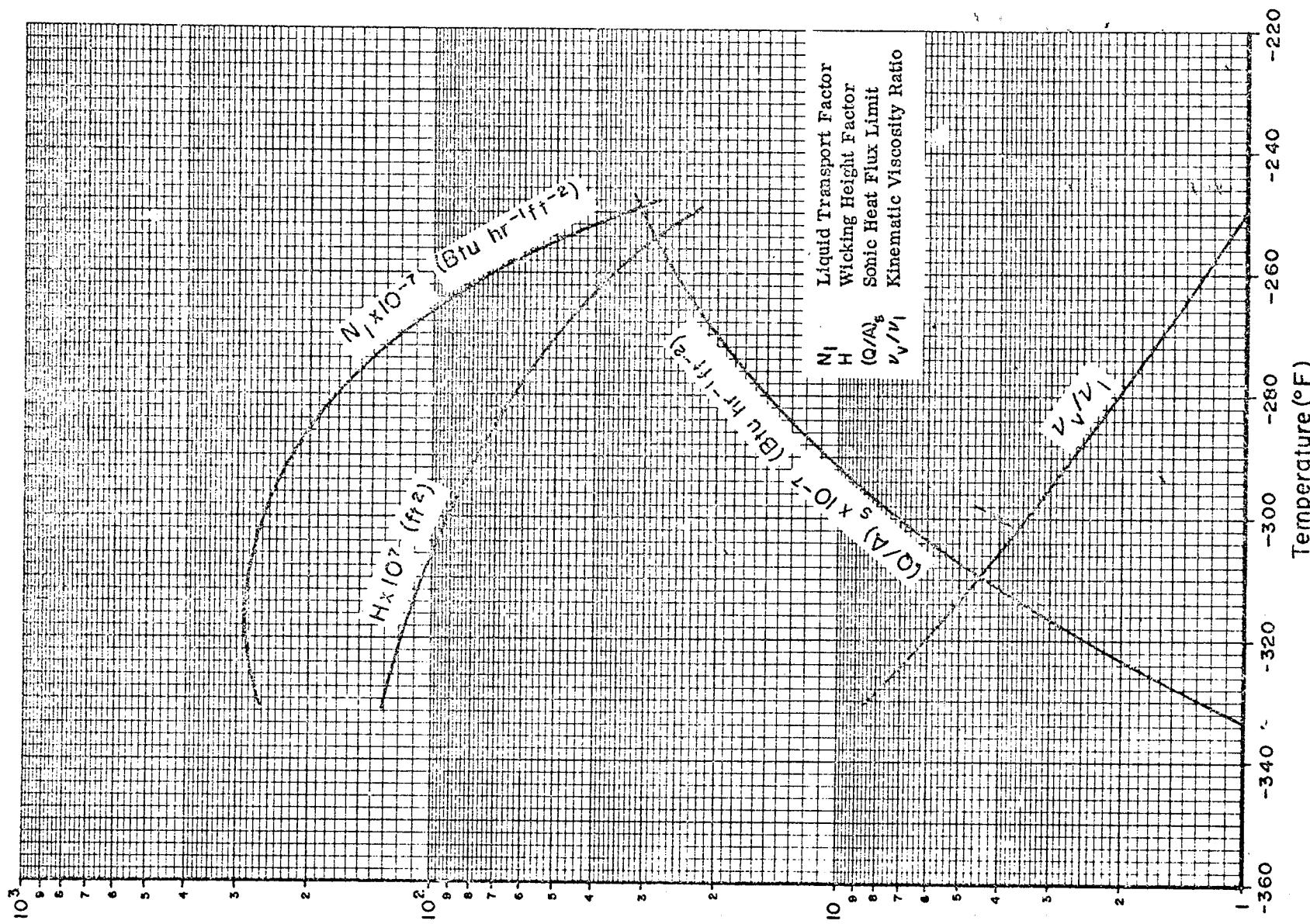
Heat Pipe Design Parameters of Nitrogen (SI Units)



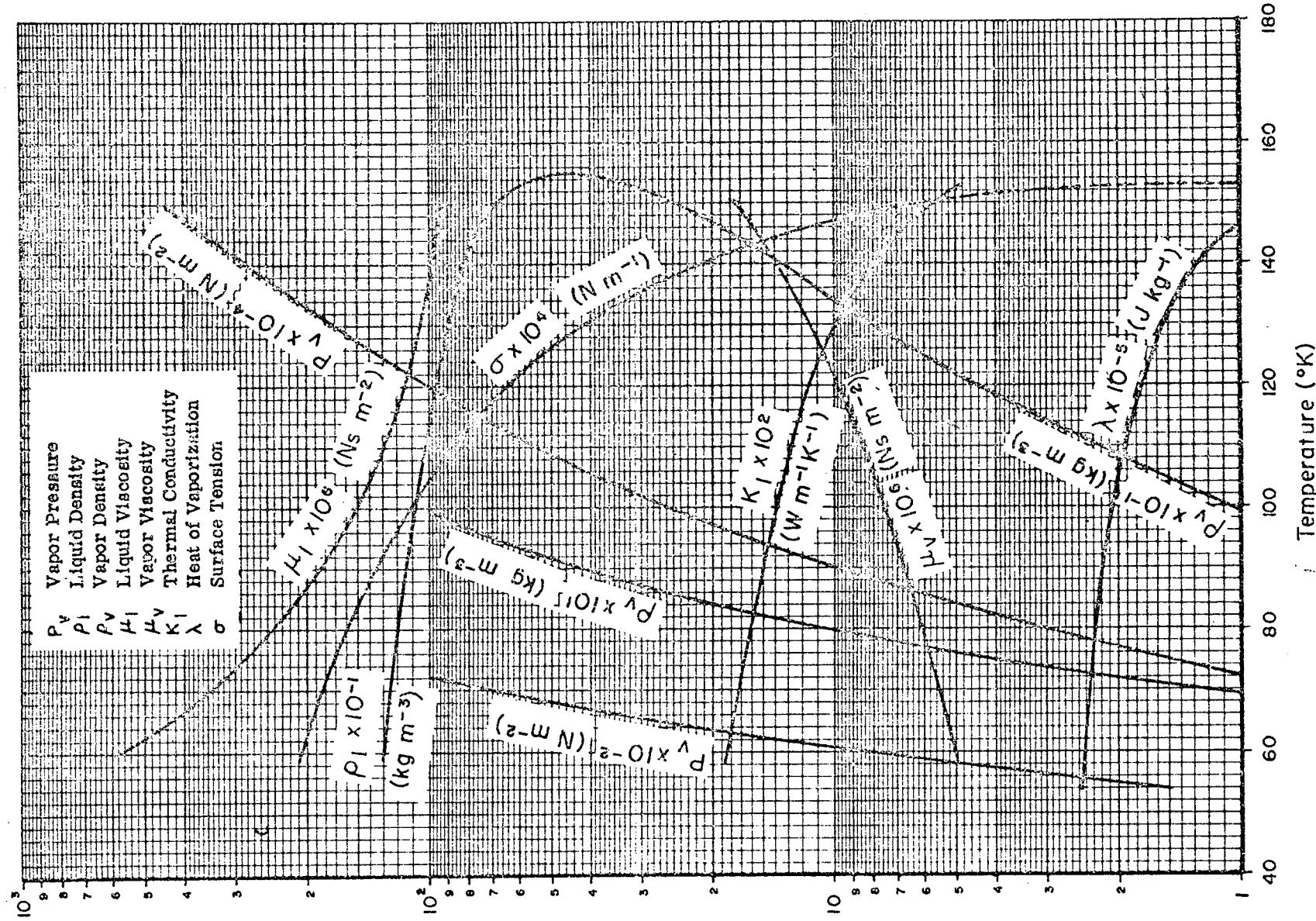
### Fluid Properties of Nitrogen (British Units)



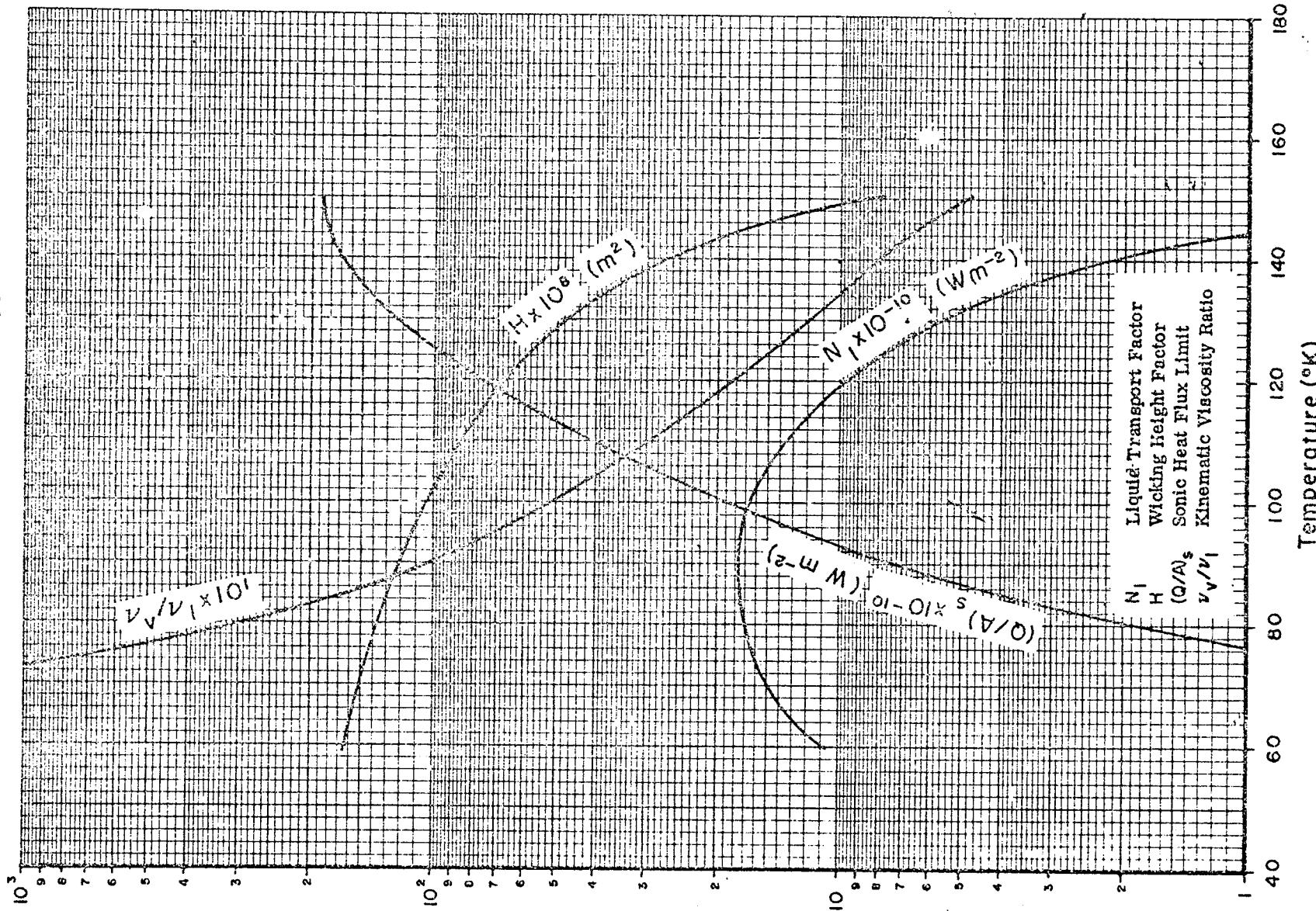
Heat Pipe Design Parameters of Nitrogen (British Units)



### Fluid Properties of Oxygen (SI Units)

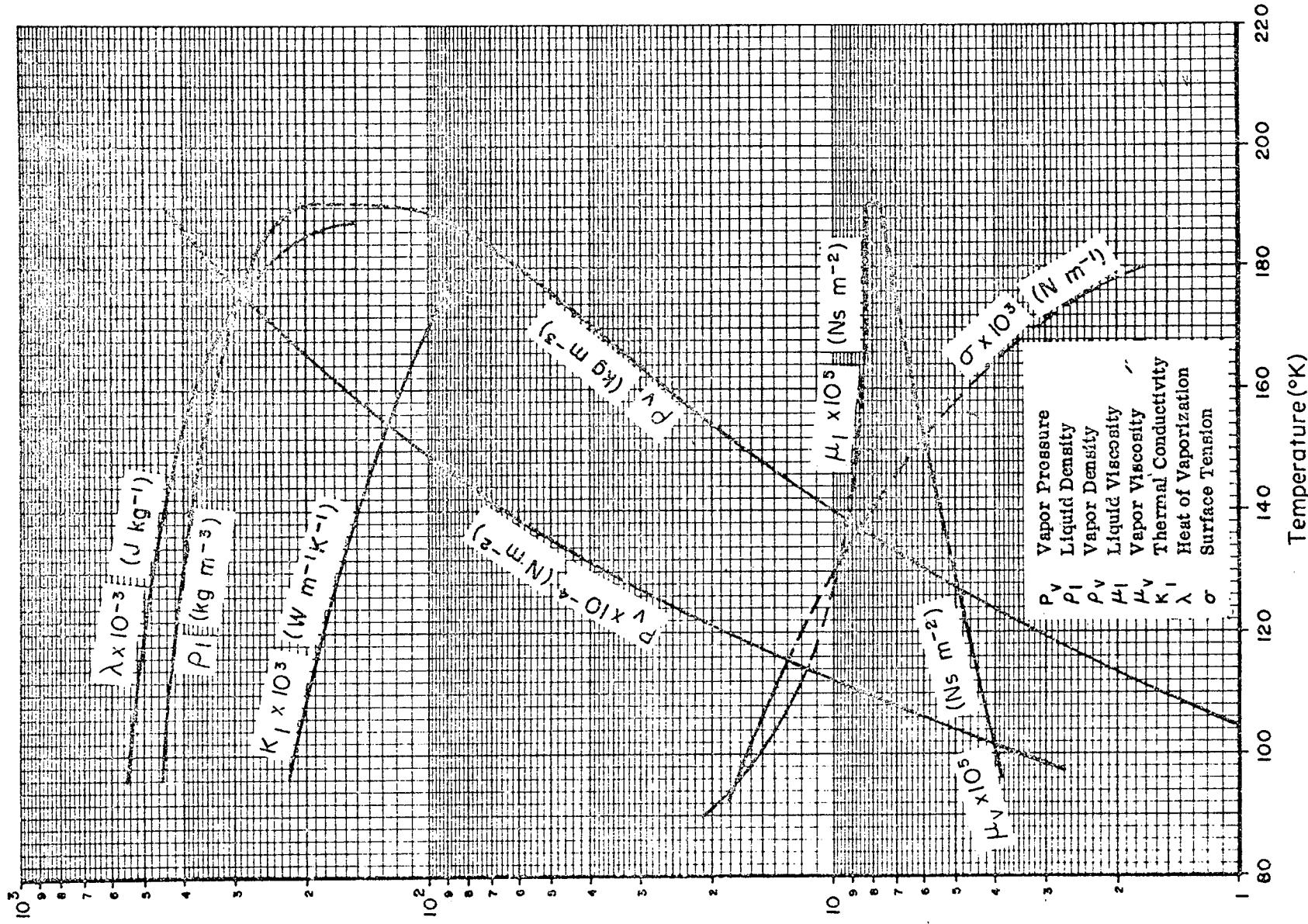


## Heat Pipe Design Parameters of Oxygen (SI Units)

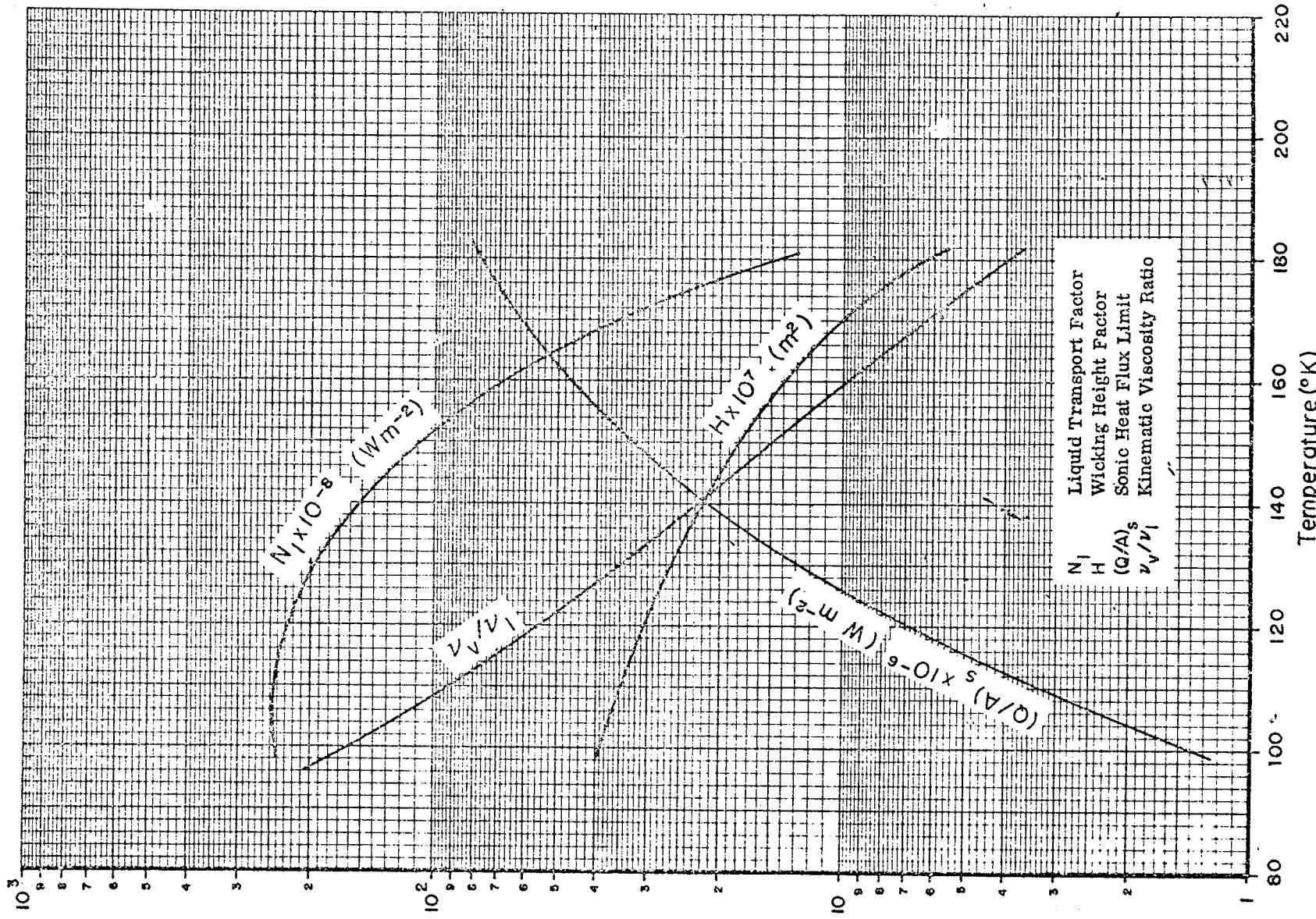


三  
一  
四

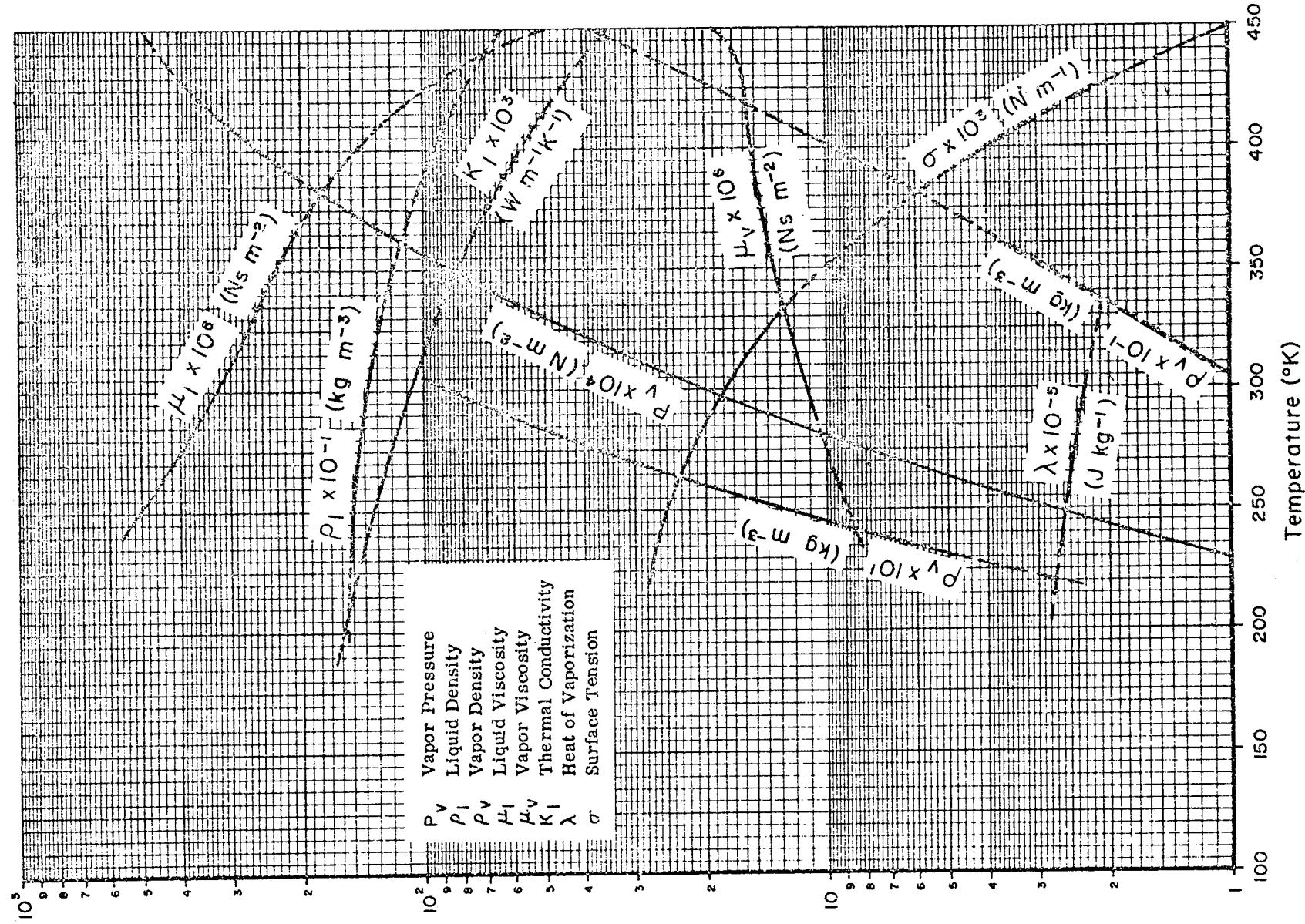
Fluid Properties of Methane (SI Units)



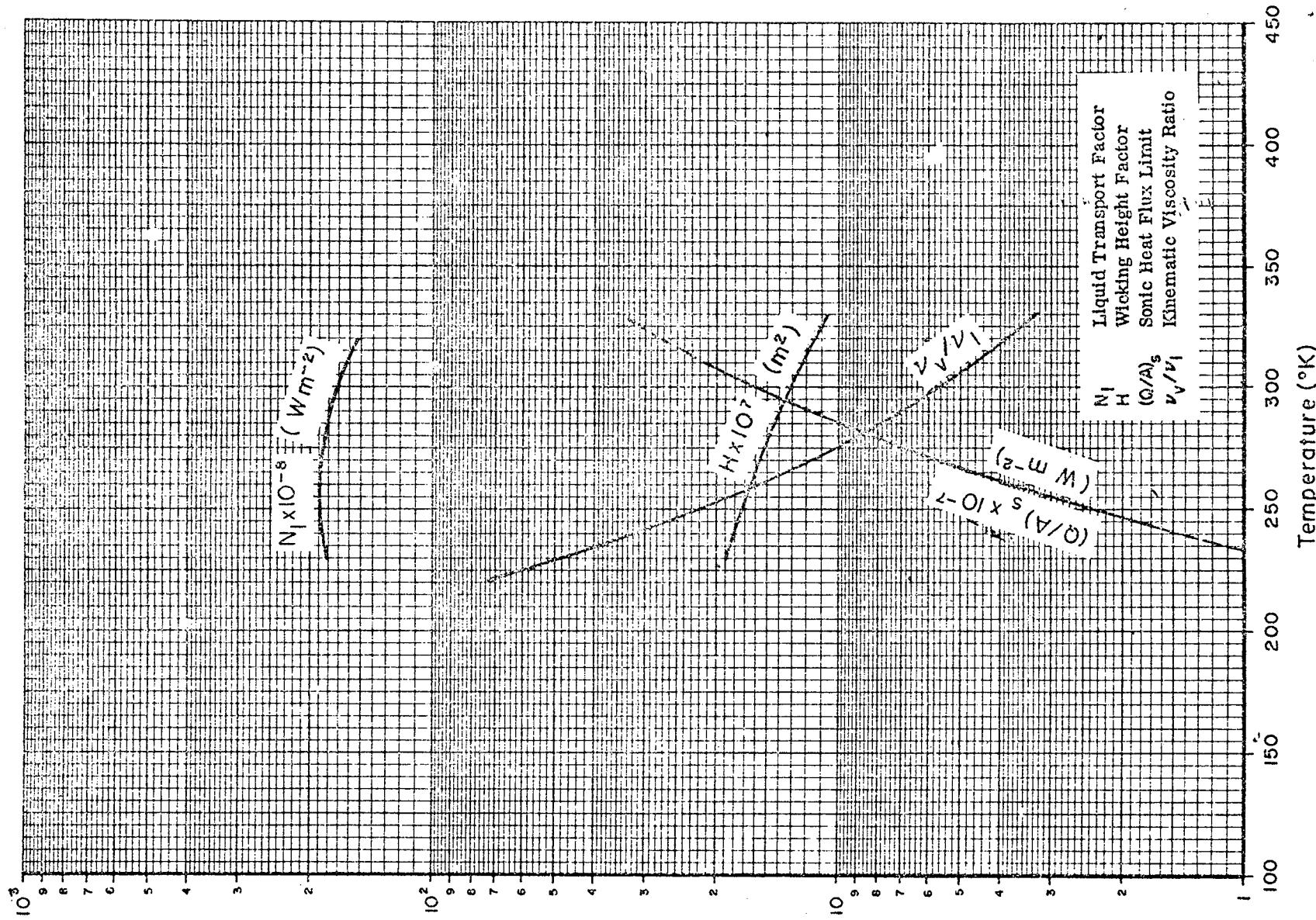
Heat Pipe Design Parameters of Methane(SI Units)



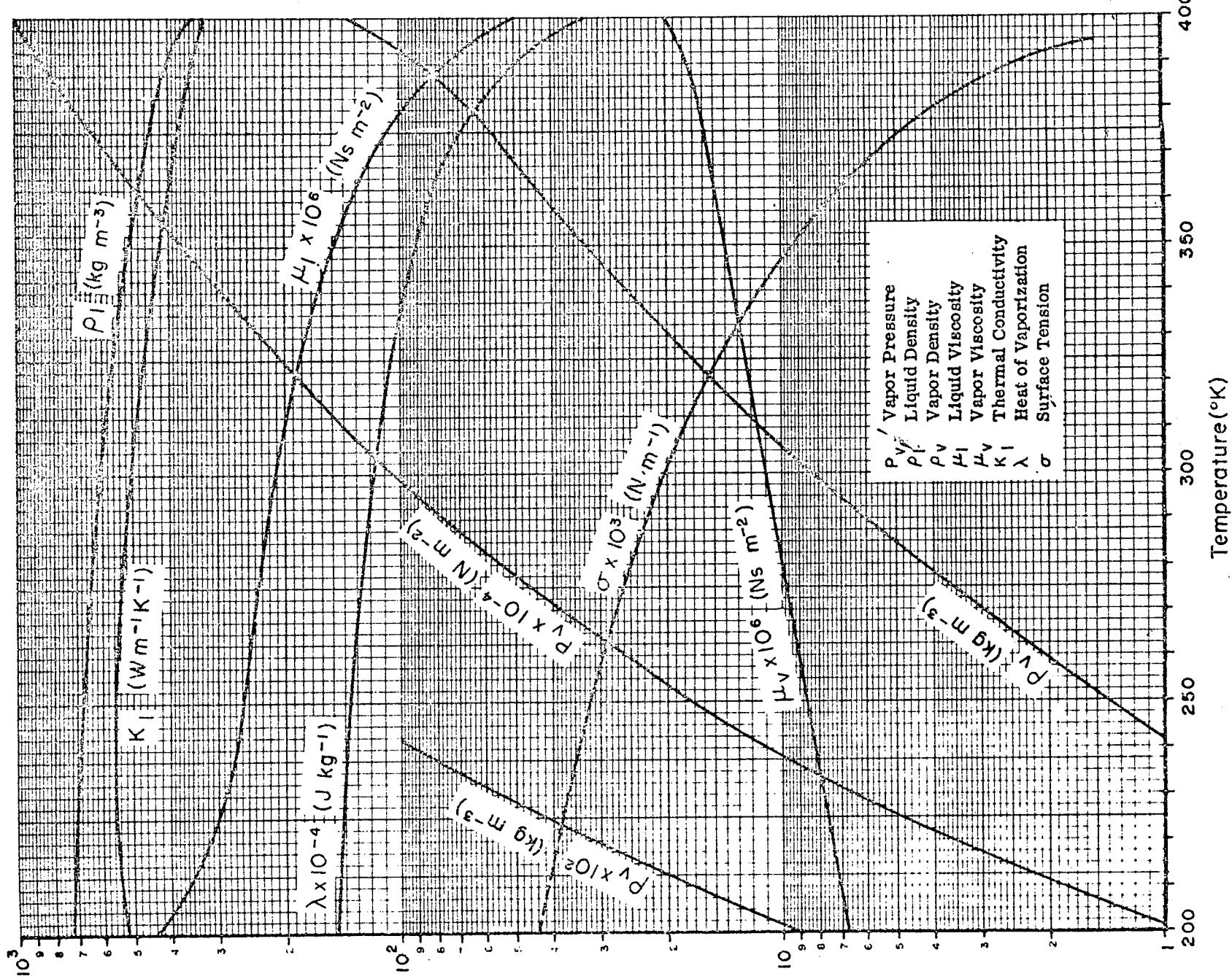
Fluid Properties of Freon-21 (SI Units)



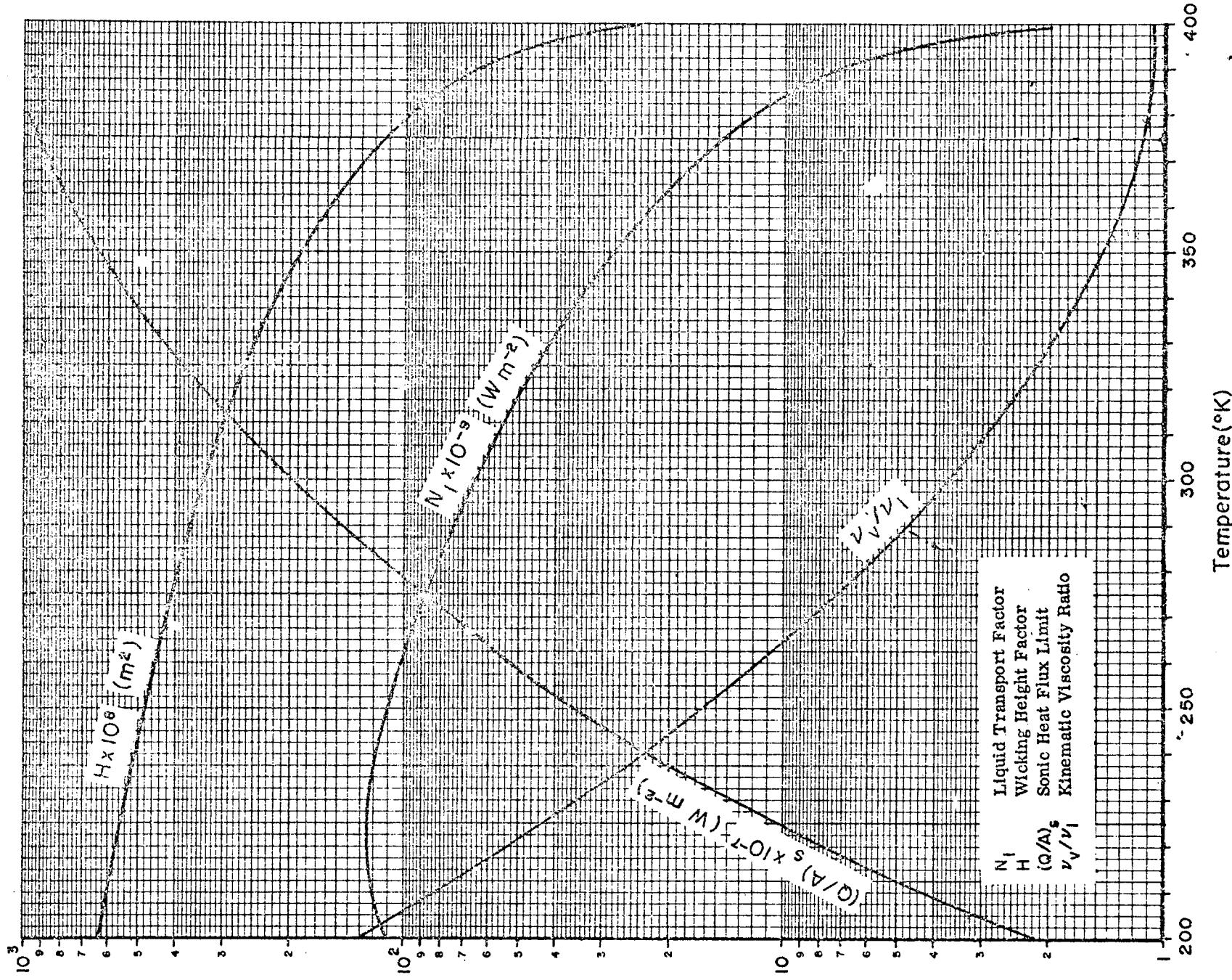
Heat Pipe Design Parameters of Freon-21 (SI Units)



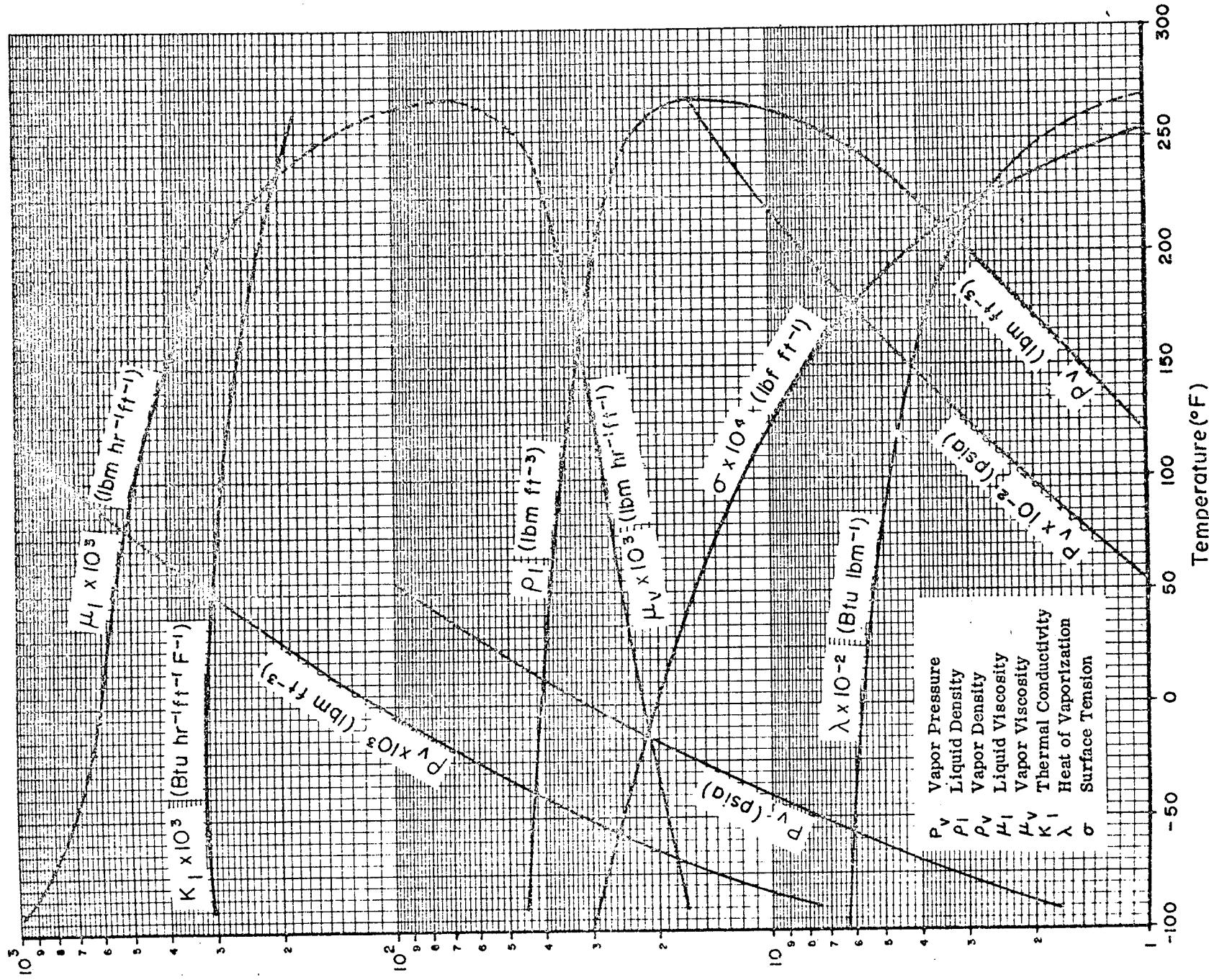
Fluid Properties of Ammonia (SI Units)



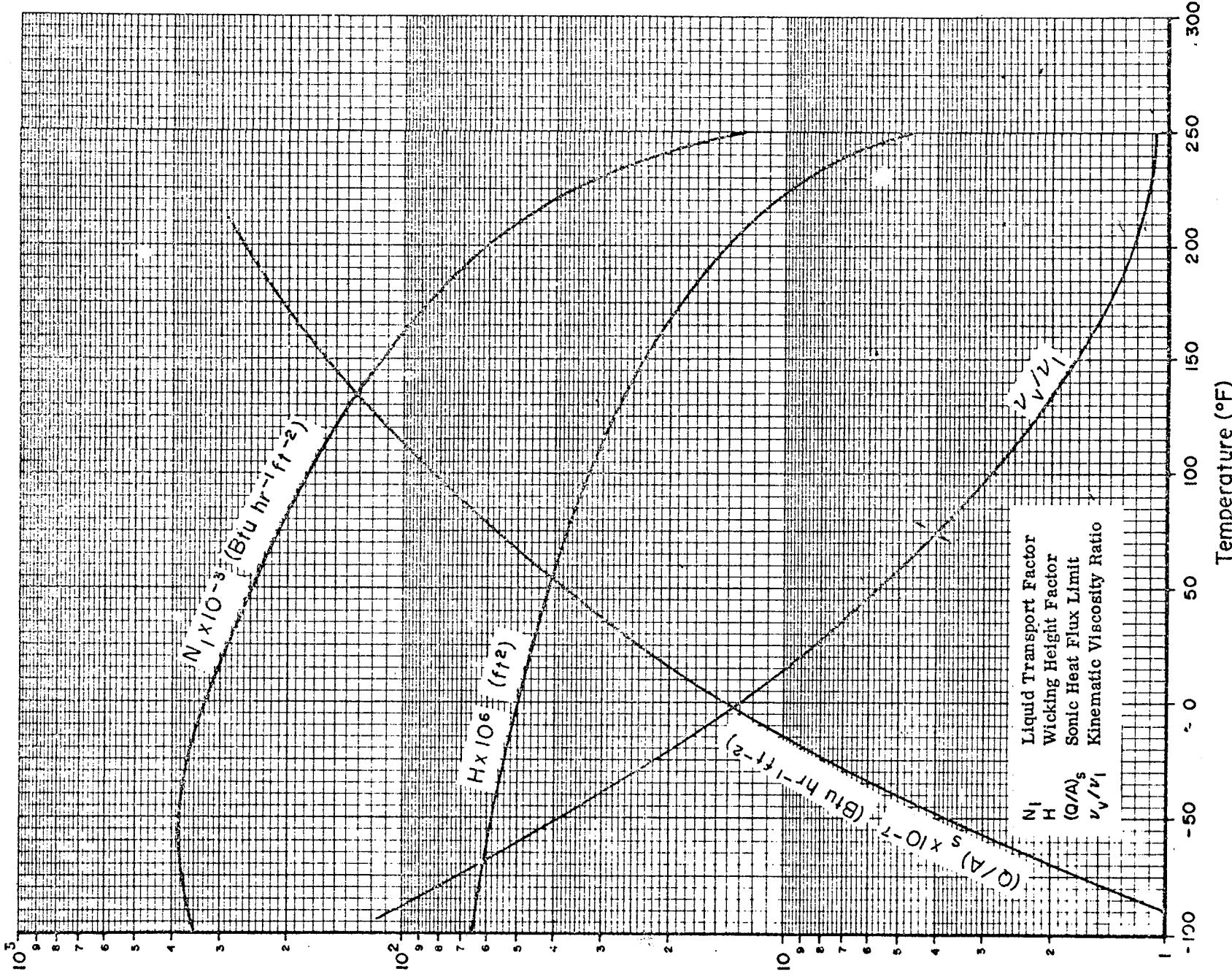
Heat Pipe Design Parameters of Ammonia (SI Units)



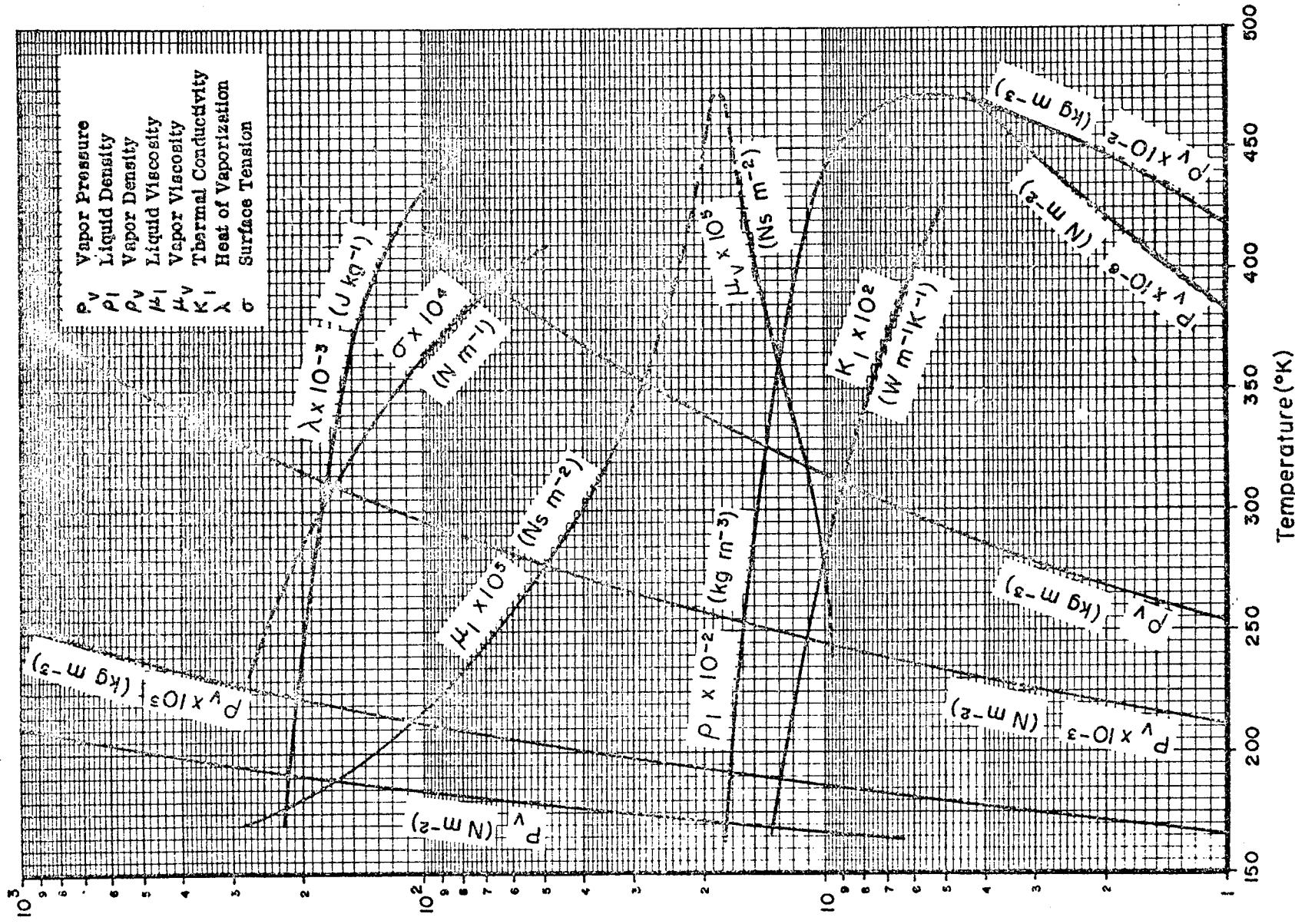
Fluid Properties of Ammonia (British Units)



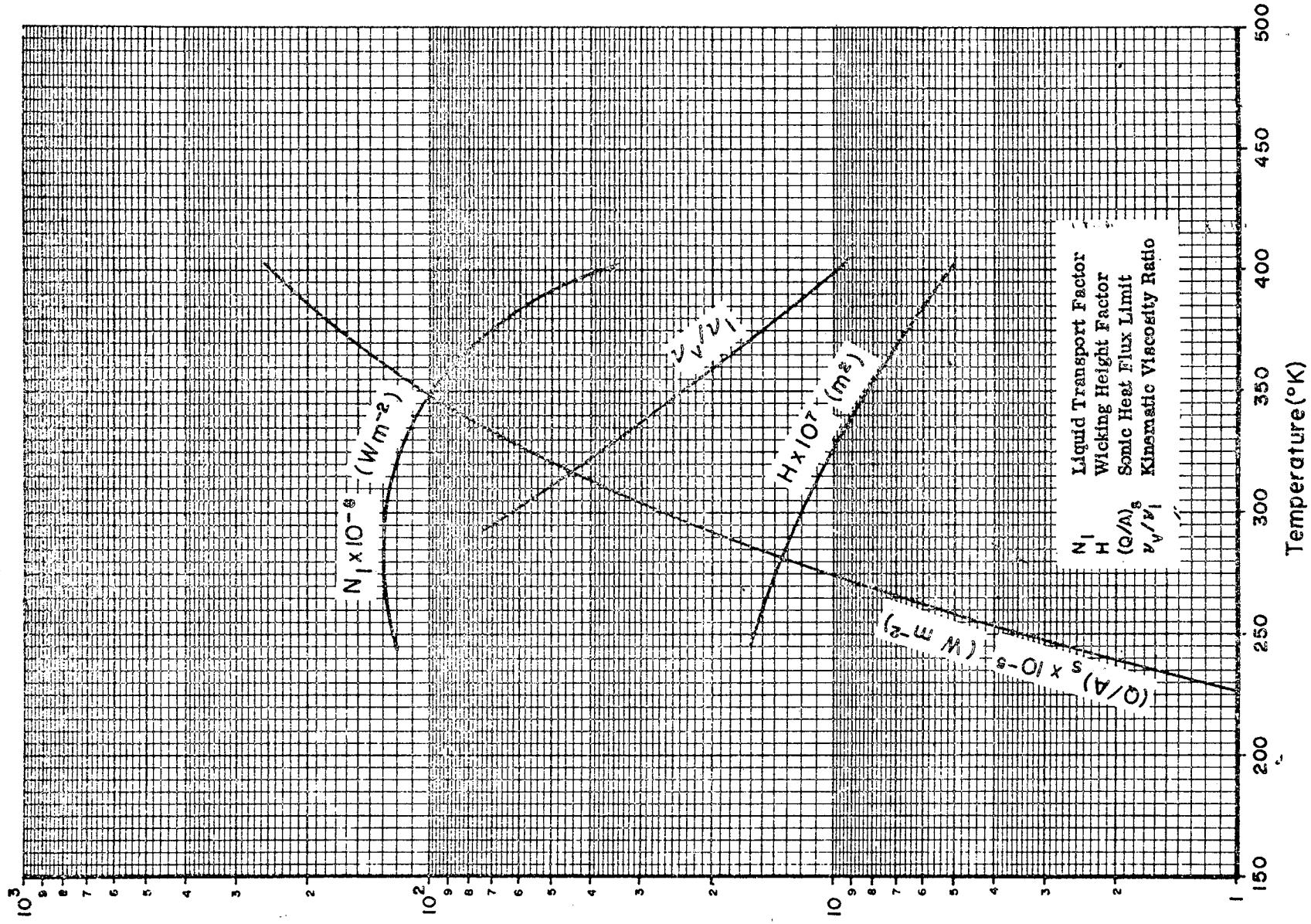
Heat Pipe Design Parameters of Ammonia (British Units)



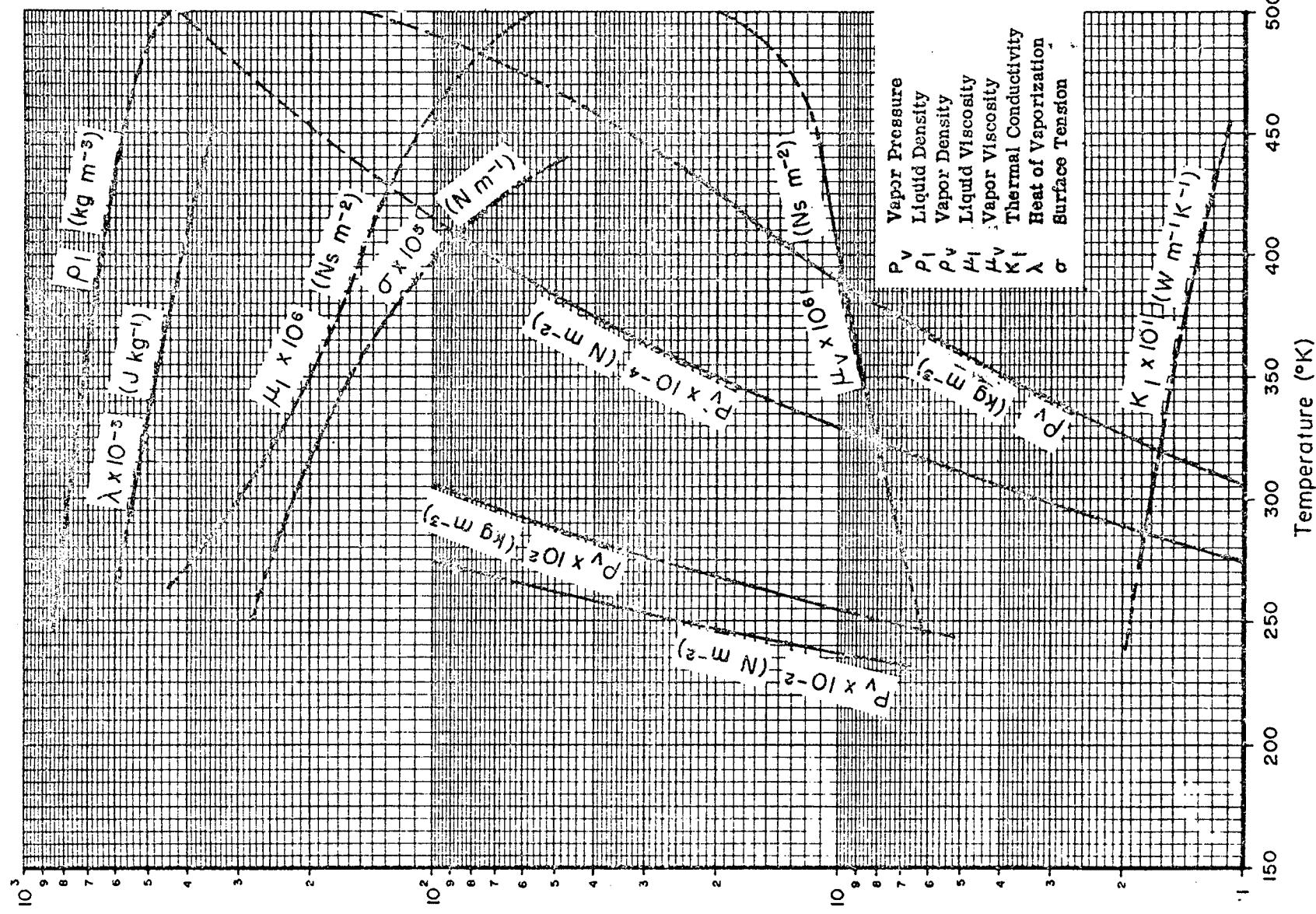
### Fluid Properties of Freon-II (SI Units)



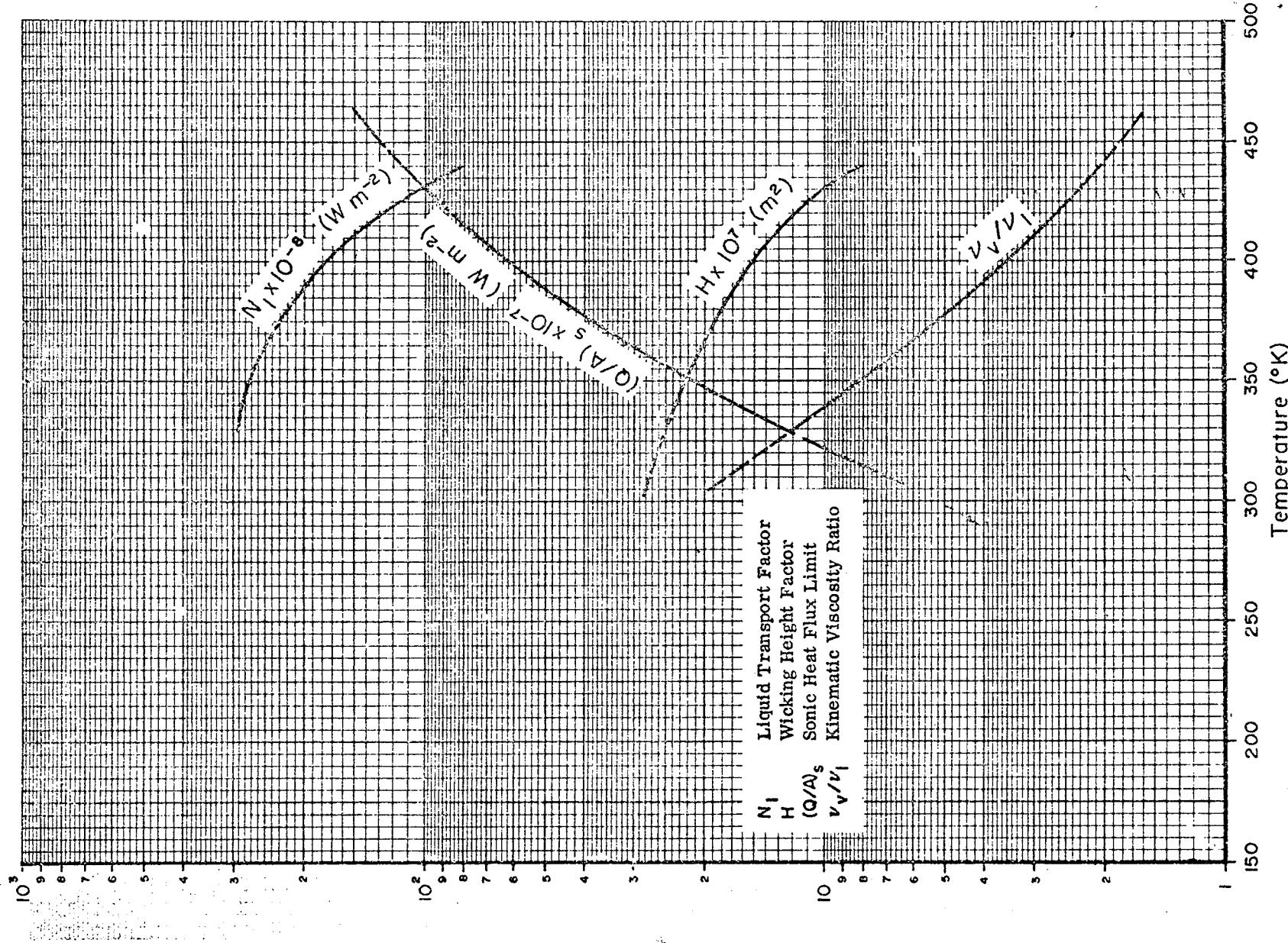
### Heat Pipe Design Parameters of Freon - 11 (SI Units)



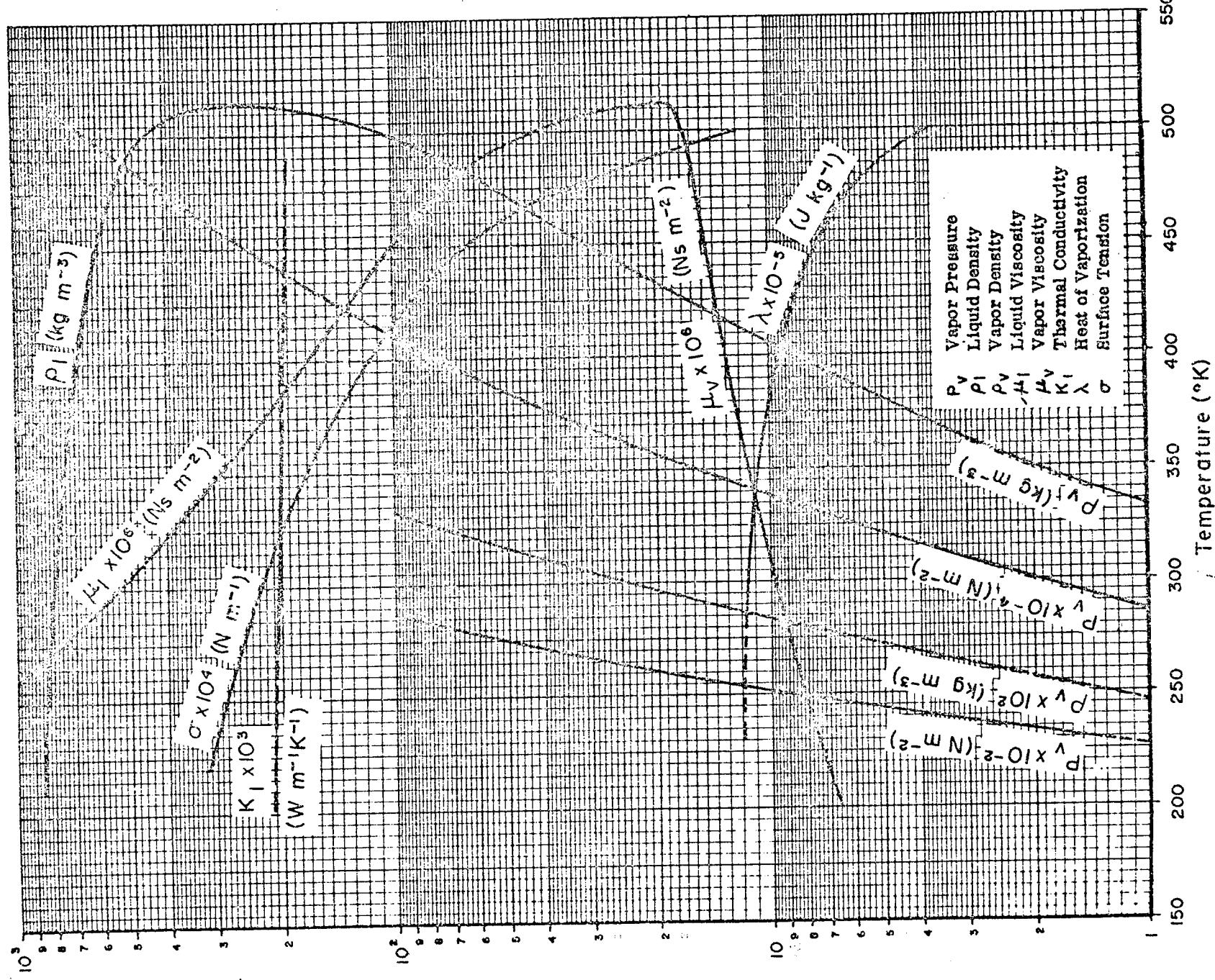
### Fluid Properties of Acetone (SI Units)



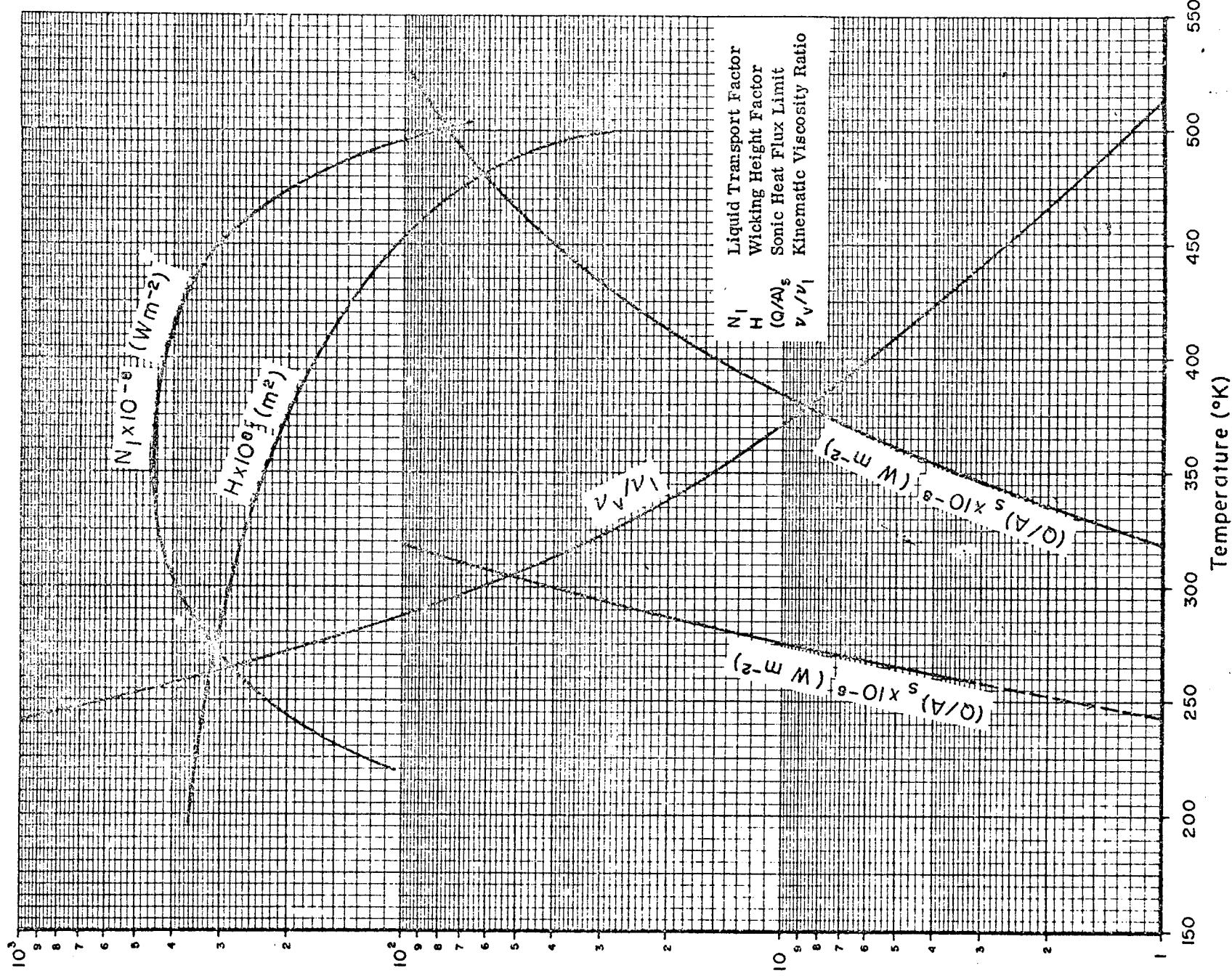
### Heat Pipe Design Parameters of Acetone (SI Units)



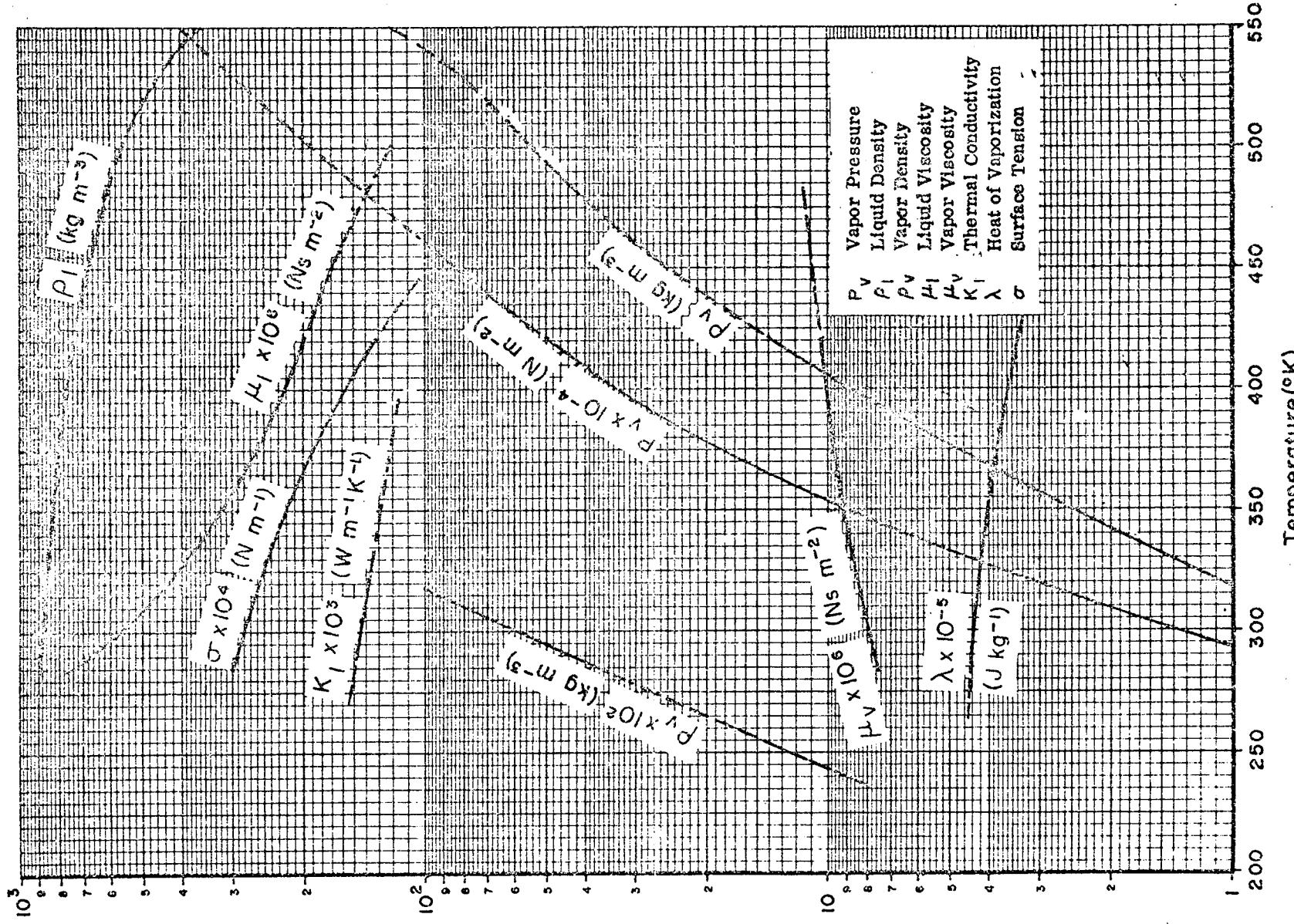
### Fluid Properties of Methanol (SI Units)



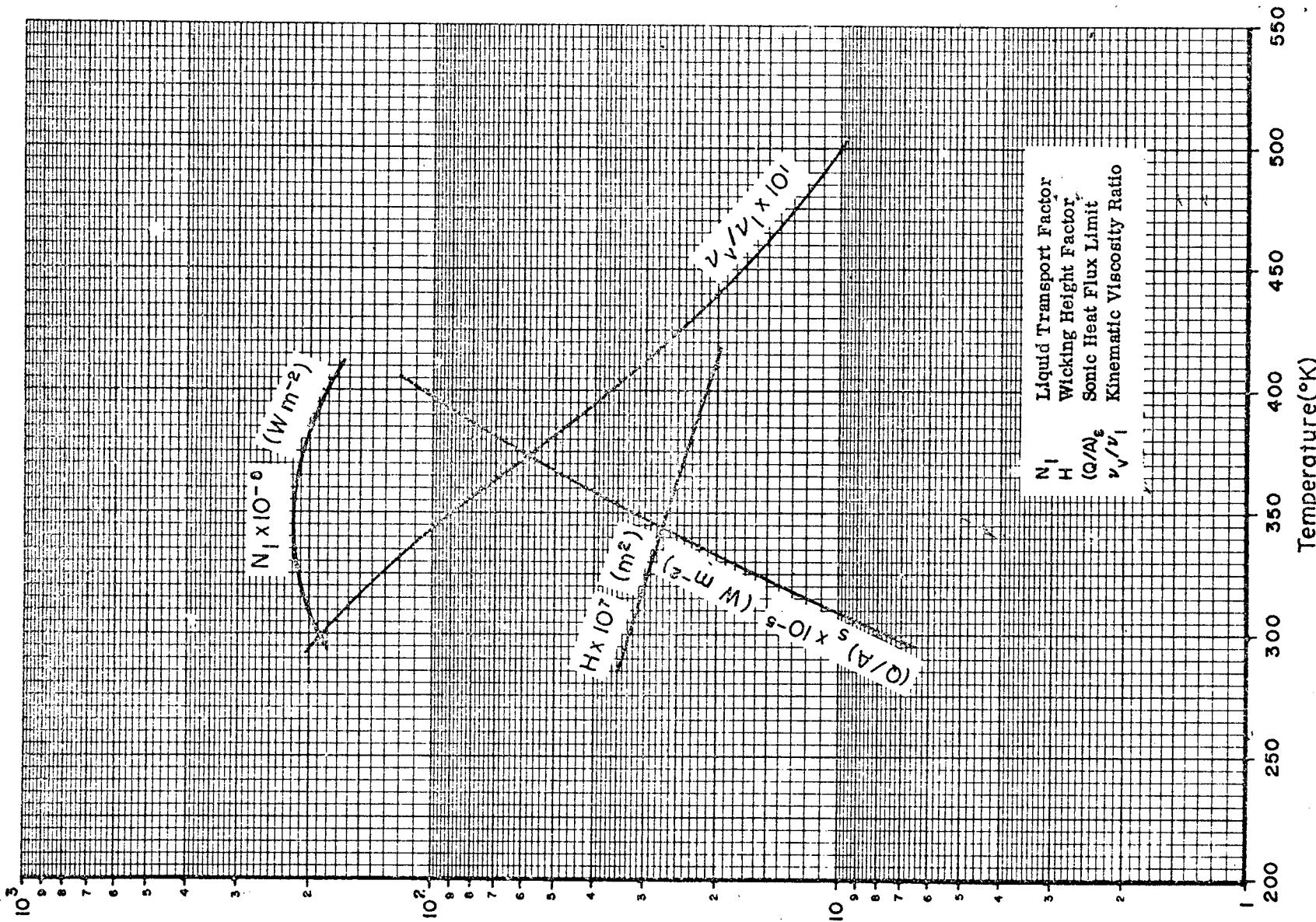
Heat Pipe Design Parameters of Methanol (SI Units)



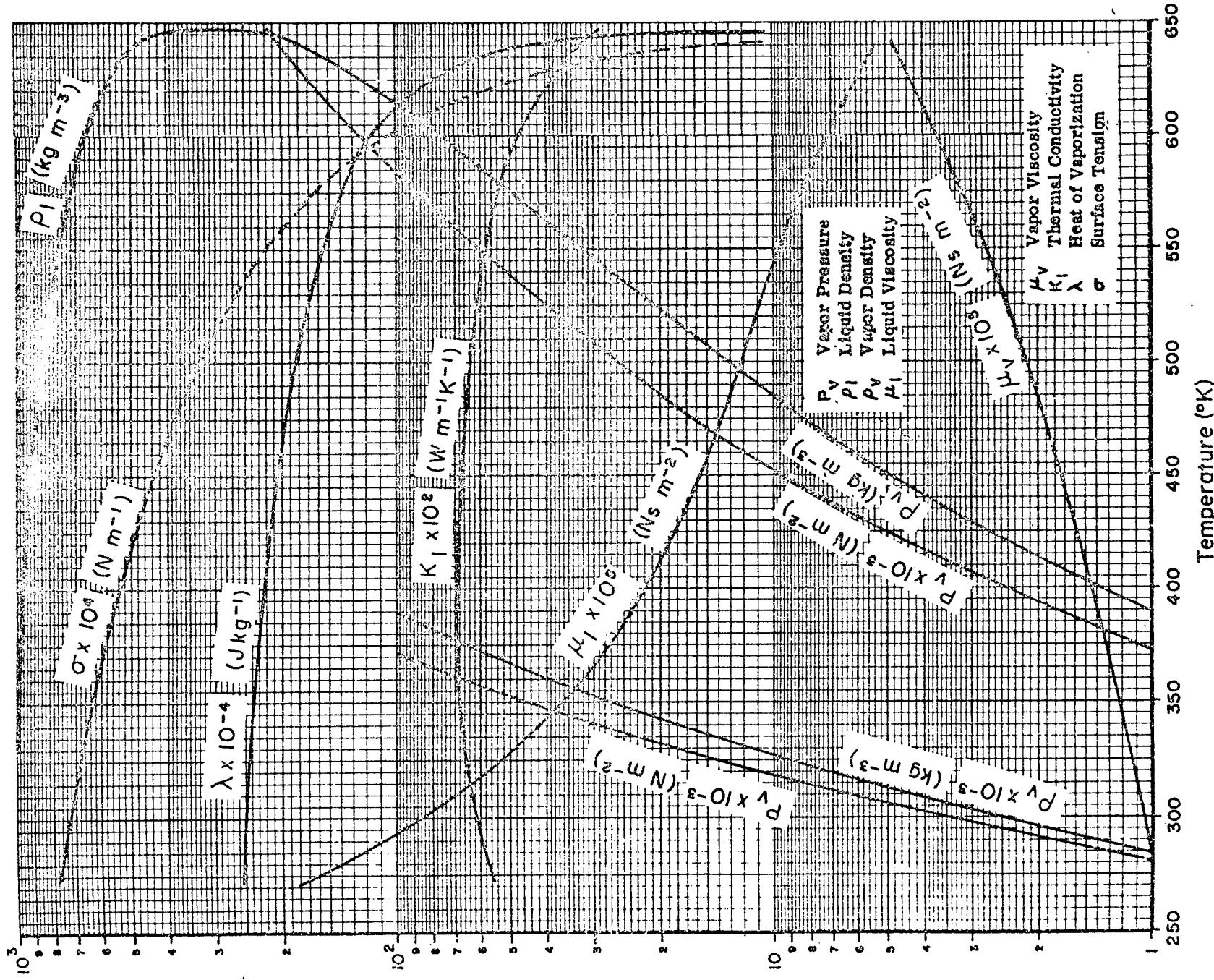
### Fluid Properties of Benzene (SI Units)



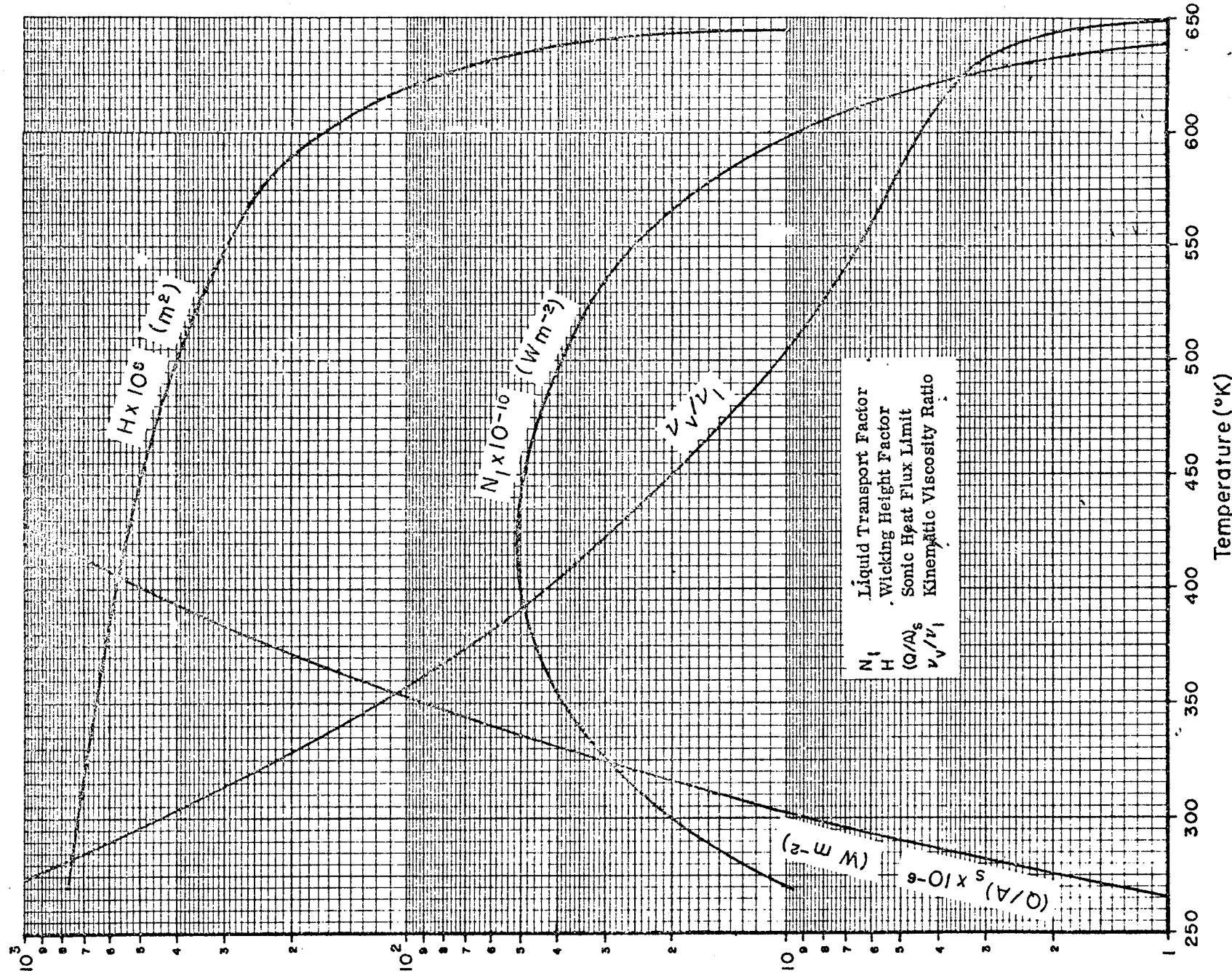
Heat Pipe Design Parameters of Benzene (SI Units)



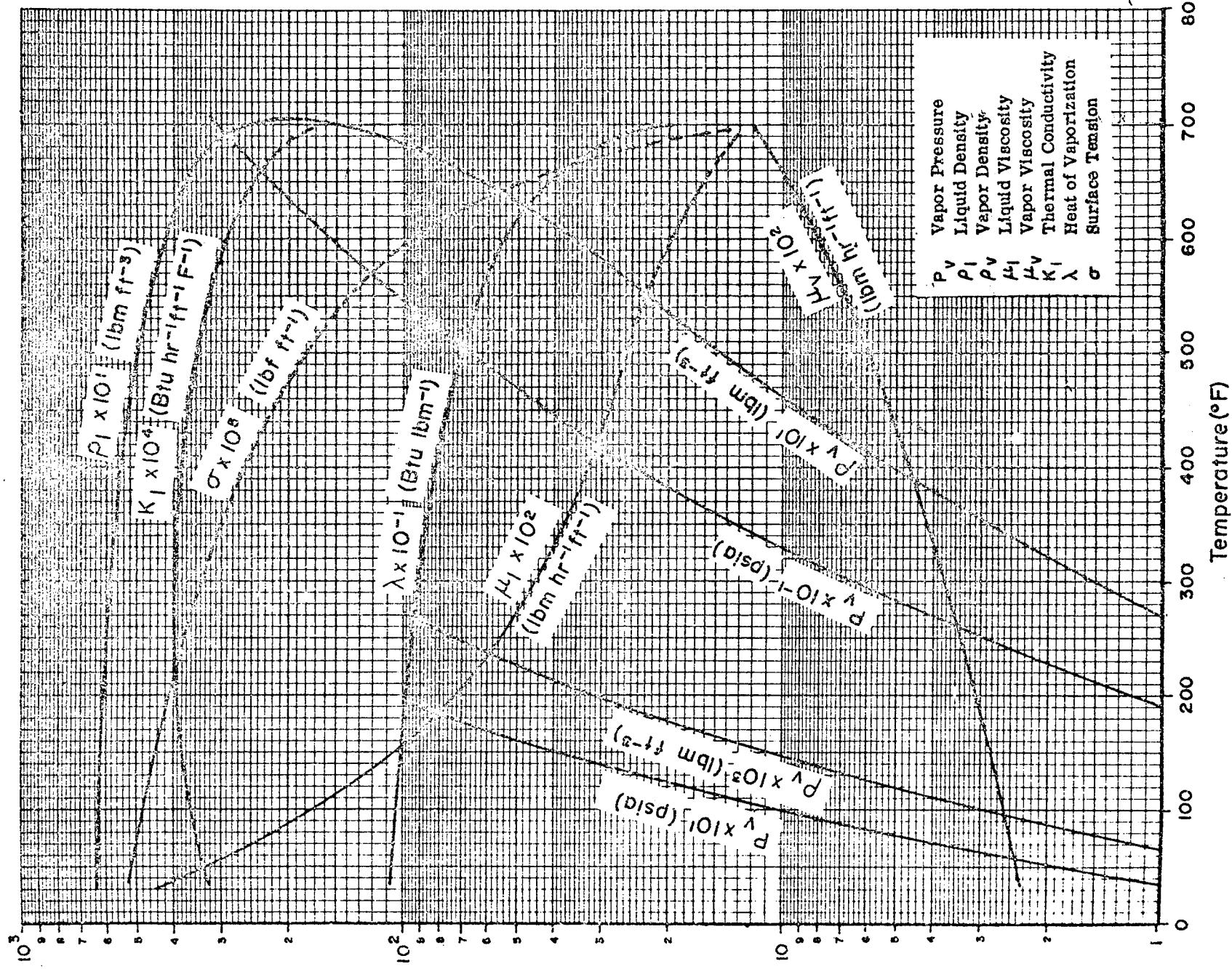
## Fluid Properties of Water (SI Units)



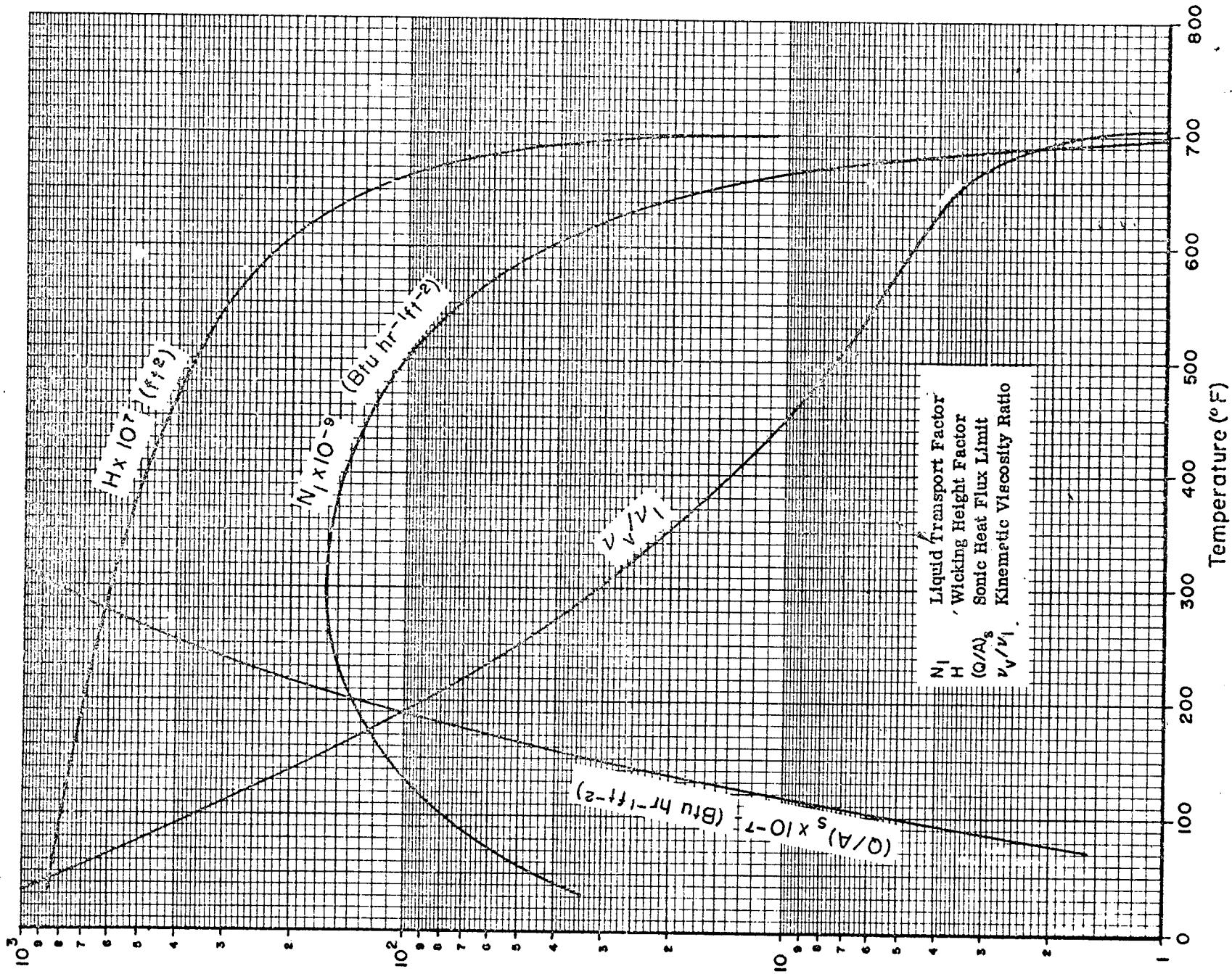
Heat Pipe Design Parameters of Water (SI Units)



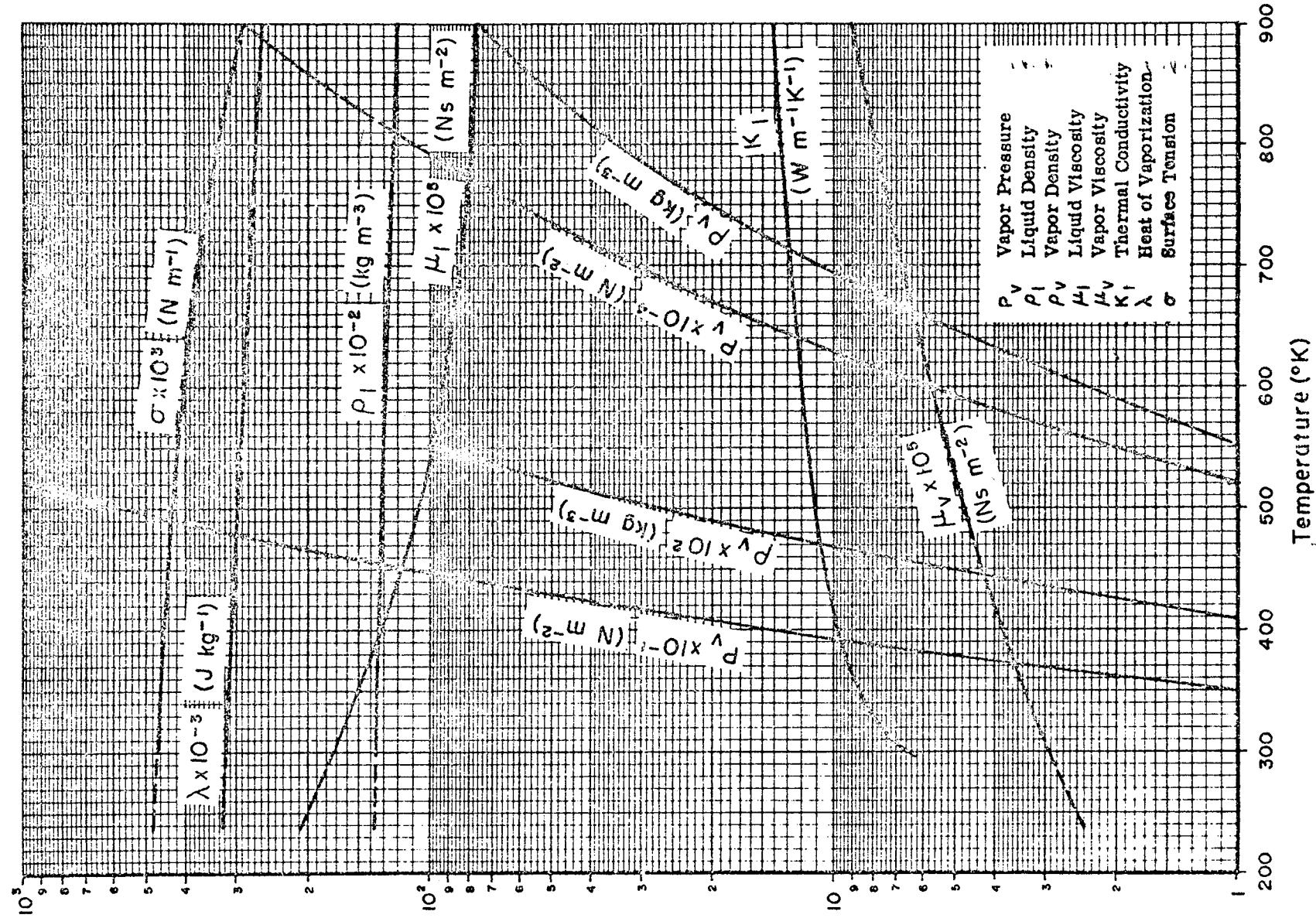
## Fluid Properties of Water (British Units)



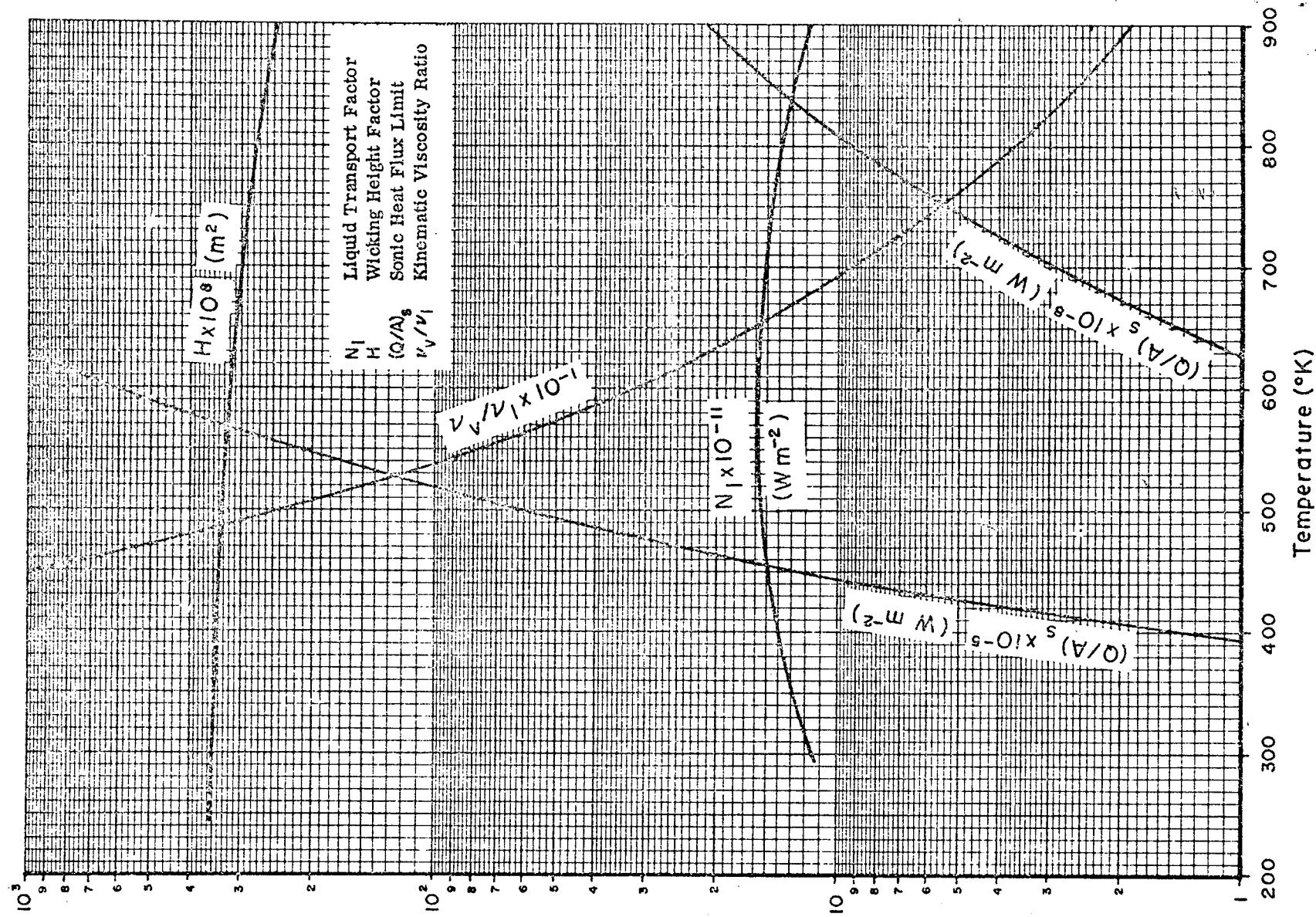
Heat Pipe Design Parameters of Water (British Units)



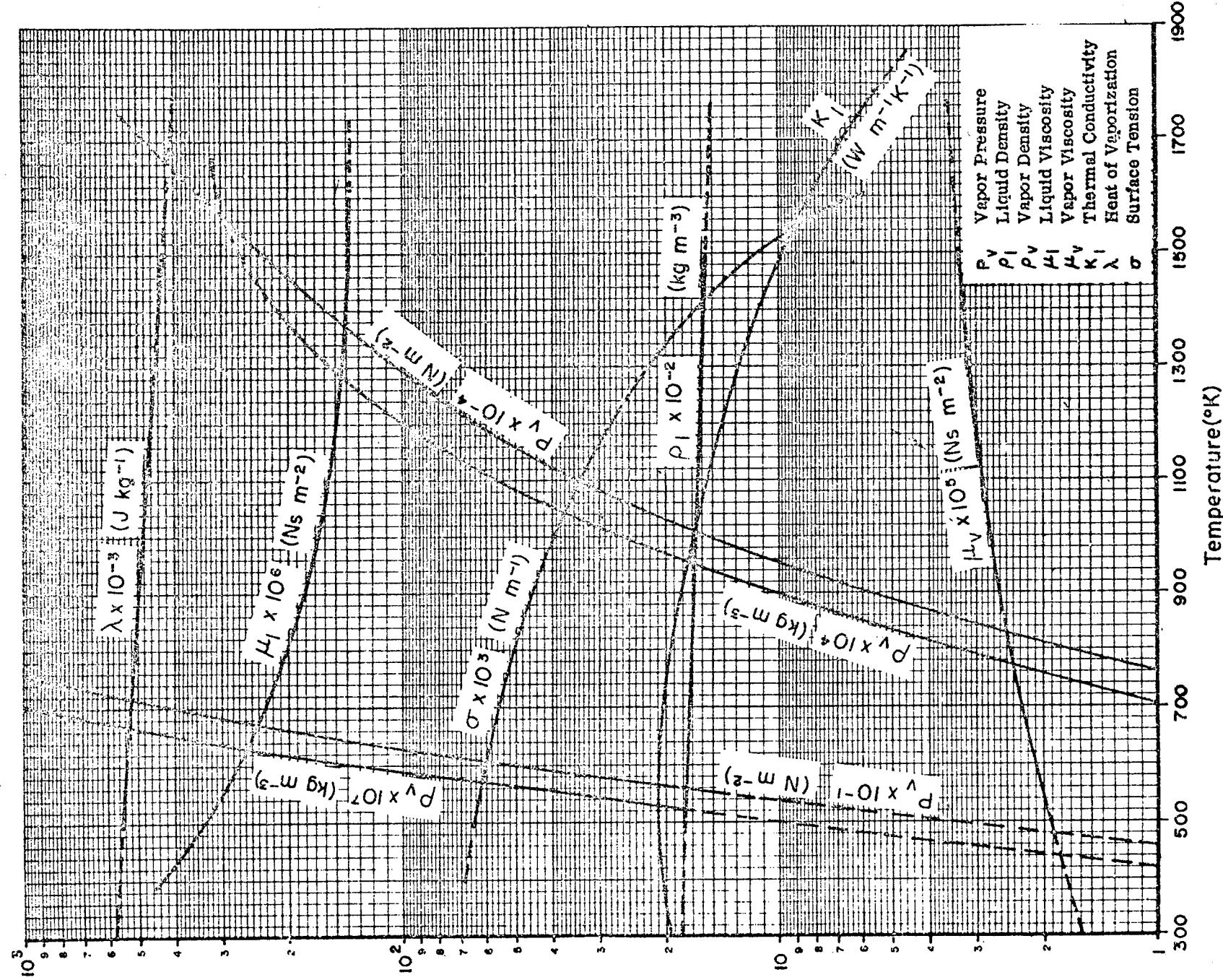
### Fluid Properties of Mercury (SI Units)



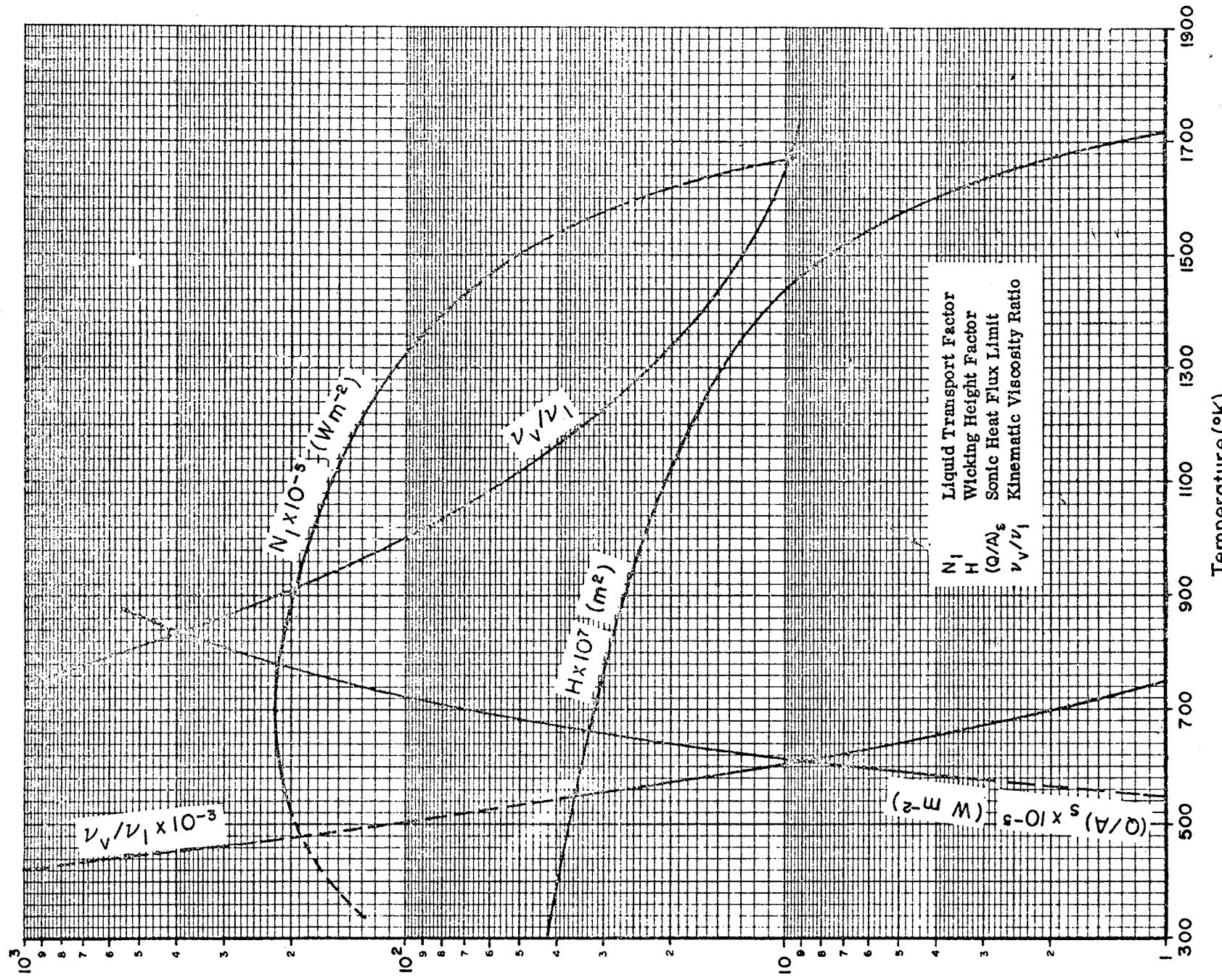
Heat Pipe Design Parameters of Mercury (SI Units)



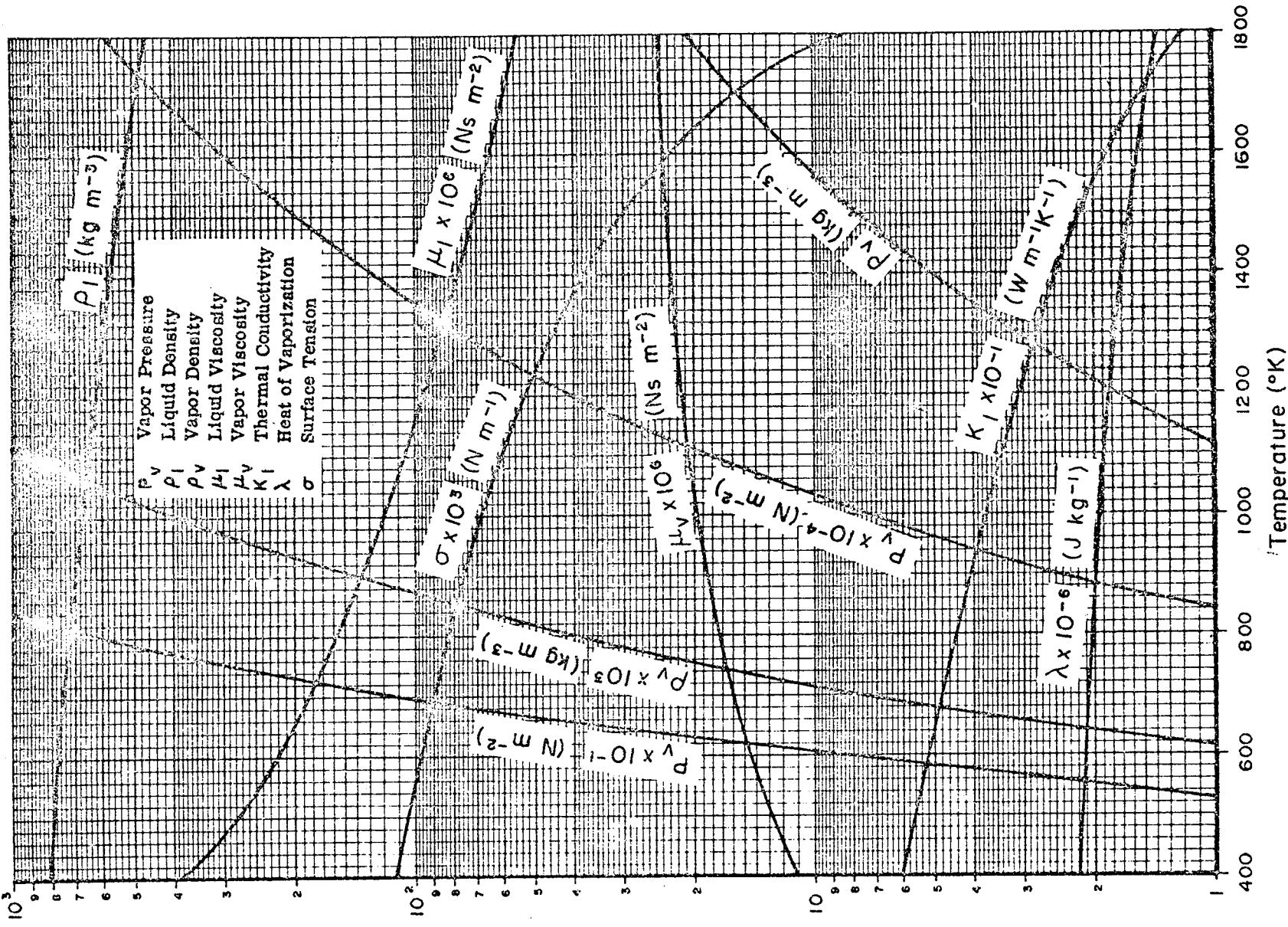
## Fluid Properties of Cesium (SI Units)



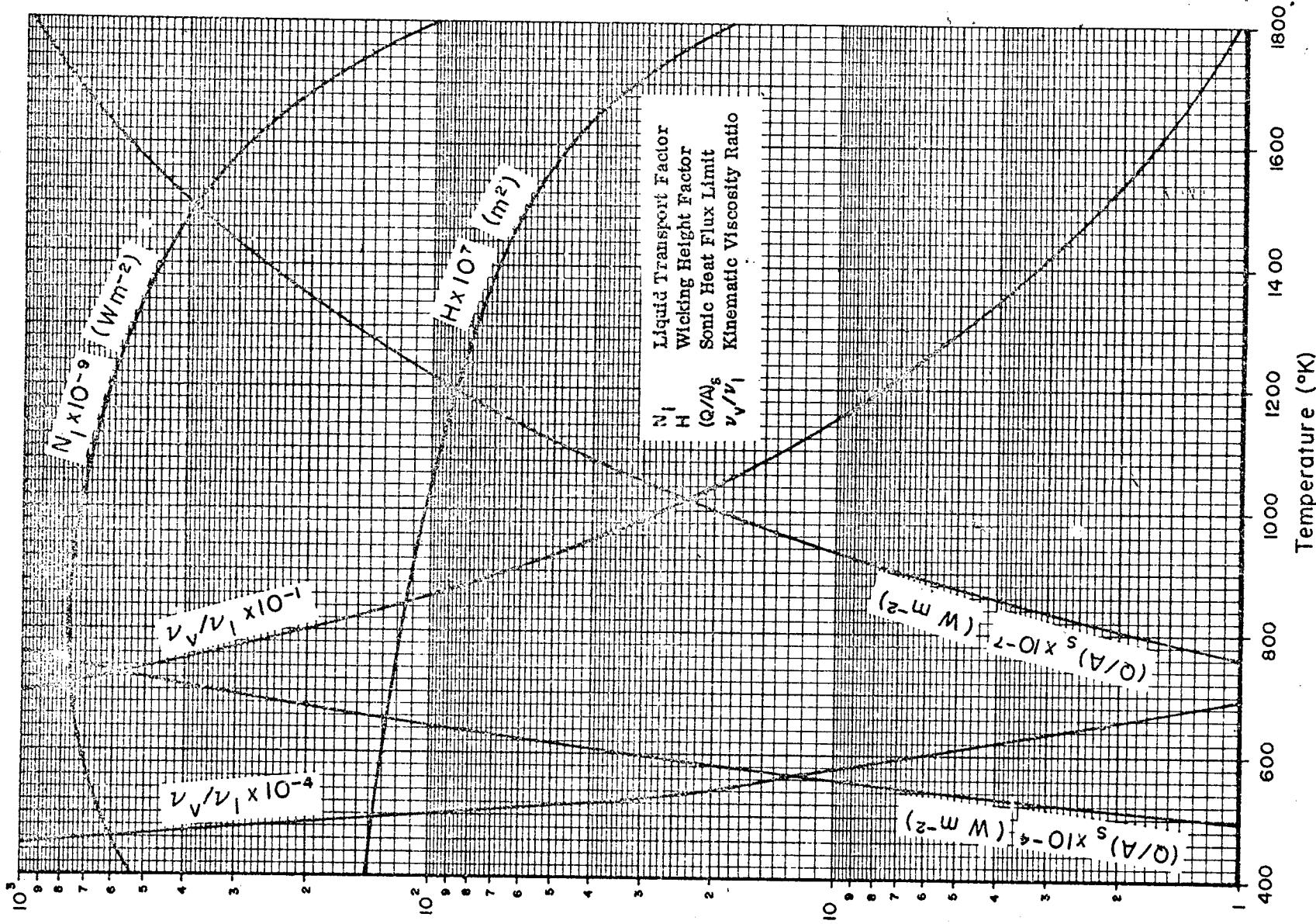
Heat Pipe Design Parameters of Cesium (SI Units)



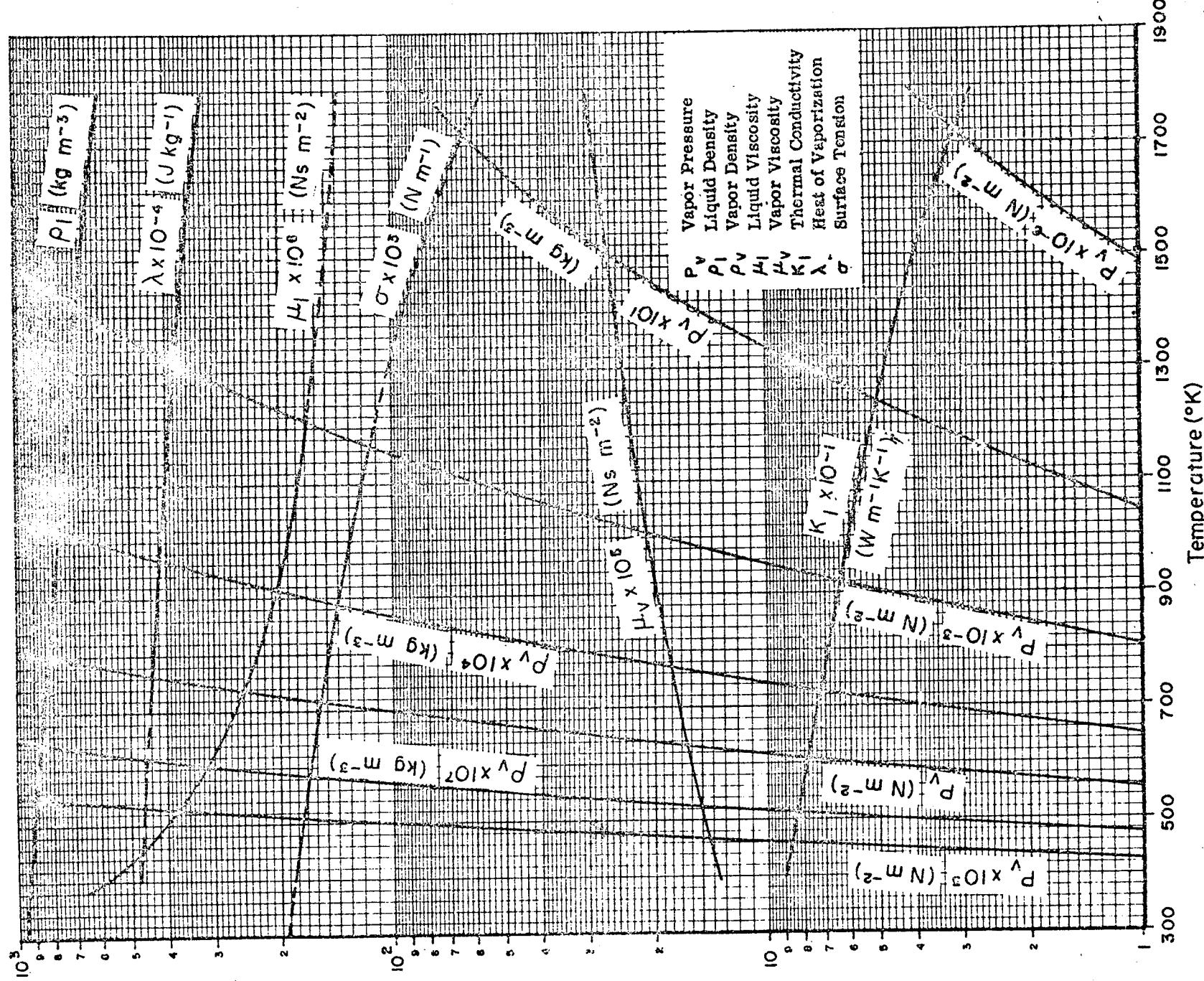
### Fluid Properties of Potassium (SI Units)



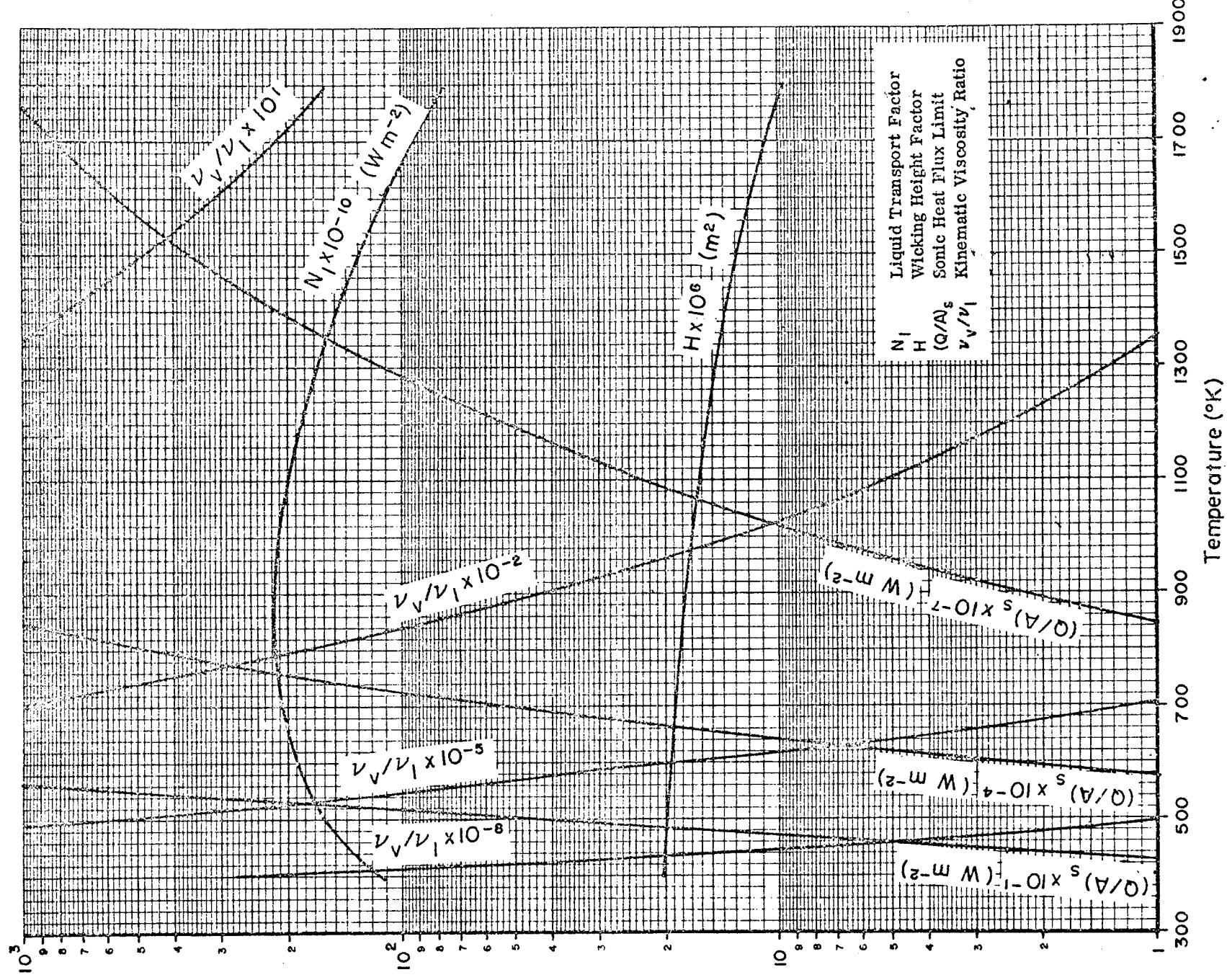
Heat Pipe Design Parameters of Potassium (SI Units)



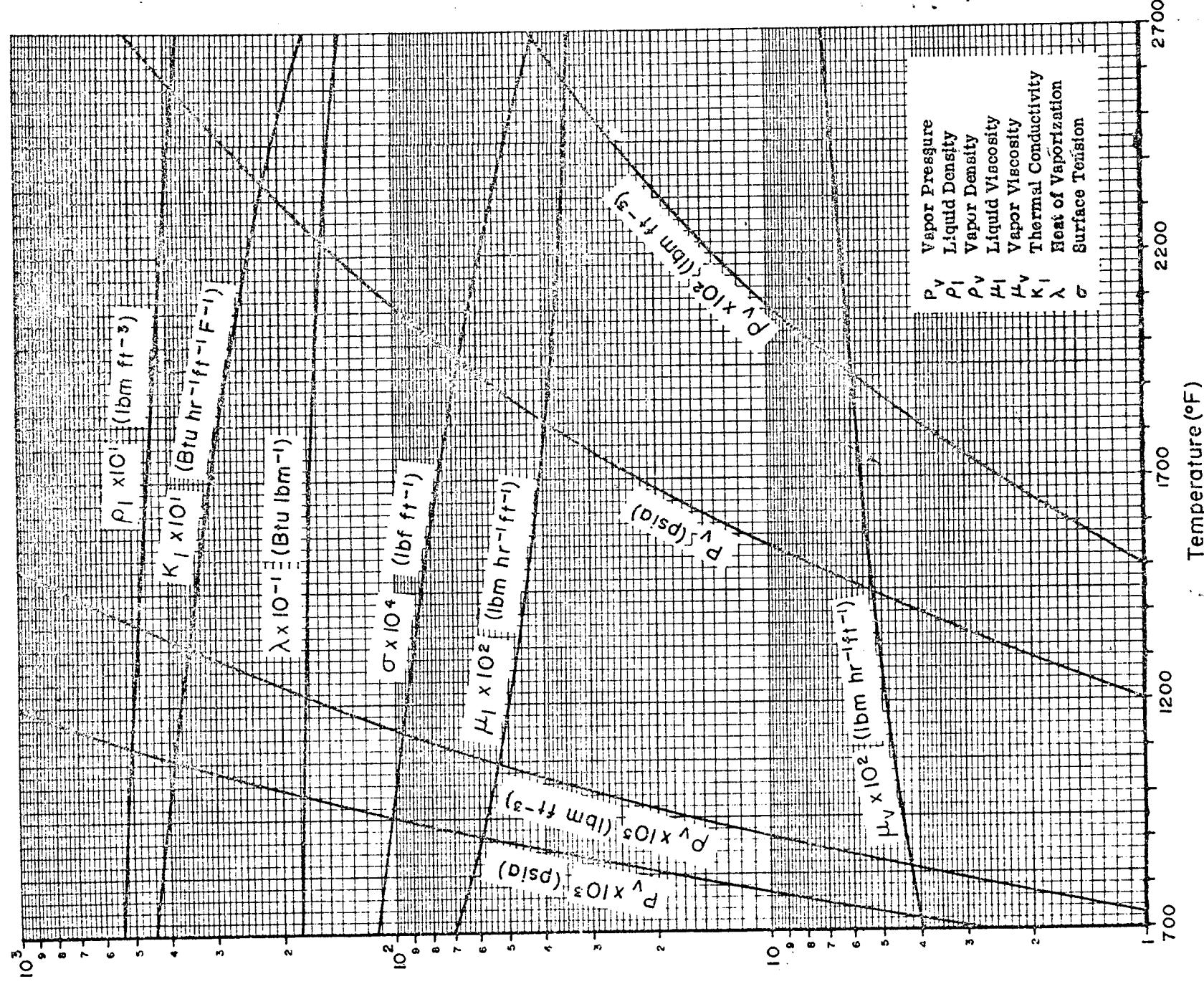
## Fluid Properties of Sodium (SI Units)



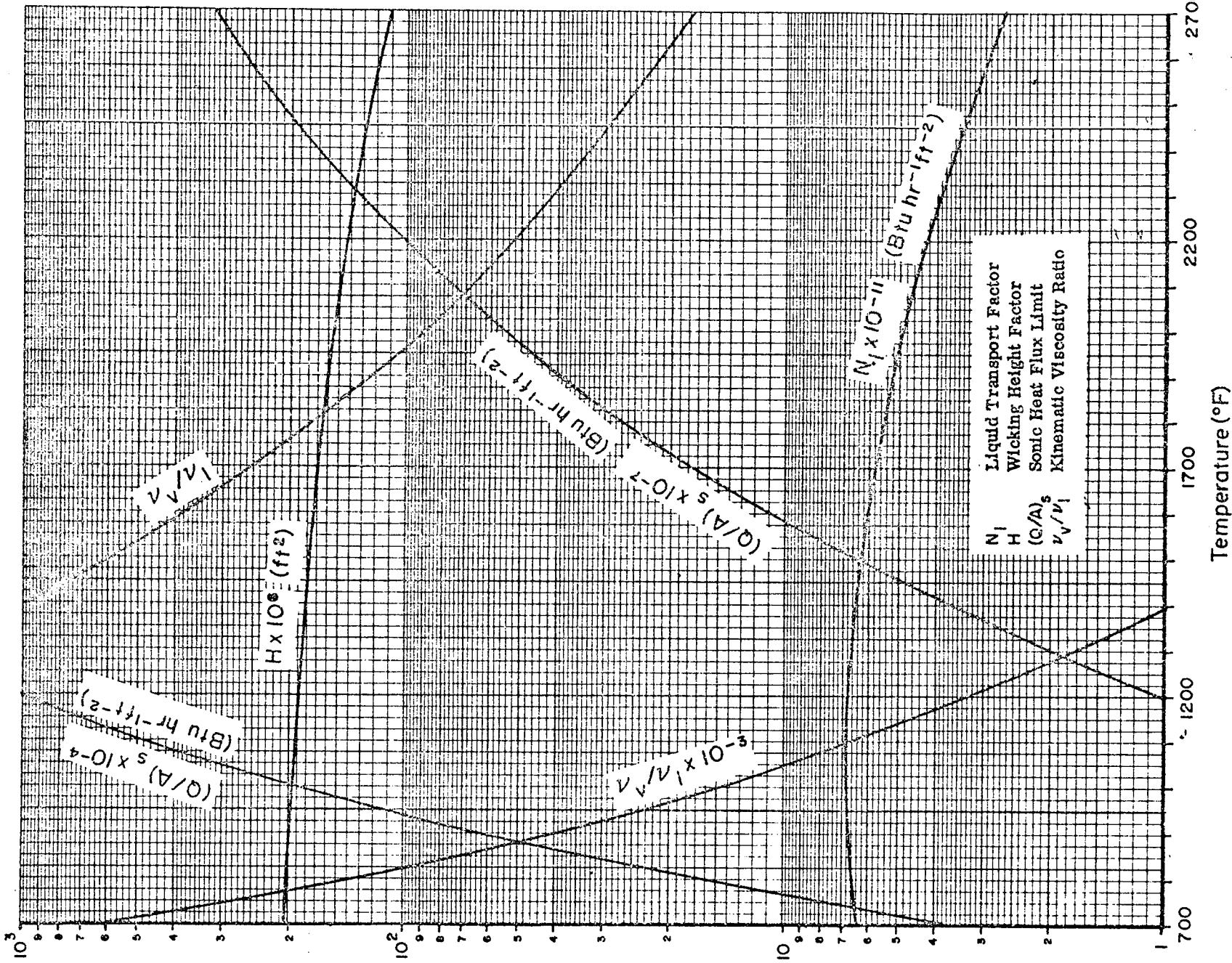
Heat Pipe Design Parameters of Sodium (SI Units)



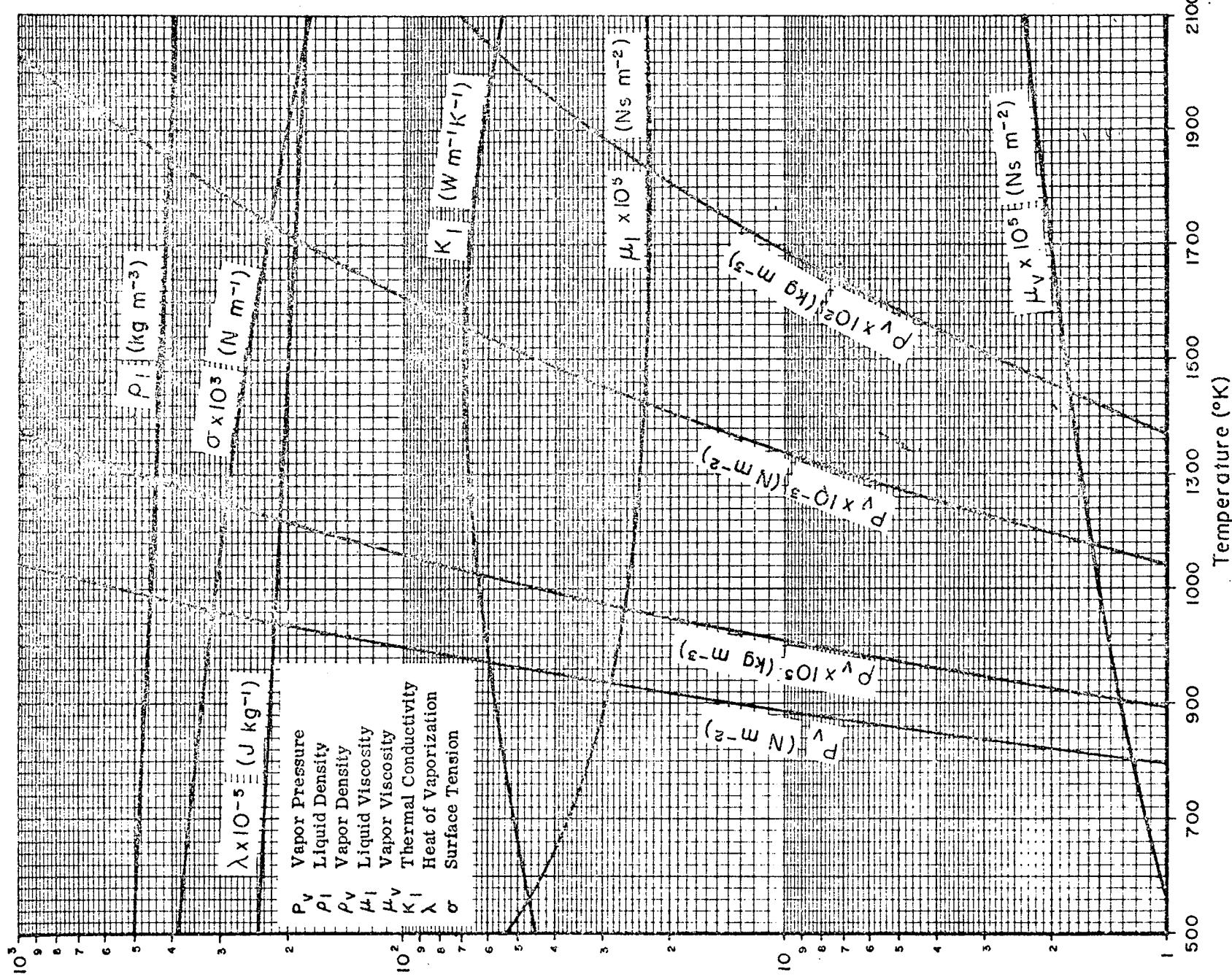
### Fluid Properties of Sodium (British Units)



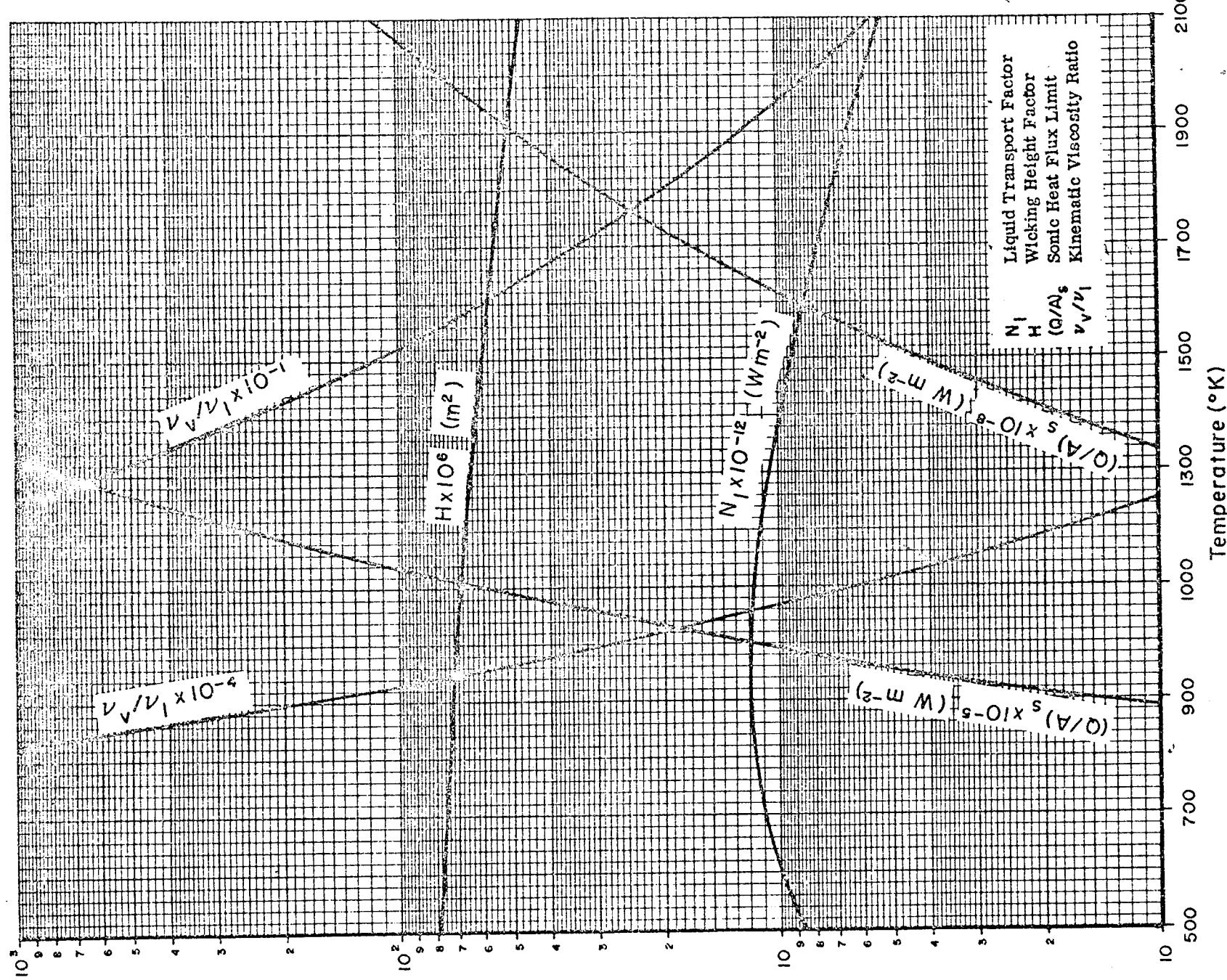
Heat Pipe Design Parameters of Sodium (British Units)



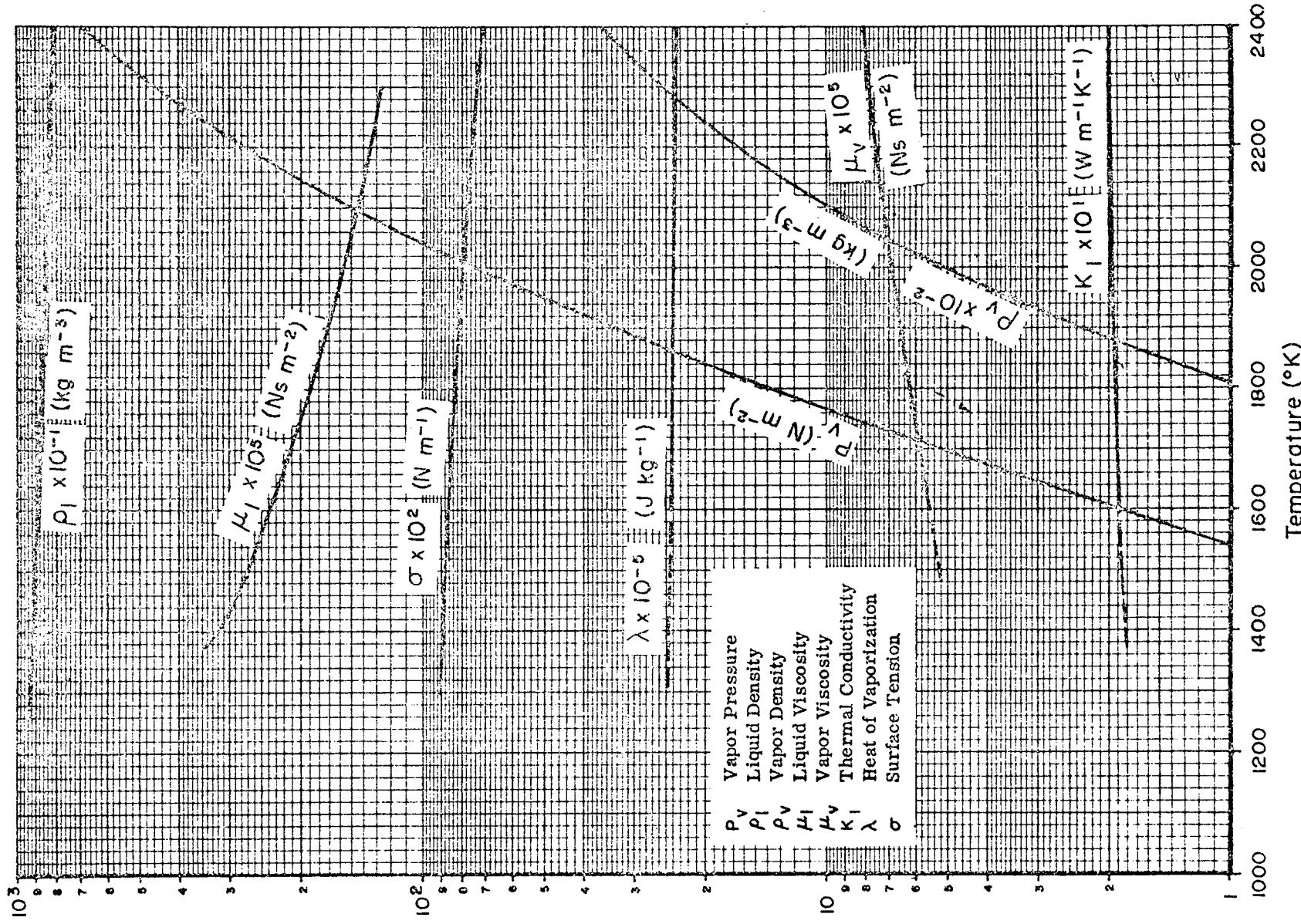
## Fluid Properties of Lithium (SI Units)



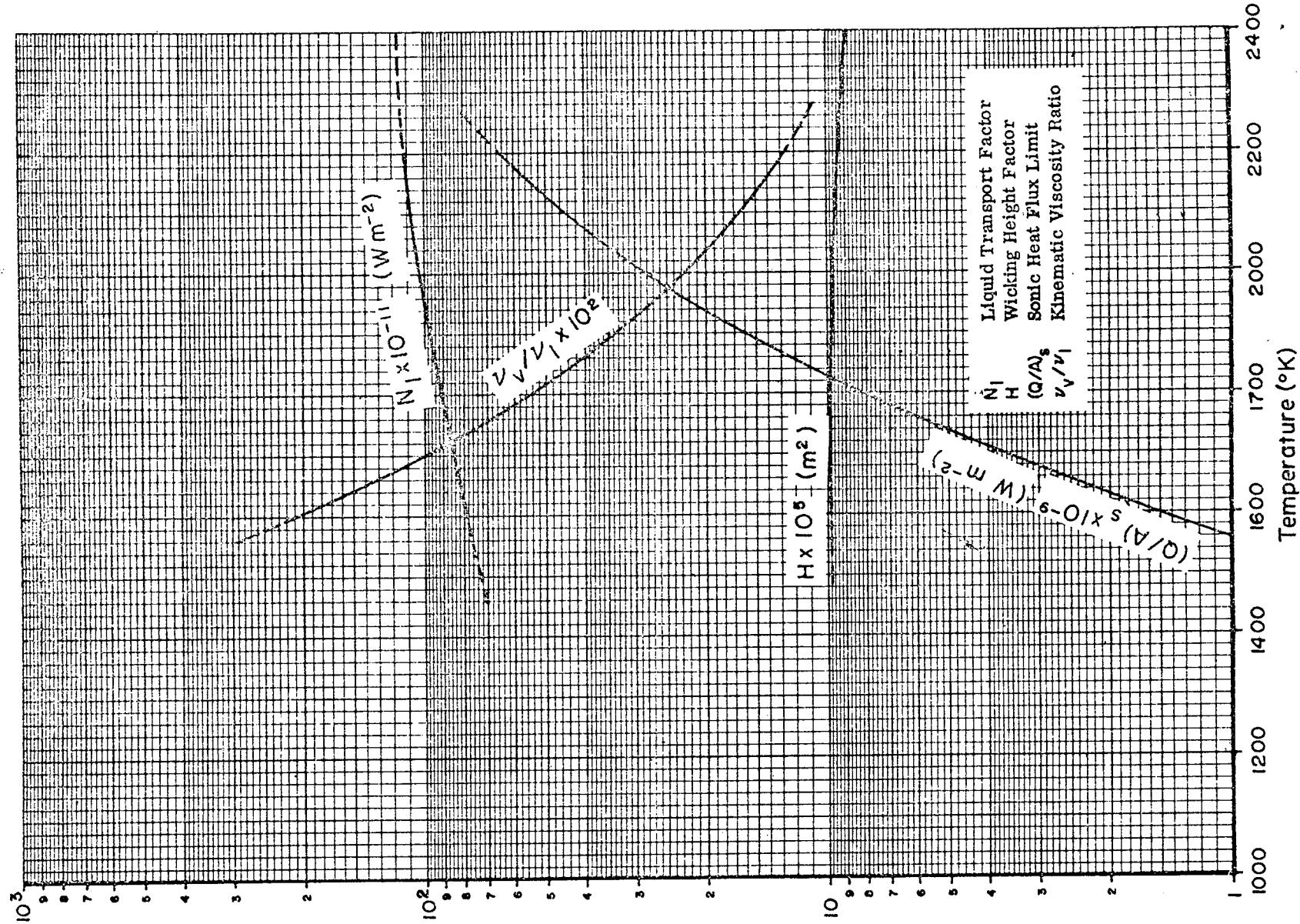
Heat Pipe Design Parameters of Lithium (SI Units)



## Fluid Properties of Silver (SI Units)



Heat Pipe Design Parameters of Silver (SI Units)



M. 1 Introduction

In order to ensure long system lifetime, compatibility must be established between heat pipe working fluid, wall material, wick material, and weld or brazing material. The wide variety of candidate materials for each of these items open many possible interactions which must be considered in the preliminary design.

The use of materials which are incompatible may affect the performance of the heat pipe in various ways. For example, if a reaction occurs and one of the products is a noncondensable gas, it will separate from the operating fluid vapor and collect in the condenser, effectively reducing the condenser heat transfer area. In arterial wick configurations this gas can break the continuity of the fluid column in the artery, causing a burnout condition by restricting fluid flow to the evaporator.

If a reaction product is a solid, it will tend to plug the wick in the evaporator area -- again leading to burnout. Reaction products can also have substantial effects on fluid properties; e.g.,  $\text{Na}_2\text{O}$  in Na causes a very marked increase in viscosity compared to that of the pure liquid metal.

The structural integrity of the container may be decreased as a result of dissolution of the wall material and thereby reduce the strength of the wall or, in severe cases, cause the wall to be penetrated. Even if the container does not completely dissolve, undesirable reactions may form compounds with the working fluid thus increasing the probability of stress cracking, etc.

Certain types of corrosion tend to be restricted to certain temperature regimes. Low temperature corrosion in heat pipes has usually been found to be electrochemical in nature, while high temperature corrosion has usually been observed to be a solution process.

The most common types of heat pipe compatibility problems are listed in Table M-1. From these it can be seen that a few basic questions should be applied to all suggested structural material/fluid combinations.

Effects	Causes
Decrease in Heat Pipe Conductance	Noncondensing gas reaction product Outgassing of container, wall, wick, or fluid Decomposition of working fluid generating noncondensing gas
Decrease in Heat Pipe Transport Capability	Wick plugged with solid precipitate and unable to transport working fluid Fluid flow disrupted by gas bubbles in wick Decrease of wick wettability due to chemical reactions Decrease in surface tension of liquid due to dissolved reaction products Increase in viscosity of fluid due to dissolved reaction products Wick dissolved and unable to transport working fluid
Failure of Container Wall	Galvanic corrosion of container wall Solubility of container wall in working fluid

Table M-1: General Compatibility Problems in Heat Pipes

- Do they react chemically with each other at the operating temperature? (This includes the formation of alloys and intermetallic compounds.)
- Will they tend to set up a galvanic cell?
- Are any of the materials soluble in the working fluid at the operating temperature?
- Will any of the structural materials catalyze the decomposition of the working fluid at the operating temperature?

The following sections cover the most common types of compatibility problems. However, since the level of corrosion which can be tolerated in a heat pipe is so small, the results of most ordinary corrosion studies can only be used as a guide to the intelligent selection of heat pipe materials. Each new combination of materials must still be proven by performing life tests.

#### M. 2 Low Temperature Corrosion

Most metals are found in nature as ores, and energy must be supplied to reduce them to the metallic state. This suggests that the metallic state is a high energy state; and, consequently, metals will generally combine with other substances to revert to a lower energy state. This basic process is generally referred to as corrosion. According to thermodynamics, the driving force is the difference between the Gibbs Free Energies,  $\Delta G$ , of the reactants and products (31). For any reaction,  $\Delta G$  is related to the equilibrium constant,  $K_e$ , for the reaction:

$$\Delta G = -RT \ln K_e$$

The reactions involve the transfer of electrons between the chemical species. A definite electromotive force is associated with such an exchange between two species. The emf is related to the Gibbs Free Energy by:

$$\Delta G = -nFE$$

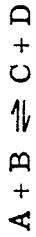
where  $F$  is the Faraday number and  $n$  is the number of electrons transferred. The

combination of Equations M-1 and M-2 yields:

$$E = \frac{R T}{n F} \ln K_e$$

M-3

For the reaction,



Equation M-3 would be expressed as:

$$E = \frac{R T}{n F} \ln \frac{(C)(D)}{(A)(B)}$$

Thus, if the reaction expressed by Equation M-4 proceeds to the right, the product of the concentrations of C and D are larger than the product of the concentrations of A and B. The electromotive force, E, is then positive. Similar reasoning shows that if the reactants are present to a greater extent than the products at equilibrium (the reaction does not occur) the emf will be negative.

Extensive tables of the characteristic emf's of many electrochemical reactions in various solutions have been presented in a number of references (22) (25) (31). A short list of some common materials in the order of their decreasing activity in aqueous solutions is given in Table M-2.

The reader is referred to works on chemical thermodynamics (31) for a thorough discussion of the utilization of such data. Special attention must be given to determine whether the tables being used give oxidation or reduction reactions in their format, since the emf's are of opposite sign in the two cases. The farther apart two materials are in this table, the more likely they are to cause a corrosion reaction if they are exposed to a common liquid bath.

The fact that the emf indicates that a reaction can take place does not necessarily ensure that it will take place. In electrochemical reactions, the rate is generally determined by the current flow; and this is subject to many variables (23), e. g., surface configuration, deposition of products, diffusion rates of current carrying species, etc. Thus, even though thermodynamic considerations indicate that the

M-4

M-5

M-4

Table M-2: Relative Electrochemical Activity of Some Common Materials Relative to Hydrogen

EMF	Material	Alloys/Condition	Material	Alloys/Condition
2.34	Magnesium		0.23	Lead
0.76	Zinc		0.23	Tin
0.63	Alclad 3003	Clad with 6061, 7075	0.20	Nickel
0.54	Aluminum Alloys	5056, 3003, 1100, 6061-T6	0.20	Monel
0.49	Cadmium		0.18	Copper
0.48	Aluminum Alloys	7075, 6061-T4	0.20	Bismuth
0.45	Aluminum Alloys	2014-T6, 2024-T3	0.24	Stainless Steel
0.40	Steel	Mid	0.24	Stainless Steel
0.35	Iron	Wrought	0.24	Nickel
0.25	Stainless Steel	316 (Passive)	0.24	Monel
0.19	Iron	Cast	0.24	Silver
0.25	Solder	50% Tin, 50% Lead	0.82	Chromium
0.25	Stainless Steel	304 (Active)	1.3	Gold
0.25	Stainless Steel	316 (Active)	1.3	Platinum

reaction should proceed spontaneously, kinetic factors may cause it to proceed at an extremely slow rate.

Emf differences can occur between different concentrations of a single species as well as between separate species (31). Different concentrations of a single species occur in a heat pipe between the condenser and the evaporator because of the concentrating effect of the evaporation process on dissolved materials.

In water heat pipes the presence of a small amount of dissolved air is very detrimental, not only because the air is swept to one end of the heat pipe to act as a gas plug but also because the presence of oxygen in aqueous solutions generally increases the reaction rate of galvanic processes (23).

Some metals owe their stability to the presence of a continuous coat of oxide, usually amorphous, on their surfaces (27). This is the case for aluminum, stainless steel, and the super-alloys (Inconel, Hastelloy, etc.). Aluminum is protected by a tightly adhering layer of aluminum oxide, while the alloys are covered with an amorphous layer of chromium oxide. As long as these coatings remain intact the metals seem very unreactive. But, if they are exposed to substances which dissolve the oxide, they generally corrode rapidly. (For instance, aluminum is attacked rapidly when exposed to a sodium hydroxide solution.)

### M. 3      High Temperature Corrosion

#### M. 3.1      Oxygen Corrosion

If a metal does not form a tightly adhering coating of oxide, it will often corrode in air at an accelerating pace as the temperature is increased. This is due to the direct oxidation of the base metal. The exact mechanism of attack is still argued (23) (37).

The presence of oxides (or other impurities) can also affect the corrosion resistance in other ways. Some oxides (especially alkalies) can dissolve a protective coating off the base metal and thus increase the rate of reaction, while other oxides can form tightly bound barrier coatings and thus inhibit corrosion. Brewer (3) gives thermodynamic data on many oxides. From the values of the free energies of formation,

estimates can be made of the relative stabilities of the oxides of the fluid and the structural materials (29) (30). Use of these properties has been made in the purification of some liquid metal heat pipes as discussed in Section M. 4.

### M. 3.2 Simple Solution Corrosion

A common phenomenon is the formation of a simple solution of the container material in the liquid. This type corrosion leads to uniform thinning of the wall unless some constituents of the alloy are preferentially dissolved. In this latter case the surface becomes pitted. Attempts have been made to treat such solution attacks theoretically, but the rather involved equations which result are usually of such a nature that errors of a few percent in some of the physical properties used result in errors of orders of magnitude in the prediction of the solution rates (8).

Normally, the rate of solution is limited by the mechanisms involved in transferring the solid atoms (molecules) into the bulk of the solvent. This transfer involves two steps: the crossing of a surface barrier, and the diffusion through the boundary layer in the liquid. If the first step is the controlling one then the rate of corrosion will be independent of the rate of circulation of the working fluid. However, if the second mechanism is controlling, the hydrodynamic conditions can have a more pronounced effect on corrosion rates. Thus, if the flow rate is such that diffusion will not occur against it, the solution will become saturated at the evaporator as the solvent continues to become vapor and solute particles will precipitate out. Normally, the most significant effect of this type of corrosion is the plugging of the flow channels rather than loss of metal at the opposite end of the heat pipe. With low flow rates, a reverse effect can be observed in which the wall material dissolves readily at the hot end; but diffusion results in a saturated solution at the lower temperatures of the condenser, which then becomes plugged.

Another type of concentration gradient mass transfer can occur if metals which can form alloys or compounds are used in the heat pipe. Then, if one metal dissolves and is transferred in the fluid to where it can form an alloy or compound, it will never build up to a high enough concentration in the liquid to slow or stop the rate of solution; and thus failure will occur as a result of the destruction of the wick or the formation of a hole in the container wall.

From the preceding discussions, it is obvious that extreme care must be exercised in order to minimize impurities in the manufacture of heat pipes. Even after compatible materials have been selected, one must normally be very careful to remove adsorbed and/or dissolved impurities which could cause problems once the completed heat pipes are in operation.

The exact amount and type of impurity which can be tolerated will be determined by the individual heat pipe application. A few of the more common problems and some of the techniques which have been utilized to overcome them are discussed briefly in the following paragraphs.

In the high temperature heat pipes, one of the most prevalent problems is the presence of oxides. If this oxide is on the wall of the heat pipe, much of it can usually be removed by means of elevated temperature outgassing under a hard vacuum. If, on the other hand, the oxide is in the liquid metal then distillation of the liquid into the heat pipe can be used (11) (19) to minimize the introduction of oxides into the final assembly. The addition of a getter (a material which has a greater affinity for the impurity than the operating system) has also been successfully utilized (20) to isolate the oxygen and then seal it off from the rest of the system. A related approach (4) involves the operation of the heat pipe for a period of time to collect the impurities in a sacrificial evaporator and then cutting off the evaporator to remove the collected impurities. A heat pipe constructed using this purification technique operated for 1000 hours with no indication of new corrosion. /

A less successful technique, which has been employed involves the addition of other metals to the working fluid as solutes. These metals were chosen on the basis that their oxides must have a higher free energy of formation than any of the oxides of the working fluid. The objective of this technique is to tightly bind up the oxygen in solution and thus prevent corrosion of the wall material. However, most of these systems (4) developed leaks in the evaporator.

Another problem encountered, especially with sodium, is the presence of large amounts of hydrogen dissolved in the as-received metal. A rather straightforward

method of removing such an impurity is to operate the assembled heat pipe with the condenser elevated and to slowly bleed off the gas through a valve on the condenser end fill tube until no more gas is observed; i. e., the temperature of the container wall is uniform (11).

Another method suggested for the removal of hydrogen is to form part of the end cap of palladium so that the hydrogen can diffuse out during operation. However, this technique has not been reduced to practice.

Absorbed gases can also be removed from low temperature working fluids by the bleeding technique. Another technique that has been used for degassing water and which has been quite successful is described in Reference 2. The water is introduced into an evacuated chamber, the water is frozen, and then the system is evacuated to approximately  $10^{-5}$  torr. The water is then warmed to about 80°F, refrozen, and the system is then reevacuated. The freeze-pump-heat cycle is repeated until no noticeable change is observed in the system pressure.

The water content of ammonia in aluminum heat pipes has been found to be critical since it results in the generation of hydrogen. Even though 50-100 ppm of water in the ammonia charge will generate only a small amount of gas, if the temperature of the heat pipe is varied over a range of about 100°F, the pressure and therefore the gas blockage will change by an order of magnitude. The water content of ammonia has been lowered to about 10 ppm by passing the ammonia through molecular sieves at a temperature at which water will be strongly absorbed on the large surface area of the sieves. A good filter must be used with such a system in order to prevent the passage of "dust" from the sieve into the heat pipe. Ultra-pure ammonia with a water content of 10-50 ppm is available commercially and can be used directly for most applications.

#### M. 5 Experimental Results

The discussions earlier in this chapter have indicated some basic compatibility considerations which must be taken into account in order to narrow down the list of candidate materials for use in a particular heat pipe design. However, it has been found through experience that many supposedly minor factors can profoundly

affect the compatibility. Therefore, experimental results remain an important part of heat pipe technology.

Table M-3 summarizes currently available experimental findings for various material combinations. Some of the tests which were used to establish this reference chart are summarized in Table M-4. Some of the techniques for corrosion prevention discussed in Section M.4 are represented in these tests. In Test Number 9, deoxidized Nb-1Zr wall was prepared by cutting off the evaporator section after the heat pipe had operated 95 hours at 1500°C. The "deoxidized" pipe which was thus formed showed very little corrosion other than some Zr depletion. Some grain growth occurred and the evaporator section exhibited some swelling, but this is a phenomenon separate from that of corrosion.

Experiments 13-22 represent the suggested technique of adding, to the working fluid, metals which exhibit higher free energies of formation for their oxides so as to "getter" the oxygen in the system. Except for calcium, all of the additives apparently accelerated the corrosion process. This is rather surprising since all of these materials have  $\Delta G$ 's of -130 to -144 kcal/mole of oxygen, while NbO has a  $\Delta G$  of only -90.5 kcal/mole of oxygen. Some penetration of lithium into the Nb walls was also found in these tests.

The highest operating temperature thus far attained has been 2000°C with Re/Ag and W-26Re/Ag heat pipes (Numbers 43 and 44). The latter exhibited negligible corrosion after 1000 hours. The rhenium pipe failed after only 365 hours, but the evidence points to the presence of foreign inclusions in the Re as the cause of failure. If this is so, pure Re pipes would seem to be capable of extended operation at 2000°C.

In the intermediate temperature range (500-1000°C), sodium has been amply demonstrated to be compatible with stainless steels, nickel, and several of the super-alloys (Numbers 25-31). Also in this temperature range is the longest successful life test reported to date -- nearly five years of continuous operation for a Ni/K system at 600°C (Number 33).

In the low temperature range (and possibly up to 700°C) the available data indicate that nearly unlimited operation can be obtained with a whole series of materials,

Table M-3. Generalized Results of Experimental Compatibility Tests

C = Compatible      \* Sensitive to Cleaning  
 I = Incompatible      # I with Austemitic SS

C = Compatible  
I = Incompatible

provided care is taken to eliminate impurities from the system. This is demonstrated rather graphically by a comparison of Numbers 61 and 62. In the first case, gas began to appear in the system soon after the start of the test; but, when the system was very thoroughly cleaned and outgassed, no signs of deterioration were observed after 3000 hours of testing. Other very good systems in this temperature range are 304 SST/Hg, Cu/H<sub>2</sub>O, Al or Fe/NH<sub>3</sub>, SST or Fe/Methanol, Cu/Dowtherm E, and Al/Freons.

Table M-4 Heat Pipe Life Test Data

No.	Wall Material	Fluid	Test Temp.	Hours of Operation (°C)	Ref.	Remarks
1	CVD <sub>1</sub> -W	Li	1600	1,000	8	No failure
2	W-26Re	Li	1600	10,000	4	No failure
3	TZM <sup>2</sup>	Li	1560	4,600	36	Evaporator leak
4	TZM	Li	1500	10,526	35	Weld leak
5	TZM	Li	1500	10,400	12	Weld failure in end cap
6	TZM	Li	1500	9,800	12	Weld failure in end cap
7	Nb-1Zr	Li	1600	132	6	
8	Nb-1Zr	Li	1500	9,000	8	
9	Nb-1Zr deoxidized	Li	1500	1,000	7	Grain growth, Zr loss, swelling
10	Nb-1Zr	Li	1350	2,300	16	
11	Nb-1Zr	Li	1100	4,300	34	
12	Nb-1Zr	Li	1000	3,670	8	
13	Nb-1Zr	Li-13Ca	1500	1,000	5	Grain growth, Zr loss, swelling
14	Nb-1Zr	Li-40Pr	1500	52	5	Evaporator leak
15	SGS <sup>3</sup> -Ta	Li	1600	1,000	9	No failure
16	Ta	Li-13Ca	1600	208	5	Evaporator leak
17	Ta	Li-40Pr	1600	94	5	Evaporator leak
18	Ta	Li-0.5Y	1600	21	5	Evaporator leak

Table M-4 Heat Pipe Life Test Data (Continued)

No.	Wall Material	Fluid	Test Temp.	Hours of Operation (°C)	Ref.	Remarks
19	Ta	Li-3Y	1600	607	5	Evaporator leak
20	Ta	Li-15Y	1600	146	5	Evaporator leak
21	Ta	Li-0.55 Sc	1600	357	5	Evaporator leak
22	Ta	Li-15 Sc	1600	16	5	Evaporator leak
23	Nb-12z	Na	1000	1,000	8	No failure, terminated
24	Nb-12z	Na	850	16,000	4	Continuing
25	304 SST	Na	800	12,760	12	No failure, terminated
26	316 SST	Na	771	11,860	12	Failed, pinhole in evaporator
27	347 SST	Na	750	1,500	20	No failure, terminated
28	304 SST	Na	732	11,500	2	No failure, terminated under program
29	Ni	Na	800	13,755	12	No failure, terminated
30	Haynes 25	Na	732	12,000	2	No failure, terminated under program
31	Hastelloy-X	Na	715	33,100	12	
32	347 SST	K	510	6,500	20	No failure, terminated
33	Ni-Al	K	600	41,000	12	Gas controlled
34	Ni	K	600	10,000	12	Gas controlled
35	Ni	K	600	6,000	12	Gas controlled
36	Nb-12z	CS	1000	1,000	8	Terminated, no failure

Table M-4 Heat Pipe Life Test Data (Continued)

No.	Wall Material	Fluid	Test Temp.	Hours of Operation (°C)	Ref.	Remarks
37	Nb-12r	CS	850	5,000	4	
38	Ti	CS	400	2,000	34	No failure, terminated
39	Ta-10W	Ca	1700	1,000	17, 18	Reflux capsule
40	304 SST	Hg	340	32,000	12	
41	347 SST	Hg	330	10,000	20	No failure, terminated
42	Re	Ag	2000	365	21	Evaporator leak
43	W-26Re	Ag	2000	1,000	4	No failure
44	W	Ag	1900	335	15	
45	Ta	Ag	1900	100	34	
46	Ta	Ag	1900	1,000	15	W wick, no failure
47	Ta	Pb	1600	1,000	8	No failure
48	CVD-W	Pb	1600	1,000	8	No failure
49	Nb	Pb	1600	3	6	Failed
50	Nb-12r	Pb	1615	23	6	Failed
51	Nb-12r	Pb	1600	19	6	Failed
52	NB-12r	Pb	1570	51	6	Failed
53	W	In	1900	75	34	
54	Cu	H <sub>2</sub> O	150	20,420	12	Continuing

Table M-4 Heat Pipe Life Test Data (Continued)

No.	Wall Material	Fluid	Test Temp.	Hours of Operation (°C)	Ref.	Remarks
55	Cu	H <sub>2</sub> O	130	> 1,400	14	Cu bronze wick, Continuing
56	Cu	H <sub>2</sub> O	115	> 2,100	14	Cu bronze wick, Continuing
57	Cu	H <sub>2</sub> O	100	19,490	12	Continuing
58	Cu (OFHC)	H <sub>2</sub> O	33	4,000	28	Triple distilled H <sub>2</sub> O, Continuing
59	Cu	H <sub>2</sub> O	80	21,360	12	Continuing
60	Cu	H <sub>2</sub> O	34	13,200	11	Continuing
61	321 SST	H <sub>2</sub> O	164	570	11	Gas generated, corrosion on walls (but see #62)
62	347 SST	H <sub>2</sub> O	91	15,000	10	Terminated
63	SST	H <sub>2</sub> O	65	8,500	2	Gas generated
64	SST	H <sub>2</sub> O	135	26,244	1	Much gas, Refrassil wick
65	SST	H <sub>2</sub> O		3,744	1	Refrassil wick, terminated
66	304 SST	H <sub>2</sub> O	35	7,000	28	KOH passivated, much gas generated
67	Ni (oxidized)	H <sub>2</sub> O	38	7,000	28	Much gas generated
68	Monel 600	H <sub>2</sub> O	38	14,000	28	Gas generated (oxidized Monel)
69	Titanium	H <sub>2</sub> O	35	14,000	28	No wick (oxidized Ti), Continuing
70	Cu	methanol	70	> 700	14	Cu Bronze wick, Continuing
71	Cu	methanol	74	24,158	1	Refrassil wick, Continuing
72	Brass	methanol	60	> 800	14	Cu Bronze wick, Continuing

No.	Wall Material	Fluid	Test Temp.	Hours of Operation (°C)	Opératior Ref.	Remarks
73	AI 6061-T6	Methanol	46	4,000	28	Gas generated, SST wick
74	AI 6061-T6	Methanol	--	--	13	Generated gas during setup
75	304 SST	Methanol	>14,250	11	Continuing	
76	304 SST	Methanol	40	16,000	28	Spectrally dried Methanol, Continuing
77	304 SST	Methanol	40	16,000	28	Spectrophotometric Methanol, Continuing
78	304 SST (oxid.)	Methanol	40	16,000	28	Spectrophotometric Methanol, Continuing
79	316 SST	Methanol	46	8,000	28	Slight gas generation
80	SST	Methanol	60	>1,650	14	Continuing
81	Fe	Methanol	33	>8,250	11	Continuing
82	Nickel 200	Methanol	35	6,000	28	Spectrally dried Methanol, Continuing
83	SST	Ethanol	60	>1,550	14	Continuing
84	AI 6061-T6	NH <sub>3</sub>	71	500	13	AI wick, no failure, terminated under contract
85	AI 6061-T6	NH <sub>3</sub>	47	10,800	11	SST artery wick, radial grooves
86	AI 6061-T6	NH <sub>3</sub>	42	2,373	11	No failure, terminated under contract
87	AI 6061-T6	NH <sub>3</sub>	49	14,000	28	SST wick, 99.999% NH <sub>3</sub> , Continuing
88	AI	NH <sub>3</sub>	48	18,120	1	AI felt wick, Continuing
89	AI	NH <sub>3</sub>	48	18,120	1	AI felt wick, Continuing
90	SST	NH <sub>3</sub>	46	18,900	1	

Table M-4 Heat Pipe Life Test Data (Continued)

Table M-4 Heat Pipe Life Test Data (Continued)

No.	Wall Material	Fluid	Test Temp.	Hours of Operation (°C)	Ref.	Remarks
91	SST	NH <sub>3</sub>	47	18,900	1	
92	Fe	NH <sub>3</sub>	35	>18,300	11	Continuing
93	Cu	Acetone	74	24,158	1	Some gas, Refrassil wick, Continuing
94	Brass	Acetone	60	>800	14	Continuing
95	Al	Acetone	110	1,700	12	Continuing
96	Al	Acetone	71	9,936	1	SST, fiber wick, no failure, terminated
97	Al 6061-T6	Acetone	33	4,000	28	Gas generated
98	304 SST	Acetone	87	14,500	12	Continuing
99	SST	Acetone	60	1,500	14	Continuing
100	Al 6061-T6	n-Butane	66	500	13	Al wick, no failure, terminated
101	Al 6061-T6	n-Pentane	158	570	13	Al wick, slight fluid discoloration, terminated
102	SST	Hexane	60	>1,200	14	Continuing
103	Al 6061-T6	n-Heptane	161	600	12	Al wick, no failure, terminated
104	Al 6061-T6	Benzene	158	570	12	Al wick, no failure, terminated
105	Al 6061-T6	Toluene	162	600	13	Small AT developed, terminated
106	Cu	C <sub>6</sub> F <sub>6</sub>	100	24,980	1	Refrassil wick, Continuing
107	Al 6061-T6	Freon 11	106	500	13	No failure, terminated
108	Al 6061-T6	Freon 11	69	500	13	No failure, terminated

Table M-4 Heat Pipe Life Test Data (Continued)

No.	Wall Material	Fluid	Test Temp. (°C)	Hours of Operation (°C)	Ref.	Remarks
109	AI 6061-T6	F-21	41	10, 000	28	Slight gas generation
110	AI 6061-T6	Freon 113	107	500	13	No failure, terminated
111	AI 6061-T6	Freon 113	69	500	13	No failure, terminated
112	Cu	Dow-A	160	20, 500	1	No failure, terminated for exam., Refrassil wick
113	Cu	Dow-A	156	26, 830	1	Refrassil wick, Continuing
114	Cu	Dow-A	149	26, 644	1	Refrassil wick, Continuing
115	SST	Dow-A	150	22, 376	1	Refrassil wick, Continuing
116	Brass	Dowtherm E	121	20, 500	11	Gas generated after 5850 hours
117	Steel cold rolled	Dowtherm E	121	20, 500	11	Gas generated after 4680 hours
118	Cu	Dowtherm E	110	>20, 500	11	Continuing
119	SST	Dow-E	128	31, 098	1	No failure, removed for analysis
120	Cu	Dow-E	~140	31, 270	1	Smintered Cu wick, Continuing
121	Cu	Dow-E	182	41, 460	1	SST wick, Continuing
122	Cu	DC-200	168	23, 000	1	SST wick, very slight mass transfer to evap. No failure, terminated for examination
123	Al	DC-200	104	18, 021	1	NI wick, Continuing
124	Cu	Dow-209	110	40, 414	1	Smintered Cu wick, Continuing
125	Cu	CP-9	149	33, 460	1	Refrassil wick, Continuing
126	Cu	Pyridine CP-32	98	10, 810	1	Ca felt wick, Continuing

Table M-4 Heat Pipe Life Test Data (Continued)

No.	Wall Material	Fluid	Test Temp.	Hours of Operation (°C)	Ref.	Remarks
127	Al 6061-T6	Pyrrole CP-32	159	550	13	Δ T developed, deposits, discolored
128	Al 6061-T6	Monsanto CP-34	160	550	13	Gas generated, discolored fluid
129	Cu	Perchloro-ethylene	93	16,670	1	Refractions wick, continuing
130	Cu	Dimethylsulfide	100	15,634	1	Some gas, Refractions wick, continuing

Notes to Table M-4

<sup>1</sup>CVD = chemical vapor deposition

<sup>2</sup>TZM = Mo-0.8Zr-0.5Ti-0.03C

<sup>3</sup>SGS = stabilized grain size

## B.0 BIBLIOGRAPHY

### B.1 Introduction

The references for all of the chapters are collected in the following pages. They are listed by chapter and generally in alphabetical order within each chapter. A few exceptions to the alphabetical order occurred with the addition of extra data after a chapter was in final form. These references were placed at the end of the list for that chapter.

A cross-reference-contents table for all of the articles referred to in this handbook follows the list of references. The first column in this table gives a quick cross-index of publications which occur in several chapters. The next sixteen columns indicate the main topics presented in each of the publications. Qualitative judgments have, of necessity, been used in determining which topics are applicable in each case. If, in the user's opinion, additional topics should be checked for a given paper he can easily add the check for his own use. Many blank lines have been left in the table, both for updating in the second edition of the Handbook and for the user's convenience in the addition of newly published works. An asterisk before a reference number in this table indicates that the publication is from the general literature and is not specifically concerned with heat pipes, as such.

This bibliography represents only the publications referred to in the text of the Handbook and is by no means an exhaustive listing. For a very thorough bibliography on heat pipes, the user is referred to the NASA sponsored "Heat Pipe Technology - A Bibliography with Abstracts" published periodically by the Technology Application Center at the University of New Mexico, Albuquerque, New Mexico.

Introduction

- I 1 Cotter, T. P., "Theory of Heat Pipes," Los Alamos Scientific Laboratory Report LA-3246-MS, February 1965
- I 2 Gaugler, R. S., "Heat Transfer Device," U.S. Patent 2,350,348, June 6, 1944
- I 3 Grover, G. M., Cotter, T. P. and Erikson, G. F., "Structures of Very High Thermal Conductivity," J. Appl. Phys., 35, 1990 (1964)
- I 4 Mechtilley, E. A., "The International System of Units - Physical Constants and Conversion Factors," NASA-SP-7012 (Rev.) 1969
- I 5 National Bureau of Standards, Administrative Bulletin, AB-64-6, Feb. 1964
- I 6 Trefethen, L., "On the Surface Tension Pumping of Liquids or a Possible Role of the Candlewick in Space Exploration," G. E. Tech. Info., Ser. No. 615 D114, Feb. 1962

Theory

T 1 Adamson, A. W., "Physical Chemistry of Surfaces," Interscience Publishers  
New York, 1960

T 2 Bennett, M. K. and Zisman, W. A., J. Phys. Chem. 74, 2309-12 (1970)

T 3 Anand, D. K. and Hester, R. B., "Heat Pipe Application for Spacecraft  
Thermal Control," Tech Memo DDC AD 662 24, NASA NG8-15338, 1967

T 4 Bienert, W. B. and Brennan, P. J., "Transient Performance of Electrical  
Feedback Controlled Variable-Conductance Heat Pipes," ASME Paper  
71-Av-27, SAE/ASME/AIAA Life Support and Environmental Control  
Conference, San Francisco, California, July 12-14, 1971

T 5 Bienert, W. B., Brennan, P. and Kirkpatrick, J. P., "Feedback Controlled  
Variable Conductance Heat Pipes," AIAA Paper No. 71-42, 6th Thermo-  
physics Conf., Tylahoma, Tenn., April 1971

T 6 Bienert, W. B., "Study to Evaluate the Feasibility of a Feedback Con-  
trolled Variable Conductance Heat Pipe," Contract No. NAS 2-5722,  
Dynatherm Corporation Rept. DTM-70-4, September 1970

T 7 Bird, R., Stewart, W. and Lightfoot, E., "Transport Phenomena,"  
John Wiley & Sons, New York, 1960

T 8 Bresslar, R. G. and Wyatt, P. W., "Surface Wetting Through Capillary  
Groves," Trans. ASME, J. Heat Transf. —, 126-132 (1970)

T 9 Chi, S. W., "Introduction to Heat Pipe Theory," George Washington  
University, Washington, D. C. (1971)

T 10 Chi, S. W. and Cygnarowitz, T. A., "Theoretical Analyses of Cryogenic  
Heat Pipes," 1970 Space Technology and Heat Transfer Conference,  
January 1970

T 11 Cotter, T. P., "Theory of Heat Pipes," Los Alamos Scientific Laboratory  
Report LA-3246-MS, February 1965

T 12 Cotter, T. P., "Heat Pipe Startup Dynamics," IEEE 1967 Thermionic  
Conversion Specialist Conference, Palo Alto, California, Oct. 30, 1967

T 13 Deverall, J. E., "Capability of Heat Pipes," Heat Pipe Technology &  
Manned Space Station Appl. Technical Interchange, Huntsville, Alabama,  
May 27, 1969

T 14 Deverall, J. E. and Kemme, J. E., "High Thermal Conductance Devices  
Utilizing the Boiling of Lithium and Silver," Los Alamos Scientific  
Laboratory, LA-3211, 1965

Theory (Continued)

T 15 Deverall, J. E., Kemme, J. E. and Florschuetz, L. W., "Sonic Limitations and Startup Problems of Heat Pipes," Los Alamos Scientific Laboratories, Report No. LA-4518, November 1970

T 16 Deverall, J. E., Salmi, E. W. and Knapp, R. J., "Orbital Heat Pipe Experiment," Los Alamos Scientific Laboratory Report LA-3714, June 5, 1967

T 17 Dynatherm Corporation, Unpublished Data

T 18 Ferrel, J. K. and Alleavitch, J., "Vaporization Heat Transfer in Capillary Wick Structures," Chemical Eng. Prog. Symposium Series V66, Heat Transfer, Minneapolis, Minn., 1970

T 19 Goring, R. L. and Churchill, S. W., "Thermococonductivity of Heterogeneous Materials," Chemical Engineering Prog. 57, No. 7, 53-59 (1961)

T 20 Hollister, M. P. and Ekern, W. F., "Performance of a Precision Thermal Control System Using Variable Conductance Heat Pipes", AIAA 7th Thermophysics Conf., San Antonio, April, 1972.

T 21 Kays, W. M., "Convective Heat and Mass Transfer," McGraw-Hill Book Co., Inc., New York, 1966

T 22 Kemme, J. E., "High Performance Heat Pipes," IEEE 1967 Thermionic Specialist Conference, Palo Alto, California, October 1967, pp. 355-358

T 23 Kemme, J. E., "Heat Pipe Capability Experiments," Proceedings of Joint AEC/Sandia Labs., Heat Pipe Conf. 1, SC-M-66-223, October 1966, pp. 11-26

T 24 Knight, B. W. and McInteer, B. B., "Laminar Incompressible Flow in Channels with Porous Walls," LADC-5309

T 25 Kreith, F., "Principles of Heat Transfer," International Textbook Company, Scranton, Pa. (1958)

T 26 Levy, E. K., "Theoretical Investigation of Heat Pipes Operating at Low Vapor Pressures," Trans. ASME, J. for Industry, November 1968, p. 547

T 27 Levy, E. K., "Effects of Friction on the Sonic Velocity Limit in Sodium Heat Pipes," ASME Paper HPT-71-022

T 28 Marcus, B. D., "Theory and Design of Variable Conductance Heat Pipes," Report No. 1, TRW 13111-6027-R0-00, Contract NAS 2-5503, April 1971

T 29 Marcus, B. D., "Theory and Design of Variable Conductance Heat Pipes," Report No. 2, TRW-13111-6027-R0-00, Contract NAS 2-5503, July 1971

Theory (Continued)

T 30 Marcus, B. D., "On the Operation of Heat Pipes," TRW Report 9895-6001-TU-000, May 1965

T 31 Marcus, B. D. and Fleischman, G. L., "Steady State and Transient Performance of Hot Reservoir Gas Controlled Heat Pipes," ASME 1970 Space Techn. and Heat Transf. Conf., Los Angeles, California, June 1970

T 32 Parker, G. H. and Hanson, J. P., "Heat Pipe Analysis," Advances in Energy Conversion Engineering ASME 1967 Intersociety Energy Conversion Conference, Miami, Florida, August 1967, pp. 857-

T 33 Reid, R. C. and Sherwood, T. K., "The Properties of Gases and Liquids - Their Estimation and Correlation," McGraw-Hill Book Co., Inc., New York (1958)

T 34 Reiss, F. E. and Schretzmann, K., "Boiling Tests with an Open Grooved Capillary Evaporator," Forschungen im Ingenieurwesen 37, 55-58 (1971)

T 35 Scheidiger, A. E., "The Physics of Flow Through Porous Media," The MacMillan Co., New York, 1960

T 36 Schlitt, K. R., "Temperature Stabilization with Heat Pipes by Varying Heat Inputs," Euratom Report No. EUR 4634d, Ispra, Italy

T 37 Shlossinger, A. P., "Heat Pipe Devices for Space Suit Temperature Control," TRW Systems Rept. No. 06462-6005-R0-00, November 1968

T 38 Soliman, M. M., Grauman, D. W. and Berenson, P. J., "Effective Thermal Conductivity of Saturated Wicks," ASME Paper No. 70-HT/SpT-40, 1970

T 39 Winter, E. R. F. and Barsch, W. O., "The Heat Pipe," in Advances in Heat Transfer, Vol. 7, Ed. by Irvine, T. F. and Hartnett, J. P., Academic Press, New York, 1971

T 40 Wright, P. E., Final Report for ICICLE Feasibility Study, Contract NAS 5-21039, RCA, Camden, New Jersey

T 41 Wyatt, T., "A Controllable Heat Pipe Experiment for the 5E-4 Satellite," Appl. Phys. Lab., Johns Hopkins University, SDO-1134 (1965)

T 42 Zisman, W. A., "Contact Angle, Wettability and Adhesion," in Advances in Chemistry Series, No. 43, Ed. by Fowkes, F. M., American Chemical Society, Washington, D.C., 1964, pp. 1-51

## Design

D 1 Bienert, W. B. and Brennan, P. J., "Transient Performance of Electrical Feedback - Controlled Variable-Conductance Heat Pipes," SAE/ASME/AIAA Life Support and Environmental Control Conference, San Francisco, Calif., July 1971

D 2 Bienert, W. B. and Kroliczek, E. A., "Experimental High Performance Heat Pipes for the OAO-C Spacecraft," SAE/ASME/AIAA Life Support and Environmental Control Conference, San Francisco, Calif., July 1971

D 3 Brennan, P. J., Trimmer, D. S., Sherman, A. and Cygnarowicz, T., "Arterial and Grooved Cryogenic Heat Pipes," ASME, Heat Transfer Div., Winter Meeting November 28, 1971, ASME Paper 71-WA-HT-42

D 4 Dynatherm Corporation, Cockeysville, Md., "Design, Fabrication and Qualification of Heat Pipes for ATS F&G," 2nd Monthly Progress Report. Contract SC68280 (Fairchild Industries), June 9, 1971

D 5 Groll, M., Brost, O., Kreeb, H., Shubert, K. and Zimmerman, P., "Power Limits, Technology, and Application of Low Temperature Heat Pipes," Forchung im Ingenieurwesen 37, 33-37 (1971)

D 6 Grumman Aerospace Corporation, Bethpage, New York, "Large Variable Conductance Heat Pipe." Contract NAS 8-27793 Marshall Space Flight Center

D 7 Kosson, R., Fembach, R., Edelstein, F. and Tawil, M., "A Tunnel Wick 100,000 Watt-inch Heat Pipe," AIAA 7th Thermophysics Conference, San Antonio, Texas, April 10, 1972. AIAA Paper 72-273

D 8 Marcus, B. D., "Theory and Design of Variable Conductance Heat Pipes," Report No. 1, TRW 13111-6027-RO-00, Contract NAS 2-5503, April 1971

D 9 Marcus, B. D.; Ibid, Report No. 2, July 1971

D 10 Marcus, B. D., Private Communication, April 1972

D 11 Moritz, K. and Pruscheck, R., "Energy Transport Limits in Heat Pipes," Chemie Ingenieur Technik 41, 30 (1969)

D 12 Shapiro, A. H., "The Dynamics and Thermodynamics of Compressible Fluid Flow", Vol. 1, p. 48, The Ronald Press Company, New York 1953

D 13 Freggens, R. A. and Langsderff, R. W., "Development of High Performance Sodium / Nickel Heat Pipes", Intersociety Energy Conversion Engineering Conference, Las Vegas, Nevada, September 1970

W 1 Bienert, W. B. and Kroliczek, E., "Experimental High Performance Heat Pipes for the OAO-C Spacecraft," SAE/ASME/AIAA Life Support and Environmental Control Conference, July 1971, San Francisco, California, ASME 71-Av-26

W 2 Bird, R., Stewart, W. and Lightfoot, E., "Transport Phenomena," John Wiley & Sons, New York, 1960

W 3 Bressler, R. G. and Wyatt, P. W., "Surface Wetting Through Capillary Grooves," Trans, ASME, J. Heat Transf., , 126-132 (1970)

W 4 Cosgrove, J. H., Ferrell, J. K. and Carnesle, A., J. Nuclear Energy 21, pp. 547-558 (1967)

W 5 Dynatherm Corporation, Unpublished Data

W 6 Ernst, D. M., "Evaluation of Theoretical Heat Pipe Performance," Thermionic Conversion Specialist Conference, Palo Alto, California, October 30- November 1, 1967, pp. 349-354

W 7 Farran, R. A. and Starner, K. E., "Determining Wicking Properties of Compressible Materials for Heat Pipe Applications," Annual Aviation and Space Conference, Beverly Hills, California, June 1968, pp. 659-669

W 8 Ferrell, J. K. and Alleavitch, J., "Vaporization Heat Transfer in Capillary Wick Structure," Chemical Eng. Prog. Symp. Series, Vol. 66, Heat Transfer Minneapolis, Minn., 1970

W 9 Florschuetz, L. W., "Brief Notes on Calculation of Liquid Pressure Drop in Heat Pipes," Los Alamos Scientific Laboratory, N-5 Tech. Memo No. 170, August 10, 1970

W 10 Freggens, R. A., "Experimental Determination of Wick Properties for Heat Pipe Applications," Proc. of 4th Intersociety Energy Conversion Conference, Washington, D.C., September 1968, pp. 888-897

W 11 Ginwala, K., Blatt, T. A., and Bilger, R. W., "Engineering Study of Vapor Cycle Cooling Components for Space Vehicles," Tech. Doc. Rept. ASD-TDR-63-582, Wright-Patterson Air Force Base, Ohio, September 1963

W 12 Gould Inc., Gould Laboratories, Brochure GLMT-101

W 13 Kays, W. M., "Convective Heat and Mass Transfer," McGraw-Hill, Co., Inc., New York, 1966

Wick Data (Continued)

W 14 Katzoff, S., "Heat Pipes and Vapor Chambers for Thermal Control of Spacecraft," Thermophysics of Spacecraft and Aeronautics, V. 20, Academic Press, New York, 1968, pp. 761-818

W 15 Kosson, R., Hemback, R., Edelstein, F. and Tawil, M., "A Tunnel Wick 100,000 Watt-Inch Heat Pipe," AIAA Thermophysics Conference, San Antonio, Texas, April 1972

W 16 Kunz, H. R., Langston, L. S., Hilton, B. H., Wyde, S. S. and Nashick, G. H., "Vapor-Chamber Fin Studies," NASA CR-812, June 1967

W 17 Luikov, A., "Heat and Mass Transfer in Capillary-Porous Bodies," Pergamon Press, New York, 1966

W 18 Marcus, B. D., "Theory and Design of Variable Conductance Heat Pipes," No. 1 TRW 13111-RO-00, Contract NAS 2-5503, April 1971

W 19 Marjon, P. L., 12th Monthly Progress Report, DOT Contract No. FH-11-7413, Dynatherm Corporation, November 1971

W 20 Phillips, E. C., "Low Temperature Heat Pipe Research Program," NASA CR-66792, June 1969

W 21 Scheidegger, A. E., "The Physics of Flow Through Porous Media," The MacMillan Co., New York, 1960

W 22 Schmidt, E., "Contribution a l' Etude des Caloducs", Ph.D Thesis, University of Grenoble, France, 1968

W 23 "Manual - Feltmetal Fiber Metal", Huyck Metals Company (now Brunswick Corporation, Technical Division)

W 24 "Metal Filter Cloth, Technical and Performance Data", Kressilk Products, Inc., Monterey Park, Calif., Julie 23, 1969.

## Fluid Properties

F 1 American Society of Heating, Refrigeration, and Air Conditioning Engineers, "Handbook of Fundamentals" (1967)

F 2 Chi, S. W., "Mathematical Modeling of Cryogenic Heat Pipes", Final Report NASA Grant No. NGR09-005-071, Catholic University of America, Sept. 1970

F 3 Deverall, J. E., "Mercury as a Heat Pipe Fluid", Los Alamos Scientific Laboratory, LA-4300-MS, January, 1970

F 4 Deverall, J. E., Kemme, J. E., and Florschuetz, L. W., "Sonic Limitations and Startup Problems of Heat Pipes", Los Alamos Scientific Laboratory, LA-4518, November, 1970

F 5 DuPont Product Information Bulletins B-2, C-30, B-32, D-27, D-27B, T-11, and DP-5

F 6 Etherington, H., Ed., "Nuclear Engineering Handbook", McGraw-Hill Book Co., Inc., New York (1958)

F 7 Frank, S., Smith, J. T. and Taylor, K., "Heat Pipe Design Manual", Martin Marietta Corporation, Nuclear Division Report 3288 (1967)

F 8 Gerrels, E. E. and Larson, J. W., "Brayton Cycle Vapor Chamber (Heat Pipe) Radiator Study", NASA CR-1677, February, 1971

F 9 Grosse, A. V., "Thermal Conductivity of Liquid Metals", TID-21737 (1964)

F 10 "International Critical Tables", McGraw-Hill Book Co., Inc., New York (1929)

F 11 Jackson, E. B., Ed., "Liquid Metals Handbook-Sodium (NaK) Supplement", TID 5227 AEC-Department of the Navy (1955)

F 12 Johnson, V. J., Ed., "A Compendium of the Properties of Materials at Low Temperature (Phase I) - Part I, Properties of Fluids", WADD Technical Report 60-56, Part I, July, 1960

F 13 Keenan, J. H. and Keyes, F. G., "Thermodynamic Properties of Steam", 31st Printing, John Wiley & Sons, Inc., New York (1958)

F 14 Kreith, F., "Principles of Heat Transfer", International Textbook Company, Scranton, Pa. (1958)

F 15 Lange, N. A., Ed., "Handbook of Chemistry", 10th Ed., McGraw-Hill Book Co., Inc., New York (1961)

F 16 Lyon, R.N., ED., "Liquid Metals Handbook", NAVEXOS P-73 (Rev.) (1952)

Fluid Properties (Continued)

F 17 National Bureau of Standards, Circular No. 142, "Tables of the Thermodynamic Properties of Ammonia" (1945)

F 18 Reid, R. C. and Sherwood, T. K., "The Properties of Gases and Liquids - Their Estimation and Correlation," McGraw-Hill Book Co., Inc., New York (1958)

F 19 Schins, H. E. J., "Liquid Metals for Heat Pipes, Properties, Plots, and Data Sheets," Euratom Report EUR 3653e (1967)

F 20 Scallon, T. R., Jr., Carpitella, M. J., and Blomstrom, L. E., "Long Life High Reliability Thermal Control Systems Study - Data Handbook," NAS8-26252

F 21 Smithells, C. J., "Metals Reference Book," Vol. 3, Plenum Press, New York (1967)

F 22 Tapper, F., et al, Thermophysical and Transport Properties of Liquid Metals, AFML-TR-65-99 (1965)

F 23 Varljen, T. C., "A Computer - Subroutine to Generate the Thermophysical Properties of Space-Power System Working Fluids," WANL-TME-1838, November, 1968

F 24 Weatherford, W. D., et al, "Properties of Inorganic Energy Conversion and Heat Transfer Fluids for Space Applications," WADD TR 61-96 (1961)

Materials Compatibility

M 1 Basiulis, A. and Filler, M., "Operating Characteristics and Long Life Capabilities of Organic Fluid Heat Pipes," AIAA 6th Thermophysics Conference, April 26-28, 1971. (AIAA Paper No. 71-408)

M 2 Bienert, W. B., Private Communication

M 3 Brewer, L., "The Thermodynamic Properties of the Oxides and Their Vaporization Processes," Chemical Reviews - 1-75, 1953

M 4 Busse, C. A., "Heat Pipes for Thermionic Space Power Supplies," Proc. 3rd Int'l. Conf. on Space Technology, Rome (1971)

M 5 Busse, C. A., "Heat Pipe Thermionic Converter Research in Europe," 4th Intersociety Energy Conversion Engineering Conference, Washington, D.C. September 1969

M 6 Busse, C. A., Caron, R. and Cappelletti, C., "Prototype of Heat Pipe Thermionic Converters for Space Reactors," Proc. of 1st Int'l. Conf. on Thermionic Electrical Power Generation, London, 1965

M 7 Busse, C. A., Geiger, F., Quataert, D., "Status of Emitter Heat Pipe Development at Ispra," IEEE Con. Record of Thermionic Specialist Conference, 1970

M 8 Busse, C. A., Geiger, F., Quataert, D., Potschke, M., "Heat Pipe Life Tests at 1600°C and 1000°C," 1966 IEEE Thermionic Specialist Conference Houston, Texas, pp. 149-58

M 9 Busse, C. A., Geiger, F., Strub, H., Potschke, M. and Kraft, G., "High Temperature Lithium Heat Pipes," 2nd Int'l. Conf. on Thermionic Electrical Power Generation, Euratom Rept. EUR 4210 f.e., 1968, pp. 495-506

M 10 Deverall, J. E. and Kemme, J. E., "Satellite Heat Pipe," Los Alamos Scientific Laboratory Report LA-3278-MS, January 1965

M 11 Dynatherm Corporation, Unpublished Data

M 12 Eastman, G. Y., "The Heat Pipe - A Progress Report," 4th Intersociety Energy Conversion Engineering Conference, Washington, D.C., September 1969, pp. 873-8

M 13 Gerrels, E. E. and Larson, J. W., "Brayton Cycle Vapor Chamber (Heat Pipe) Radiator Study," NASA CR-1677, February 1971

M 14 Groll, M., Brost, O., Kreeb, H., Schubert, K. and Zimmerman, P., "Power Limits, Technology, and Application of Low Temperature Heat Pipes," Forschung im Ingenieurwesen 37, 33-37 (1971)

Materials Compatibility (Continued)

M 15 Grover, G. M., Kemme, J. E., and Keddy, E. S., "Advances in Heat Pipe Technology," Proceedings 2nd Int'l. Conf. Thermionic Electrical Power Generation, Stresa, Euratom Rept. EUR-4210, f.e., Ispra, Italy, 1968, pp. 477-90

M 16 Harbaugh, W. E., "The Development of an Insulated Thermionic Converter-Heat Pipe Assembly," RCA Rept. AF APL TR-67-45 (1967)

M 17 Johnson, G. D., "Compatibility of Various High Temperature Heat Pipe Alloys with Working Fluids," IEEE 1968 Thermionic Conversion Specialist Conf., Framingham, N.Y. (1968), pp. 258-65

M 18 Johnson, G. D., "Corrosion Studies of Liquid Metal Heat Pipe Systems at 1000°C to 1800°C." In Draley, J. E., and Weeks, J. R., "Corrosion by Liquid Metals," Plenum Press, N.Y. (1970), pp. 321-37

M 19 Kemme, J. E., "Heat Pipe Capability Experiments," Los Alamos Scientific Laboratory Rept. LA-3585-MS, October 1966

M 20 Kemme, J. E., Quarterly Status Report on Space Electric Power R&D Program, July 31, 1971, Los Alamos Scientific Laboratory Rept. LA-4746-MS

M 21 Kemme, J. E., Quarterly Status Report on Space Electric R&D Program for period ending Jan. 31, 1969, Pt. 1, Los Alamos Scientific Laboratory Rept. LA-4109-MS

M 22 Lange, N. A., "Handbook of Chemistry," 9th Ed., Handbook Publishers, Inc., Sandusky, Ohio, 1956

M 23 LaQue, F. L. and Copson, H. R. (Eds.), Corrosion Resistance of Metals and Alloys, 2nd Ed., American Chemical Society Monograph Series No. 158, Reinhold Publishing Corp., New York, 1963

M 24 Lommel and Chalmers, Trans. ASME, 215, 499 (1959)

M 25 Lyman, T., "Metals Handbook," 8th Ed., American Society for Metals, Metals Park, Ohio (1961)

M 26 Lyon, R. N. (Ed.) Liquid Metals Handbook - NAVEXOS P-733 (Rev.) USGPO June 1952

M 27 MacLennan, McMillan and Greenblatt, "Corrosion of Aluminum and Aluminum Alloys in High Temperature Water," 1st Int'l. Congress on Metallic Corrosion London, April 1961

M 28 Marcus, B. D., Private Communication, April 1972

Materials Compatibility (Continued)

M 29 Margrave, J. L., "Thermodynamic Calculations, 1. Free Energy Functions and Heat Content Functions," *J. Chem. Education* 32, 520-4 (1955)

M 30 Margrave, J. L., "High Temperature - A Tool for the Future," Stanford Research Institute, Palo Alto, California (1956), pp. 87-106

M 31 Moelwyn-Hughes, E. A., "Physical Chemistry," 2nd Ed., Pergamon Press, New York (1964)

M 32 National Bureau of Standards Circular 500, "Selected Values of Chemical Thermodynamic Properties" (1952)

M 33 Quataert, D., "Investigations of the Corrosion Mechanism in Tantalum-Lithium High Temperature Heat Pipes by Ion Analysis," *Forsch. Ing. Wes.* 37, 37-38 (1971)

M 34 Ranken, W. A. and Kemme, J. E., "Survey of Los Alamos and Euratom Heat Pipe Investigations," IEEE Conf. Record of 1965 Thermionic Conversion Specialist Conf., San Diego, California, October 1965, pp. 325-336

M 35 Rouklove, P., Comment in Proceedings of 2nd Int'l. Conf. on Thermionic Electrical Power Generation, Stresa, Eurathom Rept. EUR 4210, f.e., Ispra, Italy (1968), p. 494

M 36 Shefsiek, P. K. and Ernst, D. M., "Heat Pipe Development for Thermionic Application," 4th Intersociety Energy Conversion Conference, Washington, D.C. (1969, pp. 879-887

M 37 Wagner, C. J., *J. Electrochem Soc.* 99, 369 (1952)

Computer Codes

C1 Chi, S. W., "Mathematical Modeling of Cryogenic Heat Pipes," Final Report NASA Grant No. NGR09-005-071, Catholic University of America, September 1970

C2 Edwards, D. K., Fleischman, G. L., and Marcus, B. D., "User's Manual for the TRW GASPIPE Program," NASA CR-114306, April 1971

C3 Lyon, R. N., Ed., "Liquid Metals Handbook," NAVEXOS P-73 (Rev.) (1952)

C4 Schins, H. E. J., "Liquid Metals for Heat Pipes, Properties, Plots, and Data Sheets," Euratom Report EUR 3653e (1967)

C5 Skrabek, E. A. and Bienert, W. B., "Heat Pipe Design Handbook," NASA Contract NAS9-11927, Dynatherm Corporation Report No. 72-3, August 1972

C6 Stallings, R. D. and Collett, J. F., "Heat Pipe Design Program," Lockheed Electronics Corp., TN-675-44-00275

C7 Wright, J. P., "Computer Program for the Design and Analysis of Heat Pipes," North American Rockwell, Space Division, Report No. SD72-SA-0001, January 1972

Bibliography

B1 Feldman, K. T., Jr., Ed., "Heat Pipe Technology - A Bibliography with Abstracts," Technology Application Center, University of New Mexico, Albuquerque, New Mexico, Published Quarterly, March 1971

Table B-1. Cross-Reference -Contents Table

Table 8-1. Cross Reference Contents Table (Continued)

Pages marked with \* refer to figures, and pages marked with # refer to tables.

Blake-Kozeny Equation, W-10, W-11\*  
 Blasius' Law, T-17  
 Body forces, T-6, T-7, T-13, T-14\*, T-17  
 Capillary heat transport limit, T-15ff, T-23ff, T-30, D-17ff  
 Capillary pressure, T-6, T-8, T-11, T-20  
 Capillary pumping requirement (and gravity), T-23  
 Capillary priming, W-14  
 Clapeyron Equation, T-87  
 Cleaning, M-8  
 Compatibility, M-1ff, D-38  
 causes, M-2#  
 Composite wicks (see wicks)  
 Configuration selection, D-65  
 Contact angle, T-8, T-9\*, T-10ff  
 Container design, D-64  
 Conversion factors, I-20  
 Corrosion (see compatibility)  
 low temperature, M-3ff  
 high temperature, M-6ff  
 Darcy's Law, T-11, T-12, T-15  
 Dynamic environment, D-14  
 Entrainment limit, T-33, D-16, D-30  
 Fluid inventory, D-68  
 Fluid (see working fluid)  
 Gravity (see body forces)  
 Heat exchange, T-7  
 Heat flow rate/mass flow rate, T-21, D-18  
 Heat flux, experimental, D-32#  
 Heat flux limit, T-34, D-16, D-30  
 Heat pipes, comparison with conductors, D-2ff  
 Heat, input, non-uniform, T-30  
 Heat transfer, T-36ff, T-37\*  
 Heat transfer coefficient, T-42, D-48#  
 requirements, D-37  
 Heat transport capability factor, T-23ff, D-4ff, D-25ff  
 closed form solution, T-27ff  
 Heat transport factor, T-23ff, D-5, D-24ff  
 Hydraulic diameter, T-12, T-15  
 Interfacial pressure, T-4, T-8, T-11, T-19, T-22, D-18ff  
 max., T-20  
 Life tests, M-9ff, M-11#, M-13ff#  
 Length, effective, T-30  
 Liquid transport factor, T-29, F-2, D-25ff, D-36\*  
 Liquid transport capabilities, D-35ff  
 Man rating, D-9  
 Material selection, D-54  
 Mechanical interfacing, D-9  
 Mass transfer, T-7, T-21 (& heat transfer)  
 Nucleate boiling, T-34ff  
 Nucleation tolerance parameter  
 Operating principle, T-1ff, T-2\*  
 Permeability, T-12  
 composite wicks, W-13#, W-12#  
 estimate, W-5ff, W-11\*  
 experimental values, W-25ff#  
 measurement techniques, W-20ff  
 physical requirements, D-8  
 Pore radius, T-8, T-9\*  
 effective, grooves, T-10  
 circular capillary, T-10  
 wire mesh, T-10  
 Porc size (see pore radius)  
 Performance limit evaluation, D-16  
 Porosity, T-12, T-16

estimate screens, W-9  
 capillaries, parallel cylindrical, W-5  
 closed rectangular channels, W-5, W-7\*  
 concentric annuli, W-6, W-8\*  
 grooves (see open rectangular channel(s))  
 open rectangular channels, W-6  
 packed spheres, W-10  
 screen (see wire mesh)  
 wire mesh, W-10, W-11\*  
 experimental, W-25ff#  
 Poiseuille's Law, T-12

Pressure  
 critical, F-3#  
 gradient, T-6, T-7, T-19ff, D-18  
 liquid, T-11, T-13  
 vapor, T-15, T-16, T-17

operating, D-33  
 Radial evaporative heat flux, max., T-34  
 Reynold's number, axial, T-17  
 radial, T-16

Reliability, D-15  
 Radius, effective pore, D-27  
 estimate, W-1ff  
 cylindrical, W-1  
 felts (fibrous), W-5

grooves, rectangular, W-3  
 semicircular, W-3  
 triangular, W-3

screen (see wire mesh)  
 sintered particles (see spheres)  
 spheres, packed, W-4

wire mesh, W-4  
 experimental data, W-25ff#  
 measurement techniques, W-15ff

sonic limit, T-31, F-2, D-16, D-29  
 velocity, T-32  
 surface tension, T-4, T-8ff

Structural considerations, D-55  
 Static capillary height, D-21  
 Stagnation temperature, T-32

Temperature  
 operating range, D-11, D-31  
 uniformity, D-13  
 sensitivity, D-15

boiling, F-3#  
 critical, F-3#  
 melting, F-3#

Testing  
 acceptance & qualification, D-13  
 ground, D-13

Thermal conductance, T-38ff, D-47  
 evaporation, T-41  
 external, T-38  
 vapor flow, T-41  
 wall, T-38  
 wick, T-39

Thermal conductivity  
 wick effective, T-40, D-47  
 thermal environment, D-14  
 Thermal load, D-11  
 Transient behavior, D-15  
 Transients, T-18

wicked reservoir, T-79  
 non-wicked reservoir, T-79  
 feedback, T-80

Tortuosity factor, T-13  
Transport length, D-7  
Variable conductance control technique, T-44ff, T-62  
condenser flooding with gas, T-45, T-47ff  
condenser flooding with liquid, T-82  
Liquid flow control, T-65  
vapor flow control, T-85  
Variable conductance heat pipes, D-58ff  
active control, T-47, T-69  
control parameter effects, T-52  
diffusion effects, T-69  
Front front model, T-69  
diffuse front model, T-71ff  
numerical analysis, T-74ff  
feedback controlled, T-46, T-60ff  
electrical, T-65ff  
mechanical, T-63  
self controlled, T-46, T-53ff  
non-wick reservoir, T-57ff  
wicked, uncontrolled reservoir, T-56ff  
wicked, temperature controlled reservoir, T-59  
variable set point, T-67ff  
Viscosity, T-12ff  
Kinematic, ratio of, F-2  
corrosion, effect, M-1  
Wicks  
Working number, T-33, D-30  
Wicking height factor, T-29, F-2, D-27, D-37  
Wicks  
composite, W-10ff, W-13\*, W-14#, D-49  
Priming, W-12ff  
conventional, W-1ff, D-46#  
design, D-40ff  
Viscous pressure gradients, W-12ff  
Liquid, T-12ff  
Vapor, T-15ff  
Weber number, T-33, D-30  
Working fluids, M-11#  
Acetone, M-16#, F-3#, F-24\*, D-34\*, D-36\*  
Ammonia, F-3#, F-18\*ff, M-9, M-12, M-17#, D-32#, D-34\*, D-36\*  
Benzene, F-3#, F-28\*, M-18#, D-34\*, D-36\*  
Butane, M-18#  
Calcium, M-15#  
Cesium, F-3#, F-36\*, M-14#, D-34\*, D-36\*  
Dimethyl sulfide, M-20#  
Dowtherm, M-12, M-19#  
Ethanol, M-17#  
Freon-11, F-3#, F-22\*, M-12, M-18#, D-34\*, D-36\*  
Freon-21, F-3#, F-16\*, M-12, M-19#, D-34\*, D-36\*  
Freon-11,3, M-19#  
Heptane, M-18#  
Hexane, M-18#  
Hydrogen, F-3#, F-4\*, D-34\*, D-36\*  
Indium, M-15#  
Lead, M-15#  
Lithium, M-10, M-13#, F-3#, F-44\*, D-34\*, D-36\*  
Mercury, M-12, M-15#, F-3#, F-34\*, D-34\*, D-36\*  
Methane, F-3#, F-14\*, D-34\*, D-36\*  
Methanol, M-12, M-16\*ff, F-3#, F-26\*, D-34\*, D-36\*  
Neon, F-3#, F-6\*, D-34\*, D-36\*  
Nitrogen, F-3#, F-8\*ff, D-32#, D-34\*, D-36\*  
Oxygen, F-3#, F-12\*, D-34\*, D-36\*  
Pentane, M-18#  
Perchloroethylene, M-20#  
Potassium, M-10, M-14#, F-34, F-28\*, D-34\*, D-36\*  
Pyridane, M-19#  
Silver, M-10, M-15#, F-3#, F-46\*, D-34\*, D-36\*

Goldura, F-3#, F-60\*ff, T-1, M-5, M-14, D-32#, D-36\*  
Water, H-5#, F-50\*ff, M-3, M-12, M-15ff, D-32#, D-34\*  
D-36\*